THE UNIVERSITY *of* EDINBURGH

THE MAPK PATHWAY: A ROLE IN DEVELOPMENT, DISEASE AND BEHAVIOUR

Korina Anastasaki

Presented for the Degree of

Doctor of Philosophy

The University of Edinburgh

June 2011

I hereby declare that this thesis has been composed by me, this work has not been submitted for any other degree or professional qualification, the work is my own and contribution from others has been clearly indicated.

Korina Anastasaki

June 2011

Acknowledgments

The sheer existence, carrying out and finishing of this thesis would not have been possible without the immeasurable help of so many people. To all of you I am and forever will be grateful.

First, I would like to acknowledge my supervisor Liz Patton for having faith in me from the very beginning and giving me a project and a lab-home for all these years. I would not be counting my fifth year in Edinburgh if it weren't for her. Thank you for all the spoken and unspoken reasons!

I would also like to thank Ian Jackson for being the calm and rational head-supervisor and for his help on this thesis throughout the years, David Porteous for his guidance and critical reading of the manuscript, our Californian collaborators Kate Rauen and Anne Estep for the constructs and advice that kicked this project off, as well as Jeroen den Hertog for the dlx3 and hggI plasmids and Richard Marais for the CI-1040.

I fear I will forget many people, so to start with, a big thanks goes to all the HGU students and postdocs, who made lunch, TGIs, parties, life all that better! These have been the most amazing years yet! Thank you all for all of them.

A huge thank you goes out to the ever-patient and always lovely Craig Nicol, Paul Perry and Matt Pearson for the endless hours they have spent with me over a computer or a microscope trying to make science look prettier. I hope I can someday make you proud…

Our everyday life in the wet wet fish room, all the terrifying fish-jumping, brine-shrimp-eating, water-soaking accidents would not be the same without the fishy people, old and new… Super Sue, ("Biiig problem") John, Keith, Karthika, Pedro, Patricia, Sofia, Niki, Anna, David thank you for the inevitable help you must have given me but most importantly for the long chats in the injection room that made all those mornings go by so much more pleasantly.

The gratitude I have and the support I received from all the people in our fantastic lab cannot fit in a few lines but I will try to squeeze my love just this once! For all the all-nighters and early-mornings, for all the "ferocious" moments and the karate-singing, for all the incredible times of happiness or disappointment, for all the laughs and tears, for the very first experiment that ever worked and yesterday's failed IHC, for all these amazing times we all shared together that are not the memories of one person alone, I am proud and honoured to be one of you. Because of these and because of you I wrote this. This thesis is for you… Jenny, Natalie, Pia, Nicola, Kerrie, Juan, Amy, Amy, Hiro, Zhiqiang, Nick, Emma! My heroes!

There are no special thank-yous because everyone has helped in their own way so so much, but the following people made everything special for me. So, REALLY thank you to my family… my family everywhere. Firstly, to my real one in Greece

without the 25-year fully-inclusive life-, love-, moral-, money-support of whom I would simply not have had the opportunity to be the same person. Mum, Dad, Danae, Nefeli (and the rest of the 5000 cousins and uncles), you are the sole reason I am where I am…And secondly, to my even more real family, the one right here…my lovely ladies, Derya, Chloe, Emily, Carol-Anne, Sehrish, Alida, Elly, Bethan, Mousou, the boys, David, Juan, David, James, David (!), Adam, Victor, Sam and all the rest of you who make life a little bit more colourful! You all turned life upside down! I will not forget you, or anything and this is not the end…

Above all I would like to thank just two more people who have made a huge difference to me and this thesis…One has been the most dependable and helpful of all and gave me the strength to finally submit this and the other one was the biggest distraction in the world but gives me the strength to carry on… Natalie has been "my person" from day 1 and, with her permission, Alex can now take over for the rest of the days… (…if he keeps doing things in R for me. Oh! And thanks for this, too, Alex!)

Abstract to Thesis

Mutations in the RAS-RAF-MEK-ERK (MAPK) pathway give rise to a range of developmental disorders collectively referred to as the RASopathies. *De novo* germ-line mutations in patients suffering from these syndromes promote similar phenotypes, which include heart abnormalities, characteristic facial features, cutaneous malformations, gastrointestinal malfunctions, failure to thrive and a spectrum of mental retardation. Although many RASopathies patients show a propensity to develop early-onset benign and malignant tumours, Cardio-facio-cutaneous (CFC) syndrome patients do not seem to share this predisposition, with the exception of an increased number of naevi.

CFC syndrome is caused by mutations in BRAF, MEK1 or MEK2, with the majority of patients harbouring BRAF mutations. Intriguingly, both kinase-activating and kinase-impaired mutations have been identified in CFC patients. Here, I use the zebrafish system to address the activity of the CFC syndrome alleles and the MAPK pathway in a developmental context and test the potential of small molecule inhibitors to restore normal development.

I established an assay for the activity of CFC, melanoma and engineered BRAF and MEK human mutated alleles *in vivo.* Using zebrafish as an animal model organism, a panel of 31 mutant and wild-type BRAF, MEK1 and MEK2 alleles were expressed in early zebrafish embryos to assess their role in development. Irrespective of the predicted kinase activity, all embryos expressing BRAF and MEK mutant alleles reproducibly manifested the cell movement phenotype during gastrulation. Consistent with aberrant fibroblast growth factor (FGF) signalling and defective gastrulation, *in situ* hybridisation against convergence-extension markers showed misregulated convergence-extension movement patterns in CFC zebrafish embryos. Finally, I performed whole embryo RNA expression microarrays to identify genes regulated downstream of the CFC mutations, and I discuss the potential for a possible link to some of the phenotypes associated with a CFC zebrafish model.

I established that the CFC, BRAF and MEK mutant embryos are sensitive to inhibition of MEK signalling by small molecules. Importantly, a time-window of treatment was identified which was sufficient to restore normal gastrulation movements and to prevent the developmental side effects promoted by the inhibitors at later stages of development. In order to begin considering the therapeutic potential of small molecules in developmental disorders (at least in our model system), the effect of low concentrations of the inhibitors in the normal formation of diverse tissues was thoroughly examined during zebrafish development. From these studies, I identified a concentration of MEK inhibitor that could be administered in a continuous fashion to prevent CFC-associated cell movement defects during gastrulation, without additional later developmental defects.

Finally, I addressed the role of MEK-ERK signalling in a specific behavioural phenotype in zebrafish. Many RASopathies patients suffer from mental retardation and experience learning and attention difficulties. Research in our laboratory has identified a novel zebrafish behaviour induced by enhanced cAMP signalling, where the zebrafish seek shaded areas in their environment and exhibit frequent defensive shoaling behaviour. I used western blotting to establish that enhanced cAMP signalling activates the MAPK signalling pathway and, in collaboration with members our laboratory, that this phenotype can be suppressed by administration of the PD325901 MEK inhibitor. While we do not yet know the effect of CFC syndrome mutations on this behaviour, we suggest that altered MEK-ERK signalling may underlie important features of vertebrate behaviour.

Table of Contents

Chapter 1 – Introduction

“The past is the beginning of the beginning and all that is and has been is but the twilight of the dawn”
– H. G. Wells

1.1. The MAPK pathway

Cells are constantly exposed to a plethora of conditions and have developed the capacity to monitor and respond to their environment. Signals such as hormones, growth factors, stress and inter-cellular communications activate membrane receptors and their tethered signalling cascades. Such integral pathways control cell fate decisions by promoting genetic and physical changes. The RAS/RAF/MEK/ERK cascade is one of those cascades and is conserved from yeast to plants and animals (reviewed in Widmann *et al*., 1999). Triggered by extracellular stimuli, mitogen-activated protein kinases (MAPKs) transduce multiple intracellular signals (reviewed in Yoon and Seger, 2006) that control cellular growth, differentiation, proliferation, senescence and apoptosis (reviewed in Pearson *et al*., 2001). The structure of each canonical MAPK pathway is based on the function of three sequentially activated kinases: a MAPK kinase kinase (MAP3K), a MAPK kinase (MAP2K) and a MAPK.

To date, six distinct MAPK pathways have been identified, each of which promotes downstream signalling via different kinases; namely, ERK1/2, ERK3/4, ERK5, ERK7/8, JNK1/2/3 and p38α/β/γ (ERK6)/δ, respectively (reviewed in Chang and Karin, 2001). ERK5 is specifically regulated by MEK5 signalling, the p38 isoforms are directly activated by MEK3 and MEK6 and the JNK kinases are phosphorylated by MEK4 and MEK7 (reviewed in Bogoyevitch *et al*., 2004; Garrington *et al*., 1999). Interestingly and unlike the other pathways, the ERK3 and ERK7 MAPK cascades are constitutively active (reviewed in Coulombe and Meloche, 2006) with the mechanism of activation of ERK8 still remaining largely elusive (Abe *et al*., 2002) and the role of ERK4 only recently beginning to be deciphered (Rousseau *et al*., 2010). The present thesis, however, is focused on the activity of ERK1/2 MAPK signalling, whose frequent association with various human cancers and identification of cascade components as prominent oncogenes (reviewed in Kolch, 2005) have propelled its extensive characterisation and study.

1.2. Working with zebrafish

1.2.1. Advantages of the zebrafish model organism

Knockout studies on mice have been informative on the importance of MAPK components expression in cancer and development. However, the physiological role of individual MAPK pathway component mutations *in vivo* has not been explicitly tested in the framework of an animal system. Zebrafish studies provide the advantage of exploring the developmental effects of an allelic series and as embryos develop *ex utero,* they are readily observed in detail from the very first stages of development.

Zebrafish (*Danio rerio*) are small cyprinids, native to the banks and shallows of low-current rivers, ponds and paddy fields of southern and south-east Asia. They are a carnivorous species feeding mainly on small insects on the surface of the water (reviewed in Miller and Gerlai, 2011; Spence *et al*., 2008).

Zebrafish are amongst the smallest vertebrate animals with a fully developed innate and acquired immune system and have been established as a system for genetic, developmental, behavioural and pharmacological investigations. They provide a good platform to model human diseases both in genetic and functional assays and as such, they are not only an efficient complement to other mammalian models but have additional advantages over other them.

The nature of embryonic zebrafish provides key advantages from a methodological perspective and has facilitated the development of a number of technologies. Firstly, embryos are small, are fertilised *ex utero* and remain translucent throughout organogenesis. These factors together have assisted in developing sophisticated imaging that has widened our understanding of organ development and function (Auman and Yelon, 2004; Kimmel *et al*., 2001) as well as allowed image-based high-throughput screening of cancer therapeutic drugs (Evensen *et al*., 2010). Their

optical transparency has been their most exploited feature as it permits visualisation of internal organs as well as targeted tissues and single cells. For instance, expression patterns of genes with GFP-tagged promoters can be readily tracked in individual tissues via fluorescence microscopy in transgenic live embryos (**Figure 3.2.2**). Similarly, RNA *in situ* hybridisation allows for similar gene expression analysis in fixed samples (**Figure 2.2.5**).

Secondly, larvae younger than 5 dpf are fully permeable to small molecules. This allows for effective pharmacological treatment and whole body staining through passive diffusion of the molecules. Thus, zebrafish are well suited for large- and small-scale library screens, especially for those designed to identify modifiers of developmental processes. A large number of chemical screens have already been carried out in zebrafish, some of which have identified new used for established drugs (White *et al*., 2011; Yeh *et al*., 2009; reviewed in Taylor and Patton, 2010). Additionally, smaller screens have been able to shed new light on the mode of action of small molecules by elucidating their specific targets (Ishizaki *et al*., 2010). More importantly, the timing of small molecule addition and therefore the inactivation of their targets can be tightly controlled. This level of control can provide insight into the spatiotemporal regulation of individual target proteins and can deepen the understanding of normal developmental processes. The temporal control of small molecule inhibition is further explored in **Chapter 3**.

Thirdly, the prolific nature of zebrafish allows a single pair of adult fish to breed once in four to five days and produce an average of 100-300 embryos per mating. Thus, high-throughput experiments greatly benefit from abundance of progeny.

Moreover, embryonic development is fully completed at 5 days postfertilisation (dpf) and their rapid embryonic maturation rate allows for quick screening of embryonic phenotypes. This provides a vast array of developmental information that can be easily assessed by direct observation. Finally, establishment of adult transgenic lines is relatively fast as individuals reach adulthood within 3 months. In addition, the size

of adult zebrafish, smaller than 4 cm, and low cost allow thousands of fish to be maintained in a relatively small space.

1.2.2. Genetic and transgenic models

Large-scale genetic screens and more recently chemical modifier screens have been carried out to generate a large number of transgenic and knockout animals (reviewed in Amsterdam, 2006). In the last decade, the zebrafish community has increased in size allowing for the development of a large collection of publicly available resources. Such tools include an annotated zebrafish genome sequence, gene expression atlas, microarray platforms and central sources of mutant and transgenic lines.

Gene knockout technology in zebrafish has been more challenging than in mammalian models due to the absence of homologous recombination. However, both temporary gene silencing and permanent gene disruption are available options. A simplistic and effective approach to gene silencing in developing embryos is via the use of morpholino oligonucleotides (MOs). The latter are short oligonucleotides injected at the single cell-stage embryo and are designed to hybridise with mRNA, either impeding its translation (translation block MO) or its proper splicing (splice-site MO).

Generation of stable knockout lines can be achieved both by genetic and chemical approaches. Zinc finger nucleases (ZFNs) act by specifically binding to zebrafish DNA and creating double strand breaks in the sequence of interest (Miller *et al*., 2007). However, the cost, difficulty of design and time dedicated to optimisation are significant and limit the use of this technique.

A different technology aiming to create knockout lines is chemical mutagenesis. Mutagenesis screens are easily and cost-effectively carried out. This approach induces random point mutations in the genome and identification of specific mutations relies on sequencing of genes of interest. High-throughput ENU

mutagenesis (Solnica-Krezel *et al*., 1994) and TILLING (targeting induced local lesions in genomes) projects (Stemple, 2004) are ongoing and have, to date, established tens of knockout lines, available upon request.

A final way to study of the effect of individual mutations in a physiological framework is through zebrafish transgenics. Zebrafish represent an ideal model to transiently express a mutant gene of interest to assess its role during development in the context of a wild-type or mutant individual. Direct injection of the coding mRNA into a single cell-stage embryo promotes ubiquitous expression albeit short-lived (**Figure 2.2.3**). Additionally, studying genes in a tissue-specific microenvironment is possible by expressing transgenes under tissue-specific promoters (**Figure 2.2.7**). Finally, making use of the transposon Tol2, DNA sequences are randomly but stably incorporated in the zebrafish genome (Kawakami *et al*., 2004).

1.2.3. Zebrafish as a model for human diseases

With all these resources in hand, zebrafish are becoming an ever-relevant model to study human diseases. The initial focus of the zebrafish field was on developmental biology. However, the identification of a large number of mutant phenotypes resembling human disorders in two initial large genetic screens (Driever *et al*., 1996; Mullins *et al*., 1996) changed the way zebrafish was approached in research. Immediate attention was shifted towards the histological and genetic similarity between zebrafish and humans that share major genes and signalling pathways as well as tumour histopathology (Amatruda *et al*., 2002). Zebrafish models of human cancer include HRAS (Santoriello *et al*., 2010) and $BRAF^{V600E}$ melanoma models (Patton *et al*., 2005) and KRAS rhabdomyosarcoma models (Langenau *et al*., 2007).

The conservation is not limited to neoplasia formation. Early embryogenesis, development and body axis formation are governed by molecular processes conserved across vertebrates. For example, neurulation and further neural crest cell migration and differentiation are integral to the proper formation of the heart, craniofacial structures, melanocytes and glial populations. The specific roles of

neural crest cell populations are discussed in further detail in **Chapter 3** (Section **3.1.8**).

Finally, zebrafish are increasingly being used in behavioural studies. A large number of tests have been developed to assess social aspects of zebrafish behaviour, including anxiety, social interaction (shoaling), fear, learning and memory (reviewed in Norton and Bally-Cuif, 2010). Such behavioural genetic studies focus on the relationship between genes or even specific mutations and a quantifiable manifested behavioural phenotype. Their main scopes are both to understand the behavioural aspect of human disorders as well as rapidly identify compounds that alleviate or ameliorate behavioural symptoms. A series of behavioural studies introducing a novel link between MAPK regulation and zebrafish behaviour is presented in **Chapter 4**.

Taken together, it becomes evident that zebrafish offer a platform for highly controlled *in vivo* experimentation and for development of new techniques. In the scope of this project, the zebrafish system will be used aiming to advance comprehensive understanding of developmental processes and disease-promoting mechanisms upon modulation of the MAPK signalling in a physiological framework.

Chapter 2 - The Activity of CFC Alleles *In Vivo*

“Somewhere, something incredible is waiting to be known”
- Carl Sagan

2.1. INTRODUCTION

2.1.1. Signalling down the MAPK cascade

In the presence of extracellular signals transmembrane receptor tyrosine kinases dimerise resulting in their autophosphorylation. The receptor phosphorylation promotes the activation of the RAS-SOS-GRB2 complex, a step that initiates a cascade of serial downstream phosphorylation events (reviewed in Orton *et al*., 2005). In more detail, in their active GTP-bound state, the human RAS proteins (HRAS, KRAS and NRAS) recruit the cytosolic RAF kinases (BRAF and C-RAF) to the plasma membrane and activate them by binding to the RAS-RAF binding domain (reviewed in Wellbrock *et al*., 2004). Phosphorylated C-RAF and BRAF, in turn, stimulate MEK1 and MEK2. Finally, the activated MEK kinases phosphorylate ERK1 and ERK2. Phospho-ERK1/2 (pERK1/2) further signal to several cytosolic pathways as well as translocating to the nucleus to phosphorylate transcription factors such as c-Myc, Ets-1 and Stat-3 (**Figure 2.1.1**).

As pERK triggers multiple biochemical signals and has a key role in the cell cycle progression (reviewed in Kolch *et al*., 2005), it is vital that the output of the MAPK cascade is regulated by positive and negative feedback loops. This tight control is enforced by components of both the MAPK pathway itself and parallel pathways. For instance, to inhibit its over-expression, ERK negatively signals back to SOS-GRB2 turning the pathway "off" (Kamioka *et al*., 2010). Additionally, downstream effectors of ERK affect the activation of individual MAPK pathway components. Dual specificity phosphatase (DUSP) proteins, achieve ERK1/2 de-phosphorylation (Jeffrey *et al*., 2007) with the cytoplasmic DUSP6, in particular, acting as a potent negative regulator of FGF/MAPK (Zhang *et al*., 2010). PAK tightly controls MEK activation by C-RAF and high pERK levels inhibit PAK to terminate the association (Eblen *et al*., 2004). pERK can also trigger a positive feedback loop by inactivating the RAF kinase inhibitor protein (RKIP) (Shin *et al*., 2009), a protein that prevents the BRAF-MEK complex formation (Yeung *et al*., 2000).

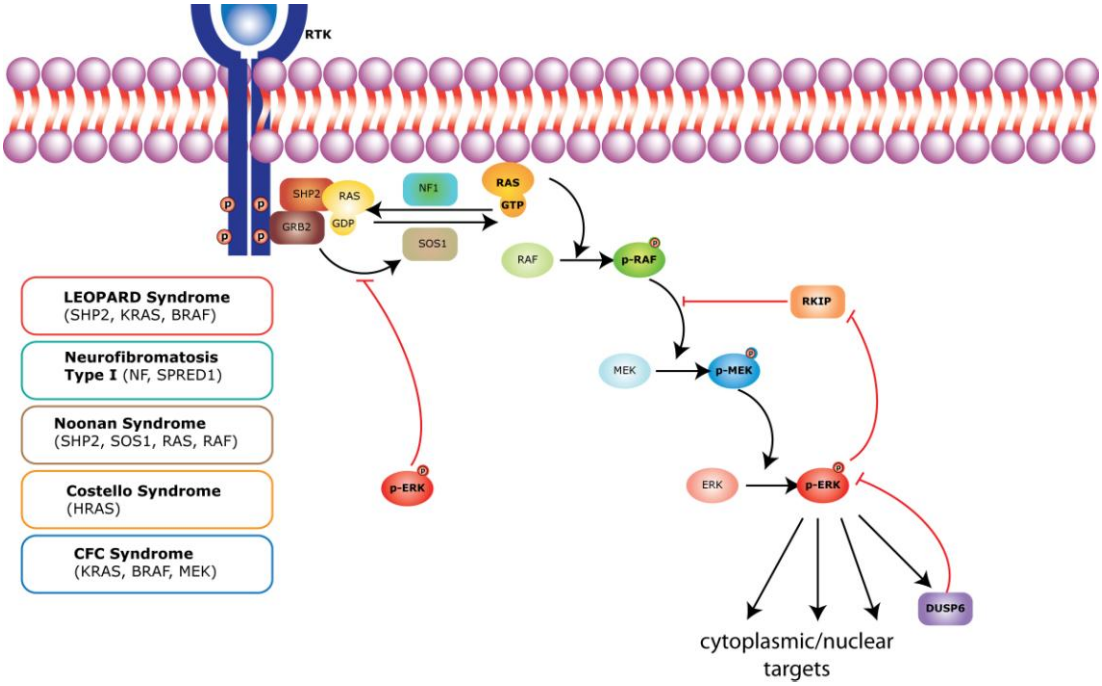

Figure 2.1.1 *The MAPK pathway*

Schematic illustration of the MAPK pathway and some of its regulatory feedback loops. The components of the pathway that are mutated in the RASopathies spectrum are highlighted in separate boxes.

Control of MAPK signalling and specific expression of its components are crucial to ensure proper development and health. This becomes more evident when studying a number of different oncogenic and developmental diseases propagated by germ-line or somatic mutations of RAS/MAPK pathway genes (reviewed in Burkitt Wright and Kerr, 2010; Aoki *et al*., 2008; Bentires-Alj *et al*., 2006). To that end, further *in vivo* models would greatly benefit the understanding of how the RAS/MAPK pathway responds in cases of misregulation.

2.1.2. The MAPK pathway in the onset of "RASopathies"

Oncogenes are misregulated in cancer but it is not uncommon that, under normal conditions, they are essential for development and survival. The MAPK pathway has been the subject of extensive research for the past two decades due to the high mutation incidence of its components in human cancer. Recently, though, germ-line

mutations have been identified in genetic developmental syndromes (reviewed in Bentires-Alj *et al.,* 2006).

By virtue of the patients' phenotypic overlap the medical genetic disorders of the MAPK pathway were collectively referred to as the neuro-cardio-facio-cutaneous (NCFC) syndromes (reviewed in Bentires-Alj *et al.,* 2006). However, this term has been updated to "RASopathies" to reflect the genetic overlap between the disorders (reviewed in Tidyman and Rauen, 2009). The RASopathies spectrum includes the cardiofaciocutaneous syndrome (CFC), Costello syndrome (CS), Noonan syndrome (NS), LEOPARD syndrome (LS), Neurofibromatosis Type 1 (NF1) and Legius syndrome.

Even though diagnosis of some patients is facilitated by the presence of characteristic features, symptom overlap and the progressiveness of the diseases renders discrimination between cases of NS, CS and CFC increasingly challenging. For example, children diagnosed with CS at birth present more CFC-like features as they grow older (Zenker *et al.,* 2007). A CFC index was generated in the past decade to distinguish CFC patients (Kavamura *et al.,* 2002) but diagnosis is frequently mostly based on molecular data of the patients. A precise map of specific genotype-to-phenotype correlations is still being delineated but, to date, each disorder has been coupled with disease-causing genes (**Table 2.1.1**). CFC is driven by mutations in *KRAS*, *BRAF*, *MEK1* and *MEK2*, CS by *HRAS* mutations, NS by *SOS1*, *PTPN11*, *KRAS* and *CRAF* mutations, NF1 by neurofibromin mutations, LEOPARD syndrome by *PTPN11* and *CRAF* mutations and Legius syndrome by *SPRED1* (Brems *et al*., 2007; Zampino *et al.,* 2007; Rodriguez-Viciana *et al.,* 2006; Niihori *et al.,* 2006; Aoki *et al.,* 2005). A diagram highlighting the genes correlated with each syndrome is illustrated in **Figure 2.1.1**. Misdiagnosis is common but can be fundamental as with some syndromes there is a high risk of cancer development.

2.1.2.1. Noonan Syndrome

Noonan Syndrome (NS) (MIM ID #163950, #609942, #610733, #611553, #613224) is a genetic condition affecting between 1 in 1,000 and 1in 2,500 people (reviewed in

van der Burgt, 2007). NS was first described as a separate disorder in 1968 (Noonan, 1968) and both its features and the underlying molecular genetics have since been closely examined. The majority of cases are caused by germ-line, missense gain-of-function mutations in PTPN11 (Tartaglia et al, 2010) although gain-of-function mutations in SOS1 (Roberts et al, 2007; Tartaglia et al, 2007; Zenker et al, 2007; Ferrero et al, 2008), KRAS (Schubbert et al, 2006; Kratz et al, 2009), NRAS (Cristea et al, 2010) and CRAF (Pandit et al, 2007; Razzaque et al, 2007) have been more recently identified (**Table 2.1.1**).

2.1.2.1.1. Clinical Symptoms and Cancer Predisposition

The phenotypic spectrum of NS is variable leading to the belief that the condition is widely under-diagnosed. Interestingly, the severity of the symptoms is attenuated with time and patients can live an independent adult life. NS is best characterised by facial anomalies, congenital heart defects and short stature. Typical facial symptoms include eye hypertelorism, down-slanting eyelids, epicanthal folds and ocular ptosis (reviewed in Zenker *et al*., 2007), which can lead to poor vision. Moreover, low-set ears, flat nasal bridge, webbing of the neck and short curly hair are typical of NS. Cardiac abnormalities are almost universal, with pulmonary valve stenosis having the highest incidence, followed by atrial septal defects and hypertrophic cardiomyopathy (Croonen *et al*., 2008; Ferrero *et al*., 2008). Individuals usually fail to thrive, especially during their early ages, as they experience severe feeding difficulties (Shah *et al*., 1999). General muscle weakness (hypotonia) is prominent which may be a leading cause of speech delay and mild learning difficulties. Some males experience cryptorchidism and delayed puberty (Ferrero *et al*., 2008).

NS is not correlated with increased cancer risk. Nevertheless, patients, often, develop multiple giant cell lesions of the jaw, most commonly the maxilla and the mandible, and other bone or cartilaginous tissues (Bertola *et al*., 2001; Tartaglia *et al*., 2010). More rarely, NS patients are diagnosed with juvenile myelomonocytic leukaemia (Bader-Meunier *et al*., 1997; Fukuda *et al*., 1997; Choong *et al*., 1999).

2.1.2.2. LEOPARD Syndrome

LEOPARD Syndrome (LS) (MIM ID #151100, #611554) is an acronym describing the most common manifestations of the disorder (Gorlin *et al*., 1969): multiple Lentigines, Electrocardiographic conduction abnormalities, Ocular hypertelorism, Pulmonic stenosis, Abnormal genitalia, Retardation of growth, and sensorineural Deafness. Lentigines are benign melanocyte hyperplasias that, unlike common moles (naevi), reside in a single layer below the epidermis. Onset of LS is driven by dominant loss-of function missense mutations in PTPN11 (Digillio *et al*., 2002) and C-RAF (Pandit *et al*., 2007). LS is a sporadic disorder with around 200 reported cases world-wide, but this is, likely, a mis-representation as many patients are undiagnosed due to lack of lentiginosis.

2.1.2.2.1. Clinical Symptoms

LS symptoms become evident in childhood and are progressive with time. Typical facial appearance in LS patients is characterised by hypertelorism, flattened nasal bridge and low set ears. Occasionally, patients present with eyelid ptosis, prominent lips and extra skin, which leads to neck webbing (Somerville and Bonham-Carter, 1972). Cardiovascular anomalies affect 75% of the patients, who suffer from hypertrophic cardiomyopathy and pulmonary valve stenosis (Limongelli *et al*., 2007; Digillio *et al*., 2006; Sarkozy *et al*., 2004). Individuals with LS are developmentally delayed, experience late puberty and cryptorchidism, very commonly display thoracic abnormalities and can, less frequently, present with skeletal problems such as scoliosis, mandibular deformities and joint hyper-flexibility (Gorlin *et al*., 1990). Moreover, up to a quarter of LS patients are diagnosed with sensorineural deafness (Sarkozy *et al*., 2004), while a third experience mild learning difficulties (Digillio *et al*., 2006).

The most characteristic features of LS are lentigines; flat, pigmented loci of melanocyte accumulation. Lentigines are normally correlated with old age and sun exposure. In LS patients however, they typically appear before 5 years of age, their

count increases with time and they occupy large areas of the face and upper body part. Additionally, congenital or late-development café-au-lait spots are observed, which appear darker than the ones on NF1 patients.

Although cancer incidence is not high, a few LS patients have been diagnosed with malignant tumours such as myelodysplasia, acute myelogenous leukaemia neuroblastoma and melanoma (Merks *et al*., 2005; Shishima *et al*., 2007).

2.1.2.3. Neurofibromatosis Type 1

Neurofibromatosis (NF) is a medical term describing two different conditions; NF Type 1 and NF Type 2. Neurofibromatosis Type 1 (MIM ID #162200) is one of the most common genetic disorders in the UK, with one in 2,500 born infants being diagnosed with a driver mutation (Huson *et al*., 2008; reviewed in Williams *et al*., 2009). It is caused by inherited or sporadic germ-line mutations of the NF1 gene.

2.1.2.3.1. Clinical Symptoms

Unlike other RASopathies, NF1 patients do not demonstrate severe facial or cardiac abnormalities, with the exception of relative macrocephaly (Clementi *et al*., 1999) and high blood pressure (Zinnamosca *et al*., 2010).

NF1 symptoms develop in early ages and mostly affect the skin, without causing further complications. These features include an increased amount of freckling, commonly around the armpits and the groin, more than six café-au-lait spots and Lisch nodules, harmless brown pigmentation speckles in the iris of the eyes (McGaughran *et al*., 1999). The disease, however, takes its name from the early development of neurofibromas, benign tumours growing on or under the skin along nerves throughout the body. The neurofibromas can be soft or rigid in texture and, in most cases, cause no distress to the patient. Although their number or size can increase dramatically with age, neurofibromas generally remain non-cancerous (reviewed in Ferner *et al*., 2007; Williams *et al*., 2009).

2.1.2.3.2. NF1 tumours are associated with learning difficulties and malignancy

NF1 is related with increased morbidity as sometimes neurofibromas can cause more prominent problems. Development of neurofibromas on the optic or the otic nerves can promote learning difficulties as a direct result of compromised vision and hearing. Moreover, neurofibromas on optic nerves can lead to the establishment of optic gliomas, benign growths, which could impair vision and require surgical attention (Daginakatte *et al.*, 2007; Dasgupta *et al.*, 2005). Nevertheless, optic gliomas can spontaneously regress leading to amelioration of vision (Parsa *et al*., 2001). During adolescence or adulthood, some of the patients develop new malignant peripheral nerve sheath tumours (King *et al*., 2000) as well as leukaemia and brain tumours (reviewed in North, 2000).

2.1.2.3.3. Neurofibromatosis-Noonan syndrome

Neurofibromatosis-Noonan syndrome (NFNS) (MIM ID #601321) is a distinct condition from NF1 and NS and results in a combination of the clinical features manifested in the two syndromes. Although mutations in NF1 are the major driving force for the onset of this syndrome (De Luca *et al*., 2005), a few patients with concurrent mutations in NF1 and PTPN11 have been identified (Thiel *et al*., 2009; Bertola *et al.*, 2005). NFNS symptoms can deviate slightly between patients, but generally include neurofibroma development, short stature, ptosis, learning disabilities, muscle hypotonia and, sometimes, atrial anomalies.

2.1.2.3.4. Legius Syndrome

Legius syndrome (MIM ID #611431) is a disorder only recently identified as a separate entity (Pasmant *et al*., 2009) as a result of heterozygous dominant mutations in SPRED1 (Brems *et al*., 2007; Pasmant *et al*., 2009). Correct diagnosis of this syndrome is important in genetic counselling as Legius syndrome symptoms are much milder and prognosis is better. Examined individuals have a normal facial

appearance, an increased count of café-au-lait spots and typical NF1 freckling. Additionally, patients lack neurofibromas and Lisch nodules but present with lipomas and learning disabilities.

2.1.2.4. Costello Syndrome

Costello syndrome (CS) (MIM ID 218040) was first described in 1977 (Costello, 1977). Due to the phenotypic overlap between CS and cardiofaciocutaneous syndrome (CFC), a number of CFC patients had been mis-diagnosed in the past. However, currently CS onset is only thought to be triggered by *de novo* autosomal dominant mutations in a single gene, HRAS (Kerr *et al*., 2008; Aoki *et al*., 2005).

2.1.2.4.1. Clinical Symptoms

CS is characterised by distinctive craniofacial characteristics, cardiac and skin anomalies, as well as mental retardation. Typical facial features are coarse and include, flattened nasal bridge, epicanthal folds, full, prominent lips and a large mouth (reviewed in Hennekam, 2003). Cutaneous manifestations are distinctive and confirm CS diagnosis. CS patients' hair appears to be curly and sparse and premature ageing or hair loss have been reported. Moreover, presentation of loose, redundant skin, mostly on the neck, as well as deep palmar and plantar creases is almost universal (reviewed in Hennekam, 2003). The skin itself is very soft, hyperpigmented with a high propensity to develop papillomata, benign, exophytic epithelial lesions. Papillomata are very common within this group and preferentially form around cavities of the body, usually, around the mouth, nares, ears and perianal region (reviewed in Costello *et al.*, 1996).

Frequently, CS promotes skeletal anomalies, most strikingly thoracic malformations, cyphoscholiosis and joint hyper-flexibility, which give CS patients a characteristic posture and short stature. Additionally, bad dental structure and osteoporosis are features of CS (White *et al*., 2005). Although, failure to thrive is characteristic in infants, due to exceptional feeding difficulties, normal body weight is gained later on in life. Despite the fact that overall development is delayed and that the majority

experience intellectual and learning deficits (Kawame *et al*., 2003), the patients' sociable skills and friendliness are outstanding (Axelrad *et al*., 2004).

2.1.2.4.2. Severe complications associated with CS

Most CS patients exhibit severe cardiac abnormalities. Congenital pulmonary valve stenosis, cardiac hypertrophy and arrhythmia are the most frequently observed conditions and require tight medical attention (Lin *et al*., 2002). Moreover, CS patients have a high propensity of forming cancerous and non-cancerous tumours from very early on in life (Gripp *et al.,* 2005; reviewed in Hennekam *et al.,* 2003). The most common non-malignant tumours associated with this disorder are papillomas. Nevertheless, malignant lesions are frequent and develop very early in life. They include paediatric cancers such as rhabdomyosarcoma (cancer of muscle tissue) (Gripp *et al.,* 2002; Feingold *et al.,* 1999) and neuroblastoma (cancer of nerve cells) (Selcen *et al*., 2001; Kerr *et al*., 1998), as well as transitional cell carcinoma of the bladder (Gripp *et al.,* 2000; Franceschini *et al.,* 1999), a highly uncommon condition for young aged individuals.

2.1.2.5. Cardiofaciocutaneous Syndrome

The cardiofaciocutaneous syndrome (CFC) (MIM ID #115150, #190070, #164757, #176872, #601263) is one of the most severe disorders of the RASopathies spectrum. It was first characterised in 1986 by Reynolds and colleagues (Reynolds *et al.,* 1986) on 8 patients of previously undefined congenital malformations. Approximately 200 patients have been reported since and the precise prevalence of the disorder can only be estimated to not exceed 400 individuals worldwide.

2.1.2.5.1. Mutations in BRAF and MEK give rise to CFC syndrome

Until recently, diagnosis was solely based on physical appearance and the presence of non-classical examples of patients (Kavamura *et al.,* 2003; Kavamura *et al.,* 2002) caused controversy on the diagnosis, rendering the CFC diagnostic index requisite (Kavamura *et al.,* 2002). Nevertheless, ambiguous cases still cannot be readily resolved without molecular evidence.

On the basis of the clinical features similarity, CFC was thought to be an extreme variant of NS. Half of the recorded cases of Noonan syndrome (NS) and the vast majority of the LEOPARD patients have missense mutations in PTPN11, the gene encoding for the protein tyrosine phosphatase SHP2 (Tartaglia and Gelb, 2005) However, after close screening of CFC patients, no PTPN11 mutations were found in any of the individuals (Musante *et al.,* 2003; Ion *et al.,* 2002) leading other groups to sequence different genes in the MAPK pathway.

Niihori and colleagues sequenced the coding sequences of HRAS, KRAS and NRAS from 43 CFC patients only to find two mutations in KRAS that had not been previously identified in cancer (Niihori *et al.,* 2006). Moreover, they identified eight mutations in BRAF. At the same time, Rauen and colleagues identified *de novo* germ-line mutations in BRAF, MEK1 and MEK2 (Rodriguez-Viciana *et al.*, 2006). The eleven missense BRAF mutations were either clustered in the cysteine-rich region in CR1 or in the protein kinase domain (**Figure 2.1.2A**). With the exception of two ($BRAF^{G469E}$ and $BRAF^{F595L}$), none of the mutations had been described in cancer patients. Two activating mutations of MEK1 were identified, one lying within the kinase ($MEK1^{Y130C}$) domain and one outside ($MEK1^{F53S}$). Finally, MEK2 harboured an analogous mutation to $MEK1^{F53S}$, $MEK2^{F57C}$ (**Figure 2.1.2B**). Thus, the capacity to perform mutation analyses of RAS/MAPK pathway genes can be a useful tool in the prediction and correct diagnosis of the conditions. Understanding the activity of the key regulators of the developmental disorders can be enlightening in treatment design.

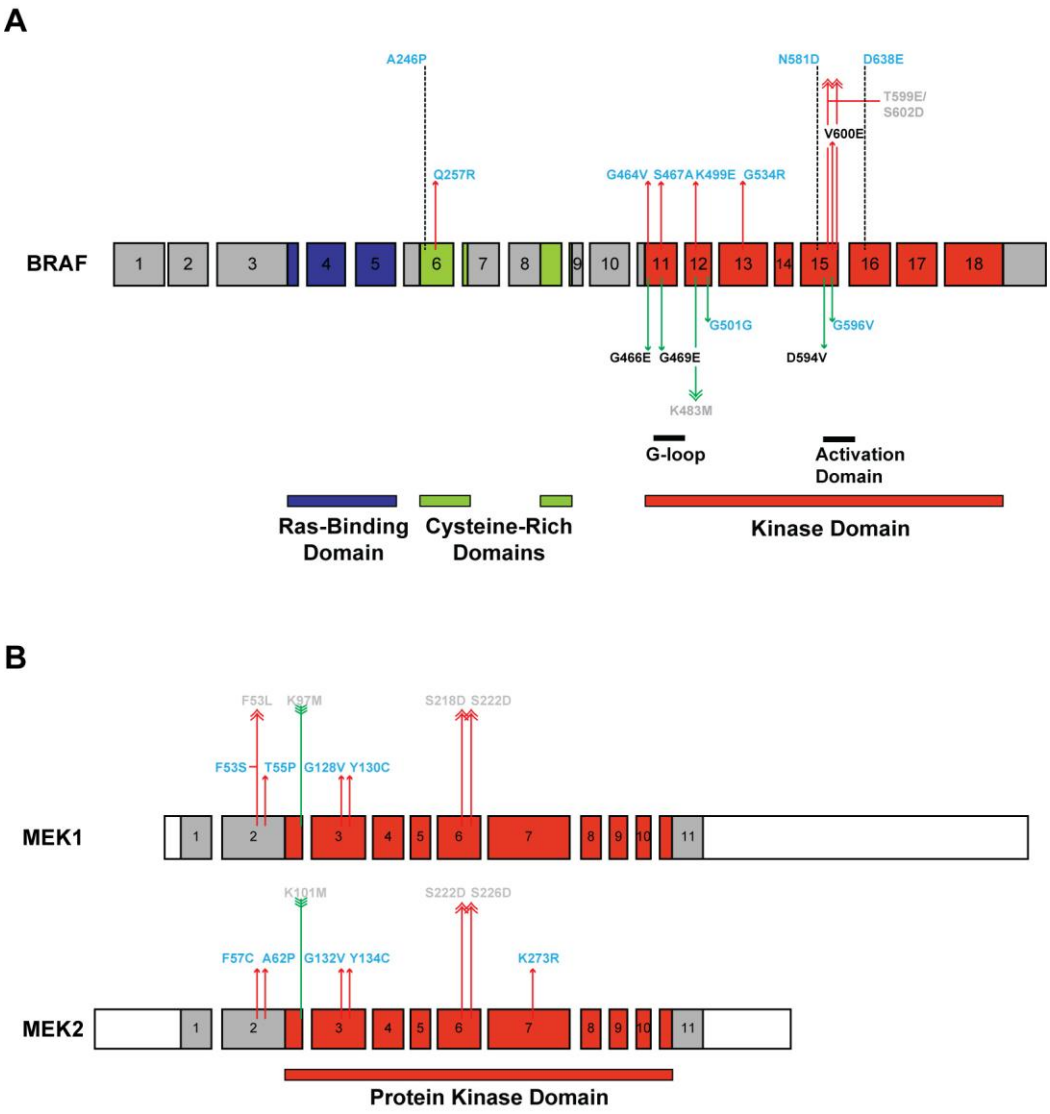

Figure 2.1.2 *Summary of allelic mutations of human BRAF, MEK1 and MEK2*

Primary structures of human BRAF (A), MEK1 and MEK2 (B) highlighting the mutations identified in CFC (light blue) and melanoma (black) patients, as well as engineered mutations (grey). Each numbered box illustrates a coding exon. Blue, green and red shading of the exons represent the Ras-binding domain (A), cysteine-rich domains (A) and the protein kinase domains (A, B), respectively. Red arrows with double arrowheads represent mutations rendering the protein constitutively active and green arrows with double (A) and triple (B) arrowheads represent substitutions leading to a kinase dead protein.
A Allelic substitutions illustrated above the linear BRAF sequence represent kinase-activating mutations (red arrows) and mutations conferring undetermined activity levels to the protein (dashed lines). Allelic substitutions positioned below the BRAF sequence represent kinase inactivating mutations (green arrows).
B Kinase-activating (red arrows) and kinase-inactivating (green arrows) allelic substitutions are illustrated above the linear representations of MEK1 and MEK2.

(Adapted from Rodriguez-Viciana et al., 2006)

2.1.2.5.2. Clinical features of cardiofaciocutaneous syndrome

The sporadic occurrence of the disease causes a characteristic set of features that mainly affect heart formation (cardio-), facial structures (facio-), skin and hair tissues (cutaneous). The patients are usually of short stature and fail to thrive, as a direct result of oral feeding aversion. A range of mental retardation is observed, but in most cases it is mild (Schulz *et al*. 2008).

The individuals have a distinguishing facial appearance, presenting with relative macrocephaly, significant hypertelorism and palpebral ptosis, a wide nasal bridge and low set ears with prominent helices (Kavamura *et al*., 2002). Dental malformations are also representative of this disease although they are not universal.

Ectodermal anomalies are outstanding and have been crucial factors in the clinical diagnosis of CFC. The absence of eyebrows and eyelashes and distinctive dark, woolly curly hair are very common. More characteristically, the diverse skin anomalies of the patients include keratosis pilaris, hyperkeratosis mostly of the palms and soles of the feet, ichthyosis (scaly skin), eczema and ulerythema ophryogenes (Siegel *et al*., 2010).

Severe heart defects are the most restrictive to the patients as cardiac complications lead to increased mortality in the first months of life (reviewed in Roberts *et al.*, 2006). Pulmonary valve stenosis, atrial and ventricular septal defects and hypertrophic cardiomyopathy present in most cases of CFC.

Although BRAF, a gene very frequently mutated in human melanoma, is often the cause of CFC, skin cancer development has not been recorded in this group of patients. Intriguingly, however, more than 20% of affected individuals show an abnormally elevated count of melanocytic naevi, a number that steeply increases with age (Siegel *et al*., 2010). CFC patients are not in an increased risk of cancer, with only two reported patients with diagnosed acute lymphoblastic leukaemia (Makita *et al*., 2007; Van den Berg and Hennekam, 1999).

2.1.2.6. RASopathies target the same tissues but each pathway component has a unique role

Close examination of the syndrome-driven symptoms reveals that disturbance of different components of the same pathway does not always translate to the same phenotypic outcome. Interestingly, however, all the diseases of the spectrum target the same tissues but affect them in different ways (**Table 2.1.1**). The multiple effectors of MAPK pathway components may account for the heterogeneity within the spectrum. Moreover, different genes might be particularly important in different tissues and their mutation might cause specific sensitivities to the patient.

Although the mutations causing the various syndromes are being constantly delineated, the mechanism of action that promotes individual mutations to give rise to different phenotypes remains elusive. Kinase activity levels (e.g. impaired activity $BRAF^{G596V}$ mutant versus high activity $BRAF^{Q257R}$ mutant) are sometimes unrelated to the severity and extremity of the clinical symptoms in CFC, NS and LS (Rodriguez-Viciana *et al.,* 2006; Aoki *et al.,* 2005; Kontarides *et al.,* 2005). Despite the rarity of the syndromes, the presumptive complexity underlying the MAPK pathway signalling has encouraged focused research on the components giving rise to the disorders. The fact alone that each syndrome presents different features suggests a unique role for each step of the signalling cascade.

			Syndrome					
			CFC	CS	NS	NF1	LS	NFNS
Mutated Gene		SOS1			✓			
		NF1				✓		✓
		PTPN11			✓		✓	
		HRAS		✓				
		KRAS	✓		✓			
		C-RAF			✓		✓	
		B-RAF	✓					
		MEK1	✓					
		MEK2	✓					
Facial	General	Large forehead	✓	✓	✓			✓
		Flat nasal bridge	✓	✓	✓		✓	✓
		Relative macrocephaly	✓			✓		✓
		Ptosis	✓		✓		✓	✓
	Eyes	Down-slanting eyelids	✓		✓			✓
		Epicanthal folds	✓		✓			
		Ocular hypertelorism	✓		✓		✓	✓
		Affected vision	✓		✓	(✓)		✓
	Ears	Low-set ears	✓	✓	✓		✓	✓
		Rotated ears	✓		✓			
	Mouth	Dental abnormalities	✓		✓			✓
		Prominent lips		✓				
		Jaw anomalies			✓		✓	
Cardiac		Pulmonary valve stenosis	✓	✓	✓		✓	✓
		Hypertrophic cardiomyopathy	✓	✓	✓		✓	✓
		Ventricular septal defects	✓		✓		✓	✓
		Tachycardia		✓				
		Arrhythmia		✓			✓	
		Atrial septal defects	✓		✓		✓	
		Blood clotting/ bruising			✓			
		Increased blood pressure				✓		
Muscular	General	Hypotonia	✓	✓			✓	
	Speech	Deep/hoarse voice		✓				
		Speech difficulties		✓	✓	✓		
	GI tract/ Feeding	Feeding difficulties	✓	✓	✓			
		Projectile vomiting			✓			
		Oral aversion	✓	✓	✓			
		Intestinal malrotation						
		Gastro-oesophageal reflux	✓	✓				
Neurological	CNS	Seizures	✓	✓		✓		
		Abnormal EEG	✓	✓				✓
		Hydrocephalus	✓	✓				
		Deafness (neural)				(✓)	✓	
	Learning/ Behaviour	Learning difficulties	✓	✓	✓	✓	✓	
		Mental retardation/ Intellectual disabilities	✓	✓				

Cutaneous Features	Skin	Neck webbing			✓			
		Extra skin		✓	✓		✓	
		Thick skin	✓					
		Soft skin		✓				
		Premature skin ageing		✓				
		Eczema	✓					
		Papillomata		✓				
	Cutaneous demonstrations	Neurofibromas				✓		✓
		Increased pigmentation	✓	✓				
		Nevi	✓					
		Freckling				✓		✓
		Lentigines					✓	
		Café-au-lait spots	✓			✓	✓	✓
		Lisch nodules				✓		✓
	Hair quality	Sparse/absent eyelashes/ eyebrows	✓					
		Curly hair	✓	✓				
		Sparse hair	✓	✓				
		Premature hair loss		✓				
Skeletal Abnormalities		General bone defects	✓	✓	✓	✓	✓	✓
		Short stature	✓	✓	✓	✓	✓	
		Thorax malformations			✓		✓	
		Delayed bone development		✓				
		Osteoporosis/ Osteopenia		✓		✓		
		Joint hyperflexibility		✓				
		Cyphoscholiosis		✓				
		Scoliosis		✓		✓		✓
General Growth	Growth	Retardation of growth	✓	✓	✓		✓	
		Failure to thrive	✓	✓				
		Growth hormone deficiency	✓	✓				
	Genitalia	Cryptorchidism		✓	✓		✓	
		Delayed puberty		✓	✓		✓	
Oncogenicity		Rhabdomyosarcoma		✓				
		Neuroblastoma		✓			✓	
		Early-onset transitional cell carcinoma of the bladder		✓				
		Optic glioma				✓		
		Myeloid dysplasia					✓	
		Leukaemia				✓	✓	✓
		Melanoma					✓	
		Brain tumours				✓		

Table 2.1.1 *Phenotypic spectrum of the RASopathies*

Abbreviations: GI: Gastrointestinal, CNS: Central nervous system, EEG: Electroencephalogram

2.1.3. Zebrafish embryogenesis

2.1.3.1. Gastrulation movements

Malfunction of key signalling cascades such as the MAPK pathway often affects the progression of normal development. Study of early embryogenesis stages in zebrafish can elucidate the role of such cascades in early developmental processes. Gastrulation is the period of time in embryonic development during which the blastula precursors of the three germ layers, ectoderm, endoderm and mesoderm, are relocated to reach their final positions (reviewed in Solnica-Krezel, 2005). In zebrafish, it starts at about 4 hours postfertilisation (hpf) at the "high" stage (Kimmel *et al*., 1995) and lasts for almost 6 hours, until the "tail bud" stage (Kimmel *et al*., 1995).

Four major cell movements are required for its successful completion, each one of which confers a different effect on the shape of the embryo. Epiboly is the movement during which the dividing cells proliferate downwards towards the vegetal pole of the embryo, thus covering the surface of the yolk. It causes posterior migration of the cells, and embryo expansion (reviewed in Lepage and Bruce, 2010). Emboly or involution promotes inward folding of the dividing cell layer. This movement ensures that mesodermal and endodermal precursor cells fold at the blastopore to create the internal layers (Solnica-Krezel, 2006). Convergence movements narrow the dorsoventral axis of the embryo while extension causes dividing cells to move upwards elongating the anteroposterior axis (**Figure 2.1.3**). Proper control of all four cell migration movements is required for correct embryonic anteroposterior and dorsoventral axis patterning and normal further development. For instance, the cells at the axial mesoderm of the zebrafish embryo converge a little and extend a lot to achieve normal midline development. In summary, the gastrulation stage ensures that the ectoderm layer is in the surface of the embryo, the mesoderm becomes the middle layer and the endoderm is positioned internally (reviewed in Solnica-Krezel, 2005).

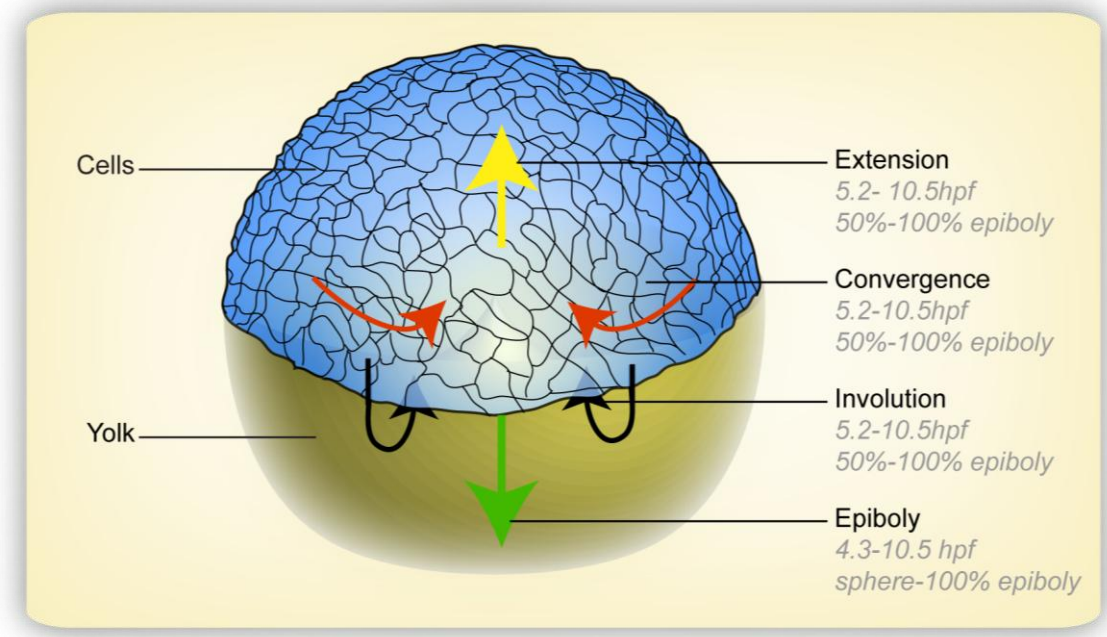

Figure 2.1.3 *Schematic representation of a gastrulating vertebrate embryo at 50% epiboly.*

The blue mesh top represents the dividing cells and the orange bottom represents the yolk. The different coloured arrows illustrate the four separate cell movements occurring during embryonic gastrulation. The time periods (hpf) and developmental stages of their activity are noted under each cell movement.
(Yellow arrow: Extension; Red arrows: Convergence; Black arrows: Involution; Green arrow: Epiboly)

2.1.3.2. Gastrulation defects in zebrafish embryogenesis

Proper completion of gastrulation and cell movement orientation depend largely on the activity of the Mapk pathway. Cellular proliferation is promoted by insulin-like growth factors via the Fgf/Mapk and PIP3 pathways (Pozios *et al.*, 2001). After the mesodermal layer specification by *nodal* signalling, Fibroblast growth factor (Fgf) signalling maintains tissue patterning (reviewed in Schier and Talbot, 2005). Fgf signalling promotes dorsal and dorsolateral effects in a morphogen-like manner (Furthauer *et al.*, 1997). This means that the mesodermal tissue furthest away from FGF expression will have a ventral fate, whereas precursor cells around areas of high FGF expression will give rise to more dorsal-like structures (**Figure 2.1.4 A**).

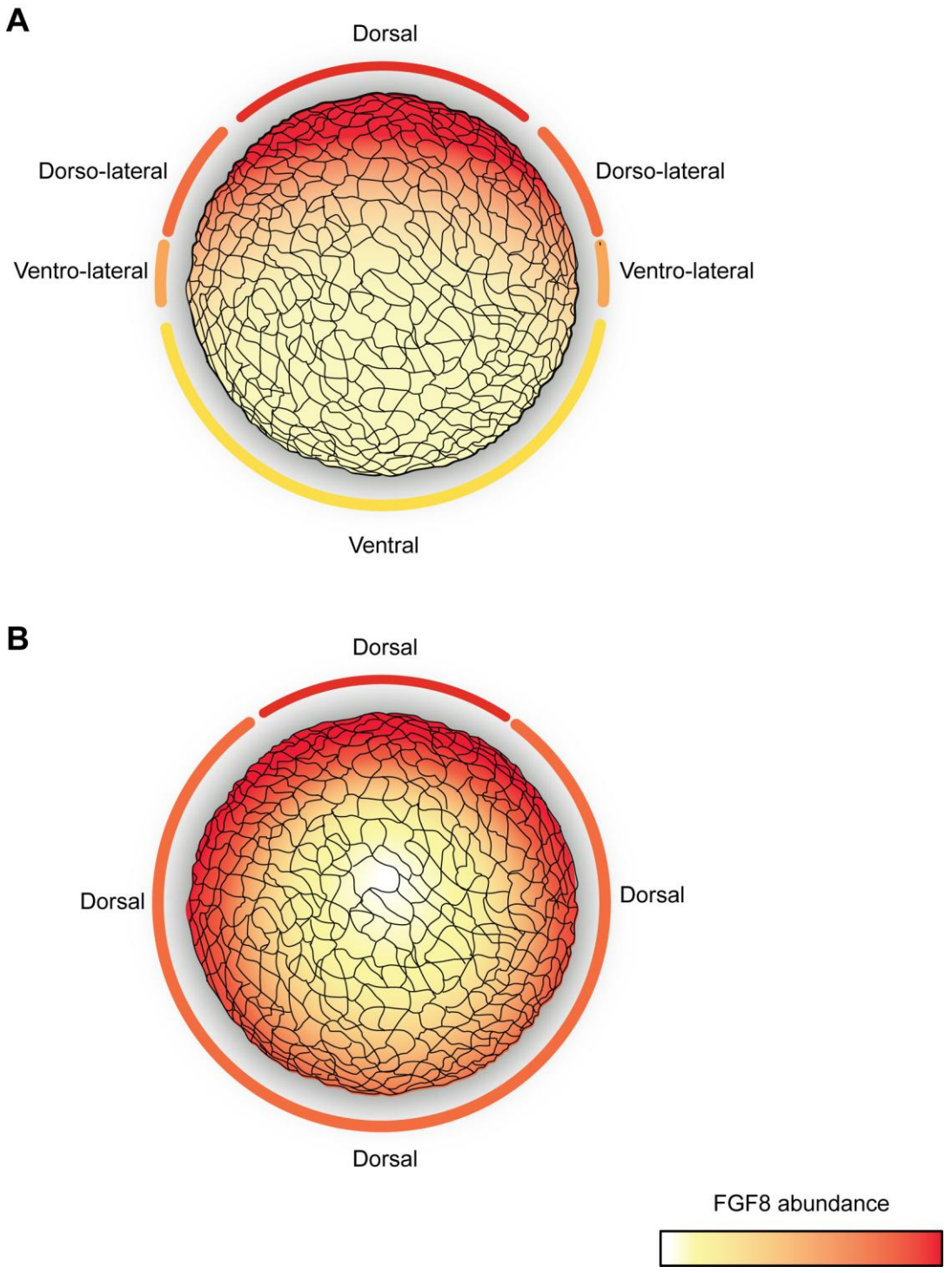

Figure 2.1.4 *Fgf8 presence dictates dorsoventral axis of the embryo*

A Fgf8 acts as a morphogen driving dorso-ventral axis orientation. Areas expressing high levels of FGF8 protein become more dorsalised, whereas no FGF expression triggers a ventralised fate.
B Fgf8 mis-expression leads to an entirely dorsalised embryo.

Additionally, zebrafish provides a robust system to study phenotypes caused by Fgf/Mapk pathway misregulation in early gastrulation. Ectopic Fgf disorientates the fate of the dividing cells (**Figure 2.1.4 B**) leading to an elongated embryonic phenotype at the end of gastrulation (Furthauer *et al.*, 2004). In detail, Fgf8 over-expression promotes embryo dorsalisation due to Bmp downregulation. The opposite effect, embryo ventralisation, can be achieved by over-expression of the Mapk pathway phosphatase Mkp3 (Shinya *et al.*, 2001), or the Mapk pathway inhibitor Sef (Furthauer *et al.*, 2002).

2.1.3.3. Expression profiling of MAPK components in zebrafish

The function and early expression of MAPK pathway components are conserved between vertebrates. Therefore, expression data from large scale or focused studies give insight to spatiotemporal regulation and activity of the Mapk pathway genes in zebrafish. Mapk cascade gene products are maternally deposited and ubiquitously expressed until the end of gastrulation. However, after somitogenesis and by 2dpf membrane-bound components such as Fgfr1 (Rohner *et al*., 2009; Thisse and Thisse, 2005), Nf1 (Padmanabhan *et al*., 2009 PNAS) and Ptpn11 (Razzaque *et al*., 2007) as well as the cytosolic C-raf (Razzaque *et al*., 2007) and Erk1 (Krens *et al*., 2006; Thisse and Thisse, 2004) become specific to the head region. Membrane-bound Grb2 and H-ras a are neuronally expressed (Thisse and Thisse, 2004), whereas K-ras (Liu *et al*., 2008), Braf and Mek2 expression (Thisse and Thisse, 2005) is thought to be ubiquitous throughout embryogenesis. Finally, Erk1 and Fgfr1 are prominently expressed in the pharyngeal arches (Thisse and Thisse, 2005). No expression profiles have been generated, to date, for *sos1*, *mek1* and *erk2*.

2.1.4. Aims

2.1.4.1. Establishing an *in vivo* bioassay to test activity of disease alleles

BRAF and MEK germ-line mutations promote CFC in human patients. Using the simplicity of the developing zebrafish embryo, I aimed to determine if the same mutations affect early development in zebrafish. To that end, I over-expressed an array of human CFC, naevi and melanoma disease alleles in one-cell stage zebrafish and directly observed the early patterning and structure of the embryos.

2.1.4.2. Drawing genotype-to-phenotype conclusions

The different point mutations studied confer alternate kinase activity levels to the protein *in vitro*. In order to establish whether there is a genotype-to-phenotype correlation between protein activity levels and phenotypic severity I expressed a panel of BRAF and MEK allelic variants (kinase-activating, kinase-inactivating, kinase-dead) in wild-type zebrafish embryos and compared their phenotypes.

2.1.4.3. Testing the oncogenic potential of BRAF CFC alleles

Although somatic *BRAF* mutations are prevalent in premalignant melanocytic lesions (naevi) and melanoma, CFC patients harbouring germ-line *BRAF* mutations are not at increased risk of developing cancer. As sometimes CFC and neoplastic mutations overlap, I aimed to test the oncogenic potential of BRAF CFC alleles. For this study, I specifically expressed the different BRAF alleles in melanocytes of wild-type zebrafish and assessed their naevus-driving potential.

2.2. RESULTS

The work presented in this chapter has been published and the relevant publication has been attached in **Appendix II** with permission from the journal.

2.2.1. Similarity of human and zebrafish BRAF, MEK1 and MEK2

The zebrafish genome has been fully sequenced and genomic resources are becoming more widely available. The ninth zebrafish genome assembly, Zv9, was made public from the Wellcome Trust Sanger Institute in Ensembl e60 in November 2010. The final gene set contains 24,020 protein-coding genes and 38 pseudogenes. The majority of the sequencing results were based on clone data and the remaining gaps were filled using new RNA sequencing technology and aligned zebrafish cDNAs.

The known zebrafish *braf, mek1* and *mek2* cDNA and amino acid (aa) sequences were aligned against the equivalent human sequences using the BLASTn and BLASTp programmes in the NCBI database, accordingly. The graphical illustrations were generated in R.

Zebrafish and human cDNAs were similar. Zebrafish *braf* cDNA (2737bp) was longer than the human *BRAF* cDNA (2480bp) but shared 75% sequence identity. *mek1* (2093bp) was 77% identical to *MEK1* cDNA (2642bp) and the aligned cDNA sequence of *mek2* (2787bp) was 79% identical to *MEK2* (1734bp) (**Figure 2.2.1**).

Braf is 817aa long as opposed to the shorter 766aa human BRAF. Upon alignment, 636/763aa (84%) were identical and the overall sequence similarity was 87%. Mek1 (395aa) and MEK1 (393aa) were identical in 348/393aa, with an overall sequence similarity of 95%. Finally, Mek2 (397aa) and MEK2 (400aa) shared 86% sequence identity and were 92% similar (**Figure 2.2.1**).

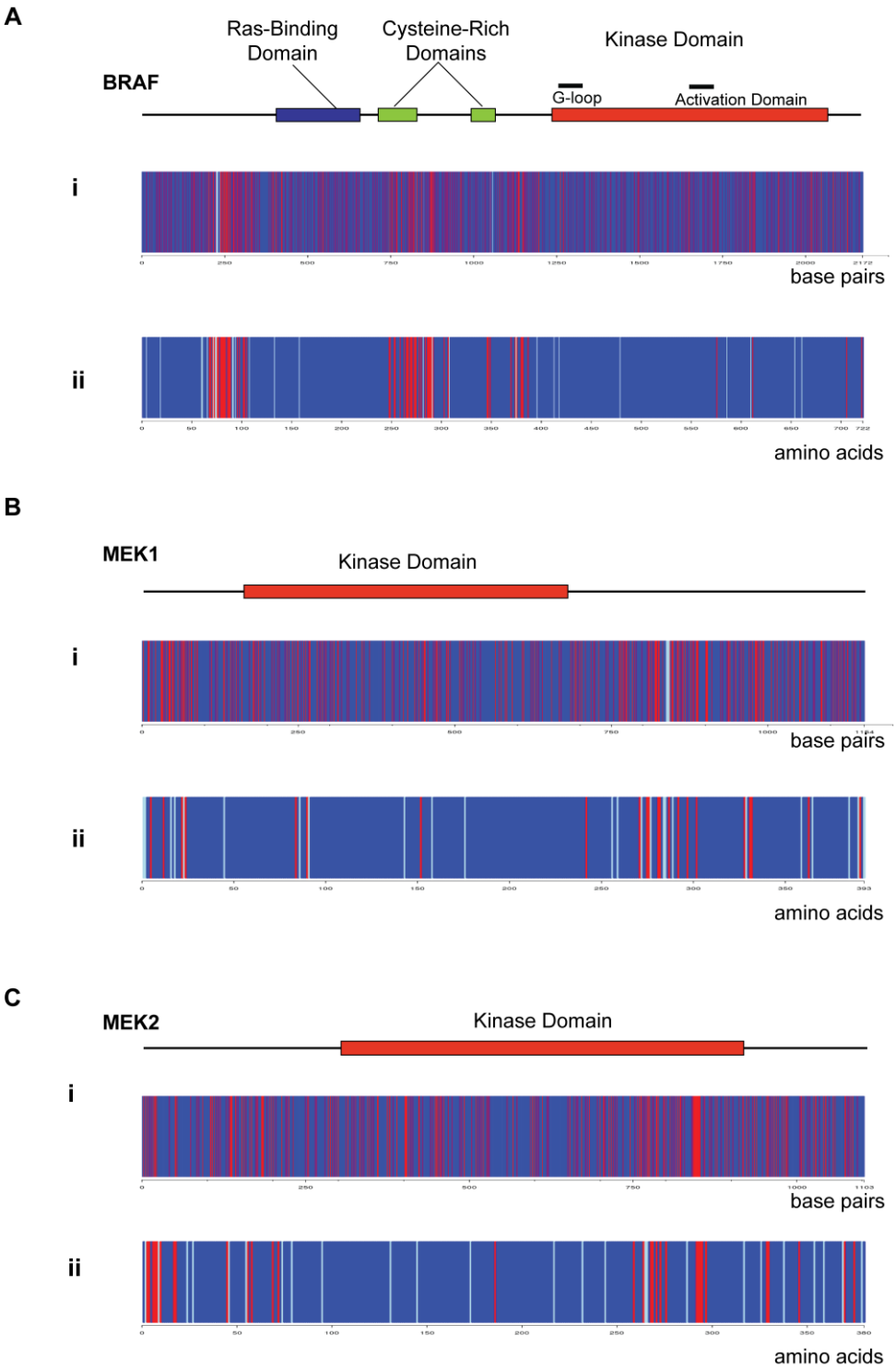

Figure 2.2.1 *Overlap between zebrafish and human BRAF, MEK1 and MEK2 sequences*

(***Figure 2.2.1***)
Diagrams depicting identity between cDNA (Ai, Bi, Ci) and amino acid sequences (Aii, Bii, Cii) of BRAF (A), MEK1 (B) and MEK2 (C). The functional domains of each protein are shown above the alignments.
Ai, Bi, Ci Sequence identity of human compared to zebrafish cDNA. Blue: identical; Red: mismatch; Grey: mismatch coding for the same amino acid. **Aii, Bii, Cii** Amino acid identity between zebrafish and human proteins. Blue: identity; Red: mismatch; Grey: similarity in amino acid function.

2.2.2. Mutations along the RAF-MAPK pathway are active in vivo

The Fgf-Ras-Mapk pathway is of integral importance in early embryogenesis, as Fgf signalling levels govern the patterning of the dorso-ventral axis (Solnica-Krezel, 2005). Ectopic expression of the normally stringently regulated Fgf proteins during gastrulation promotes dysfunctional convergence cell movements (Furthauer *et al*., 1997, 2002, 2004). As epiboly, involution and extension movements are not affected by the loss of dorso-ventral orientation, activated FGF signalling results in embryo elongation (Furthauer *et al*., 2002).

Based on the understanding of MAPK pathway importance in early development and the practical uses of having an established readout for gastrulation defects, I used the zebrafish system to test the *in vivo* significance of BRAF, MEK1 and MEK2 CFC alleles in a developmental context.

2.2.2.1. BRAF CFC and melanoma alleles promote developmental abnormalities in zebrafish

In order to determine whether human CFC and melanoma disease mutations have an effect on zebrafish development, mRNA from a small panel consisting of BRAF allelic variants were injected into one-cell stage zebrafish wild-type embryos. The mRNA was carrying the wild-type (WT) human BRAF protein, the most common melanoma mutation and highly kinase-activating $BRAF^{V600E}$, the most common CFC and activating mutation $BRAF^{Q257R}$ and the kinase-impaired melanoma and CFC mutation $BRAF^{G596V}$. The injected individuals were closely monitored from early gastrulation.

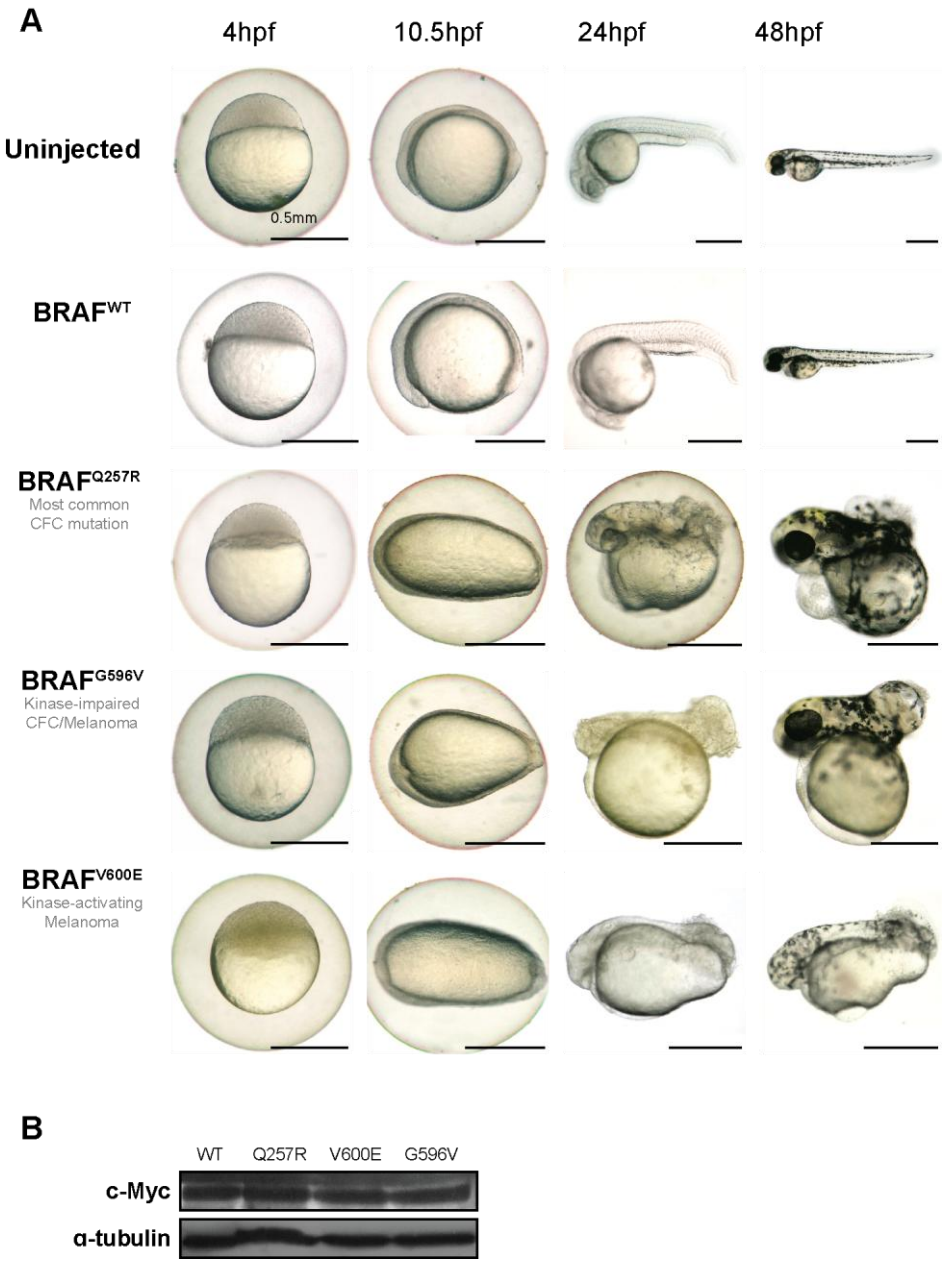

Figure 2.2.2 *CFC and melanoma BRAF disease alleles are active* in vivo

A Embryos over-expressing BRAF disease alleles had specific developmental phenotypes that can be followed during development. Embryos injected with mRNA expressing $BRAF^{CFC}$ alleles ($BRAF^{Q257R}$, $BRAF^{G596V}$) and melanoma alleles ($BRAF^{G596V}$, $BRAF^{V600E}$) were elongated at 10.5hpf when compared to the uninjected controls and the embryos expressing the wild-type BRAF protein. Mutations in BRAF promoted shortening of the antero-posterior axis, yolk extension defects and general developmental toxicity in 24 and 48hpf embryos.
B Immunoblotting illustrating similar levels of BRAF mRNA expression in injected embryos. The mRNA constructs were myc-tagged and injected BRAF expression levels were detected by western blotting. α-tubulin was used as a loading control.

Development of the embryos over-expressing BRAF mutations was compared to that of embryos injected with WT human *BRAF* mRNA as well as to the development of their untreated siblings. Whereas early cell movements were unaffected in all injected embryos, it became apparent by the end of gastrulation that both CFC and melanoma alleles were active *in vivo* (**Figure 2.2.2A**). At the tail-bud stage (10.5hpf) all embryos injected with *BRAF* mutant alleles were significantly elongated, similarly to embryos experiencing ectopic MAPK signalling (Furthauer *et al*., 2002).

By 24hpf the body axis of the BRAF-expressing embryos was much shorter than the control larvae, with a characteristic loss of posterior structures and prominent cranial hypomorphism. Additionally, CFC and melanoma allele-expressing individuals presented with yolk extension defects.

At 48hpf, the malformed embryos had not increased in size but were not developmentally delayed based on observations of heart development, blood circulation and normally acquired pigmentation.

Most remarkably, over-expression of the wild-type BRAF protein did not cause any defects and embryos appeared indistinguishable from their un-injected siblings, suggesting that the injection process itself and the human mRNA levels were not toxic to zebrafish development. All BRAF proteins synthesised from the injected mRNA were myc-tagged and western blotting revealed that their expression levels were similar in all treatment groups (**Figure 2.2.2 B**).

2.2.2.2. All zebrafish embryos expressing BRAF, MEK1 and MEK2 allelic variants exhibit the same elongation phenotype at the end of gastrulation

Like in human melanoma, the BRAF-CFC mutations result in both kinase-activating and kinase-impaired activities, whereas all MEK CFC mutations are kinase active (Rodriguez-Viciana *et al*., 2008; Rodriguez-Viciana *et al*., 2006; K.A. Rauen, unpublished data). As irrespective of the kinase activity levels of the expressed protein all three BRAF allelic variants promoted the same phenotype in gastrulating

embryos, it was of interest to determine whether other available human and engineered mutations would have the same effect on zebrafish development. To that end, a library of more than thirty kinase-active and kinase-impaired BRAF, MEK1 and MEK2 allelic variants (Rodriguez-Viciana *et al*., 2008; Rauen *et al*., 2006; Rodriguez-Viciana *et al*., 2006), including human CFC, melanoma and engineered mutations, was assessed for its *in vivo* activity (**Table 2.2.1**). Notably, kinase-impaired mutations confer a lower activity to the kinase compared to the wild-type protein but do not inactivate it like the kinase dead mutants do.

Gene	*Amino acid change*	*Predicted* in vitro *activity*	*Disease*	*Developmental phenotype in zebrafish (n)*
BRAF	Wild type	Wild type	N/A	no (0/40)
	A246P	Not determined	CFC	yes (31/57)
	Q257R	Kinase-activating	CFC	yes (83/95)
	G464V	Kinase-activating	CFC	yes (25/45)
	S467A	Kinase-activating	CFC	yes (49/57)
	K483M	Kinase dead	CFC	yes (34/44)
	K499E	Kinase-activating	CFC	yes (23/44)
	G534R	Kinase-activating	CFC	yes (33/38)
	N581D	Not determined	CFC	yes (23/51)
	D594V	Kinase-impaired	Melanoma	yes (43/56)
	G596V	Kinase-impaired	CFC/ Melanoma	yes (86/104)
	T599E/S602D	Constitutively active	Engineered	yes (36/73)
	V600E	Kinase-activating	Melanoma	yes (68/84)
	D638E	Not determined	CFC	yes (66/89)
MEK1	Wild type	Wild type	N/A	no (0/40)
	F53L	Constitutively active	Engineered	yes (16/33)
	F53S	Kinase-activating	CFC	yes (20/33)
	T55P	Kinase-activating	CFC	yes (26/45)
	K97M	Kinase dead	Engineered	yes (45/62)
	G128V	Kinase-activating	CFC	yes (22/35)
	Y130C	Kinase-activating	CFC	yes (30/45)
	S218D/S222D	Constitutively active	Engineered	yes (45/55)
	ΔN3DD	Constitutively active	Engineered	yes (41/60)
MEK2	Wild type	Wild type	N/A	no (0/40)
	F57C	Kinase-activating	CFC	yes (31/42)
	A62P	Kinase-activating	CFC	yes (25/39)
	K101M	Kinase dead	Engineered	yes (39/52)
	G132V	Kinase-activating	CFC	yes (45/72)
	Y134C	Kinase-activating	CFC	yes (30/54)
	S222D/S226D	Constitutively active	Engineered	yes (33/49)
	K273R	Kinase-activating	CFC	yes (42/63)

Table 2.2.1 *The panel of CFC, melanoma and engineered alleles used in this bioassay*

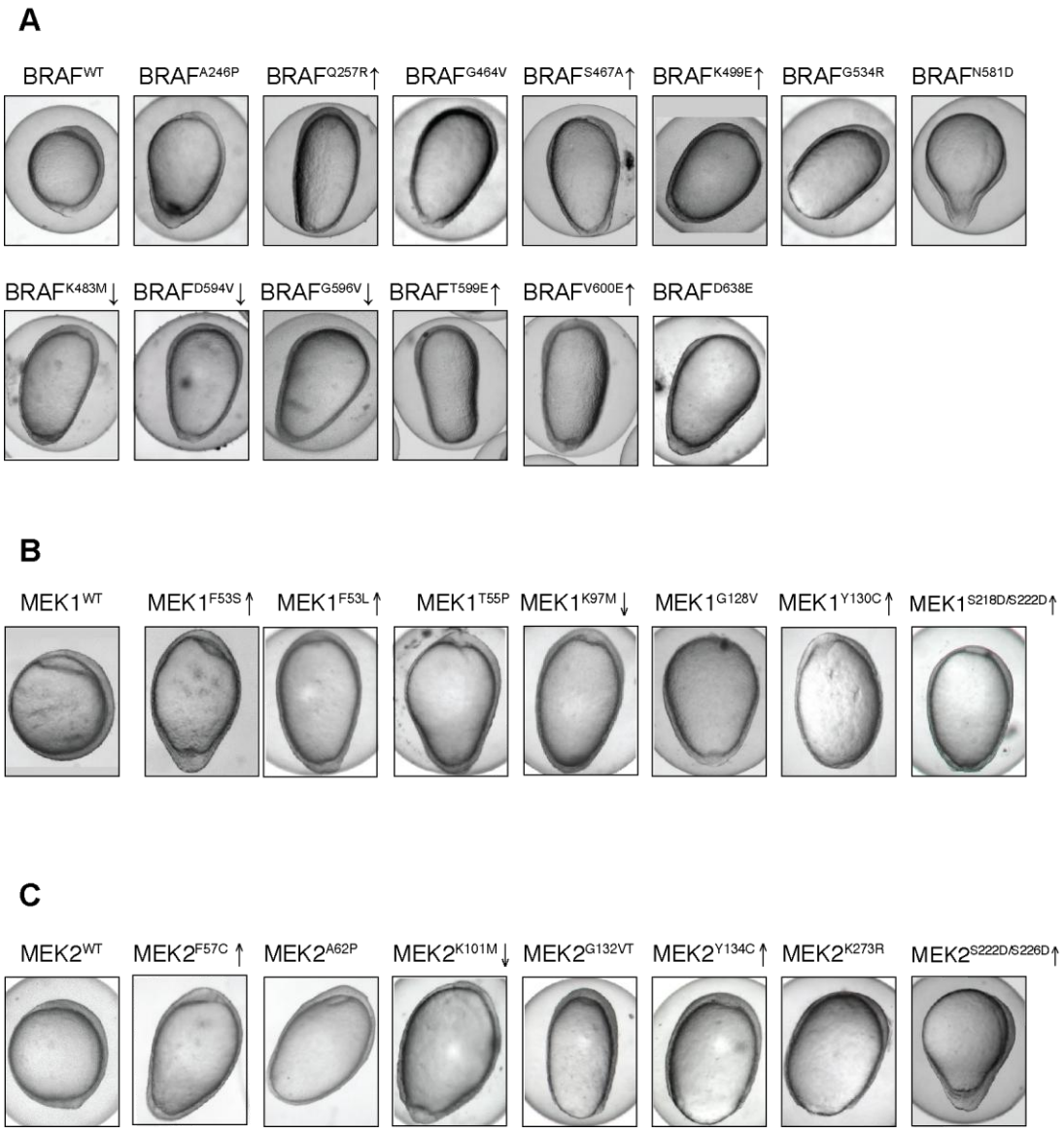

Figure 2.2.3 *Testing the in vivo activity of BRAF, MEK1 and MEK2 constructs*

A-C All thirteen mutant forms of BRAF, including the $BRAF^{K483M}$ kinase dead variant (**A**), seven MEK1 (**B**) and seven MEK2 mutant proteins (**C**) promoted embryonic elongation at 10.5hpf. Notably, over-expression of the wild-type proteins had no effect in embryonic development.
Arrows next to the amino acid substitutions represent the activity level conferred to the kinase as a result of each mutation, compared to the wild-type protein.

Thirty-one allelic variants were sub-cloned into destination vectors from their original plasmids, kindly sent by Dr. Katherine A. Rauen (UCSF) (refer to **Chapter 6; Materials and Methods**). In order to test the elongation-promoting capacity, mRNA was *in vitro* transcribed from all vectors. One-cell stage wild-type zebrafish

embryos were injected with human mRNA from the library and were, subsequently, scored for their elongation status at 10.5hpf. To introduce a tighter control to the experiment and minimise the effects that individual embryos may have had on phenotypic outcomes, a minimum of two (and most commonly four) separate injection sets were performed on each embryo collection batch (i.e. injection of two or more mRNA samples in one embryo pool).

Initially, BRAF CFC, melanoma and engineered alleles were assessed and allelic variants were found to promote embryo elongation at the tail bud stage irrespective of their activity levels (**Figure 2.2.3A**). Embryos expressing mutated forms of MEK1 and MEK2 proteins they were, also, elongated at the same stage (**Figure 2.2.3B, C**). Intriguingly, constitutively active ($BRAF^{T599E/S602D}$, $MEK1^{S218D/S222D}$, $MEK2^{S222D/S226D}$) or kinase-dead ($BRAF^{K483M}$, $MEK1^{K97M}$, $MEK2^{K101M}$) protein-expressing individuals displayed an identical elongation phenotype. Importantly, none of the WT proteins triggered a phenotype. This suggested that, unlike their *in vitro* predicted activity, kinase-active and kinase-impaired alleles promote the same developmental outcome *in vivo*. In fact, western blotting of zebrafish embryonic lysates against pErk and total Erk protein confirmed that all BRAF and MEK alleles caused Erk activation (**Figure 3.2.3**).

2.2.3. Over-expression of multiple disease alleles has an additive phenotypic effect in development

SHP2 mutations identified in Noonan and LEOPARD syndrome patients also act by activating or in-activating downstream signalling. Additionally, generated shp2 zebrafish mutants have both gain- and loss-of-function phenotypes (Jopling *et al.*, 2007). However, in our model all the mutations tested acted as gain-of-function *in vivo*, irrespective of their predicted *in vitro* activity.

To elucidate the mode of action of activating and kinase-impaired mutations from our library, sub-optimal levels of combinations of CFC kinase-active, CFC kinase-impaired and WT BRAF and MEK proteins were expressed in wild-type embryos.

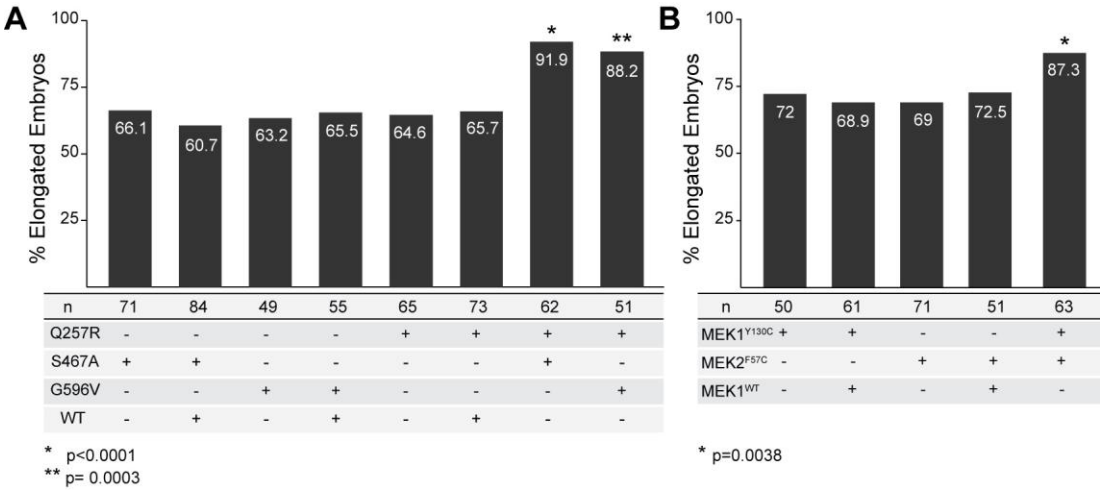

Figure 2.2.4 *Over-expression of sub-optimal doses of two mutation variants has an additive effect in the embryonic elongation phenotype*

A Histogram supporting that BRAF kinase-active and kinase-impaired alleles promote additive effects during development. Embryos were co-injected with combinations of suboptimal doses of kinase-active ($BRAF^{Q257R}$, $BRAF^{S467A}$) and kinase-impaired ($BRAF^{G596V}$) CFC alleles or $BRAF^{WT}$ mRNA. Co-expression of the wild-type protein with the CFC mutations did not alter the proportion of elongated embryos at 10.5hpf when compared to the embryos expressing the CFC alleles alone. Co-expression of two disease alleles resulted in a significant increase in the number of elongated embryos at 10.5hpf: $BRAF^{Q257R}$ with $BRAF^{S467A}$ ($p < 0.0001$) and $BRAF^{Q257R}$ with $BRAF^{G596V}$ ($p = 0.0003$) as indicated by $\chi 2$ tests.
B Histogram illustrating the additive effect promoted by co-expression of sub-optimal concentrations of MEK1 CFC ($MEK1^{Y130C}$) and MEK2 CFC ($MEK2^{F57C}$) alleles. Co-injection of $MEK1^{Y130C}$ and $MEK2^{F57C}$ caused a significant increase ($p=0.0038$) in the numbers of embryos with an elongated phenotype when compared to embryos co-expressing CFC alleles and $MEK1^{WT}$.

The numbers in the bars indicate the percentages of elongated embryos; n is the number of injected embryos in each set.

The activating mutation $BRAF^{Q257R}$ was co-expressed with the kinase-active $BRAF^{S467A}$ and the kinase impaired $BRAF^{G596V}$. The kinase-active $MEK1^{Y130C}$ was co-expressed with the kinase-active $MEK2^{F57C}$. As an internal control, each allelic variant was, also, expressed alone or alone with either $BRAF^{WT}$ or $MEK1^{WT}$, accordingly. The percentage of elongated individuals in cohorts co-expressing two disease alleles was compared to that of embryos expressing a mutant allele and its equivalent wild-type protein.

Co-injection of CFC disease alleles with $BRAF^{WT}$ or $MEK1^{WT}$ promoted similar levels of embryo elongation as those in cohorts of embryos expressing the sub-optimal level of the disease allele alone (**Figure 2.2.4 A,B**). These percentages ranged from 60.7% ($BRAF^{S467A}$) to 72% ($MEK1^{Y130C}$). In contrast, the combination of two kinase-activating alleles as well as one kinase-activating and one kinase-inactivating allele promoted a highly significant increase (as indicated by chi-squared tests) in the number of elongated embryos at 10.5hpf ($BRAF^{Q257R}$-$BRAF^{S467A}$ 91.9%; $BRAF^{Q257R}$-$BRAF^{G596V}$ 88.2%; $MEK1^{Y130C}$-$MEK2^{F57C}$ 87.3%). The proportion of these elongated embryos is directly comparable to the levels observed in optimally injected individuals. This suggests that all kinase activity level mutations act as gain-of-function mutations during zebrafish development.

2.2.4. Embryonic elongation starts around 7hpf

The importance of early cell movements in correct axis patterning as well as the involvement of the FGF/MAPK cascade in this process have been highlighted in a number of embryonic zebrafish models (Furthauer *et al*., 2002, 2004). Moreover, convergence-extension defects have been recorded in zebrafish embryos lacking proper Shp-2 (Jopling *et al*., 2007) and Erk (Krens *et al*., 2008) signalling.

To identify the point when embryo elongation first became apparent, the early development of a control un-injected embryo was directly compared to an embryo injected with the most common CFC mutation ($BRAF^{Q257R}$) (**Figure 2.2.5A**). The closely monitored embryos were imaged every 20 minutes, from the beginning of gastrulation (4hpf) until the tail bud stage (10.5hpf). Early divisions and cell movements were identical between the two groups until 7hpf. After the 7.5hpf time-point the appearance of the injected embryos started to deviate from the wild-type embryos, with the yolk becoming increasingly more elongated every hour. By 10.5hpf the embryos had the characteristic elongated phenotype.

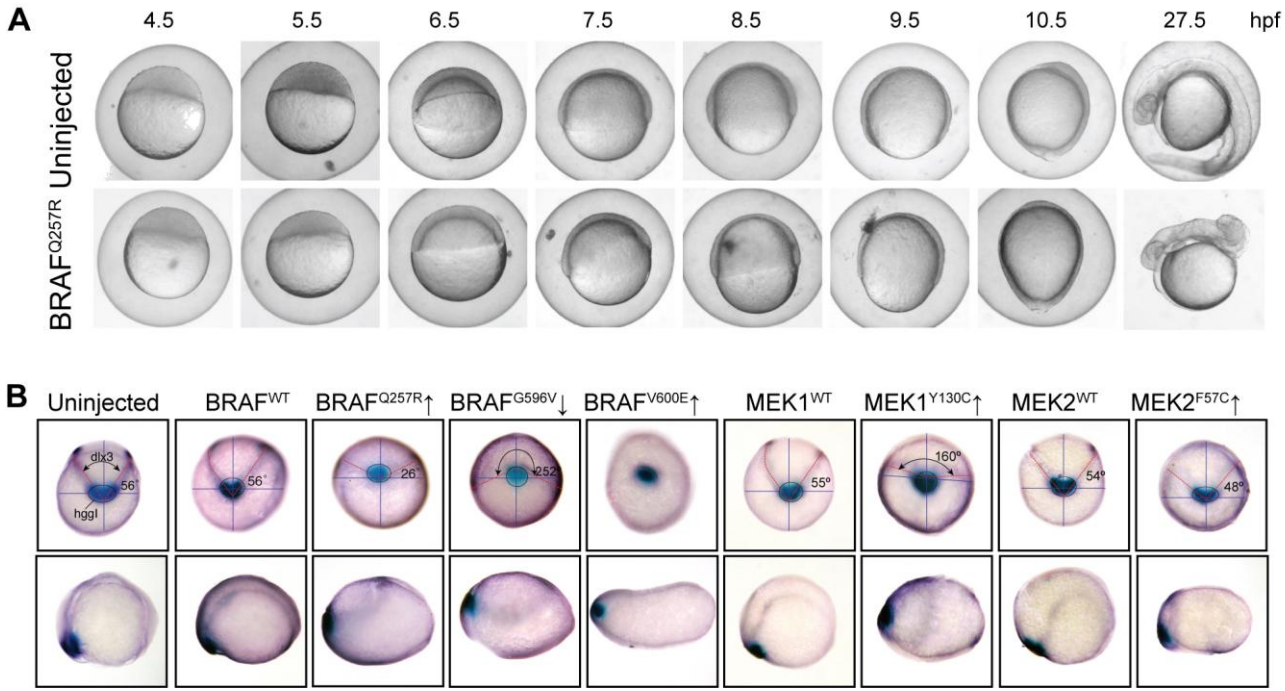

Figure 2.2.5 *Gastrulation cell movement defects cause the elongation phenotype*

A Time-course still images of developing embryos. The top panel shows the normal development of an uninjected control wild-type embryo. The lower panel illustrates the development of an embryo over-expressing $BRAF^{Q257R}$, the most common CFC allele. The injected embryos were indistinguishable from the controls until 8.5hpf when their body axis started elongating and at 10.5hpf the embryos had the characteristic phenotype. By 24hpf the embryos were visibly shorter, lacking a significant part of their posterior structures, had an enlarged cardiac oedema and the yolk failed to extend properly.
B Dlx3 and HggI in situ hybridisation staining revealed convergence-extension movement defects in all embryos expressing disease alleles, but not the wild-type proteins. The angle of Dlx3 expression (red dashed lines) relative to the embryo midline (horizontal blue line) was calculated for every embryo. Notably, embryos injected with $BRAF^{V600E}$ do not show any Dlx3 expression. The lower panel shows side views of the same embryos as the ones directly above them.

2.2.5. Embryonic elongation originates from convergence-extension defects

To determine whether the various BRAF and MEK mutations have a direct effect on convergence-extension movements, whole-mount *in situ* hybridisation (WISH) against specific convergence-extension markers was performed. Elongated embryos expressing a sub-panel of disease allelic variants were collected at the tail-bud stage, were processed and were hybridised with probes for Dlx3, expressed at the neuronal plate margin, and HggI, the hatching gland and anterior-posterior axis marker.

The pattern of the embryos expressing the WT proteins was the same as that of the un-injected control embryos (**Figure 2.2.5B**). The angle of the Dlx3 pattern in reference to the embryo size and the HggI expression, however, was dramatically altered in all elongated embryos. Namely, the angle of Dlx3 relative to the horizontal midline of the embryo was widened in embryos expressing $BRAF^{Q257R}$, $BRAF^{G596V}$ and $MEK1^{Y130C}$ but narrower in $MEK2^{F57C}$-embryos. Interestingly, Dlx3 expression was completely absent in $BRAF^{V600E}$ embryos. HggI expression levels remained unaffected in all embryos. Taken together, these findings indicate that the disease alleles tested cause major disruptions in convergence cell movements.

2.2.6. Interruption of BRAF signalling by *c-raf* knockdown does not prevent embryonic elongation

BRAF mutant proteins in melanoma cell lines harbouring kinase-impaired BRAF mutations are thought to signal through C-RAF to activate downstream targets of the RAS-RAF-MAPK pathway (Wan *et al*., 2004). *c-raf* knockdown through injection of a specific translation block morpholino oliogonucleotide (MO) resulted in embryos that, by 3dpf, had a smaller head, close proximity of the otoliths, heart pericardium enlargement and minor atrioventricular valve malfunctions as well as yolk extension defects and curvature of the posterior structures (**Appendix I-1**), all in accordance with previously defined morphant phenotypes (Razzaque *et al*., 2007).

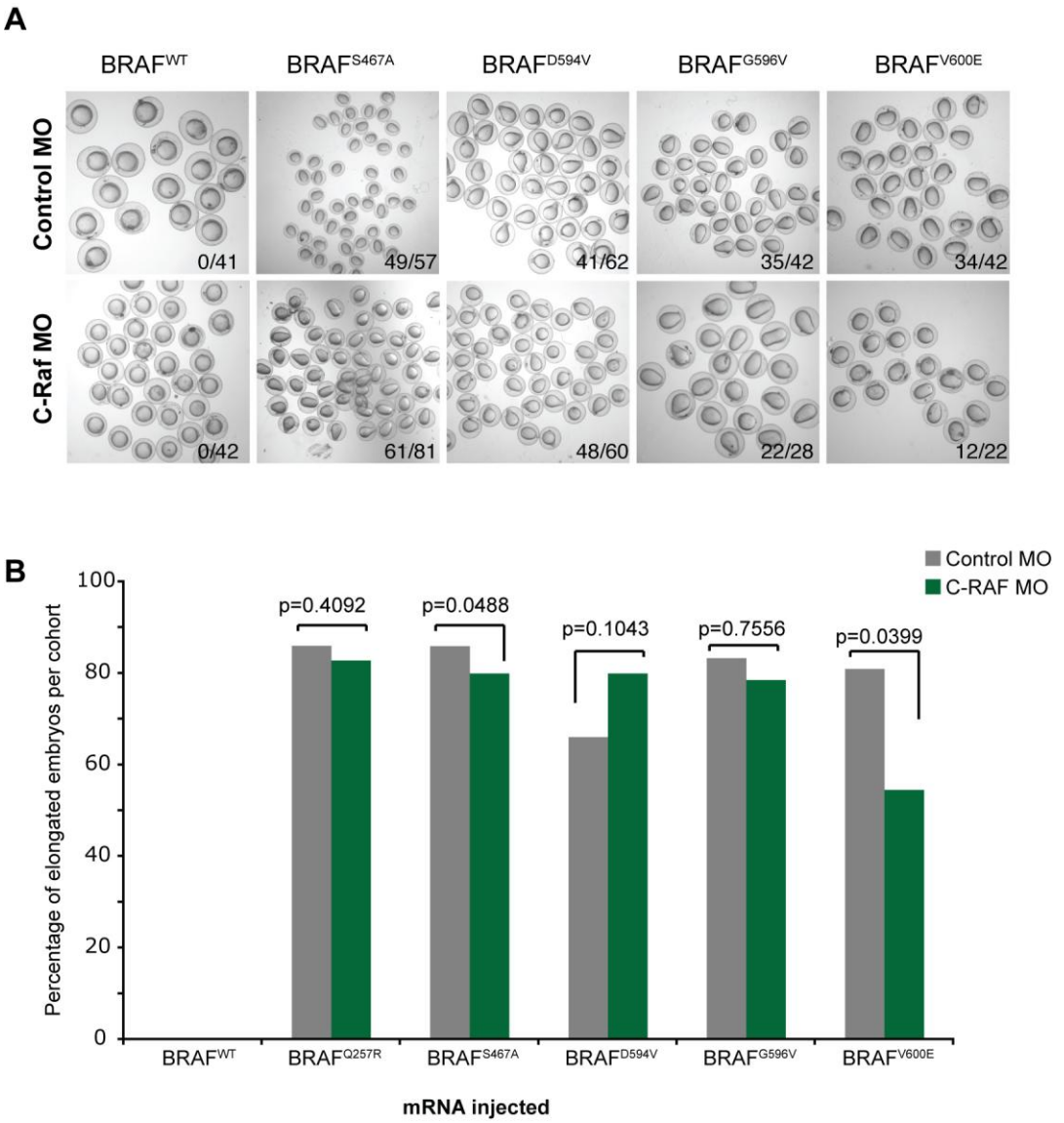

Figure 2.2.6 *C-raf morpholino does not rescue BRAF mRNA phenotype after co-injection*

A The top panel shows 10.5hpf embryos injected with human $BRAF^{WT}$, $BRAF^{S467A}$, $BRAF^{D594V}$, $BRAF^{G596V}$ and $BRAF^{V600E}$ mRNA and a control morpholino (MO). Embryos over-expressing mutated forms of the protein were elongated, unlike the $BRAF^{WT}$-expressing samples. The lower panel shows that co-injection of the mRNA and a C-raf MO led to similar levels of embryo elongation as their paired controls.
B Histogram showing the percentage of elongated embryos in each injection set (corresponding to injections in panel A). Grey bars represent embryos injected with the respective mRNA alone and the green bars represent embryos co-injected with mRNA and C-raf MO. The p values for each experimental set were calculated using the two-tailed Fisher's exact t-test and were not considered to be statistically significant to the $p<0.001$ level. The $BRAF^{WT}$ category was excluded from this calculation as no embryos were elongated.

To test whether C-raf is responsible for the downstream activation of MEK in the presence of impaired activity BRAF mutation, a sub-panel of BRAF allelic variants ($BRAF^{Q257R}$, $BRAF^{S467A}$, $BRAF^{D594V}$, $BRAF^{G596V}$, $BRAF^{V600E}$) were co-expressed with a C-raf translation block MO. Doubly injected embryos were tested for their elongation status at the tail bud stage and were compared to embryos expressing the disease alleles with a control fluorescein MO (**Figure 2.2.6**). Based on the two-tailed Fisher's exact t-test, the levels of elongation incidence were not significantly altered in the presence of the C-raf MO to the $p<0.001$ level. The number of elongated embryos co-injected with $BRAF^{V600E}$ and C-raf MO was reduced compared to the individuals expressing $BRAF^{V600E}$ alone, but due to the low numbers and mortality of doubly injected embryos the reduction in elongation incidence was not considered C-raf MO-dependent.

2.2.7. Oncogenic potential of CFC BRAF alleles

As with many of the RASopathies, CFC is a progressive disorder with physical symptoms becoming more severe with time. Sometimes undiagnosed at birth, CFC patients acquire a vast range of disease manifestations as they get older. Although CFC syndrome is not traditionally correlated with high cancer risk, a number of patients present with an increased count of skin naevi, which could be viewed as benign lesions. The established bioassay described above clearly demonstrated the activity of transient expression of BRAF disease alleles during embryogenesis. To better understand the ability of CFC alleles to drive malignancy, stable and more permanent activity of BRAF allelic variants has to be tested in the context of an adult organism.

To achieve that, I sub-cloned a sub-panel of BRAF variants under the melanocyte-specific *mitfa* promoter in a way that the constructs were flanked by Tol2 transposon sequences. Co-injection of wild-type embryos with a mix of the DNA plasmids and Tol2 transposase mRNA promoted random incorporation of the generated DNA in the fish genome. One-cell stage wild type (AB and TL) embryos were injected with

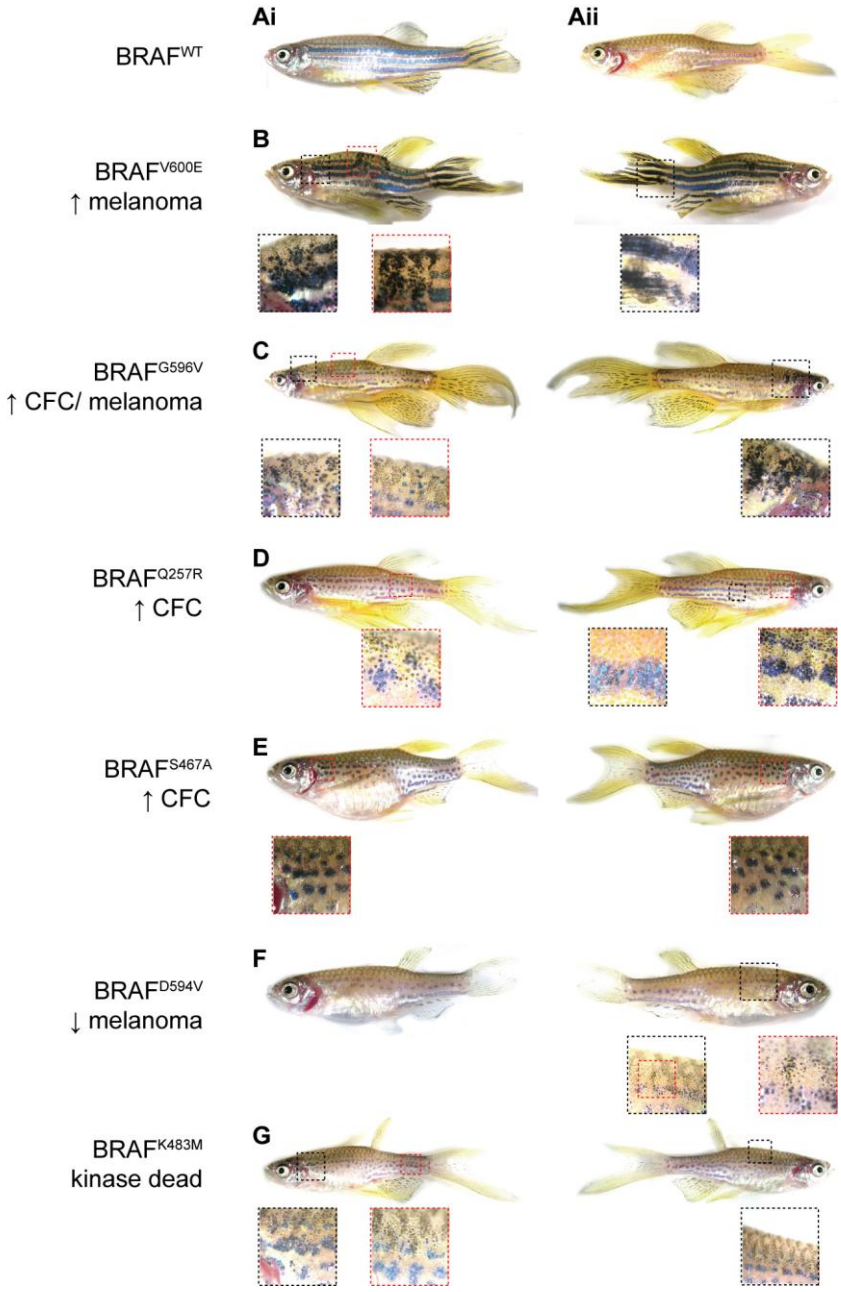

Figure 2.2.7 *Assessment of the oncogenic potential of BRAF disease allelic variants*

Illustration of fish expressing different human BRAF disease variants under the melanocyte-specific promoter, *mitfa*. Expression of mitfa-BRAF^{V600E} is sufficient to drive extensive ectopic pigmentation/naevi (**B**). The kinase-impaired mutant BRAF^{G596V} drove ectopic melanisation in vivo, as well (**C**). Small deviation from the wild-type patterning was observed in mosaic fish expressing BRAF^{Q257R}, BRAF^{S467A}, BRAF^{D594V} and BRAF^{K483M} (**D-G**).
Panel **A** shows control adult fish expressing mitfa-BRAF^{WT} on two different wild-type backgrounds. AB fish present with a striped pigmentation pattern (**Ai** and **B**) and TL Leopard have spots (**Aii**, **C-G**). Panels **B-G** illustrate the two sides of the same fish. The areas outlined by the dotted boxes are colour-coded and magnified below each fish. Arrows after the amino acid substitutions indicate the kinase activity of the mutant protein compared to the WT BRAF.

mitfa-BRAF^{WT}, mitfa-BRAF^{Q257R}, mitfa-BRAF^{S467A}, mitfa-BRAF^{K483M}, mitfa-BRAF^{D594V}, mitfa-BRAF^{G596V} and mitfa-BRAF^{V600E}. The embryos were grown into adulthood and were monitored regularly for abnormal pigmentation patterning (**Figure 2.2.7**).

Fish expressing Mitfa-driven BRAF^{WT} developed as wild-type individuals and had no overt phenotype. From one and a half month of age, the fish expressing the most highly activating BRAF^{V600E} mutation under the *mitfa* promoter had obvious aberrant melanisation with multiple loci of naevi formation. By two months, the naevi had grown and the fish were covered in dark spots (**Figure 2.2.7B**). Most strikingly, BRAF^{G596V}, a kinase-impairing mutation present in CFC and melanoma patients, was able to promote naevi formation (**Figure 2.2.7C**). This was the first incidence of an inactivating variant driving abnormal melanisation. This observation underpins the importance of studying a vast array of alleles irrespective of their predicted *in vitro* activity as even inactivating mutations can have, as in this case, a high oncogenic potential. Progression from a benign naevus to malignant melanoma requires acquisition of multiple driving somatic mutations. Therefore, it would be interesting to express BRAF^{G596V} alongside common melanoma mutations to assess the allele's true oncogenicity. Fish injected with the rest of the constructs did not present with obvious naevi. However, the strict pigmentation pattern observed in the vast majority of wild-type adults was frequently disturbed (15-20%) in the injected individuals.

With the exception of BRAF^{V600E} and BRAF^{G596V} the oncogenic potential of CFC alleles was low. However, what became clear by monitoring the injected fish is that all phenotypes observed (naevi/ ectopic melanocytes/ disturbed pattering) were progressive (**Figure 2.2.8**). The fish expressing BRAF^{G596V} in their melanocytes initially demonstrated only a few ectopic melanised spots that later developed to larger naevi covering the fish (**Figure 2.2.8**).

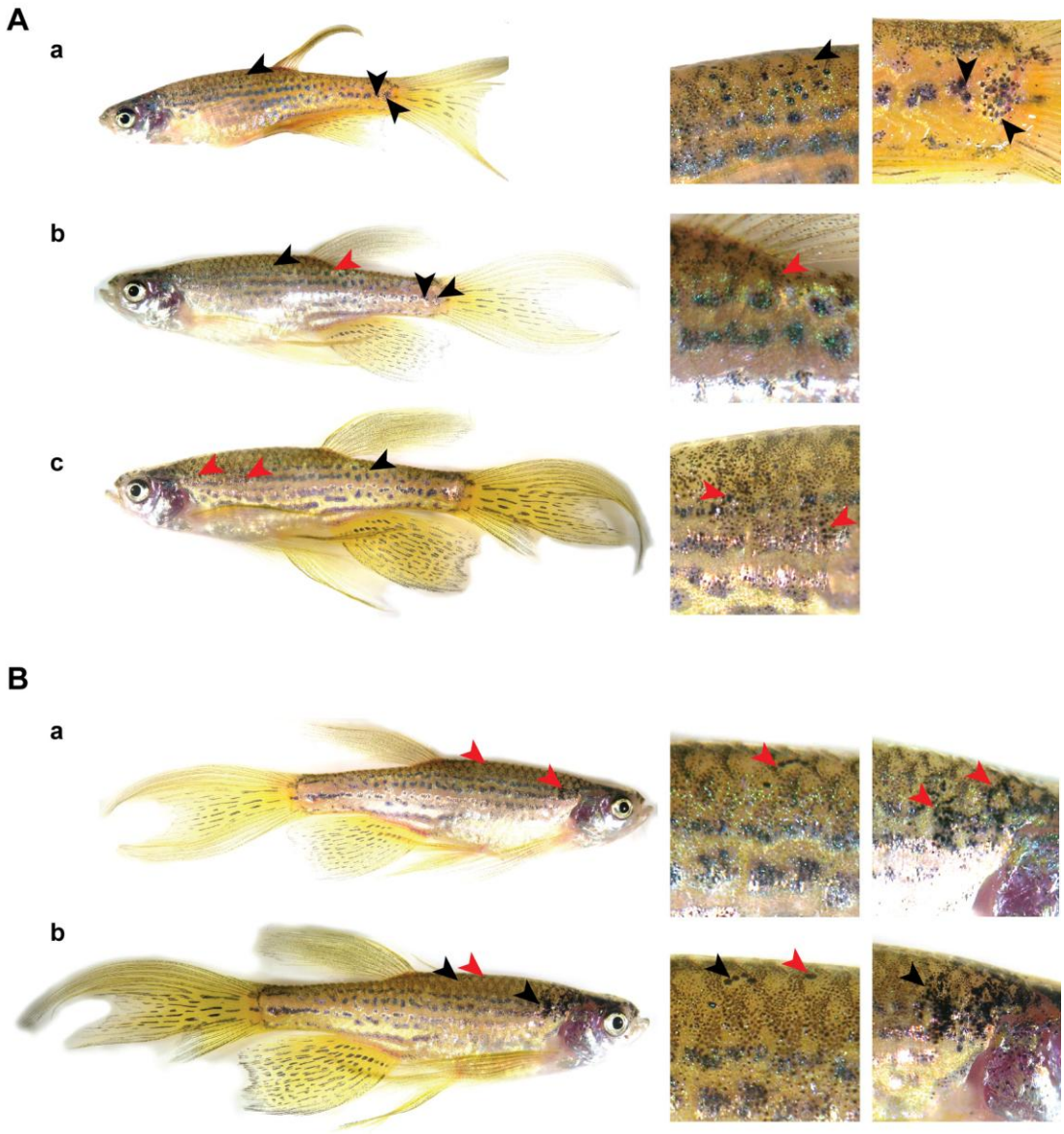

Figure 2.2.8 *Progressive ectopic melanisation of mitfa-BRAF^{G596V} fish*

A Left lateral view of a mitfa-BRAF^{G596V} fish over two months. Substantial ectopic pigmentation (naevi) (black arrowheads) was observed from two months (a) in fish with melanocyte-expressing BRAF^{G596V}. By three months of age (b), the ectopic pigmentation pattern persisted (black arrowheads) but, also, new sites of nevi appeared (red arrowheads). At four months (c), the fish had acquired more new naevi (red arrowheads).
B Right lateral view of the same fish at three (a) and four (b) months showing the appearance of new nevi (red arrowheads) that were not present earlier.

Close-up images on the right highlight the progressive development of naevi.

2.3. DISCUSSION

This work addressed the activity of CFC and other disease mutant alleles in a developing vertebrate organism. The mutations evaluated included 18 human CFC and three melanoma alleles all of which caused a similar developmental phenotype, irrespective of their predicted kinase activity. Wild-type zebrafish embryos were injected at the single cell stage either with human mRNA harbouring a disease allele, or with wild-type control mRNA and the phenotypes of the embryos were assessed ad the end of gastrulation (**Figures 2.2.2, 2.2.3**). Localised expression of Fgf/Mapk signalling is tightly controlled during normal development. This ensures proper shaping of the gastrulating embryos. As all kinase-active and –impaired variants triggered elongation, convergence-extension movements were monitored in disease allele-expressing individuals. All BRAF and MEK variants interfered with gastrulation movements in a comparable manner, suggesting a similar downstream mode of action. This observation could possibly explain why diverse mutations across different genes can lead to the same clinical symptoms in CFC syndrome.

2.3.1. Wild-type levels of BRAF and MEK signalling are imperative for proper gastrulation

BRAF allele substitution in CFC and melanoma naturally promotes both increased and decreased kinase activity to the protein by altering the physical accessibility to the kinase domain (Wan *et al*., 2004). Unlike melanoma patients, BRAF mutations identified in CFC syndrome are not solely clustered around a specific domain. Both kinase-activating and –inactivating mutations have been identified in the kinase domain, the activation segment, the cysteine-rich domain of the conserved region 1 (CR1) and the glycine loop in exon 11 (domains highlighted in **Figures 2.1.2A, 2.2.1**; Rodriguez-Viciana *et al*., 2006).

While the mutations are distributed more widely than in melanoma, some mutations have overlapping functions. In particular, germ-line $BRAF^{G596V}$ promotes CFC while somatic $BRAF^{G596V}$, in the presence of a second mutation, can cause melanoma onset (Rodriguez-Viciana *et al*., 2006). The notion of mutations overlapping between syndromes is not novel. For instance, the same K-RAS allelic substitution has been identified both in a patient with CFC (Niihori *et al*., 2006) and Noonan syndrome (Schubbert *et al*., 2006).

Consistent with human clinical evidence, the current *in vivo* assay suggested that both increased and decreased activity BRAF, MEK1 and MEK2 CFC alleles disrupt the signalling of the MAPK cascade, promoting gastrulation defects. It became clear that disturbing normal MAPK signalling early in development had detrimental effects initially in the axis patterning and later in tissue formation. The dorsalisation of embryos at 10.5hpf was translated into severe shortening of the antero-posterior axis of the larvae at 24hpf (**Figure 2.3.1**).

The entire panel of allelic variants caused embryo elongation. The fact that over-expression of the human wild-type proteins alone did not promote any morphological or molecular changes suggests, firstly, that the embryo elongation was not an artefact of the RNA injection of human mRNA and, secondly, that the embryos can cope in the presence of elevated amounts of a foreign protein without affecting the activity of the pathway or the progression of development. In the framework of this assay, all the mutations were activating, irrespective of their *in vitro* or *in silico* predicted kinase activity.

It was of interest to test whether early gastrulation movements were affected by the expression of disease alleles, as embryo dorsalisation results from Fgf-signalling disruption. HggI expression remained unaffected in all groups of embryos suggesting that convergence movements were not disrupted. Dlx3 expression, however, was widely modified in the embryos injected with the disease alleles, but not in those injected with the wild-type form of the human protein. Therefore, while convergence

carried on as normal, extension cell movements were enhanced, thus causing the elongated phenotype. The fact that convergence disruption is even greater than Shp2 zebrafish mutants may indicate a different mode of action of Braf and Mek during gastrulation.

2.3.2. Kinase-impaired mutants do not signal through C-raf to promote Mek activation

Low activity BRAF mutants signal through C-RAF to activate the MEK and subsequently ERK in tumour cell lines (Dumaz *et al*., 2006; Garnett *et al*., 2005; Wan *et al*., 2004). In the present study, kinase-inactivating allelic variants such as $BRAF^{D594V}$ and $BRAF^{G596V}$ promoted embryo elongation. This suggests that they activated the pathway less optimally than the WT protein but sufficiently to affect gastrulation progression.

To examine whether C-raf was, indeed, the mediator between impaired activity BRAF proteins and MEK1/2, kinase-inactivating BRAF variants were expressed in a C-raf knockdown background (**Figure 2.2.6**). The C-raf morpholino used was designed based on published data and morphant phenotypes were consistently reproduced (Razzaque *et al*., 2007). However, the reduction of endogenous C-raf levels did not prevent the elongated phenotype. This finding is in contrast with the previously speculated theory of BRAF-C-RAF dimerisation (Rushworth *et al*., 2006) and is suggestive of an alternative mode of pathway activation. In addition, a constitutively active C-RAF mutant (kind gift from Dr. Eric Holland, NY) failed to cause embryo dorsalisation (data not shown), suggesting that this bioassay is independent of C-raf signalling.

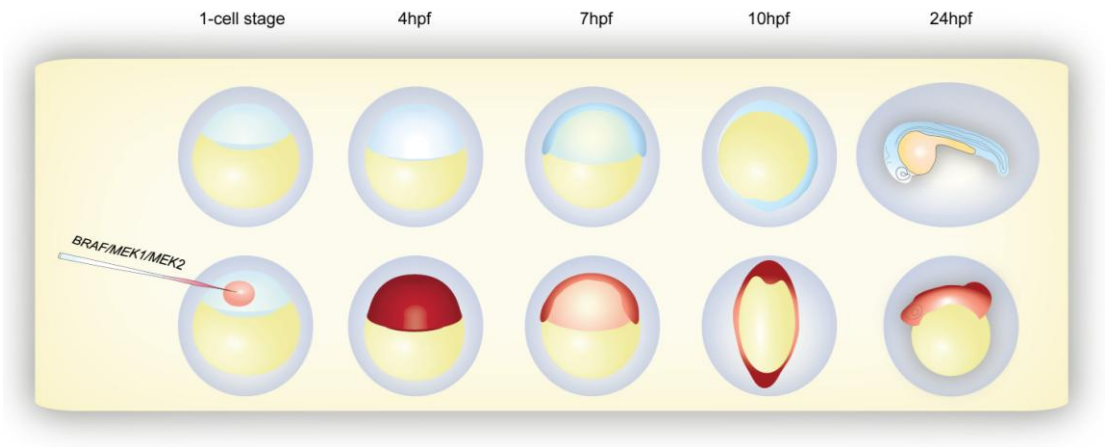

Figure 2.3.1 *Schematic overview of in vivo activity of BRAF, MEK1 and MEK2 mutant alleles*

Injection of one-cell stage wild-type embryos with a mRNA expressing mutant but not WT human BRAF, MEK1 and MEK2 proteins disrupted normal gastrulation movements and caused dorso-ventral axis defects at 10hpf and significant shortening of the embryo by 24hpf.

The top panel illustrates the development of control, untreated embryos. Red cell lineage represents injected embryos.

2.3.3. All CFC disease variants act as gain-of-function mutations *in vivo*

It is not unusual for gain-of-function (gof) and loss-of-function (lof) mutations to advance similar clinical phenotype in different patients (Bentires-Alj *et al*., 2006; Keilhack *et al*., 2005). Conversely, gof and lof mutations of the same gene can lead to the onset of separate disorders. In the case of SHP2, germ-line gof mutations cause Noonan syndrome (NS) whereas lof mutations are found in LEOPARD syndrome (LS) (Stewart *et al*., 2010; reviewed in Edouard *et al*., 2007). Additionally, Shp-2 knockdown as well as expression of NS and LS mutations give rise to comparable phenotypes both in zebrafish and *Drosophila melanogaster* models of the diseases (Oishi *et al*., 2009; Jopling *et al*., 2007; Oishi *et al*., 2006). There is presently no established correlation between kinase activity levels of MAPK components and symptom severity. Therefore, *in vitro* protein activity cannot be used as a reliable predictor of patient phenotype.

Co-expression of sub-optimal levels of CFC BRAF and MEK disease alleles promoted an additive effect in terms of aberrant phenotype incidence (**Figure 2.2.4**).

Similarly, the presence of two mutations in the MAPK pathway can have an additive clinical outcome. For example, a severely affected NFNS patient had a *de novo* PTPN11 and an inherited NF1 mutation, and only one parent showed mild features of neurofibromatosis type I (Thiel *et al*., 2009). Unlike NS and LS zebrafish models, where gof and lof mutations cancel each other out upon simultaneous expression (Jopling *et al*., 2007), concurrent presence of kinase-inactivating and kinase-activating BRAF and MEK mutations significantly enhanced elongation frequency. These findings strongly support that all CFC allelic variants are activating the MAPK pathway and act as gof mutations *in vivo*.

2.3.4. CFC alleles may have a low-penetrance oncogenic potential

BRAF is often mutated in a range of cancer patients. Mutations arise in approximately 7% of all human cancers and, more strikingly, in 66% of malignant melanomas (Davies, 2002). The most frequent missense point mutation occurs at the valine 600 (V600) and the most common substitution, V600E, confers a 500-fold kinase activity increase to the protein (Wan *et al.,* 2004). $BRAF^{V600E}$ is found predominantly in pre-malignant naevi (Pollock et al. 2003), benign senescent lesions that normally would not progress to melanoma (Michaloglou *et al.,* 2005; Bennet, 2003). However, $BRAF^{V600E}$ is present in more than 80% of primary and metastatic melanoma patients and its elevated oncogenic potential when specifically expressed in melanocytes, has, previously, been assessed (Patton and Zon, 2005; Patton *et al*., 2005).

Moreover, engineered MEK alleles promote transformation in cancer studies (Lemieux *et al*., 2009; Komatsu *et al*., 2006; Mansour *et al*., 1994). However CFC mutations in MEK1 and MEK2 were the first MEK mutations to be identified in a human disease. It is only very recently that activating MEK1 mutations were identified in ovarian cancer (Estep *et al*., 2007; Bian *et al*., 2004).

Despite the germ-line mutations in BRAF and MEK, CFC patients are not thought to be at an increased risk for cancer. Nevertheless, their propensity to develop high

numbers (commonly over 100) (Tidyman and Rauen, 2010) of naevi poses the question whether CFC mutations possess increased oncogenicity. Having a previously established system to evaluate the potential of BRAF allelic variants to drive ectopic naevi formation, I tested the oncogenic effect of an array of CFC, melanoma and engineered BRAF mutations.

For the first time, mosaic melanocyte expression of a kinase-inactivating mutation identified both in melanoma and CFC patients ($BRAF^{G596V}$) was found to be sufficient to trigger extensive ectopic pigmentation (**Figures 2.2.7, 2.2.8**). Although no other variant was able to convincingly promote naevus formation, they all caused deviation from the standard defined pigmentation pattern. Most strikingly, new foci of pigment mis-patterning became apparent as the fish grew older. For instance, fish expressing $BRAF^{G596V}$ under the *mitfa* promoter developed six new distinct areas of pigmentation in two months in previously normally patterned areas (**Figure 2.2.8**). The changing melanisation of CFC allele-expressing fish could be attributed to their ongoing development but could possibly be linked to the progressive nature of CFC syndrome.

2.3.5. Concluding remarks

During this study I developed a robust bioassay that can be used as a tool to study the developmental effect of an allelic series. Using the embryonic phenotype at the end of gastrulation as the readout, the impact of the expression of multiple proteins can be easily accomplished and confirmed. Co-expressing different components of the same or different pathways can give insight into molecular and genetic interactions during gastrulation, within the physiological framework of a live developing organism.

However, this assay does not mimic the actual genetics of CFC and a better understanding of the pathway regulation can help design more realistic ways of therapeutic targeting. Although creating an animal model that more closely represents the physiology of CFC is essential, it requires time. To genetically intercept the pathway more rapidly small molecule inhibitors can be beneficial in teasing apart the mechanism of action of MAPK components as well as in approaching the possibility of pharmaceutical intervention.

Chapter 3 - Pharmacological inhibition of the MAPK pathway *in vivo*

“Cure sometimes, treat often, comfort always”
- Hippocrates

3.1. INTRODUCTION

3.1.1. The MAPK pathway as a target for drug development

The role of oncogenic MAPK signalling in driving the initiation, progression and maintenance of cancer has made this pathway a priority target for drug development (reviewed in Pratilas and Solit, 2010). Aberrant upregulation of the pathway is noted in numerous neoplasias and confers enhanced survival, independent of growth factor binding, and metastatic ability. So far, the key components of the pathway (receptor tyrosine kinases, RAS, RAF and MEK) have been the molecular targets of chemical antagonists. Small molecules acting as potent inhibitors have already been identified, some of which are being successfully used in human clinical trials (Chapman and Miner, 2011; reviewed in Weickhardt *et al*., 2010; reviewed in Sebolt-Leopold, 2008).

The MAPK pathway endorses pro- and anti-apoptotic signals depending on the cell type and amongst other processes activated ERK1/2 controls regeneration, migration and cell shape changes (reviewed in Winter-Vann and Johnson, 2007). Thus, MAPK signalling and, by extension, its inhibitors are predicted to be primarily active in tissues undergoing regeneration or have rapid turnover rates. For example target tissues include the skin and the gastrointestinal tract. Moreover new advances delineate novel MAPK regulators through RNA interference library screening (Friedman *et al*., 2006). Therefore, with new knowledge at hand and focused study of already described endogenous inhibitors construction of new drugs for the pathway becomes more approachable.

Development of new drugs specifically designed for the treatment of the RASopathies is mostly inhibited by the rarity of the disorders. However, recycling the use of already FDA-approved anti-cancer drugs or compounds in clinical trials provides a route to the possibility of RASopathies treatment (reviewed in Rauen *et*

al., 2011; reviewed in Sebolt-Leopold, 2008). Systemic therapy in young children can reduce the elevated output of the activated MAPK pathway thereby reducing the symptom severity of the patients. In the following section I will discuss the design of various inhibitors of the FGF/MAPK cascade developed to target cancerous lesions and highlight the compounds that could offer therapeutic potential for the RASopathies spectrum.

3.1.2. Cell membrane receptor inhibition

3.1.2.1. FGFR family in disease

The mammalian fibroblast growth factor receptor (FGFR) family is highly conserved amongst vertebrates and consists of four members, while a fifth one has been recently characterised in humans (Sleeman *et al*., 2001). The receptors share sequence and structural similarity but perform distinct functions in different tissues (reviewed in McIntosh *et al*., 2000). Overall, FGFRs play a central role in development, angiogenesis and wound healing. Their aberrant expression leads to constitutive activation of the FGF/MAPK pathway and occurs through three mechanisms: point mutations, chromosomal translocations and gene amplifications.

Most FGFR-related tumours arise due to gene amplifications. Over-expression of FGFR1-3 is a leading cause for the onset of rhabdomyosarcoma (FGFR1), breast (FGFR1, 2), ovarian (FGFR1), gastric (FGFR2) and bladder cancer (FGFR1, 3). Point mutations are most commonly associated with endometrial (FGFR2), bladder and cervical cancer (FGFR3). Translocations are identified in leukaemia (FGFR1), lymphoma (FGFR1) and myeloma (FGFR3) development (reviewed in Turner and Grose, 2010).

FGFRs predominantly activate the RAS/MAPK pathway (Corson *et al*., 2003) both in physiological and tumourigenic conditions. Coupled with their great involvement in cancer progression the design of compounds that block their function has increased.

3.1.2.2. FGFR germ-line mutations

Like the RASopathies, gain-of-function FGFR germ-line mutations promote the onset of a spectrum of genetic disorders (Lajeunie *et al*., 2006). All syndromes affect the embryonic development of branchial arches and as such result to similar clinical manifestations involving cartilage and bone malformations. The disorders include Crouzon syndrome (FGFR2, 3) (OMIM #123500) (Reardon *et al*., 1994), Jackson-Weiss syndrome (FGFR1, 2) (OMIM #123150) (Jabs *et al*., 1994), Pfeiffer syndrome (FGFR1, 2) (OMIM #101600) (Rutland *et al*., 1995) and Apert syndrome (FGFR2) (OMIM #101200) (Anderson *et al*., 1998; Moloney *et al*., 1996; Park *et al*., 1995; Wilkie *et al*., 1995).

FGFR2 mutations are responsible for the onset of craniosynostosis (Kan *et al*., 2002), the most important common feature between the syndromes. This condition causes infant skull sutures to fuse prematurely impeding proper cranial development. Similarly to the RASopathies, the branchial arches syndromes are progressive in severity due to bone growth with increasing age. Craniofacial and tooth formation is prominently disturbed and characteristic facial features include widely spaced eyes and low set ears.

3.1.2.3. Somatic mutations are targeted with chemical compounds

Many different FGFR alterations have been reported to be involved in cancer progression (reviewed in Turner and Grose, 2010). Carcinogenic FGFRs are mostly associated with bladder cancer, with almost half the reported cases harbouring an FGFR3 mutation (van Rhijn *et al*., 2002; Cappellen *et al*., 1999). Interestingly, most somatic mutations identified in patients with FGFR-induced tumours are the same as the germ-line mutations promoting thanatophoric dysplasia, a developmental disorder of the FGFR spectrum (van Rhijn *et al*., 2002). Overlap between the same variant causing melanoma in somatic mutations and CFC syndrome in germ-line mutations has been observed with the $BRAF^{G596V}$ allele.

Inhibition of FGFRs has clinical significance especially in tumourigenic lesions with amplified FGFR expression, like breast and bladder cancer. Small molecule compounds have been generated to block the activated receptor tyrosine kinases *in vitro* and *in vivo*. However, the majority of the drugs are not FGFR-selective. Due to their structural similarity, most inhibitors target FGFRs, vascular endothelial growth factor receptors (VEGFRs) and platelet-derived growth factor receptors (PDGFRs) at a similar dosage (reviewed in Hynes and Dey, 2010). An example of a broad-range anti-angiogenic drug is Dovitinib (Sarker *et al*., 2008) currently in clinical trials against solid tumours (Loriot *et al*., 2010).

Affecting a large spectrum of kinases has been beneficial in impeding tumour progression in cancer patients but it is important to be able to selectively target a single protein. To this end, antibodies may become useful in inhibiting single FGFRs in cancer patients (Qing *et al*., 2009; Sun *et al*., 2007). Additionally, ligand traps are compounds that selectively inhibit the binding of different ligands to their respective receptor tyrosine kinases, thereby completely impeding mitogen-dependent activation of the molecular cascades downstream of the receptors. Such ligand traps have already entered clinical trials (ClinicalTrials.gov identifier: NCT01244438).

3.1.2.4. FGFR-selective inhibitors

SU5402 (**Figures 3.1.1, 3.1.2**) and PD173074 were identified through a chemical library screen for their ability to inhibit autophosphorylation of FGFR1 and phosphorylation of ERK1/2 in NIH 3T3 cells at low concentrations (Mohammadi *et al*., 1998; Mohammadi *et al*., 1997). Resolution of the crystal structure of the FGFR1 kinase domain confirmed the ATP-competitive interaction of the compounds with the catalytic domain of the receptor (**Figure 3.1.1**). Importantly, both agents exhibit high specificity for FGFR1. They do not block the activation of epithelial growth factor receptors (EGFRs), PDGFRs or insulin receptors. However they can potently inhibit VEGFRs. The specificity to FGFR and VEGFR relies on the presence of an asparagine residue in the hinge region of the kinases. Binding to this particular amino

acid promotes structural changes stabilising the binding loop of the receptor (Mohammadi *et al*., 1997).

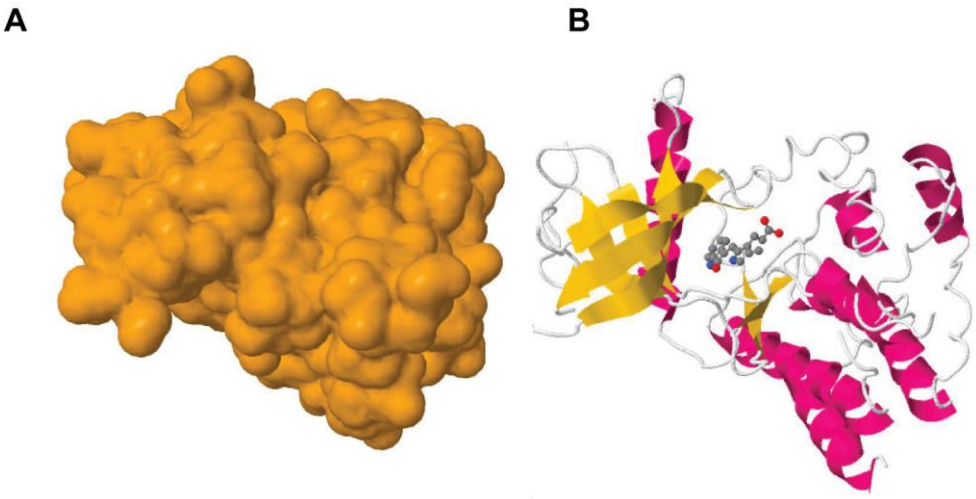

Figure 3.1.1 *Illustration of FGF receptor 1 (FGFR1) bound to the inhibitor SU-5402*

A Three-dimensional reconstruction of the surface of FGFR1.
B Schematic illustration of FGFR1 and SU-5402 in the binding pocket of the receptor. The secondary structures of FGFR1 are highlighted in magenta (α helices) and yellow (β sheets). The small molecule inhibitor is shown in a plain ball and stick style. Carbon, nitrogen and oxygen atoms are represented by grey, blue and red balls, respectively.

Both images were generated using the Jmol version 12.0.18 application on RCSB Protein Data Bank (PDB reference 1FGI).

SU5402 and PD173074 are soluble chemical agents selective for FGFR that are predominantly used in animal and *in vitro* work. Breast tumour cell lines with activating mutations or FGFR amplifications showed increased sensitivity to PD173074 treatment (Turner *et al*., 2010; Koziczak *et al*., 2004). Similarly, growth, survival and migration of non-small cell lung carcinoma lines were inhibited by SU5402 treatment (Fischer *et al*., 2008). Both SU5402 and PD173074 have been able to induce apoptosis in multiple myeloma cell lines (Grand *et al*., 2004) and mouse models (Paterson *et al*., 2004) as well as in bladder cancer tumour cell lines (Lamont *et al*., 2011) with activated and amplified FGFR1 and FGFR3.

Most features of the branchial arch syndromes are surgically corrected and patients are not treated with active FGFR inhibitors. However, treatment of a mouse model of Crouzon syndrome with an FGFR inhibitor (PD173074) promoted normal skull development (Perlyn *et al*., 2006). This is encouraging for the developmental syndromes field and suggests the possibility of pharmacological craniosynostosis patients treatment

Small molecule inhibitors of other receptor tyrosine kinases are being used successfully either as second line of treatment (e.g. Gefitinib inhibiting EGFR in non-small cell lung carcinoma) or are in advanced clinical trials (e.g. bevacizumab targeting VEGFR in non-small cell lung carcinoma and renal cancer) (reviewed in van Meter and Kim, 2010, reviewed in Shao *et al*., 2010).

3.1.3. RAS inhibition

Increased activity of the cascade can also be triggered by mutations downstream of the tyrosine kinase receptors. RAS proteins, H-RAS, N-RAS and K-RAS, are frequently mutated in a variety of human cancers. Constitutive activation of RAS either as a result of a mutation or of continuous growth factor stimulation is imperative for tissue transformation and tumour growth. This is further supported by the fact that single correction of RAS-driven aberrant signalling reverses malignant transformations even in the presence of additional genetic mutations. For the past twenty years researchers have tried to prevent the activation of this component in the scope of anti-cancer drug development (reviewed in Krens *et al*., 2010; Saxena *et al*., 2008; Konstantinopoulos *et al*., 2007; reviewed in Sebolt-Leopold and Herrera, 2004).

3.1.3.1. Mode of RAS inactivation

The oncogenicity of RAS depends on activated RAS (Ras-GTP) binding to the inner cell membrane (Kohl *et al*., 1993; James *et al*., 1993). Attachment to the plasma membrane is ensured by post-translational modifications such as prenylation (Reuter

et al., 2000). This process entails the stable attachment of a farnesyl (15 carbon-) or geranylgeranyl (20 carbon-) group to the cysteines at the carboxyl end of the protein.

RAS membrane association is promoted by the prenylation of a characteristic CAAX (Cysteine- Aliphatic amino acid- Aliphatic amino acid- any amino acid) motif at the carboxyl terminal of the kinase. Without this step, RAS is restricted to the cytoplasm and downstream activation of the pathway is impeded. Mutations of the protein anchoring site or introduction of inhibitors of the farnesyl transferase enzyme block RAS activation and, thus, MAPK pathway signalling.

3.1.3.2. Development of post-translational modification inhibitors

Farnesyl transferase inhibitors (FTIs) have been successful in preventing tumour progression in h-ras transgenic mice and mice xenografted with fibroblasts harbouring *h-ras* mutations (Liu *et al*., 1998). Some FTIs have been evaluated in clinical trials (Alsina *et al*., 2004; Cortes *et al*., 2003; Morgan *et al*., 2003). However, they have not shown high clinical efficiency and the response to the treatment was incomplete (Alsina *et al*., 2004). This may be accounted for by the fact that FTIs only inhibit farnesylation and the most commonly mutated K-RAS and N-RAS kinases undergo a different type of end modification, geranylgeranylation (Rowel *et al*., 1997; Whyte *et al*., 1997; Zhang *et al*., 1997).

To that end, a new inhibitor was developed to target all three orthologues. Farnesylthiosalicylic acid (FTS), also known as salirasib, competitively occupies the RAS-docking sites on the cell membrane impeding RAS-GTP anchorage and promoting its degradation (reviewed in Gana-Weisz *et al*., 2002; Weisz *et al*., 1999; Haklai *et al*., 1998). FTS has been the most successful in uncoupling all RAS proteins from the cell membrane and promoting RAS-independent growth *in vivo* and *in vitro* (Jansen *et al*., 1999; Weisz *et al*., 1999). FTS inhibits tumour formation both in mice xenograft experiments (Zundelevich *et al*., 2007; Jansen *et al*., 1999; Weisz *et al*., 1999) and after direct oral administration (Haklai *et al*., 2008) most importantly without causing any toxicity to the animals.

Being the only active compound against K-RAS and N-RAS, coupled with the lack of adverse side effects at physiological doses (reviewed in Gana-Weisz *et al*., 2002) rendered FTS a good potential candidate for clinical trials. It has already been entered in phase I and II clinical trials against non-small cell lung carcinoma, lung adenocarcinoma and pancreatic cancer (Clinical trial identifier: NCT00531401; Tsimberidou *et al*., 2009; reviewed in Bustinza-Linares *et al*., 2010).

Further obstruction of RAS post-translational modifications also seems promising. Inhibiting ICMT, the protein that methylates RAS after proteolytic cleavage of its CAAX motif, halts cellular transformation (Bergo *et al.,* 2004) and potent inhibitors are being developed against it, like cysmethynil, (Winter-Vann *et al.,* 2005).

3.1.3.3. FTIs and FTS against RASopathies

Neurofibromin 1 is encoded by the NF1 gene and acts as a Ras-GTP-ase activating protein. Its implication in the onset of Neurofibromatosis Type I (NF1) has been previously discussed (Chapter 2). The activity of NF1 exons 23-29 promotes RAS inactivation by hydrolysing the active GTP-bound RAS to the inactive GDP-bound protein (Ballester *et al*., 1990; Martin *et al*., 1990). Mutations leading to neurofibromin 1-depletion promote perpetual RAS activation and tumourogenicity.

NF1 patients develop a plethora of tumours, which are accounted for by the cellular increase of RAS-GDP. Thus, administration of FTIs presented as a potential treatment for some NF1-related symptoms. Indeed, FTIs blocked the oncogenic growth of neurofibromin 1-deficient malignant cell lines (Mahgoub *et al*., 1999; Kim *et al*., 1997; Yan *et al*., 1995). Later studies further supported NF1 treatment through RAS inhibition as the more effective FTS inhibitor restored normal RAS-GTP levels, halted tumour growth and reversed the malignancy of NF1 mutant cells (Barkan *et al*., 2006).

3.1.4. RAF inhibition

After the identification of BRAF as an oncogene and its frequent implication in multiple cancer types (Davies *et al.*, 2002), community interest was shifted towards identifying therapeutic agents against RAF kinases. Although the members of the RAF family are structurally similar, their activity and expression patterns differ (Chapter 2). This together with the fact that Raf proteins are interacting both positively and negatively with a complicated network of downstream effectors, render the simultaneous inhibition of all three kinases more difficult.

3.1.4.1. Inhibitors of C-RAF are not specific

From all the small molecule inhibitors directed against RAF, only one has been entered in clinical trials. The C-RAF inhibitor BAY 43-9006 (Sorafenib) competes with ATP to bind to C-RAF and BRAF pockets (Lyons *et al*., 2001). It has been entered into Phase I, II and III trials (Wilhelm *et al*., 2006; Lee and McCubrey, 2003; reviewed in Bollag *et al*., 2003) with manageable side effects. The drug promoted gastrointestinal and cutaneous reactions (Hotte *et al*., 2002), common side effects to inhibitors of the MAPK pathway.

However, pERK was only partially suppressed following sorafenib treatment and inhibition effectiveness depended on the tissue type examined (Clark *et al*., 2005; Strumberg *et al*., 2005). Moreover, the compound lacked in specificity (Wilhelm *et al*., 2004) and failed to induce a response in BRAF-specific tumours such as melanoma. This is likely to be the case as the small molecule binds to the inactive form of BRAF and the malignant protein may be less sensitive to inhibition (Wan *et al*., 2004). Kinase assays supported that sorafenib was preferentially selective for growth factor receptors like VEGFR2-3, PDGFR and KIT (Wilhelm *et al*., 2004) and not RAF. Despite the lack of MAPK inhibition, the compound had great success in prohibiting renal and hepatocellular carcinoma in clinical trials (Escudier *et al*., 2009; Escudier *et al*., 2007; Strumberg *et al*., 2005).

3.1.4.2. Targeting specific BRAF mutant conformations

BRAF mutations are most frequently identified in melanoma (Satyamoorthy *et al*., 2000; Davies *et al*., 2002) but are also prevalent in colorectal (Yuen *et al*., 2002), ovarian (Singer *et al*., 2003) and thyroid cancer (Kimura *et al*., 2003). The majority of the mutations result in the substitution of the valine at the amino acid 600, which causes a structural change to the protein. $BRAF^{V600E}$ mutations highly enhance the kinase activity by mimicking the active conformation of the activation loop of the protein (Wan *et al*., 2004).

After the crystallisation of BRAF (Wan *et al*., 2004), second generation RAF inhibitors were developed. The structure of the most promising inhibitor PLX-4032 was based on the conformation of $BRAF^{V600E}$ thus exhibiting very high specificity for the mutant and not the wild type kinase (Tsai *et al*., 2008). In initial studies, melanoma cell lines treated with PLX-4032 were positively responsive to the inhibitor (Sala *et al.,* 2008). The drug soon entered clinical trials against metastatic melanoma with great success in promoting non-toxic growth regression and inhibiting metastasis (reviewed in Wellbrock and Hurlstone, 2010). It is currently in Phase III trials.

Despite the increased patient responsiveness, drug resistance with PLX-4032 was common and developed in as little as two months of treatment (Tuma, 2011). Two mechanisms of resistance have been characterised. In some patients, the cells compensated for the loss of BRAF activity by making use of parallel pathways (Johannessen *et al*., 2010). C-RAF and COT directly activated downstream MAPK signalling in a BRAF-independent manner. Alternatively, secondary oncogenic mutations affecting the MAPK cascade arose to promote resistance (Nazarian *et al*., 2010). Two patients with N-RAS and PDGFR mutations have been reported to date.

3.1.5. MEK inhibition

MEK kinases have a seminal role in the promotion of the MAPK pathway and the further transduction of proliferative or apoptotic signals. MEK1/2 have been described as oncogenes by virtue of the tumourigenic potential of their constitutively active forms *in vitro* (Hoshino *et al*., 1999; Cowley *et al*., 1994; Mansour *et al*., 1994). It is possible to target both kinases simultaneously based on their highly homologous sequence and structure (**Figure 3.1.2; Figure 3.1.3**).

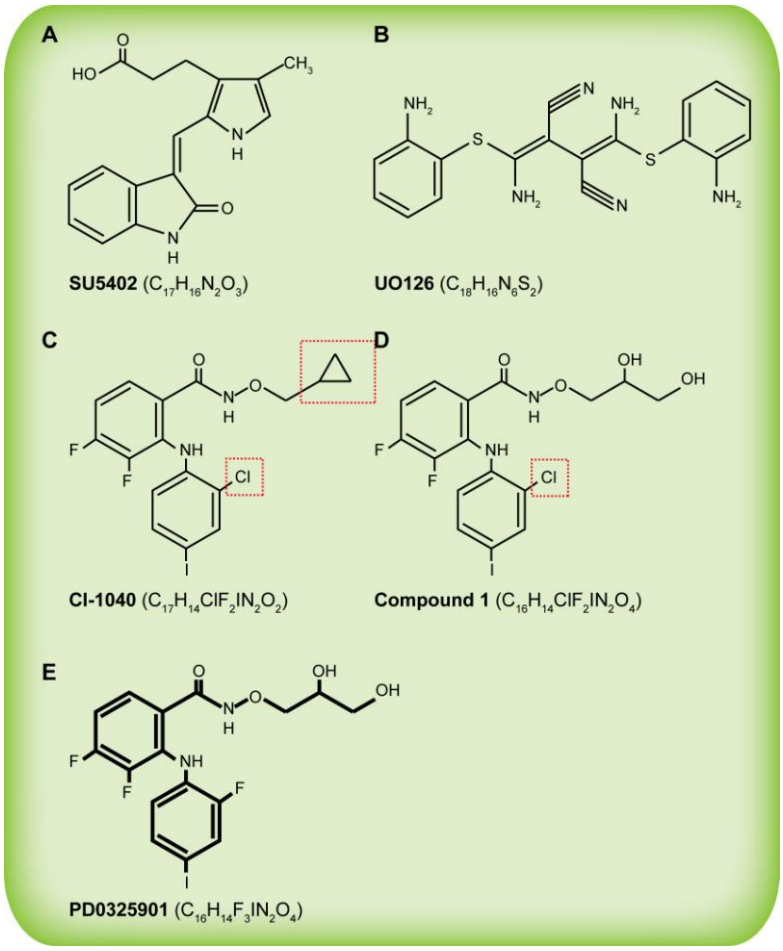

***Figure 3.1.2** Chemical structures of small molecule inhibitors*

Representations of the structures of small molecule inhibitors of the FGF/MAPK pathway.
A The FGF receptor inhibitor SU5402
B-E The MEK1/2 inhibitors UO126 (B), CI-1040 (C), Compound 1 (D) and PD032501 (E). The red dotted boxes are highlighting the chemical differences between CI-1040 and Compound 1 and their derivative PD0325901 (bold).

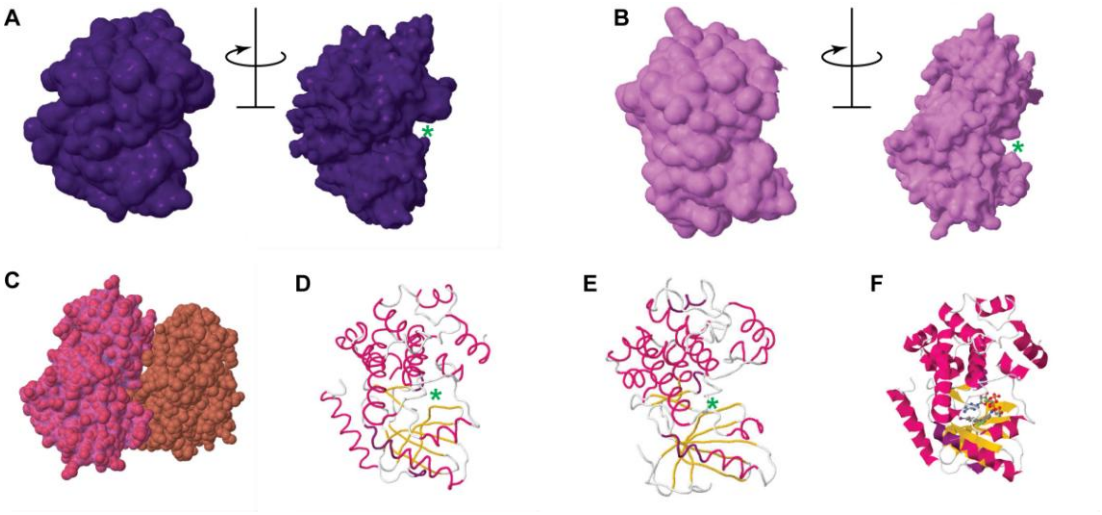

Figure 3.1.3 *Illustrations of MEK1 and MEK2*

A, B Three-dimensional reconstructions of MEK1 (A) and MEK2 (B) from different angles. The images on the right of each panel illustrate the same molecules rotated anti-clockwise, thus revealing the opening of the binding pocket (green asterisk).
C Illustration of a MEK2 homodimer. For clarity purposes the hue of each MEK2 monomer is altered.
D, E Simplified representations of the secondary structures of MEK1 (D) and MEK2 (E). Oriented at similar angles to each other the structural similarity of the proteins is apparent. The structures illustrated are α helices (magenta), β sheets (yellow) and the binding pocket (green asterisk).
F PD0325901 bound to MEK1
All images were generated using the Jmol version 12.0.18 application on RCSB Protein Data Bank (PDB references MEK1: 3EQG; 3EQG; MEK2: 1S9I).

3.1.5.1. Partial success with the first MEK inhibitors

With only two known effectors, ERK1 and ERK2, MEK1 and MEK2 were initially targeted with PD98059 (Dudley *et al.*, 1995). The development of this small molecule inhibitor advanced the study and understanding of the MAPK pathway by the academic community. A more potent inhibitor, UO126 (**Figure 3.1.2**), was generated shortly after PD98059 (Ahn *et al.*, 2001; Favata *et al.*, 1998) but neither were administered during clinical trials due to their rapid turnover rate.

The first drug to successfully block tumour growth *in vivo* was the non-ATP competitive inhibitor CI-1040 (**Figure 3.1.2**). Oral administration of CI-1040 effectively impeded up to 80% of colon tumour growth in mice (Sebolt-Leopold *et al.*, 1999). CI-1040 treatments of zebrafish embryos promoted defined

developmental phenotypes that resemble CFC syndrome defects (Grzmil *et al.*, 2007). Namely, heart development, body axis and craniofacial cartilage structures were vastly affected.

After its initial success in animal models (Sebolt-Leopold *et al*., 1999) and its high specificity for MEK1/2 (Davies *et al*., 2000), CI-1040 entered Phase I and II clinical trials (Rinehart *et al*., 2004; Allen *et al*., 2003). The drug successfully inhibited ERK phosphorylation at doses well tolerated by patients, some of whom showed evidence of tumour regression. It has, however, been proposed that CI-1040 preferentially inhibits proliferation of thyroid tumours harbouring BRAF or RAS mutations (Liu *et al.*, 2007). This is a possible explanation as to why the drug only halted tumour growth without being overtly successful in causing tumour regression in clinical trials. Additionally, as the compound was rapidly metabolised the trials were terminated.

3.1.5.2. Second generation MEK inhibitors enter clinical trials

The design of PD0325901 was based on CI-1040 and as such is biologically and structurally (**Figure 3.1.2**) very similar. PD0325901 is equally selective for MEK1 and MEK2 as CI-1040 but is more potent in inhibiting MEK both *in vitro* and *in vivo* (reviewed in Sebolt-Leopold, 2008). The enhanced activity of the drug is attributed to its improved stability and increased solubility. This was achieved by optimising the compound's core and modifying its side chain (Barrett *et al*., 2008). PD0325901 treatment has been effective in a range of human tumours. It has been tested in clinical trials for patients with MAPK-activated solid tumours, breast cancer, colon cancer, melanoma and non-small cell lung carcinoma (Haura *et al*., 2010; LoRusso *et al*., 2010; clinical trial identifiers: NCT00147550; NCT00174369).

3.1.5.3. MEK inhibitors are highly selective

MEK1/2 inhibition has proven to be the most highly selective one as the developed small molecule compounds failed to sufficiently inhibit a spectrum of other kinases (Davies *et al*., 2000). CI-1040 can only additionally inhibit MEK5 at a concentration

100 times higher than MEK1/2 (Mody *et al*., 2001). Blocking MEK with small molecules *in vitro* effectively inhibits the activity of mutant BRAF resulting in growth arrest and apoptosis (Solit *et al*., 2006). This suggests that the cancerous cells are addicted to BRAF, a notion referred to as oncogene addiction.

Crystallisation of the kinase domain of MEK1 and MEK2 identified the presence of an inhibitor-binding domain, unique to MEK1/2 kinases (Ohren *et al*., 2004). This site is directly adjacent to the ATP-binding pocket. Resolution of the structure revealed that simultaneous binding of ATP and the inhibitor is possible. This association leads to conformational changes of the protein without suppressing its kinase activity. In detail, CI-1040 and PD0325901 binding disrupts the catalytic site of the protein by stabilising the naturally occurring inactive conformation of the activation loop and helix C. The possibility of the presence of analogous binding pockets in other kinases facilitates the design of new non-ATP competitive drugs (non-classical kinase inhibitors) (Tecle *et al*., 2008).

3.1.5.4. MEK inhibitors and RASopathies

The development of high specificity and efficacy MEK inhibitors offers therapeutic potential in the RASopathies field. Such drugs function by impeding the activation of ERK. As all germ-line mutations identified in this spectrum are mostly upstream of MEK and in the case of 25% of CFC patients are in MEK, halting the downstream output of the pathway has the potential of restoring physiological MAPK signalling levels. Indeed, pre-natal PD0325901 administration to a mouse model of Noonan syndrome (NS) with a homozygous SOS1 mutation reduced both lethality and the severity of the phenotypes (Chen *et al*. 2010). Additionally, post-natal MEK inhibition of a different NS mouse model harbouring C-RAF mutations overtly improved the NS features of the animal (Wu *et al*., 2011). Both studies are encouraging and support the benefits of reducing MAPK pathway activity by administering systemic therapy after birth.

Agent	*Class*	*Target*	*Clinical Trials*
Dovitinib	Multitarget agent	FGFR, PDGFR, VEGFR	✓
SU5402	ATP-competitive FGFR inhibitor	FGFR, VEGFR	×
PD173074	ATP-competitive FGFR inhibitor	FGFR, VEGFR	×
Gefitinib/ Erlotinib	ATP-competitive RTK inhibitor	EGFR	✓
Sunitinib	Multitarget agent	PDGFR, VEGFR2, KIT, FLT3	✓
Bevacizumab	Monoclonal antibody	VEGFR	✓
Salirasab	Farnesylation inhibitor	KRAS, NRAS	✓
17-DMAG	Hsp90 inhibitor	Hsp90 (C-RAF, $BRAF^{V600E}$)	✓
Sorafenib	Multitarget agent	PDGFR, VEGR2/3, KIT, FLT3, C-RAF, BRAF	✓
PLX4032	B-RAF selective inhibitor	$BRAF^{V600E}$	✓
CI-1040	Non-ATP competitive MEK1/2 inhibitor	MEK1/2	✓
PD0325901	Non-ATP competitive MEK1/2 inhibitor	MEK1/2	✓
AZD6244	Non-ATP competitive MEK1/2 inhibitor	MEK1/2	✓

Table 3.1.1 *List of MAPK pathway inhibitors and their clinical trial status*

The drugs highlighted in bold were used in the present study

Developmental disorders other than RASopathies can profit from the study of MEK inhibition. FGFR syndromes, for instance, are phenotypically and molecularly similar to the RASopathies. An FGFR3 mosaic somatic mutation was recently identified promoting CFC reminiscing- skin softening, increased naevi count and mental impairment (Garcia-Vargas *et al*., 2008). Moreover, craniocystosis patients with activated FGFR signalling can evade FGFR drug resistance and benefit by MEK inhibition, as already demonstrated in a pre-clinical mouse model of Apert syndrome (Shukla *et al*., 2007).

3.1.6. Development of drug resistance

Inhibitor resistance is a principal issue in cancer treatment and occurs with many widely used cancer drugs. Resistance is potentially conferred by many factors. One theory is that the cancerous cells produce more of the particular protein to compensate for the loss of its function in response to treatment-induced inactivation of a particular kinase (Gorre *et al.,* 2001). Alternatively, following prolonged treatment, mutations can arise in the catalytic domain of the protein impeding optimal binding of the pharmacological agents (Kobayashi *et al.,* 2005). Finally, activity of parallel pathways can account for resistance when no mutations have developed in the targeted kinase (Wang *et al.,* 2005).

3.1.6.1. Gene amplification

FGFR1 amplification in breast cancer induces resistance to endocrine therapies (Turner *et al*., 2010). Moreover, to elucidate the mechanisms driving potential MEK inhibitor resistance a model of AXD6244-resistant colorectal cell lines was generated. In the pre-clinical model, resistance against MEK and BRAF inhibitors was achieved through amplification of the BRAF gene (Corcoran *et al*., 2010).

3.1.6.2. Development of resistance as a result of secondary mutations

The BCR-ABL fusion protein acquires resistance against the ATP-competitive imatinib (Gleevec) by developing a mutation at the threonine 315 in the kinase domain (Bishop, 2004). The mutation causes destabilisation of the activation loop and reduction in binding affinity to the drug (Gorre *et al*., 2001). An analogous mutation has been identified in the ATP-binding site of other receptor tyrosine kinases. The substitution of threonine 670 for an isoleucine impedes binding of imatinib to the cytokine receptor KIT (Tamborini *et al*., 2006). Equivalent threonine substitutions at the binding pockets of EGFR (Kobayashi *et al*., 2005; Pao *et al*., 2005) and PDGFR (Azam *et al*., 2008) are responsible for drug resistance. This mutation locus may be conserved in other tyrosine kinases, accounting for the

developed resistance against kinase-specific drugs. To avoid such resistance, HG-7-85-01 was developed to inhibit mutant and wild-type forms of kinases irrespective of the mutational status of the essential threonine. This inhibitor targets BCR/ABL, PDGFR, KIT and Src kinases (Weisberg *et al*., 2010).

3.1.6.3. Parallel components promote downstream activation

Although inhibitors may be successful in blocking the function of their targets, the signalling route is frequently circumvented in neoplasias in order to promote oncogenic growth. Activating mutations of BRAF, such as $BRAF^{V600E}$, promote cancer survival by enforcing continuous downstream signalling. Pharmacological inhibition of oncogenic $BRAF^{V600E}$ has been successful but brief (Sala *et al*., 2008). A characterised way for persistent downstream signalling in cancerous tissues harbouring BRAF mutations that lose their sensitivity to the drugs is by the activation of C-RAF. In inhibitor-resistant melanoma cells the levels of wild-type C-RAF increase and the oncogene dependency is swapped between the two RAF kinases (Montagut *et al*., 2008). In a similar manner low kinase activity BRAF mutants heterodimerise with wild-type C-RAF to achieve further MEK and ERK activation (Garnett *et al*., 2005).

Recently, a counter-intuitive form of resistance against BRAF inhibitors was described. Upon inhibition with PLX4032 and other RAF inhibitors, BRAF/MAPK signalling was blocked in cells with oncogenic BRAF but was enhanced in cells with wild-type BRAF (Poulikakos *et al*., 2010). All drugs used act by binding to the BRAF member ($BRAF^{V600E}$) of a RAF dimer (C-RAF-$BRAF^{V600E}$ or $BRAF^{V600E}$-$BRAF^{V600E}$) and inactivating it. This step, in turn, activates the other member (C-RAF). Upstream signalling (RAS) is not activated in $BRAF^{V600E}$ –dependent cells, hence reducing the concentration of activated C-RAF and the chances of transactivation of another dimer (C-RAF-C-RAF or C-RAF-B-RAF). As ERK phosphorylation depends entirely on RAS/RAF/MEK signalling, pERK levels were inhibited in a dose-dependent manner with increasing concentrations of the inhibitors. Conversely, free C-RAF heterodimers or homodimers were transactivated in treated cells with wild-type RAF, thus inducing ERK activation.

3.1.7. Overcoming drug resistance through combination therapy

3.1.7.1. Targeting multiple components of the same pathway

Developing anti-cancer drugs that promote tumour regression as single agents is a great challenge. Most malignancies arise due to or acquire multiple genetic mutations making it difficult for individual compounds to concurrently target all the defects. The use of two highly selective drugs that act on the same pathway constitutes a potential solution to the drug resistance problem. Acquisition of dual resistance would not be common, hence more studies are being focused on double targeting. This combinatorial approach has a low probability of generating an additive phenotype that is different to the one that either one of the agents would promote on their own.

In the framework of the MAPK pathway, CI-1040 interacts synergistically with 17-DMAG, an hsp90 inhibitor, to cause mitochondrial damage in leukaemia cells and reduction of the expression of the anti-apoptotic protein Bcl-x_L (Nguyen *et al.*, 2006). Additionally, targeting the VEGFR/mTOR pathway at different levels provides improved outcomes for the therapy of metastatic renal carcinoma.

3.1.7.2. Dual inhibition of different pathways

Another effective approach for clinical treatment is simultaneous targeting of all affected pathways. Tumours and cancer cell lines with activated survival-inducing FGF/MAPK signalling often present with aberrant levels of pro-apoptotic PI3K/AKT/mTOR signalling, leading to the complication of cell fate decision.

It is uncommon for two mutations to exist within the same pathway. Indeed, N-RAS and BRAF mutations are mutually exclusive (Gorden *et al.*, 2003; Davies *et al.*, 2002). Nevertheless, there is a high incidence of MAPK and phosphatidylinositol 3-kinase (PI3K) pathway mutations in melanoma cases (Dankort *et al.*, 2009; Stahl *et al.*, 2003), suggesting co-operation between the two cascades. Activating BRAF

mutations coincide with loss of PTEN (a component of the PI3K pathway) much more frequently than independent PTEN mutations arise in lesions (Michailidou *et al*., 2009; Tsao *et al*., 2004; Tsao *et al*., 2003). Conversely, PI3K (Wee *et al*., 2009) and AKT (Gopal *et al*., 2010) over-activation confer resistance to MEK inhibition. This supports that malignant progression requires aberrant regulation of both pathways. Simultaneous suppression of components of both pathways ameliorates the effectiveness of the treatment (Meier *et al*., 2007; Bedogni *et al*., 2006; Smalley *et al*., 2006).

mTOR is another serine-threonine kinase activated by extracellular stimuli and is frequently dysregulated in human cancer. Its inhibitor rapamycin (Sirolimus) has not had success in generating a response in melanoma clinical trials when administered alone (Margolin *et al*., 2005). However, mTOR inhibition combined with agents directed against the MAPK pathway prohibits tumour growth and invasion. Simultaneous treatment with sorafenib promotes sensitivity to BRAF inhibition and apoptosis (Niessner *et al*., 2011; Gedaly *et al*., 2010; Lasithiotakis *et al*., 2008). Moreover, co-treatment with PD0325901 promotes melanoma tumour regression in mice (Dankort *et al*., 2009).

3.1.8. Neural crest cell populations are targeted during aberrant MAPK signalling

It becomes evident through the study of FGFR congenital defects and the RASopathies that the phenotypes presented by the patients are closely related. The similarity of the craniofacial malformations is particularly indicative of a specific population of cells being affected by FGF/MAPK signalling modulation. Additionally, pharmacological targeting of the MAPK cascade is predominantly affecting cutaneous and gastrointestinal tract tissues, both arising from the neural crest cell (NCC) population. It can be hypothesised that the anomalies caused by chemical intervention can be the direct result of improper control of NCC maturation. If the genetic mutations and the small molecules targeting the cascade are indeed affecting the NCC it is important to understand their molecular

background. Comprehension of NCC generation, migration and differentiation can elucidate the mechanisms underlying the abnormal development and the acquired clinical manifestations promoted by dysregulated MAPK signalling.

3.1.8.1. Neural crest cell migration

Neural crest cells (NCCs) are an embryonic cell population that delaminates from the dorsal neural tube to give rise to melanocytes, smooth muscle, peripheral and enteric neurons, ganglia as well as craniofacial bone and cartilage (reviewed in Knecht and Bronner-Fraser, 2002).

In gastrulating embryos, NCCs are confined at the neural plate border. This is the site of dlx3 expression (Kaji and Artinger, 2004), which was vastly affected by the expression of CFC disease alleles in developing zebrafish (**Chapter 2; Figure 2.2.5**). This confirms that at least the NCC orientation is altered upon aberrant MAPK signalling.

Neurulation is the embryonic process that succeeds gastrulation. After its completion three separate progenitor cell layers, the ectoderm, the neural plate border and the neural plate fold within themselves at the plate border to generate the epidermis, the neural crest and the neural tube. At that point, the epithelial NCCs migrate from the dorsal neural tube to remote sites along the vertebrate embryo, giving rise to neural and non-neural cell types. During the migration process, NCCs undergo epithelial to mesenchymal transition (EMT) (reviewed in Trainor, 2005; reviewed in Chizhikov and Millen, 2004). The FGF/MAPK pathway is a key regulator of EMT and controls NC cell motility, polarity and survival (Szabo-Rogers *et al*., 2008; Abu-Issa *et al*., 2002). Attracting signals drive NCC migration to peripheral locations promoting NCC differentiation into craniofacial, cardiac and skeletal NC tissues.

3.1.8.2. Craniofacial neural crest

FGF/MAPK signalling controls the anteroposterior and dorsoventral polarity as well as the left-right asymmetry of the cranial NCC (reviewed in Minoux and Rijli, 2010).

Craniofacial NCCs move ventrolaterally to give rise to the nasal skeleton, membranous skull bones and the pharyngeal arches (PAs). The seven PAs develop into the thyroid cartilages, otoliths, odontoblasts and jaw (Cordero *et al*., 2010; Chai *et al*., 2000; reviewed in Fagman and Nilsson, 2010; reviewed in Gross and Hanken, 2008; reviewed in Knight and Schilling, 2006). In zebrafish, PAs additionally contribute to the formation of part of the gills. The craniofacial cartilage of 4dpf zebrafish embryos is composed of seven pharyngeal arches: the Meckel's cartilage (mandibular arch), the ceratohyal cartilage (hyoid arch), and the five branchial arches (**Figure 3.2.10A**).

Maintenance of pharyngeal structures is ensured by a highly controlled network of pathways and genes, which include Slug, Snail, Sox10 and c-Myc. Importantly, cranial NCC specification and maintenance is induced by MAPK signalling (Nechiporuk *et al*., 2007; Crump *et al*., 2004). FGFs are particularly essential in PA formation and development. Fgf3 and Fgf8 promote NCC survival and subsequent formation of PA3/4 (David *et al*., 2002) and PA1 (Creuzet *et al*., 2004), respectively, and the majority of their derived structures. This partly explains the scale of the impact of an FGFR3 germ-line mutation (White *et al*., 2005).

3.1.8.3. Cardiac and trunk neural crest cells

The trunk (skeletal) NCCs migrate either dorsolaterally towards the ectoderm to form melanocytes or ventrolaterally to the anterior part of the sclerotomes to form the dorsal root ganglia. These undergo further specification. Progenitors of the sympathetic ganglia, aortic nerves and adrenal medulla undergo ventral migration (Cheung *et al*., 2005). Alternatively, vagal and sacral NCCs differentiate into the parasympathetic ganglia, the glia of the enteric nervous system (reviewed in Burns *et al*., 2009).

The cardiac NCCs are situated between the cranial and the skeletal NCCs. They populate the lower hindbrain and migrate via PAs 3,4 and 6 towards the heart (reviewed in Maschhoff and Baldwin, 2000). They develop into melanocytes, the

semilunar valves, the entirety of the muscle connective tissue of the heart arteries and also contribute to the neuron population of pharyngeal arches (Jain *et al*., 2011; reviewed in Aman and Piotrowski, 2009).

In all vertebrates, the heart forms during somitogenesis when two primordia fuse to form a linear tube. The atrium and ventricle are formed when the primary tube loops asymmetrically along the left-right axis. Unlike higher vertebrates, the zebrafish heart retains the simplistic structure of two cardiac chambers and has a single blood vessel connected to the gill arches (Hu *et al*., 2000). Zebrafish NCCs originally occupy a broader region than the one normally seen in other animal models and contribute to the ventricle, the atrium, the atrioventricular junction and the bulbus arteriosus (the cardiac outflow tract) (Li *et al*., 2003; Sato and Yost, 2003).

3.1.9. Aims

Having established that CFC and melanoma alleles are active in early development, I aimed to test whether the phenotype promoted by aberrant MAPK signalling can be prevented by pathway inhibition. Making use of highly selective anti-cancer drugs currently used in clinical trials against FGFR and MEK, I treated embryos over-expressing CFC and melanoma disease alleles.

3.2. RESULTS

CFC syndrome patients exhibit symptoms that may alter or develop in severity with time. This progressive nature suggests the possibility that specific pharmacologic administration could prevent the onset of latent phenotypes. Targeted inhibition of the mutated genes' signalling, either upstream or downstream of them, might be the key to develop new therapeutic agents and consider the possibility of chemical intervention to alleviate symptoms. The work in sections 3.2.1, 3.2.2.2, 3.2.3-3.2.5 has been published and the relevant publication has been attached in **Appendix II** with permission from the journal.

3.2.1. Fgf inhibition restores normal development in embryos expressing BRAF and MEK mutations

As argued earlier, proper Fgf/Mapk signalling is indispensable for the completion of the four embryonic cell movements during gastrulation. Aberrant expression of Fgf has a prominent role both in zebrafish development and cancer. In the established bioassay embryos over-expressing active CFC and melanoma disease variants acquired identical phenotypes as individuals with ectopic Fgf (Furthauer *et al*, 2004) by the end of gastrulation. This suggested that mutations downstream of Fgf receptors (Fgfr) may feed back to activate the entire Mapk pathway and lead to similar *in vivo* outcomes to those observed in Fgf mutants. Moreover, it is plausible that endogenous activity of the Mapk pathway in conjunction with disease allele injections had an additive effect in promoting elongation. Thus, it was hypothesised that inhibiting endogenous Fgfr could suppress the abnormal gastrulation phenotype.

Embryos expressing BRAF CFC, melanoma and engineered alleles (**Figure 3.2.1A**) as well as MEK1 and MEK2 CFC and engineered alleles (**Figure 3.2.1B**) were incubated in 0.5μM SU-5402, an FGFR1 inhibitor, at the beginning of gastrulation (4hpf). The phenotype of embryos was assessed at 10.5hpf. The development of all

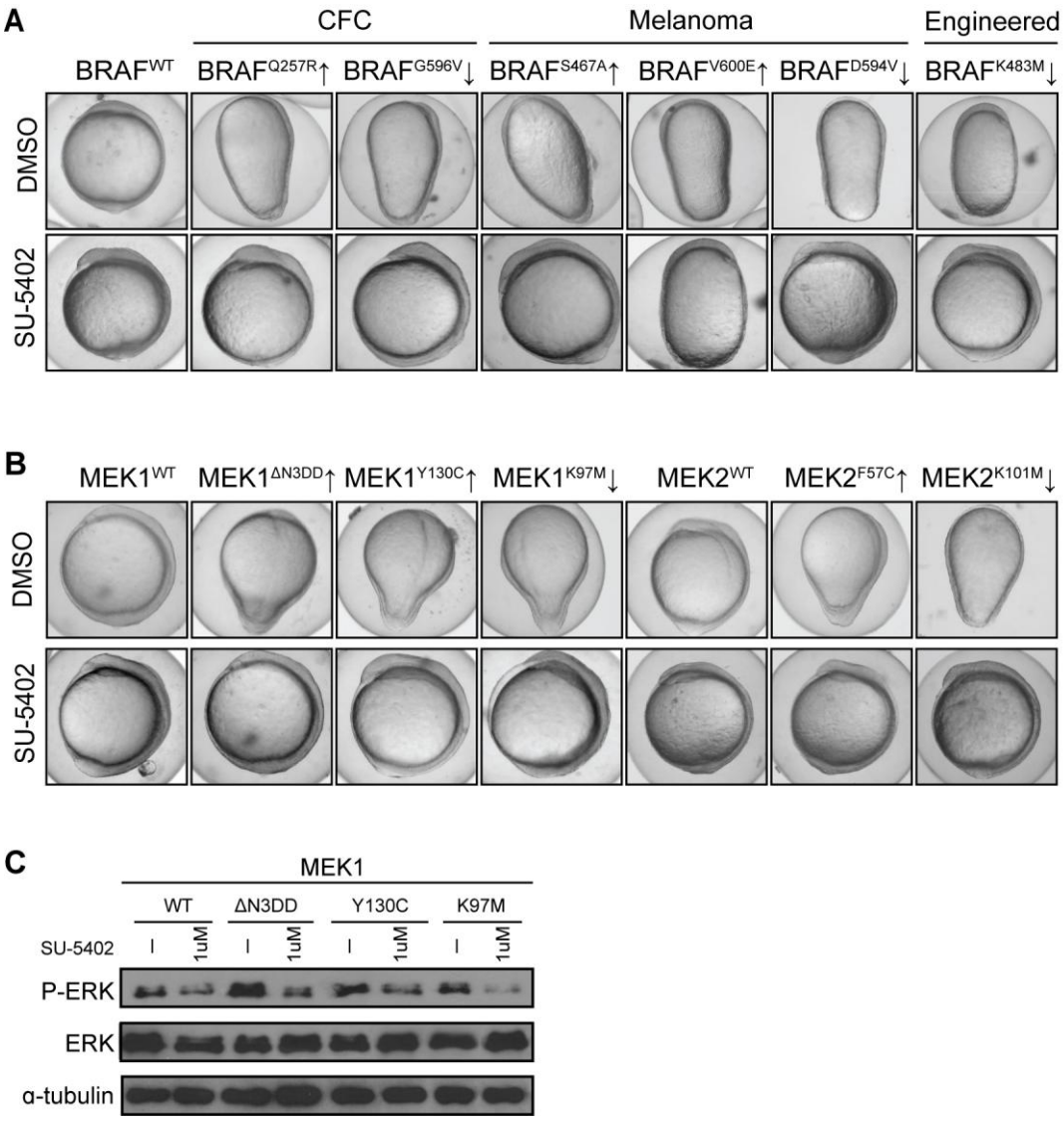

Figure 3.2.1 *Treatment of BRAF, MEK1 and MEK2 variants with SU-5402.*

A The elongation promoted by BRAF variants was pharmacologically prevented by treating with 0.5µM of the FGFR1 inhibitor SU-5402, with the exception of the developmental phenotype caused by $BRAF^{V600E}$.
B MEK1 and MEK2 disease allele-driven phenotypes were, also, prevented by SU-5402 treatment.
C Western blotting of total zebrafish lysates for Erk and p-Erk protein shows that SU-5402 treatment caused reduction of Erk phosphorylation. α-tubulin was used as a loading control.

individuals in all but one treatment groups was restored (**Figure 3.2.1**). The effect of the highly activating melanoma mutation $BRAF^{V600E}$ was not fully rescued. This finding coupled with reduction of p-Erk readout supports the hypothesis that individual BRAF and MEK mutations affect total levels of Mapk signalling, as

illustrated by western blots of treated embryos (**Figure 3.2.1.C**). Inhibition of the pathway, even upstream of the mutations, can avert their pathological output.

3.2.2. The MEK inhibitors CI-1040 and PD325901 disrupt the Mapk pathway

3.2.2.1. PD325901 decreases the expression levels of Dusp6

In order to determine whether the MEK inhibitor PD0325901 effectively prohibited Mapk activity in the developing embryo, I made use of the transgenic line *dusp6*-GFP. DUSP6 is a downstream effector of ERK1 and ERK2 and its expression depends on active MAPK signalling (Section 2.1.1). The Dusp6 expression pattern in zebrafish is visualised via the GFP reporter driven by a 10Kb region upstream of the *dusp6* gene (Molina *et al*., 2007). Using this system, I could optically ascertain whether inhibition of ERK phosphorylation coincided with a decrease in Dusp6 levels.

To examine whether the expression pattern of Dusp6 was altered, un-injected *dusp6*-GFP embryos were treated with DMSO, 0.5μM or 1.0μM of PD0325901 at 4hpf and were imaged for 20 hours using a time-lapse set up (**Figure 3.2.2**). At the shield stage (30% epiboly) Dusp6 expression is localised at the shield and the margin (Molina *et al*., 2007) a dorsal embryonic tissue giving rise to the germ ring and the tail bud. In this study, the GFP signal was, first, detected in DMSO-treated embryos at 50-60% epiboly at the axial hypoblast (white arrowheads), which derives from the shield and develops into the axial mesoderm. The expression expanded vegetally as gastrulation progressed to have a diffuse, almost ubiquitous pattern but, also, occupy specific foci such as the tail bud (yellow arrowheads). By 24hpf high levels of Dusp6 remained at the tail bud but were also detected at the midbrain-hindbrain boundary and the telencephalon (red arrowheads) (**Figure 3.2.2A**). Dusp6 patterning did not alter after PD0325901 addition but increasing concentrations of the MEK inhibitor resulted in a linear decrease and slight diffusion of the signal intensity (**Figure 3.2.2B,C**). Thus, PD0325901 seems to be down-regulating p-ERK activity *in vivo*.

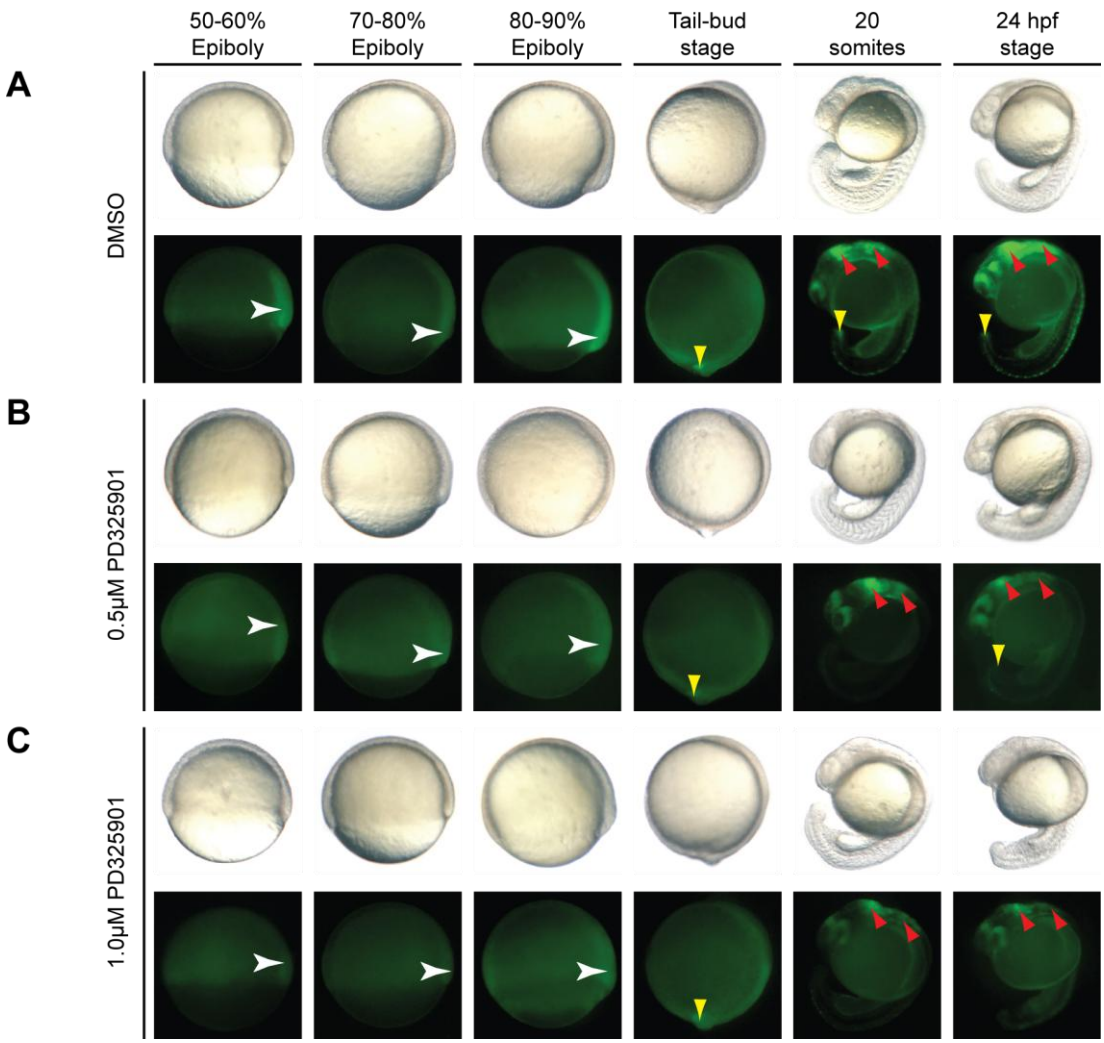

Figure 3.2.2 *Dusp6 expression appears to decrease in PD325901-treated embryos*

A Normal Dusp6 expression in developing d*usp6*-GFP transgenic zebrafish embryos treated with DMSO. The GFP signal was first detected in gastrulating embryos at 50-60% epiboly (white arrowhead). The expression area expanded towards the vegetal pole during epiboly (white arrowhead) and at the tail-bud stage the expression was more diffuse with higher expression levels at the tail bud (yellow arrowhead). By the next day (20 somites and 24hpf), high levels of Dusp6 were detected in the midbrain-hindbrain boundary and more posterior parts of the brain (red arrowheads) as well as the tail bud.
B,C Expression localisation did not alter after PD0325901 addition. However, higher concentrations of the MEK inhibitor (C) appeared to cause a decrease in signal intensity.
The brightfield images of the embryos are on the top row and their paired fluorescence images are directly below them.

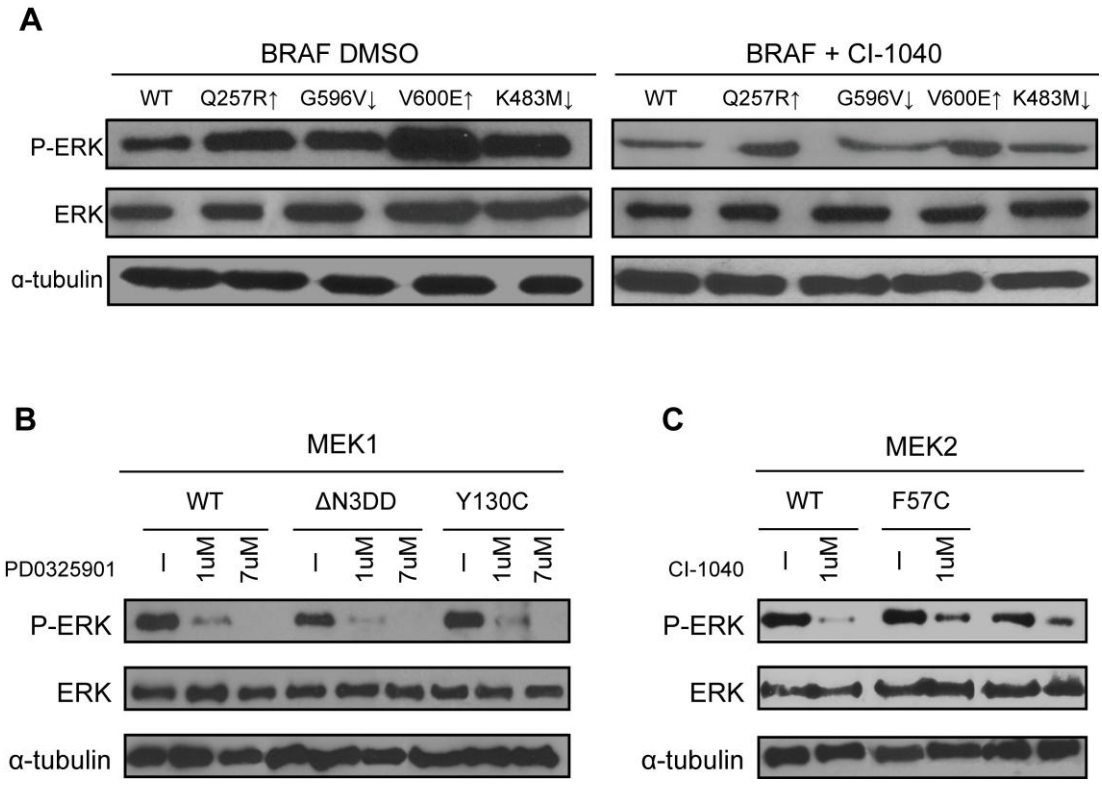

Figure 3.2.3 *The specific MEK inhibitors CI-1040 and PD0325901 are active in zebrafish*

A Immunoblotting against p-Erk demonstrates the differences in Mapk pathway activity promoted by the different mutant proteins (left panel) and the effective inhibition of the pathway by CI-1040 administration, as illustrated by the significant reduction in phospho-Erk readout (right panel). Total Erk levels remained unaffected.
B,C Immunoblotting against p-Erk demonstrates that increasing concentrations of PD0325901 (**B**) and CI-1040 (**C**) significantly decreased the activity of the Ras-Mapk pathway, with total levels of Erk being unaffected.
α-tubulin was used as a loading control.

3.2.2.2. CI-1040 and PD325901 effectively inhibited Erk phosphorylation

To molecularly confirm that MEK inhibitors were impeding Mapk signalling, CI-1040 or its derivative PD0325901 were administered to 4hpf wild-type or embryos expressing disease alleles. Immunoblotting of entire embryonic tissues against p-Erk demonstrated that the pathway was effectively inhibited after addition of the small molecule inhibitors but not of DMSO (**Figure 3.2.3**). Total Erk levels remained unaffected.

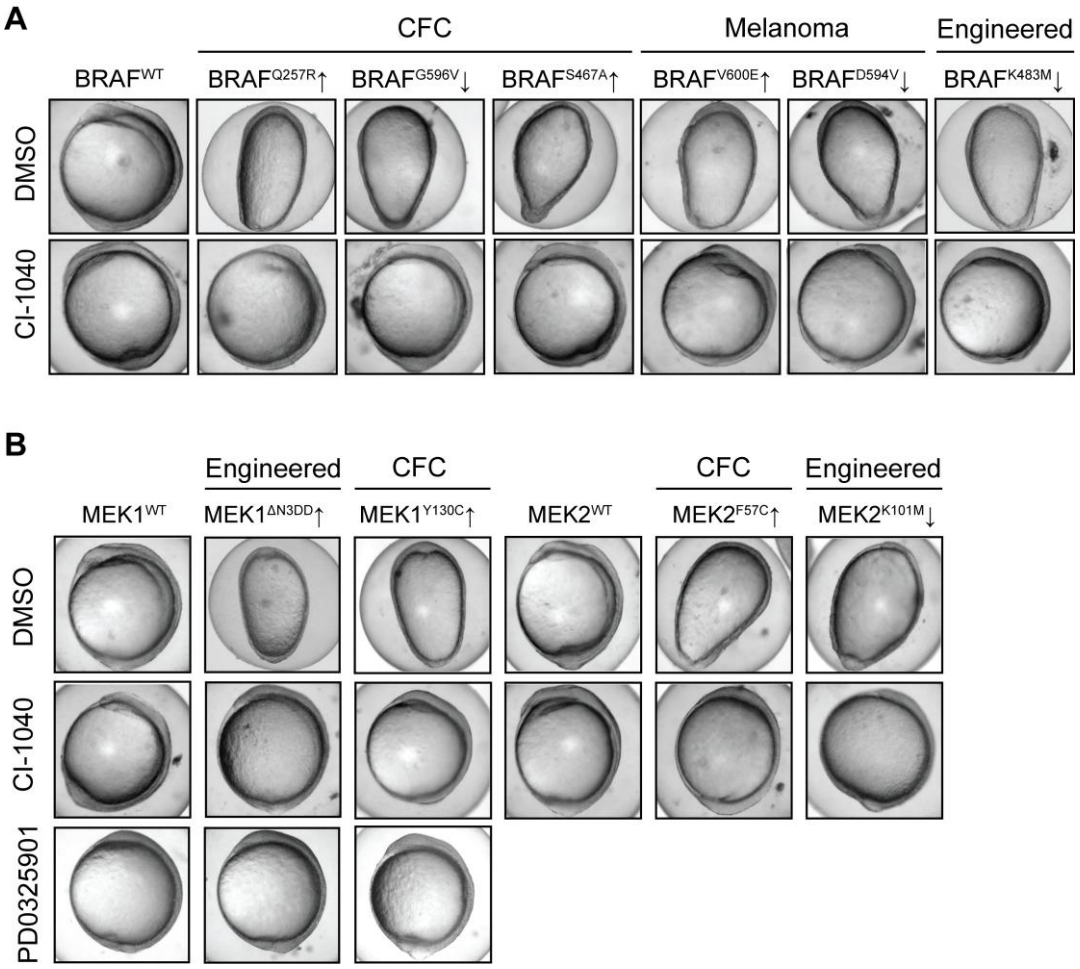

Figure 3.2.4 *CI-1040 and PD0325901 prevent elongation phenotype in all BRAF- and MEK- expressing embryos*

A The elongated phenotype of the embryos over-expressing CFC, melanoma and engineered BRAF mutations was fully prevented after incubation of the injected embryos in 1µM CI-1040 from 4hpf (the beginning of gastrulation). CI-1040 addition did not affect normal embryonic development.
B Elongation promoted by MEK1 and MEK2 disease allele mRNA at 10hpf was rescued in 100% of embryos treated with 1µM of the specific MEK inhibitors CI-1040 and PD0325901. Administration of the inhibitors alone did not affect normal development of the embryo at 10hpf.

3.2.3. Incubation of disease allele-expressing embryos in specific MEK inhibitors prevents the elongation phenotype

As suppression of Fgfr was able to partially prevent the gastrulation phenotype of BRAF and MEK-expressing embryos, I aimed to test the efficacy of selective MEK inhibitors in restoring normal development. As both available MEK inhibitors have been entered in clinical trials as chemotherapeutic agents against cancer (Haura *et*

al., 2010; Rinehart *et al*., 2004) they represent physiological agents that could be potentially administered to CFC patients. The effect on MEK inhibition has only been studied in the framework of kinase-activating mutations and supports that activating BRAF mutations confer an increased *in vitro* sensitivity to MEK inhibition (Solit *et al*., 2006). Similarly, all the CFC mutations identified to date have been activating and have been shown to be reactive to the UO126 MEK suppressor *in vitro* (Senawong *et al*., 2008).

Gene	Amino acid change	Response to small molecule treatment
BRAF	Wild type	N/A
	A246P	yes
	Q257R	yes
	G464V	yes
	S467A	yes
	K483M	yes
	K499E	yes
	G534R	yes
	N581D	yes
	D594V	yes
	G596V	yes
	T599E/S602D	yes
	V600E	yes CI-1040; no SU-5402
	D638E	yes
MEK1	Wild type	N/A
	F53L	yes
	F53S	yes
	T55P	yes
	K97M	yes
	G128V	yes
	Y130C	yes
	S218D/S222D	yes
	ΔN3DD	yes
MEK2	Wild type	N/A
	F57C	yes
	A62P	yes
	K101M	yes
	G132V	yes
	Y134C	yes
	S222D/S226D	yes
	K273R	yes

Table 3.2.1 *Responsiveness of CFC, melanoma and engineered alleles to FGF/MAPK inhibition*

To assess the sensitivity of all the disease alleles available against two specific MEK small molecule inhibitors, embryos expressing BRAF, MEK1 and MEK2 variants were incubated after 4hpf in 0.5μM CI-1040 or PD325901. Embryo elongation was recorded at 10.5hpf **(Figure 3.2.4**). 100% of the MEK inhibitor-treated embryos expressing wild-type, highly active or kinase impaired proteins were indistinguishable from the wild-type DMSO-treated embryos, whereas the elongation incidence in injected embryos incubated in DMSO was the same as previously observed. This suggested that inhibition of Mapk signalling downstream of the dysregulated gene is enough to restore normal development at 10.5hpf

3.2.4. Identification of a treatment window with CI-1040 restores normal development beyond gastrulation

The MEK suppressors were able to fully prevent elongation in embryos expressing both activating and kinase-impaired mutations. Nevertheless, prolonged drug administration has severe toxic side-effects, leading to body axis shortening, craniofacial and cardiac malformations, phenotypes similar to those displayed in CFC patients. Disease allele-expressing embryos incubated in MEK inhibitors appeared normal at 10.5hpf but suffered serious developmental anomalies by 24hpf linked to the previously published studies from our lab (Grzmil *et al*., 2007).

In order to identify a time period of drug exposure sufficient to prevent defects without disrupting development, embryos expressing the most common CFC allele, $BRAF^{Q257R}$, underwent 12 separate treatments. Each treatment was initiated at different developmental stages and varied in duration (**Figure 3.2.5**). Elongation at 10.5hpf was avoided in 100% of embryos treated from 4hpf and the aberrant phenotype was restored in fewer embryos as the treatment initiation was moved to later time points (**Figure 3.2.5B**). Importantly, a treatment window between 4.5-5.5hpf was able to restore normality both at 10.5 and at 24hpf. Interestingly, it was not the short length of the treatment that was sufficient to avert adverse development, as incubation in CI-1040 between 9.5 and 10.5hpf did not prevent elongation.

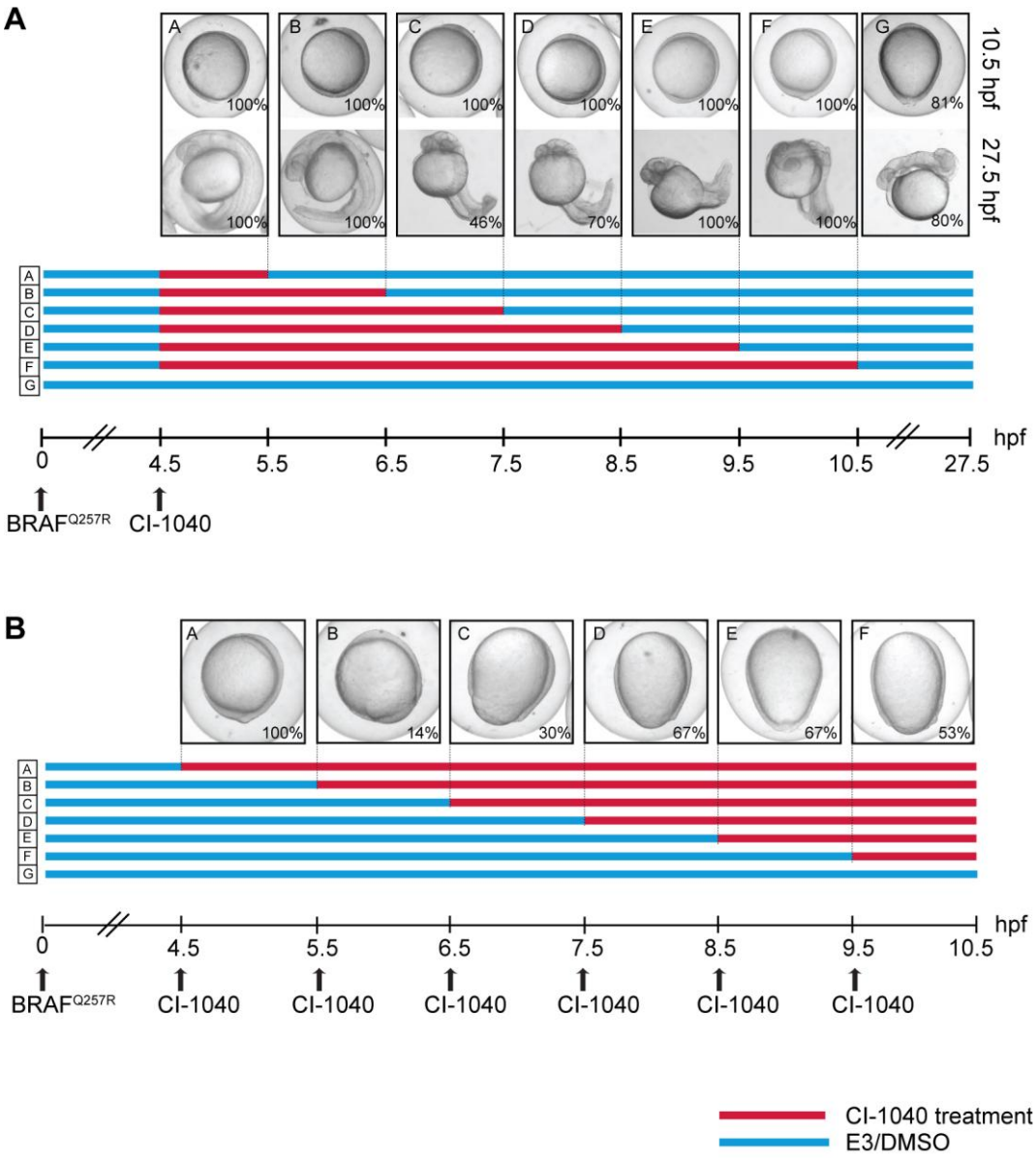

Figure 3.2.5 *Identification of a zebrafish-CFC treatment window*

A Treatments of embryos over-expressing the most common CFC variant BRAF^{Q257R} demonstrate that all CI-1040 treatments (A-F), but not the control DMSO treatment (G), prevented embryo elongation at 10.5 hpf. Only short treatments A and B restored normal development both at 10.5 and 27.5 hpf, with other drug treatments (C–F) causing additional developmental defects at 27.5hpf.
B Six additional CI-1040 treatments (A–F) and a control treatment (G) of BRAF^{Q257R} -expressing embryos showed that a specific developmental window between 4.5–5.5hpf is necessary for the prevention of zebrafish-CFC early phenotypes and sufficient to restore normal further development.
The numbers at the lower right corner of each image indicate the percentage of the elongated embryos in each set ($n \geq 30$/experiment). Blue bars represent embryo medium and red bars represent CI-1040 treatment.

3.2.5. Design of a systematic approach to identify the target tissues of PD325901 during zebrafish development

Recycling the use of cancer drugs to alleviate symptoms of congenital developmental disorders, such as the RASopathies, would be beneficial in the research and progress of the treatment of such diseases (Wilkie, 2007). Albeit very informative of early gastrulation mechanisms, isolation of the treatment window necessary to prevent toxic side-effects is not a notion that can be easily extrapolated to human care, as *in utero* CFC patient treatment is not possible during the developmental window.

To identify a dose that can be continuously administered with minimal toxicity, a deeper knowledge of the specific effects of MEK inhibitors in normal development is required. To that end, a detailed analysis was designed to determine the main tissue targets of PD032590 throughout normal zebrafish embryogenesis (**Figure 3.2.6**). Wild-type embryos were collected at six different developmental stages (4, 10, 24, 30, 48, 72hpf) and were incubated in increasing concentrations of PD0325901 (0.1μM-1.0μM). The embryos were monitored closely and were imaged daily.

Activated MAPK signalling in developmental syndromes affects the proper formation of tissues delineated from neural crest cells, including melanocytes, cardiac, craniofacial and gastrointestinal tissues. The targets of PD0325901 in developing zebrafish (Grzmil *et al*., 2007) and many MAPK pathway inhibitors used in clinical trials largely overlap with neural crest cell-derived populations. Based on this knowledge the recordings were focused on the appearance of the body axis, craniofacial structures and heart function.

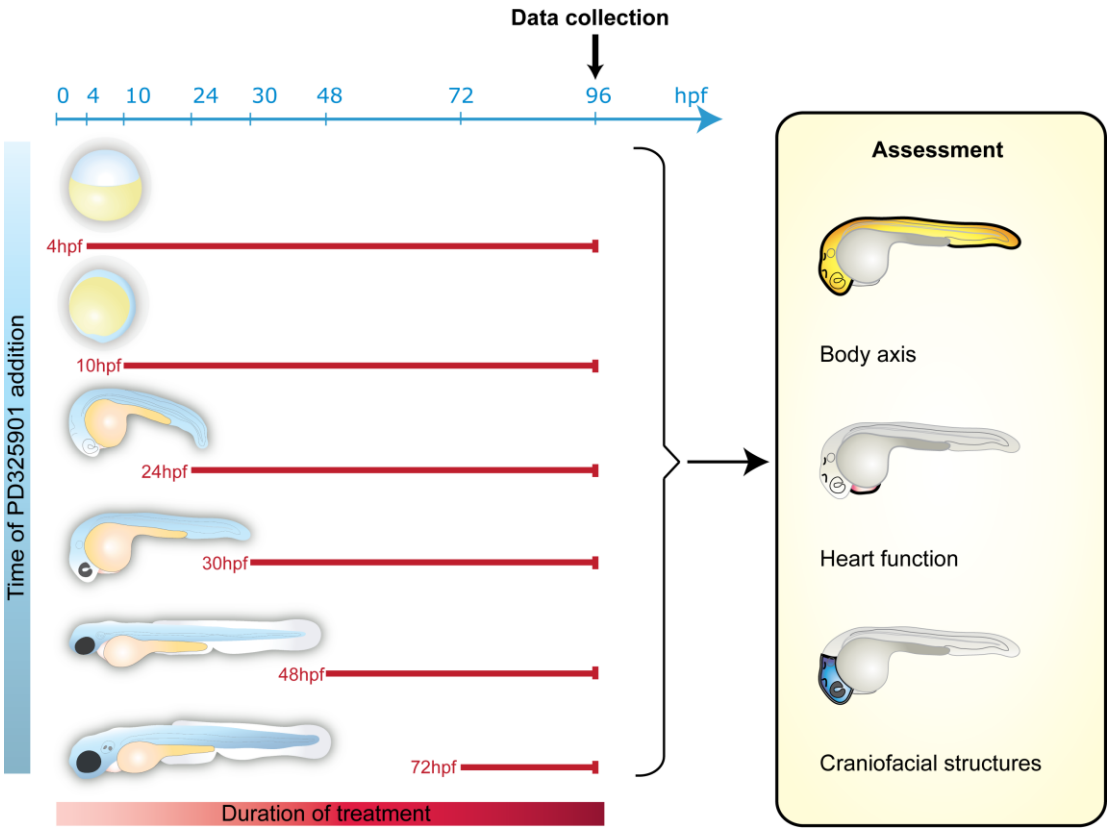

Figure 3.2.6 *Design of systematic study of the PD0325901 effects in zebrafish development*

Wild-type embryos were treated with the specific MEK inhibitor PD0325901 to identify the most affected tissues at different developmental stages. Zebrafish embryos were treated with increasing concentrations of PD0325901 (0.1-1.0µM) at six different developmental stages (4hpf, 10hpf, 24hpf, 30hpf, 48hpf, 72hpf) until 96hpf. The embryos were monitored daily and were assessed for body axis, cardiac morphology and craniofacial structure phenotypes at 4dpf (96hpf).

3.2.5.1. Universal cardiac disruption

Administration of increasing PD0325901 dosage at 4, 10, 24, 30 and 48hpf lead to heart anomalies in most embryos by 4dpf (**Figure 3.2.7**). The phenotype included cardiac oedemas and bulbus arteriosus blockage restricting the blood in the heart chambers and not letting it enter the bloodstream. The severity of the phenotype was not concentration-dependent as even 0.1µM PD0325901 caused the above symptoms. The cardiovascular system of embryos incubated in the drug at 72hpf appeared unaffected at 4dpf, but the embryos displayed the described aberrant cardiac phenotype at 5dpf, after a 48-hour incubation (data not shown).

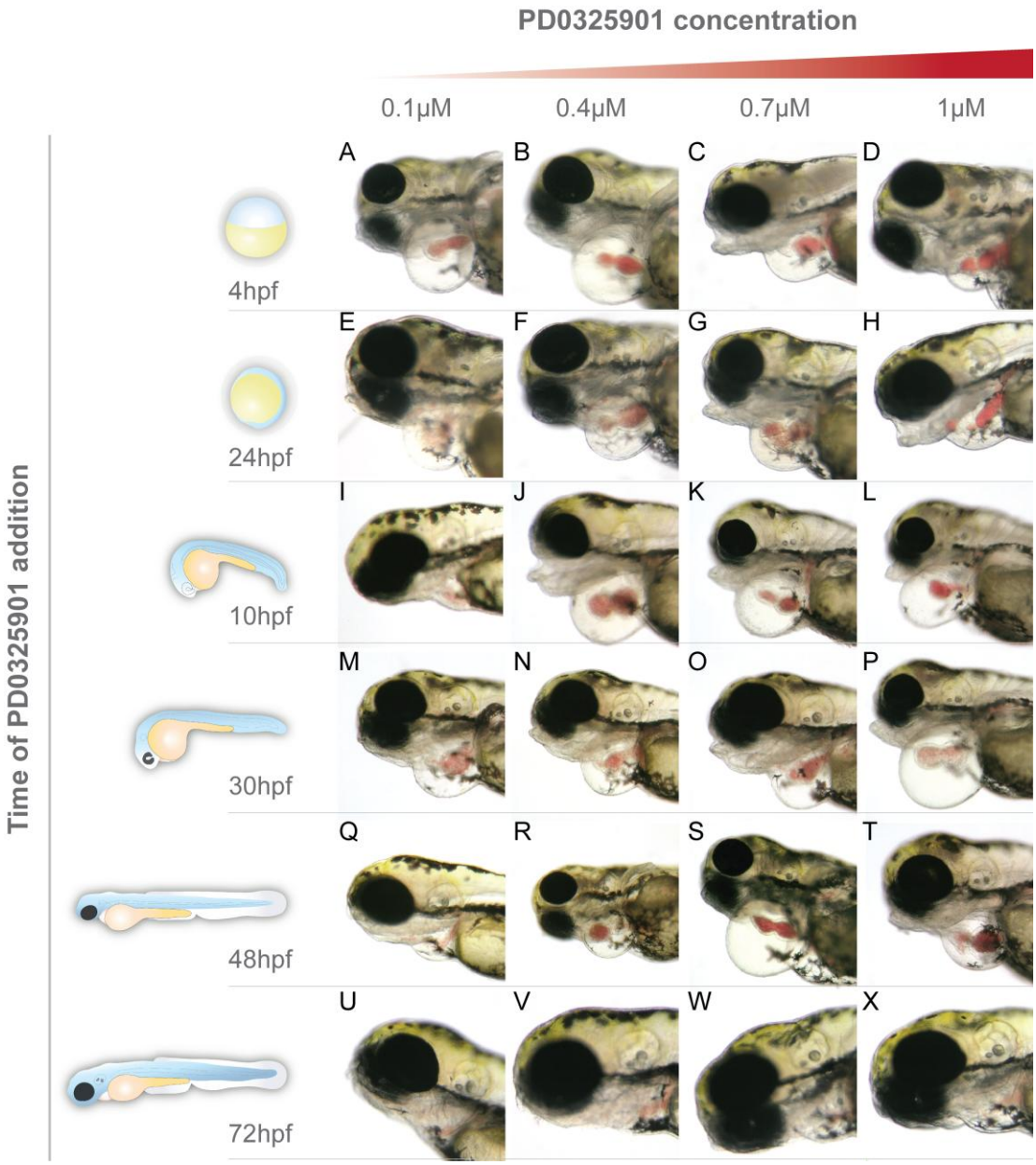

Figure 3.2.7 *PD0325901 affects cardiac function*

Lateral views of 4dpf embryos treated with increasing concentrations of PD325901. Addition of the inhibitor, even at low concentrations (0.1µM), blocked the cardiac valve and blood remained restricted in the heart chambers (A-T). Cardiac oedemas were frequently observed (A-H; J-P; R-T). Blood circulation of embryos treated at 3dpf was not affected at 4dpf (U-X).

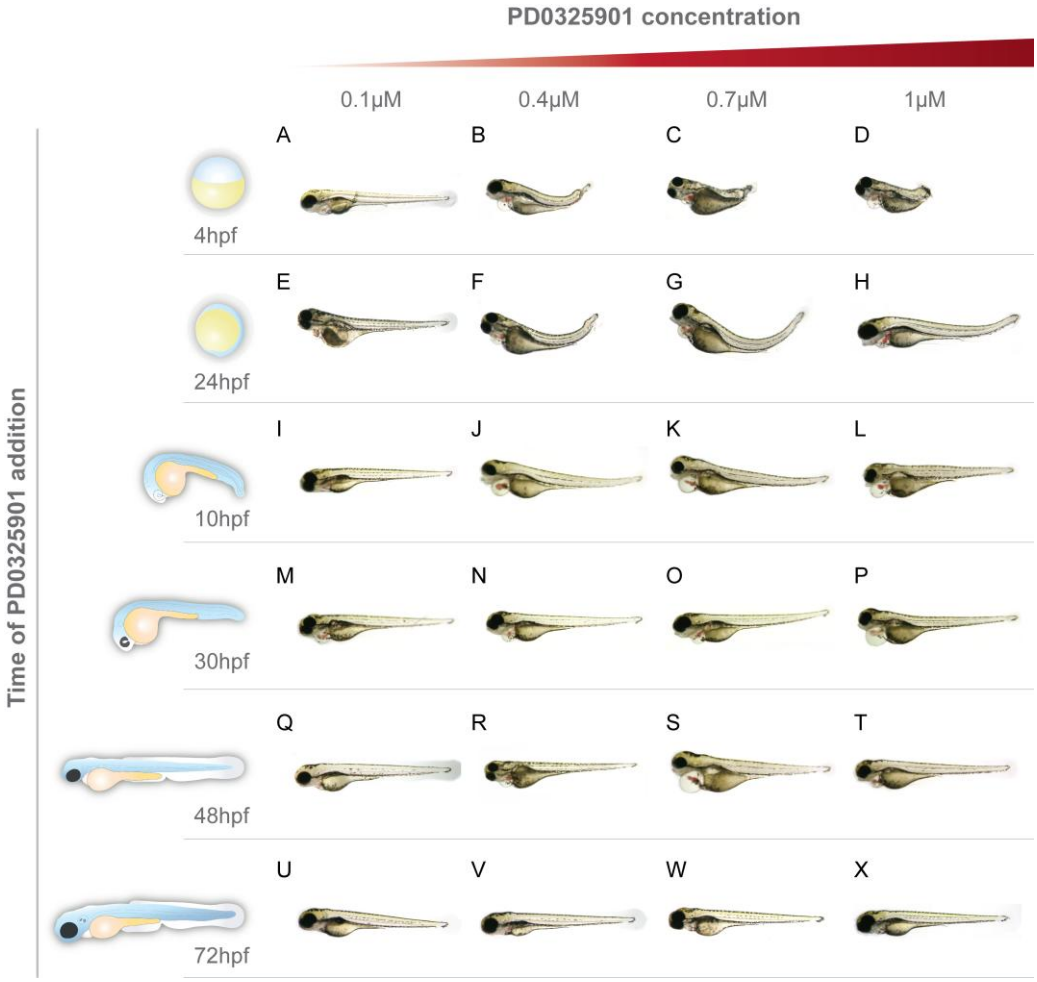

Figure 3.2.8 *Incubation in PD0325901 promotes body axis defects*

Treatment with PD0325901 from 4hpf promoted shortening of the antero-posterior axis of zebrafish embryos in a dose-dependent manner. Administration of the drug after the completion of gastrulation did not affect the size of the embryo.

3.2.5.2. Body axis is disrupted when MEK is inhibited during gastrulation

The body axis of 4dpf embryos treated with PD0325901 from 4hpf was shorter than that of their wild-type control siblings (**Figure 3.2.8**). Their A-P axis was shortened, with higher concentrations being more detrimental to body length. Individuals incubated in 0.1µM developed to normal size, whereas those incubated in 1.0µM PD0325901 were half as long. Administration of the inhibitor at later points in development had no effect on body axis formation. Thus, active MEK signalling ensures proper body axis patterning during gastrulation.

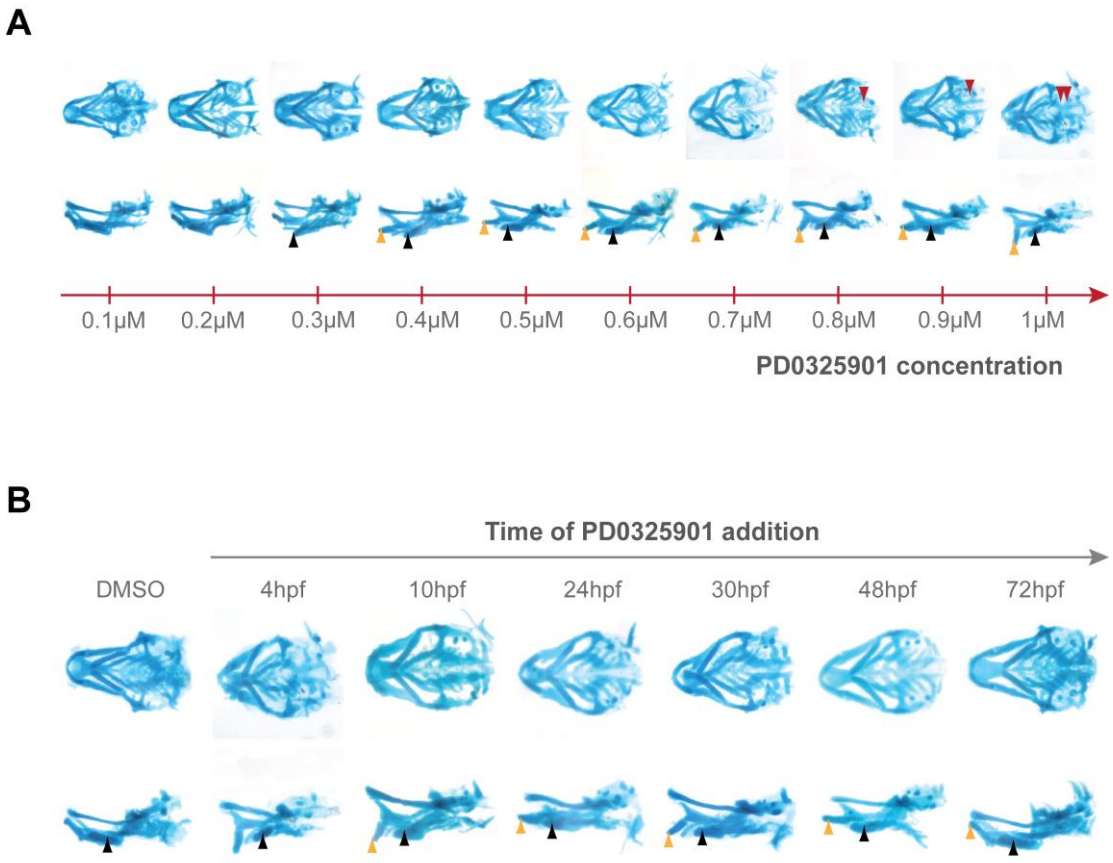

Figure 3.2.9 *PD0325901 treatments cause craniofacial structure deformities*

A Administration of increasing concentrations of the PD0325901 (0.1-1.0μM) from the beginning of gastrulation (4hpf) caused progressive malformation of Meckel's cartilage (orange arrowheads) and ceratohyal cartilage (black arrowheads), as well as loss of pharyngeal arches (red arrowheads).
B Comparison of craniofacial cartilage of 4 day old control embryos (DMSO) and embryos treated with 1μM PD0325901 added at different timepoints in development (4-72hpf). Meckel's cartilage is highlighted by orange arrowheads and ceratohyal cartilage by black arrowheads.
Top panels show ventral and lower panels show lateral views of the same specimen.

3.2.5.3. Craniofacial disruption

The jaw of zebrafish and all vertebrates derives from neural crest cells and activated MAPK signalling is required for proper specification of craniofacial components (Komisarczuk *et al*., 2008; Crump *et al*., 2004; Wilson and Tucker, 2004; Walshe and Mason, 2003). Incubation of embryos at different developmental stages in PD0325901 promoted a variety of jaw phenotypes, which were time-and dose-dependent (**Figures 3.2.9-3.2.11; Appendix I-2**).

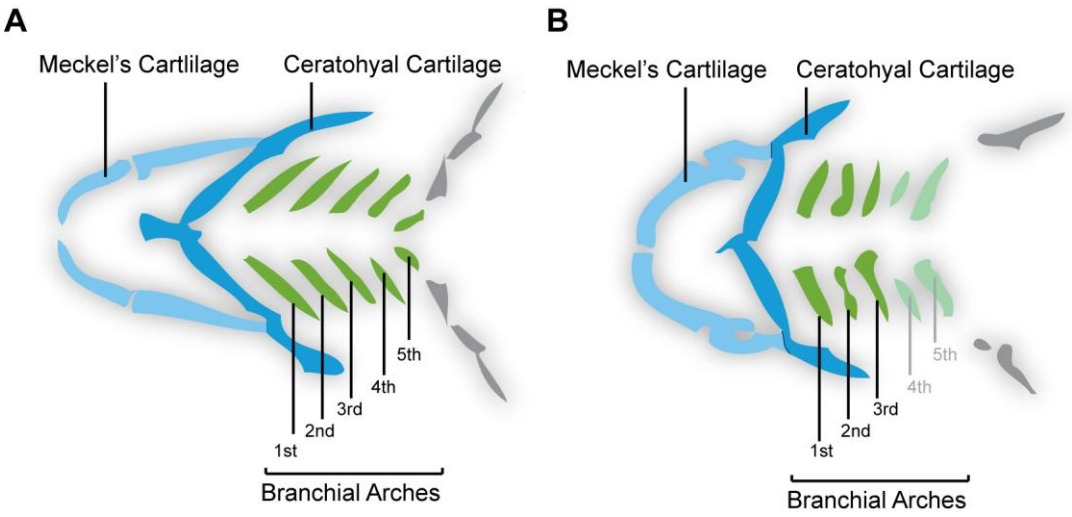

Figure 3.2.10 *Schematic illustration of zebrafish cartilage structures*

A Simplified illustration of the ventral view of a 4dpf wild-type zebrafish jaw structures. All seven pharyngeal arches are formed and are clearly distinguishable.
B Ventral representation of 4dpf zebrafish pharyngeal arches of an embryo treated with a high concentration of a MEK inhibitor. All structures are malformed, the angles of Meckel's and ceratohyal cartilage are distorted and, at concentrations higher than 0.8µM of the drugs, the 4th and 5th branchial arches are missing.
The seven pharyngeal arches represented are: Mandibular arch/ Meckel's cartilage (light blue), hyoid arch/ ceratohyal cartilage (dark blue), 1st-5th branchial arches (green), fins (grey).

Addition of the drug at 4hpf caused progressive loss of pharyngeal arch development as well as malformation of the Meckel's (MC) and ceratohyal cartilages (CH) (**Figure 3.2.9**). A schematic comparison between the jaw cartilage structures of 4dpf control and PD0325901-treated embryos clearly illustrates the angle distortion of MC and CH and the abnormally developed or absent pharyngeal arches (**Figure 3.2.10**). Embryos incubated in the drug at 10hpf were phenotypically similar to the ones treated from 4hpf, with the exception that they successfully formed all seven pharyngeal arches.

Administration of the drug at 1dpf (24, 30hpf) affected the size and angle of MC and addition of PD0325901 at 2dpf (48hpf) caused CH development anomalies. Mek inhibition in older embryos did not promote an overt craniofacial defect.

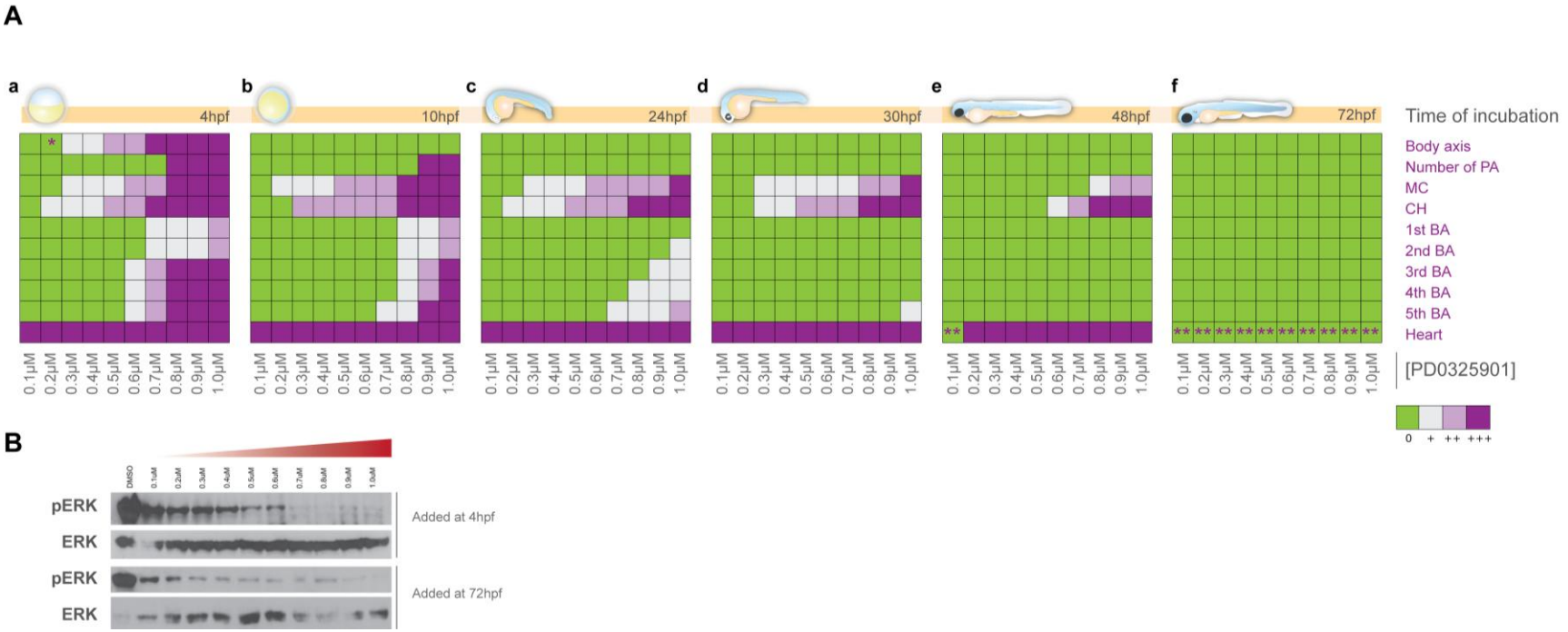

Figure 3.2.11 *Effect of addition of increasing concentrations of PD325901 at different timepoints in development*

A Heat-map of tissue sensitivity to PD325901 treatment. Each panel shows tissue sensitivity after the addition of increasing concentrations of PD325901 (0.1-1.0μM) at a different timepoint. Sensitivity to PD0325901 treatment was translated into colour (Green: No effect; Light grey: Mild effect; Pink: Intermediate effect; Purple: Severe effect). Embryos treated with 0.2μM PD0325901 from 4hpf had a normal A-P axis but showed mild malformation of the tail tip (asterisk, *). The heart valve of embryos treated with 0.1μM PD0325901 from 48hpf and with all ten concentrations of PD0325901 from 72 hpf was blocked at 5dpf (double asterisk, **).
Abbreviations: pa: Pharyngeal arches; MC: Meckel's cartilage; Ch: Ceratohyal cartilage; ba: Branchial arches.
B Increasing levels of PD325901 caused reduction in phospho-Erk levels. Immunoblotting shows phospho-Erk levels in embryos treated with increasing concentrations of PD325901 at 4hpf and at 72hpf. Erk was used as a loading control.

3.2.6. Selection of a dosage that allows continuous exposure to PD0325901 with minimal side-effects

3.2.6.1. Heat map summarises effects of PD0325901

In order to visually review all the recorded phenotypes promoted by Mek inhibition a series of "heat map" panels were generated (**Figure 3.2.11A**). In summary, embryo body axis was only affected when Mek was inhibited in early gastrulation (panels a-b). All treated embryos presented heart defects suggesting that this might be a toxic side-effect of the drug and not a developmental phenotype (panels a-e). Gastrulation was crucial to the development of the 5th branchial arch and the proper formation of the 3rd and 4th branchial arches (panels a-b).

The 24-30hpf time period was mostly critical for the proper formation and arching of the MC (panels c-d), whereas only the development of the CH cartilage was interrupted by Mek inhibition during the second day postfertilisation (panel e). Addition of PD0325901 later than 3dpf had no developmental phenotype (panel f) as all structures had already formed.

3.2.6.2. Continuous PD0325901 administration (0.2μM) restores almost normal embryonic development

After examination of the heat maps it became obvious that administration of low doses of PD0325901 from early gastrulation only distorted normal development at a minimal level. It was, therefore, possible that constant incubation of zebrafish embryos in low concentrations of the drug would not prominently interfere with development. I also hypothesised that permanent inhibition of Mek may compensate in part for the aberrant signalling caused by CFC allelic variants expression.

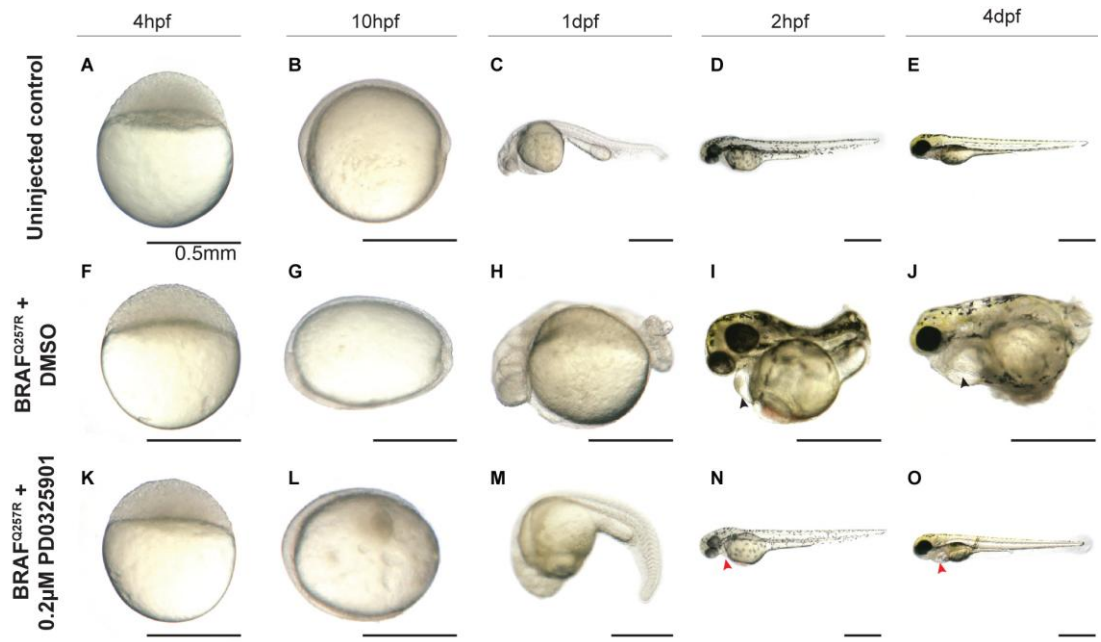

Figure 3.2.12 *Continuous administration of PD0325901 restores normality*

Embryos over-expressing the most common CFC allele $BRAF^{Q257R}$ incubated in DMSO (F-J) have a cell movement phenotype at 10hpf (G). From 1dpf (H) they had a shorter anteroposterior axis and by 2dpf (I) the cardiac disruption was evident (black arrows; I,J).
Embryos injected with the CFC allele and continuously incubated in 0.2µM PD0325901 (K-O) demonstrated mild elongation status at the end of gastrulation (L) but only a slight developmental delay at 1dpf (M). The body axis of the 2dpf embryos (N) was comparable to their wild type siblings and normal development was restored, with the exception of mild cardiac valve closure (red arrows; N,O).

To test the above hypotheses, wild-type embryos were injected with the most common CFC disease allele, $BRAF^{Q257R}$, and were continuously incubated in 0.2µM PD0325901 from 4hpf (**Figure 3.2.12**). At 10hpf, PD0325901-treated embryos were less elongated compared to control embryos (panels B,L**)**. At 24hpf the body axis of treated embryos (panel M) was almost identical to wild-type uninjected siblings (panel C) and significantly longer than $BRAF^{Q257R}$ expressing individuals (panel H). By 48hpf, incubation in PD0325901 caused a mild cardiac valve closure without other prominent side-effects.

Therefore, the drug counter-balanced the developmental effect of CFC allele mis-expression, corrected the total levels of the initially aberrant Mapk signalling and was able to restore near-normal development and survival.

3.3. DISCUSSION

Activation of the MAPK pathway leading to high levels of ERK phosphorylation is commonly described in human cancers and, recently, in the RASopathies syndromes. Mutated pathway components, such as RAF and RAS, constitute potential therapeutic targets for all patients. Better understanding of genotype-phenotype correlations with respect to cancer development and progression has advanced our ability to manufacture drugs that selectively target specific proteins (reviewed in Sebolt-Leopold and Herrera, 2004) and even specific mutations (Sala *et al*., 2008). Small molecule inhibitors have already been successfully used in clinical trials for the treatment of human neoplasias (Friday and Adjei, 2008). The presence or absence of gene mutations has become predictive of the tumour's responsiveness to given inhibitors. For instance, EGFR and KRAS mutational status in non-small cell lung carcinoma patients can predict their sensitivity to EGFR receptor inhibitors (Pao *et al*., 2005; Paez *et al*., 2004). Similarly, KRAS and BRAF mutations are strongly correlated with response to MEK inhibition in lung and ovarian cancer (Nakayama *et al*., 2008; Pratilas *et al*., 2008).

As MEK CFC mutations have been responsive to MEK and RAF inhibition in *in vitro* studies (Senawong *et al*., 2008), I wanted to examine the sensitivity of the CFC and melanoma variant spectrum to MEK and FGFR inhibitors *in vivo*. Pre-clinical testing of anti-cancer drug efficacy on zebrafish exhibiting CFC features would allow assessment of potential therapeutic agents. Here, I have been able to rescue the disease-driven gastrulation phenotype in embryos expressing CFC, melanoma and engineered alleles after administration of specific FGFR and MEK inhibitors. Importantly, I identified a treatment window sufficient to prevent any malformations and a treatment dose that restores normality upon continuous administration.

3.3.1. Small molecule inhibitors of the MAPK pathway prevent cell migration defects

3.3.1.1. FGFR inhibitor restoration of total Mapk signalling levels and possible implication of C-raf

A functional Fgf/Mapk pathway is essential for the completion of gastrulation while its over-activation promotes the described elongation phenotype. Treatment of embryos with activated Mapk signalling with the FGFR1 inhibitor SU5402 resulted in complete prevention of the elongation phenotype in almost all the cases. All mutations except $BRAF^{V600E}$ were sensitive to Fgfr inhibition. One theory to explain the rescue is that blocking Fgfr reduced the levels of total endogenous Fgf/Mapk signalling (**Figure 3.3.1**). This highlights the importance of total Mapk activity in the progression of CFC syndrome.

Another explanation for the phenotype prevention in kinase-inactivating BRAF mutants may be that in the absence of high concentrations of upstream receptor stimulation and Ras, endogenous C-raf is not activated and cannot further phosphorylate Mek and Erk (Dumaz *et al*., 2006; Wan *et al*., 2004). This would also explain why $BRAF^{V600E}$-expressing embryos were not responding to treatment. The most common BRAF mutation is promoting near constitutive activation of the kinase *in vitro* (Wan *et al*., 2004) which is RAS-independent and sufficient to drive malignant and pre-malignant transformation *in vivo* (Patton *et al*., 2005; Pollock *et al*., 2003; Davies *et al*., 2002). Moreover, the levels of *in vitro* BRAF activity conferred by the substitutions Q257R and V600E are similar (Rodriguez-Viciana *et al*., 2006). However, the fact that the effect of all CFC and engineered alleles but not that of $BRAF^{V600E}$ was rescued supports that the latter variant is more severe *in vivo*.

C-RAF exhibits an inhibitory effect against oncogenic BRAF in cell line studies by forming heterodimer C-RAF-$BRAF^{V600E}$ complexes (Karreth *et al*., 2009). The abundance of such heterodimers is decreased in human melanoma with activating

mutations and presumably in the current zebrafish bioassay, as all the disease alleles expressed are acting as gain-of-function mutations. Therefore, further restraint of C-RAF activity has the capacity to induce BRAF signalling. This notion is further supported by the fact that C-raf suppression by the use of 17-DMAG, an HSP90 inhibitor was unable to prevent the gastrulation phenotype (data not shown).

3.3.1.2. Mek inhibition prevents gastrulation phenotype

I further tested the activity of the highly selective and clinically efficient MEK inhibitors CI-1040 and PD0325901 *in vivo*. The effective blocking of Erk1/2 phosphorylation in this zebrafish model was demonstrated both optically and molecularly and was supported by the decrease in Dusp6-GFP intensity (**Figure 3.2.2**) and p-Erk levels of treated embryos (**Figure 3.2.3**). Activation of RTK-independent signalling by activated BRAF or MEK increases the levels of effectors downstream of ERK, such as its negative regulator Dusp6 (Pratilas *et al*., 2009). Lower signal intensity in the treated *dusp6*-GFP embryos and reduced ERK phosphorylation confirms lower Mapk signalling output. Importantly, both compounds were able to prevent the developmental phenotype of the CFC and melanoma alleles. I demonstrated that the gastrulation defects were avoided in 100% of injected embryos by very low concentrations of either agent (**Figure 3.2.4**) and that treatment during a short developmental window (4-6hpf) was sufficient to prevent additional drug toxicity (**Figure 3.2.5**).

3.3.2. Possibilities of PD0325901 use in developmental syndrome therapy

The budget for drug design and the resources to carry out clinical trials are real obstacles in the way of generating novel compounds to target rare congenital disorders such as CFC (Wilkie, 2007). Making use of already available anti-cancer agents that block the activity of genes mutated in developmental syndromes renders symptom treatment a possibility.

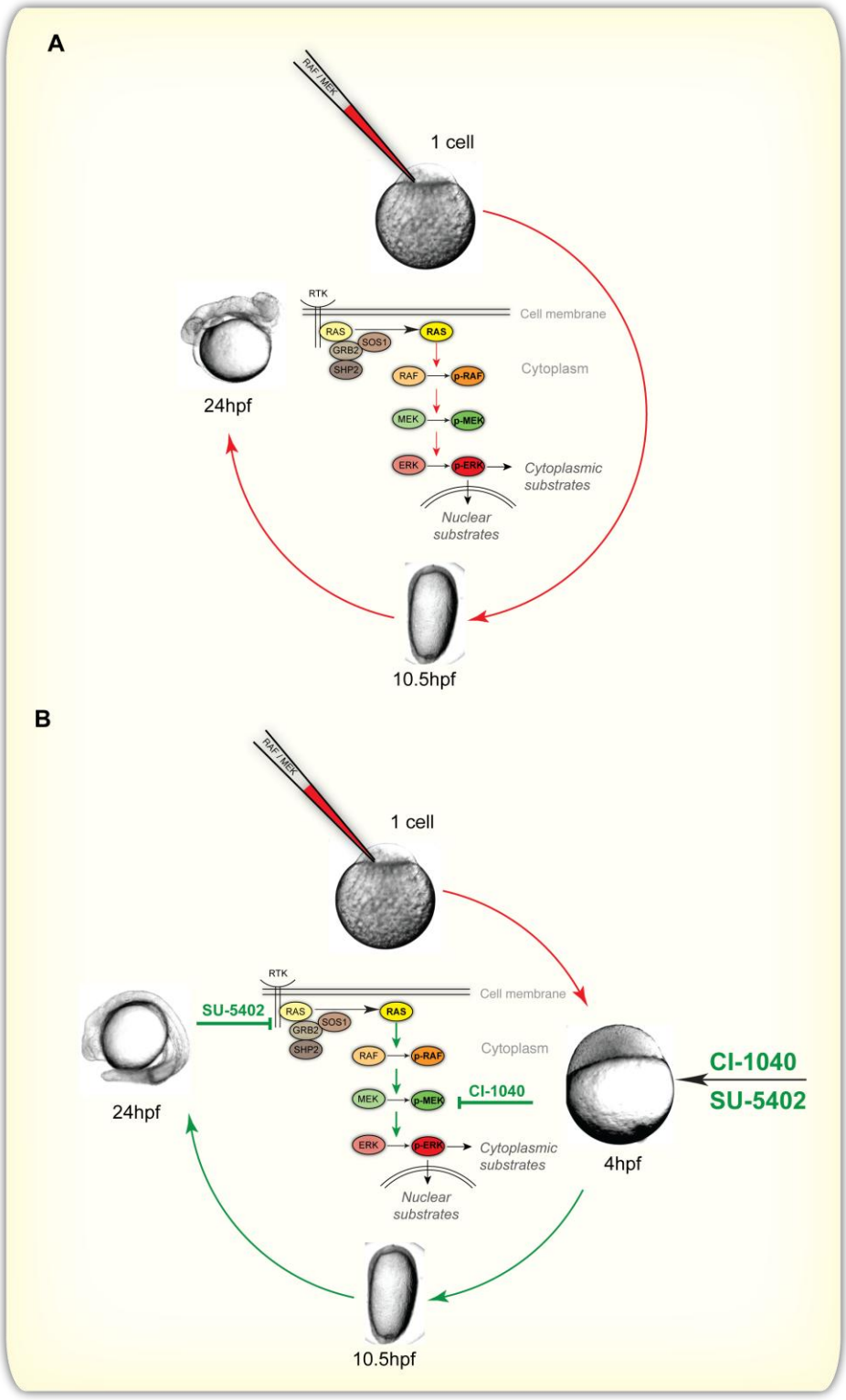

Figure 3.3.1 *Suggested mode of action of CFC-disease variants in combination with small molecule potential treatment*

(**Figure 3.3.1**)
Schematic representation of the zebrafish-based approach designed to examine the in vivo significance of BRAF and MEK CFC disease mutations.
A Microinjection of BRAF or MEK CFC variant mRNA into the single-cell zebrafish embryo promoted an elongated zebrafish embryo at 10.5hpf that led to severe further development defects, including body axis malformation, and heart defects at 24hpf.
B Treating CFC variant-over-expressing embryos with inhibitors of the FGF-MAPK signalling pathway (green) prevented aberrant development of the CFC-zebrafish embryos, possibly by restoring appropriate total levels of Mapk-signalling.

In this zebrafish model the allelic spectrum affected very early processes in embryogenesis and the treatment window is limiting. Thus, similar temporally strict *in utero* drug administration is not possible in human patients. However, treatment after birth can alleviate the severity of the CFC features and possibly decelerate the advancement of the CFC evolving symptoms (reviewed in Tidyman and Rauen, 2010). To mimic clinical treatment, I aimed to identify an optimal dose that can be continuously administered to CFC-zebrafish with minimal side effects.

3.3.2.1. Methodical characterisation of PD0325901 revealed spatio-temporal targets

In order to delineate the targets of a specific MEK inhibitor in disease, I first examined the tissues most affected by the activity of Mapk signalling during normal development of wild-type individuals. Close monitoring of treated embryos revealed that proper body axis patterning is defined very early in development, at the beginning of gastrulation (**Figure 3.2.5, 3.2.8**). Blocked Mapk signalling does not affect body length past the first hours of embryogenesis (4-6hpf).

On the contrary, incubation in all tested concentrations of PD0325901 for any period of time longer than 24 hours lead to semilunar valve blockage (**Figure 3.2.7**). This valve is responsible for blood outflow from the heart chambers and is a structure that originates from cardiac NCCs. It is, thus, possible that cardiac neural crest cell derivatives require continuous Mapk signalling to maintain their muscular functions. Alternatively, PD0325901 may chemically interfere with the lining of the heart promoting valve closure.

Cranial NCC-derived pharyngeal arches were prominently affected by Mek inhibition. Treatment with the drug at 0dpf is imperative for the formation of the branchial arches 3-5. 1dpf embryos require active Mek for proper Meckel's cartilage development and 2dpf for ceratohyal cartilage formation. This suggests that PD0325901 acts in a posterior-to-anterior direction. The most anteriorly-positioned cranial NCCs give rise to Meckel's and ceratohyal cartilage (rhombomeres 2-5) and posterior cranial NCCs contribute to the branchial arches (Schilling and Kimmel, 1994).

Evidently active Mapk signalling is required in NCC-derived tissues but PD0325901 only targets a sub-set of them. Whereas cardiac and craniofacial structures were disrupted, the pigmentation patterns and of embryos incubated in PD0325901 were unaffected. This is the opposite effect to the one observed in the *colourless* (*cls*) mutants (Dutton *et al*., 2001). In *cls*, sox-10 mutations lead to abnormal development of pigment cells, sympathetic and parasympathetic neurons but the pharyngeal arch formation is complete (Kelsh and Eisen, 2000). Therefore, I can conclude that tissues of the cranial and cardiac NCCs but not of trunk NCCs are sensitive to Mek inhibition. This hypothesis can be further validated in future studies by examining the enteric neuron formation in treated individuals.

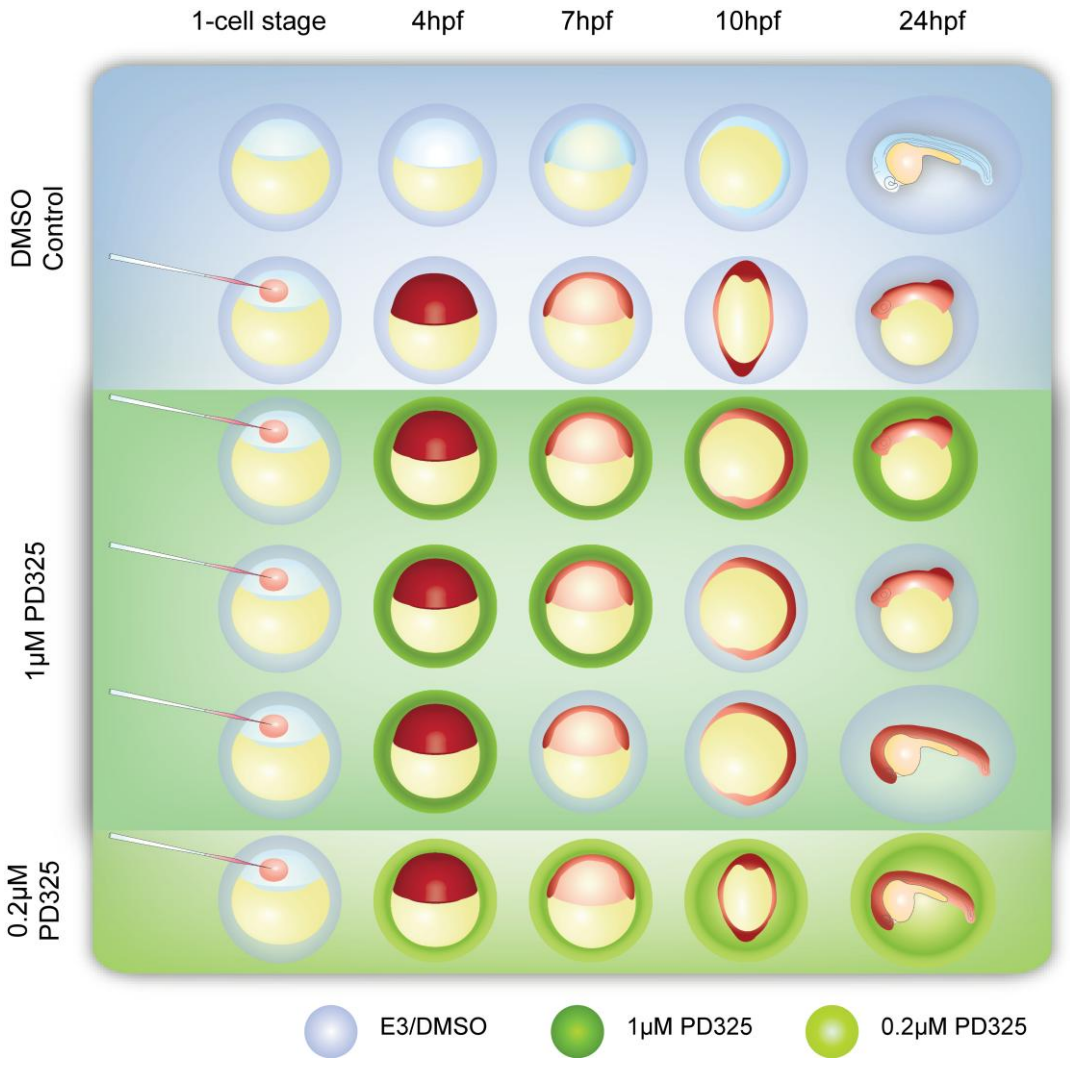

Figure 3.3.2 *Schematic overview of elongation phenotype prevention after Mek signalling inhibition.*

Injection of the most common CFC allele promoted embryo elongation at 10hpf and short body axis at 24hpf (top blue panel). Treatment of injected embryos with 1µM PD0325901 (middle green panel) from 4hpf prevented the elongation, while a treatment-window (4-6hpf) was also sufficient to prevent further developmental defects. A continuous dose of PD0325901 (0.2µM) (lower light green panel) was able to partially prevent the phenotypes at 10 and 24hpf and allowed normal development progression.

3.3.2.2. Concluding remarks

Mek inhibition efficiently restored both the cell migration phenotype in gastrulating embryos and the developmental anomalies propelled by CFC disease alleles further along in development. Most importantly, continuous treatment with 0.2µM PD0325901 from the beginning of gastrulation reversed the mutation-driven defects and was administered in a low enough dose to avoid drug toxicity (**Figure 3.2.12, 3.3.2**). As discussed in Chapter 2, CFC allele-driven Mapk over-activation causes embryo elongation at the end of gastrulation and multiple tissue malformation at later stages. It was until now hypothesised that this early cell movement defect was directly linked to the additional future phenotypes. The PD0325901- treated CFC allele-expressing embryos were slightly elongated at 10hpf. The fact that they had not completely overcome the gastrulation defect at 10hpf but appeared almost normal at 24 and 48hpf suggests that the effect of the CFC alleles is evident beyond gastrulation and that their aberrant effect can be counter-balanced by low levels of Mek inhibition.

The current work is becoming increasingly relevant to the treatment of developmental disorders of the FGF/MAPK spectrum and reinforces the notion of recycling the use of anti-cancer drugs to manage congenital defects.

Chapter 4 - MAPK in Behaviour

“Hide not your talents. They for use were made. What's a sundial in the shade?” - Benjamin Franklin

4.1. INTRODUCTION

4.1.1. Signalling network between cAMP and MAPK pathways

Multicellular organisms require the presence of both intercellular and intracellular signalling for proper development and function. This communication is achieved through the activity of various pathways. It is increasingly evident that different molecular cascades do not act in isolation but interact with each other at multiple levels within the pathway. This cross-talk controls the intensity, duration and localisation of the signalling outcome.

The MAPK and cAMP pathways are near ubiquitously expressed. Experimental data supports that they are both important in development and survival and regulate similar processes but often function to achieve different outcomes. MAPK predominantly controls cell proliferation, growth and survival (reviewed in Zhang and Liu, 2002), whereas cAMP mostly mediates tissue-specific processes such as metabolism and memory formation (Li *et al*., 2011; reviewed in Houslay, 2010). Although the latter pathway inhibits growth in most tissues (Hewer *et al*., 2011; Weinberg *et al*., 2009; reviewed in Stork and Schmitt, 2002), this is not true in the thyroid and pituitary, for example, where cell growth is stimulated by cAMP (Chiappini *et al*., 2011; reviewed in Pertuit *et al*., 2009). However, in every case it is the interconnection between the two cascades that is thought to shape and elicit a specific cellular response. Rather than functioning independently in a linear manner, the two signalling cascades are integrated in a network.

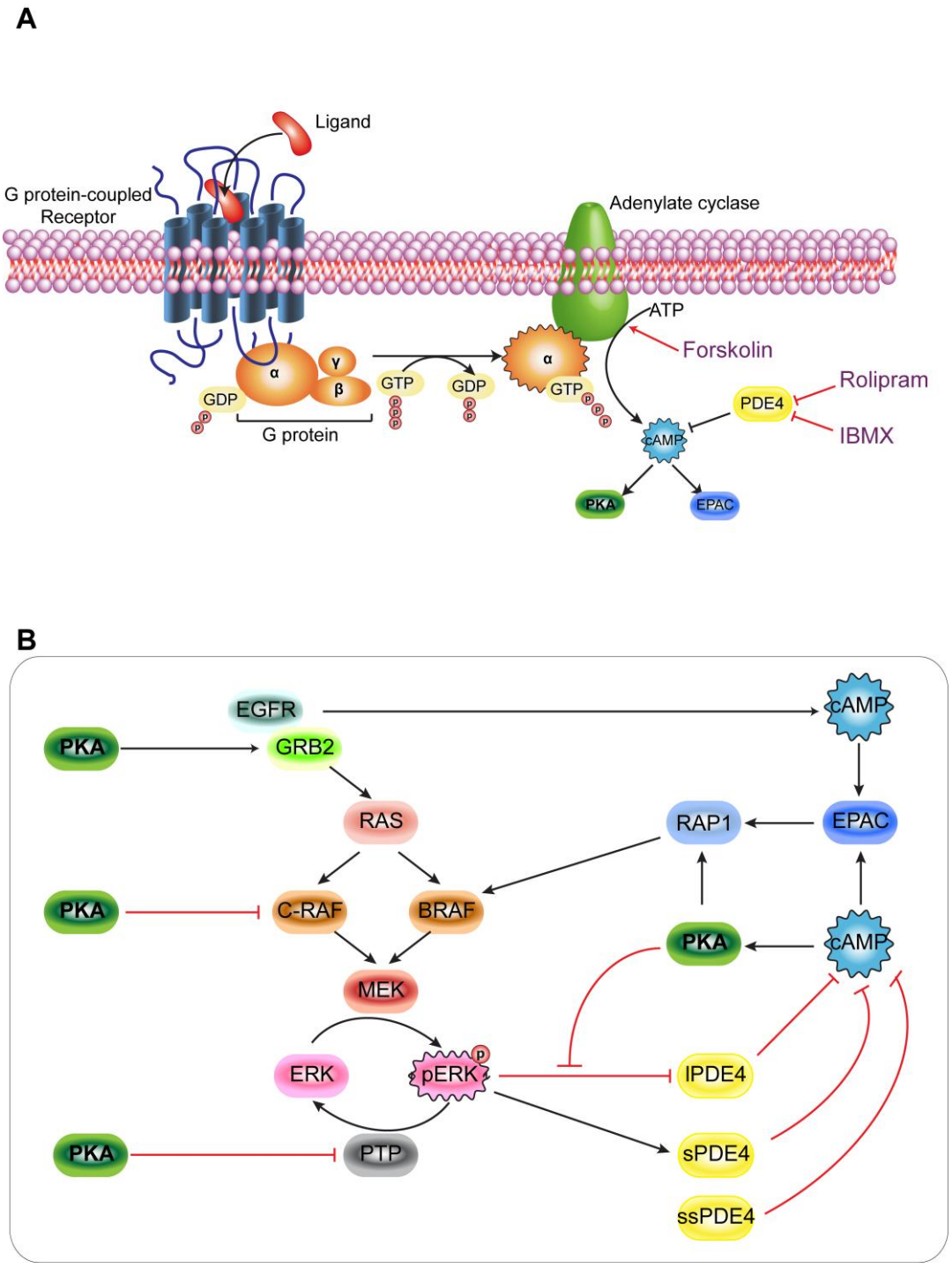

Figure 4.1.1 *The cAMP pathway and its interactions with MAPK signalling*

A Schematic diagram illustrating the mechanism of cAMP activation and its major downstream targets. Small molecule cAMP elevators are shown in purple (Forskolin, Rolipram, IBMX).

B Diagram showing common interactions between the cAMP and the MAPK pathways. lPDE4: long PDE4; sPDE4: short PDE4; ssPDE4: super short PDE4

The cross-talk between the RAS/MAPK and the cAMP/PKA pathways was first described almost twenty years ago when it was demonstrated that cAMP elevation differentially affected the activity of MAPK depending on the cell type studied (reviewed in Gertis *et al*., 2008). The complex communication between the two is yet to be fully delineated but recent studies have shed light in the understanding of the molecular connections between different cell types. The abundance of isoforms of different components of the pathways and the specificity of their intracellular localisation points towards the idea of compartmentalised signals within a cell or a tissue type (reviewed in Houslay *et al*., 2005). Such compartmentalisation and temporal control of a signalling outcome can be pivotal in cell fate determination and differentiation. Therefore, close examination of individual isoenzymes and components of the two pathways is important in the delineation of a tissue-specific signalling network. The following section will explore the various interconnection points between the MAPK and cAMP pathways (**Figure 4.1.1B**). Understanding the function of such a network would allow for better knowledge of cellular function in physiological conditions and improvement of therapeutic targeting in disease.

4.1.2. PDE4 – a mediator between two pathways

The phosphodiesterase (PDE) 4 family of enzymes consists of four genes, *PDE4A, 4B, 4C and 4D,* and represents one of eleven PDE families that act by degrading cyclic nucleotides (reviewed in Beavo and Brunton, 2002). *PDE4*s catalyse the hydrolysis of the ubiquitous second messenger molecule cyclic adenosine 3', 5'-monophosphate (cAMP), thus regulating its intracellular concentration and downstream signalling (Lynch *et al*., 2006). Downstream effectors of cAMP include protein kinase A (PKA), exchange proteins activated by cAMP (EPACs) and cAMP-gated ion channels (CNGCs) (reviewed in McCahill *et al*., 2008). There are more than 20 isoforms of *PDE4*s, each one with different and specific expression patterns, which assist in tissue and sub-cellular compartmentalisation of cAMP (reviewed in Houslay and Adams, 2003). The sheer number of different PDE isoforms, which

approximates 100, and the conservation of PDE orthologues across species underpin the importance of their function.

4.1.2.1. PDE4s protein structure

Each of the four different *PDE4* genes is encoded by an average of 20 exons and alternative splicing gives rise to a plethora of isoforms of different length (Bolger *et al*., 1997). The isoforms can be categorised into four groups based on their composition; long, short, super-short and dead-short. Each one has a unique N-terminal region, which determines the isoform sub-cellular localisation, and a highly conserved catalytic domain (reviewed in Houslay and Adams, 2003). Between these units long isoforms have two additional domains: the upstream conserved region (UCR) 1 and the UCR2. These modules have regulatory functions and further act as platforms for scaffolding proteins. Protein kinase A (PKA) phosphorylates UCR1 thereby activating PDE4 long isoforms (reviewed in McCahill *et al*., 2008). Short isoforms lack UCR1 and super-short isoforms only possess a truncated UCR2 unit. Dead-short isoforms are catalytically inactive in terms of PDE activity as they are C- and N-terminally truncated but are highly conserved (Johnston *et al*., 2004). Their function remains elusive.

The catalytic subunit of PDE4 proteins can adopt two binding states defined by its affinity to inhibitors, namely the High Affinity Rolipram Binding State (HARBS) and the Low Affinity Rolipram Binding State (LARBS). The reason for the existence of the different states is poorly understood but recent studies support that the conformational changes are driven by isoform dimerisation at the UCR1 and UCR2 regions (Richter and Conti, 2001). LARBS PDE4 is mostly expressed in peripheral tissues and the brain (Zhao *et al*., 2003a) and is involved in inflammatory responses of peripheral sites (Souness *et al*., 1997). The HARBS form is prominent in the brain and is specifically important in the hippocampus, the cortex and the olfactory bulbs (Kaulen *et al*., 1989). Administration of antidepressant drugs increases the HARBS but not the LARBS levels (Zhao *et al*., 2003b). As a result the focus has shifted towards HABS PDE4s in antidepressant tests.

4.1.2.2. PDE4s are regulated by PKA and ERK

The study of different PDE4 isoforms has revealed that alternatively spliced variants are dissimilarly regulated. UCR2 acts as an inherent constitutive inhibitor of PDE4s (Lim *et al*., 1999). Its effect can be reversed in long isoforms by PKA phosphorylation at UCR1 (MacKenzie *et al*., 2002), a domain completely absent in short and super-short isoforms. On the contrary, ERK can bind and phosphorylate the catalytic domain of all isoforms except that of PDE4A (Baillie *et al*., 2000). Interestingly, phosphorylation by ERK has varied effects on different isoforms, activating short isoforms but strongly and weakly inhibiting long and super short isoforms, respectively (MacKenzie *et al*., 2000). Nevertheless, this ERK-driven PDE4 inhibition is transient as the resulting localised cAMP elevation promotes a PKA increase and, hence, PDE4 activation. This system provides a negative feedback mechanism to control cAMP levels. Therefore, it is evident that PDE4s are acting as mediators between activated MAPK and cAMP signalling and the ratio of long to short PDE4 isoforms within a tissue plays a very important role in controlling signal dissemination (**Figure 4.1.1B**).

4.1.2.3. PDE4 inhibitors for the treatment of human disease

Due to their mediating function between two pathways, PDEs have been the target of drug development for decades with the most widely known compound being the PDE5 inhibitor Viagra (Soderlin *et al*., 1998; Boolel *et al*., 1996). However, PDE4s have the largest group of manufactured antagonists. A number of natural or chemically engineered inhibitors have been identified with anti-inflammatory, anti-depressant and memory-enhancing abilities (reviewed in Jeon *et al*., 2005).

Non-selective competitive PDE inhibitors include methylated xanthines such as IBMX, which compromise the function both of PDEs and adenosine receptors. Specific PDE4 inhibitors include Rolipram and its derivative catechol class, such as CDP840, Cilomilast and Piclamilast. The latter group have been used in the therapy of inflammatory and autoimmune (dermatitis, psoriasis, Crohn's disease, rheumatoid

arthritis, cancer), cognitive (depression, Alzheimer's disease) and pulmonary (chronic obstructive pulmonary disease (COPD), asthma) disorders (Zhang *et al*., 2006, reviewed in Houslay *et al*., 2005). More recently, they were introduced in anti-psychotic, learning and memory studies (Zhang *et al*., 2004; Zhang *et al*., 2000). The effect of PDE4 inhibitors can be phenocopied by cAMP agonists, such as Forskolin. This is a hydrophobic small molecule that increases cAMP levels by activating the enzyme adenylyl cyclase (reviewed in Insel and Ostrom, 2003).

Rolipram is a first generation competitive PDE4 inhibitor extensively used in *in vitro* and *in vivo* studies as a tool to chemically elevate cAMP. It was initially identified as an anti-depressant (Zeller *et al*., 1984) and was also used for treatment of Parkinson's disease (Parkes *et al*., 1984). The current wide use and success of Rolipram is partly due to its outstanding anti-inflammatory effects and the ability to penetrate the blood-brain barrier to target central nervous system (CNS) tissues (Nikulina *et al*., 2004). This is crucial in the management of brain cancer. PDE4A is a positive regulator of intracranial tumour growth and is over-expressed predominantly in a variety of brain tumours. Other PDE4 isoforms have been involved in a larger spectrum of neoplasias including glioblastoma (Yang *et al*., 2007), colon carcinoma (McEwan *et al*., 2007), as well as lung and breast cancer (reviewed in Marko *et al*., 2000).

4.1.2.4. Limitations of PDE4 inhibitors

Rolipram was withdrawn as a result of its short treatment windows, but second generation PDE4 inhibitors, such as Roflumilast and Cilomilast, are currently in Phase III clinical trials (reviewed in McCahill *et al*., 2008). The therapeutic advantage of elevating cAMP levels is, however, limited by the prominent side effects of the drugs, nausea and emesis, thought to be caused by the concurrent inhibition of all PDE4s.

The expression pattern of the different PDE4 genes is directly correlated with their role. Therefore, gene-specific inhibitors can maximise the focus and therapeutic success of the treatment. For example, PDE4B is mostly expressed in neutrophils and

monocytes. Thus, blocking its activity would have an anti-inflammatory effect in the treatment of asthma, psoriasis and chronic obstructive pulmonary disease. Conversely, PDE4D is a key component of central nervous system and cardiac signalling (reviewed in Houslay *et al*., 2005).

4.1.3. Receptor kinase and cAMP/PKA interaction

cAMP interacts with the epidermal growth factor receptor (EGFR) to achieve different end processes, depending on the cell lineage. Firstly, cAMP can target EGFR in a PKA-dependent manner. Over-expression of the regulatory unit of PKA alone in breast epithelial cells was able to constitutively activate the classical EGFR/RAS/MAPK pathway in the absence of a mitogen by directly binding and activating the receptor-bound protein Grb2 (Tortora *et al*., 1997). Secondly, increased muscle contraction in cardiomyocytes occurred when EGFR activated the cAMP/PKA pathway by stimulating adenylyl cyclase to generate cAMP (Sun *et al*., 1995).

4.1.4. Nf1 and cAMP/PKA interaction

As previously discussed in Chapter 2 (**Section 2.1.2.3**), neurofibromin 1 germ-line mutations promote neurofibromatosis type I and secondary somatic mutations drive the onset of nerve sheath tumours as a result of RAS/MAPK pathway over-activation. However, NF1 brain expression was recently linked to cAMP/PKA signalling (Brown *et al*., 2010). Interestingly, neurofibromin 1-depletion affects the growth and survival of central nervous system (CNS) (Hegedus *et al*., 2007) but not peripheral nervous system (PNS) neurons in a MAPK-independent manner (Brown *et al*., 2010). The cAMP elevator Forskolin and the PDE4 inhibitor Rolipram but not the MEK inhibitor PD0325901 were able to restore the morphology and survival rate of hippocampus and retinal ganglion $Nf1^{+/-}$ cells. Additionally, Rolipram increased the survival rates in mice with optic gliomas (Brown *et al*., 2010) and xenografted glioblastoma cells (Goldhoff *et al*., 2008). In combination with temozolomide and radiation, the current first line treatment for gliomas, Rolipram endorsed tumour regression (Goldhoff *et al*., 2008).

4.1.5. cAMP mediates RAF activation

4.1.5.1. cAMP inhibits C-RAF

C-RAF activation requires specific phosphorylation events, membrane recruitment by RAS and binding to various proteins such as the prolyl isomerase PIN1 and the phosphatase PP2A (reviewed in Baccarini, 2005). High cAMP levels induce C-RAF inhibition in fibroblasts, fat cells and smooth muscle cells (reviewed in Houslay and Kolch, 2000). This occurs via a PKA-C-RAF interaction. PKA constitutively phosphorylates C-RAF enforcing an inactive conformation of the kinase and interfering with its RAS binding domain (Dumaz and Marais, 2003). This, in turn, does not allow the kinase to be recruited by Ras in the cell membrane and impedes downstream C-RAF/MEK/ERK activation. Moreover, PKA-independent activation of cytosolic RAP1, a RAS-related G protein, via cAMP/EPAC results in C-RAF sequestering

4.1.5.2. cAMP activates BRAF

Interestingly, cAMP promotes MAPK activity in some cell types, including neuronal, ovarian, melanoma and pituitary cells, as well as adipocytes (reviewed in Gerits *et al*., 2008). In these tissues ERK and cAMP collaborate to elicit a functional response such as precise regulation of long-tem potentiation and circadian gene expression. Increased levels of cAMP stimulate PKA which triggers the plasma membrane-localised Rap1 allowing the latter to bind and activate BRAF (Wang *et al*., 2006).

The most well defined example of cross-talk between cAMP and MAPK pathways comes from the study of neuronal differentiation. This process requires long-term cAMP-mediated ERK activation (Yao *et al*., 1998). In this situation, extracellular stimulation of undifferentiated cells with the neuronal growth factor (NGF) triggers two separate events that affect MAPK signalling in a cAMP-regulated fashion.

Firstly, RAF/C-RAF are activated and promote ERK phosphorylation. However, C-RAF is rapidly inhibited by PKA (**Section 4.1.5.1**) impeding further downstream signalling. Secondly, NGF stimulates the RAS-related G protein RAP1, which in turn binds and enhances BRAF signalling, thus promoting a prolonged period of ERK activation (Vossler *et al*., 1997). Extracellular stimulation by a non-neuronal mitogen, such as EGF, fails to activate RAP1, thus activating the MAPK pathway only transiently and not allowing cellular differentiation to proceed.

4.1.6. MAPK and cAMP cross-talk at the ERK level

The key role of ERK in regulating the activation of PDE4s has been previously introduced (**Section 4.1.2**) and essentially presents a platform for ERK to control cAMP signalling (**Figure 4.1.1B**). Additionally, ERK1/2 activation and stimulation of its downstream targets are important in the development and function of the central nervous system (CNS). cAMP has an inhibitory role towards ERK1/2 in non-neuronal cells and activates ERK1/2 in neurons (Cavanaugh *et al*., 2001). Moreover, protein tyrosyl phosphatase (PTP) is a cytosolic negative regulator of ERK that acts by dephosphorylating active ERK and blocking its translocation to the nucleus. cAMP ultimately endorses the activated state of ERK1/2 by antagonising the function of PTP in a PKA-dependent manner (Saxena *et al*., 1999). Notably, it is this inter-connection between cAMP and ERK1/2 that determines neuronal specificity and the conservation of this connection is pivotal for neuronal survival and memory formation (Gerstner *et al*., 2009; Yao *et al*., 1998).

4.1.7. Conclusions

Different cell types exhibit different sensitivity to cAMP elevation after pharmacologic treatment and act differently in response to genetic inhibition or activation of cAMP. Drawing conclusions about cAMP interactions in a linear fashion is becoming increasingly complex. It is thus clear that cAMP compartmentalisation is regulating distinct downstream signalling networks in a tissue-specific manner.

4.1.8. Aims

An important aspect of the RASopathies lies in the presence of behavioural anomalies of patients. Having established the therapeutic efficacy of MAPK pathway inhibitors against CFC disease alleles, I aimed to assess their potential in modifying behaviour. To accomplish that, I tested the effect of the MEK inhibitor PD0325901 on the behaviour of 3dpf zebrafish embryos exhibiting a robust and reproducible Rolipram-induced, cAMP-mediated behavioural phenotype previously identified in our lab by Nicola Grant (MSc Thesis, 2010).

4.2. RESULTS

4.2.1. Characterisation of the edge effect

Small molecule inhibition of key molecular pathways can elicit behavioural outcomes. Previous work in our lab identified a highly reproducible behavioural phenotype demonstrated after effective endogenous pde4 inhibition (MSc thesis, Grant). Chemical blocking of pde4 with the small molecule inhibitor Rolipram promotes a specific phenotype in 3dpf zebrafish embryos referred to as the "edge effect". This behaviour takes its name after the rapid positioning of the Rolipram-treated embryos at the edge of their containers. Treated individuals space themselves around the Petri dish directly facing its edge **(Figure 4.2.1A, B, D**) actively swimming in the same spot to maintain their position. Upon agitation or physical stimulation embryos immediately swim against the current and seek an edge (Anastasaki *et al*., manuscript in preparation).

Embryos exhibiting this "edge effect" phenotype were scored to quantify this behaviour for subsequent experiments. Only embryos perpendicularly facing the edge of the plate with their heads fully positioned within the outer ring (**Figure 4.2.1C, D**) were scored as "edge effect"-positive. The inner edge of the outer ring (dashed lines) was defined as a circle concentric to the perimeter of the Petri dish with a smaller radius. The difference in radius length was equal to a third of a 3dpf zebrafish embryo body.

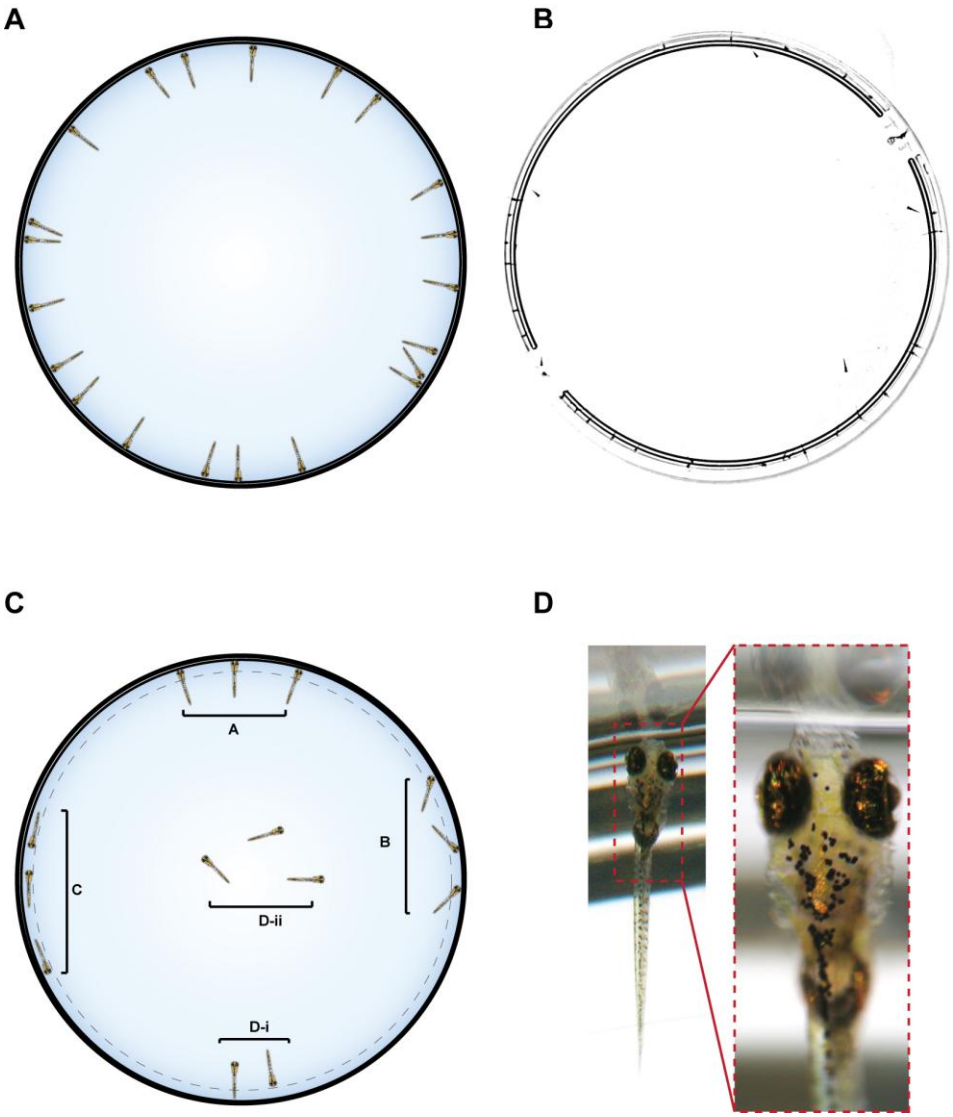

Figure 4.2.1 *Schematic diagram defining the "edge effect"*

A Illustration of the Rolipram-induced "edge effect". The treated embryos space themselves around the Petri dish to directly face the edge of the container. Once they reach this position they only move upon physical stimulation.
B Enhanced contrast brightfield image of live 3dpf embryos treated with 15μM Rolipram.
C Strict selection of embryos displaying the edge effect phenotype. Embryos swimming in the inner ring of the Petri dish (behaviour D-ii) or in the proximity of the edge (outer ring, separated by the dashed circle) but not directly facing the edge of the plate (behaviours B, C) were not counted as "edge effect"-positive in subsequent experiments. Embryos facing the edge of the plate but not adhering to it (behaviour D-i) were, also, discarded from the counts. The only "edge effect"-positive embryos are the ones displaying behaviour A.
D Brightfield image of embryo exhibiting the "edge effect" and magnification of its head region directly perpendicular to the plate wall (dotted red box).

4.2.2. Rolipram induces the "edge effect"

Administration of 15µM Rolipram but not DMSO vehicle control to wild-type embryos promoted the "edge effect" (**Figure 4.2.2**). Statistical analysis comparing the behaviours exhibited by the two treatment groups revealed a significant difference in embryo positioning after Pde4 inhibition ($p<0.0001$).

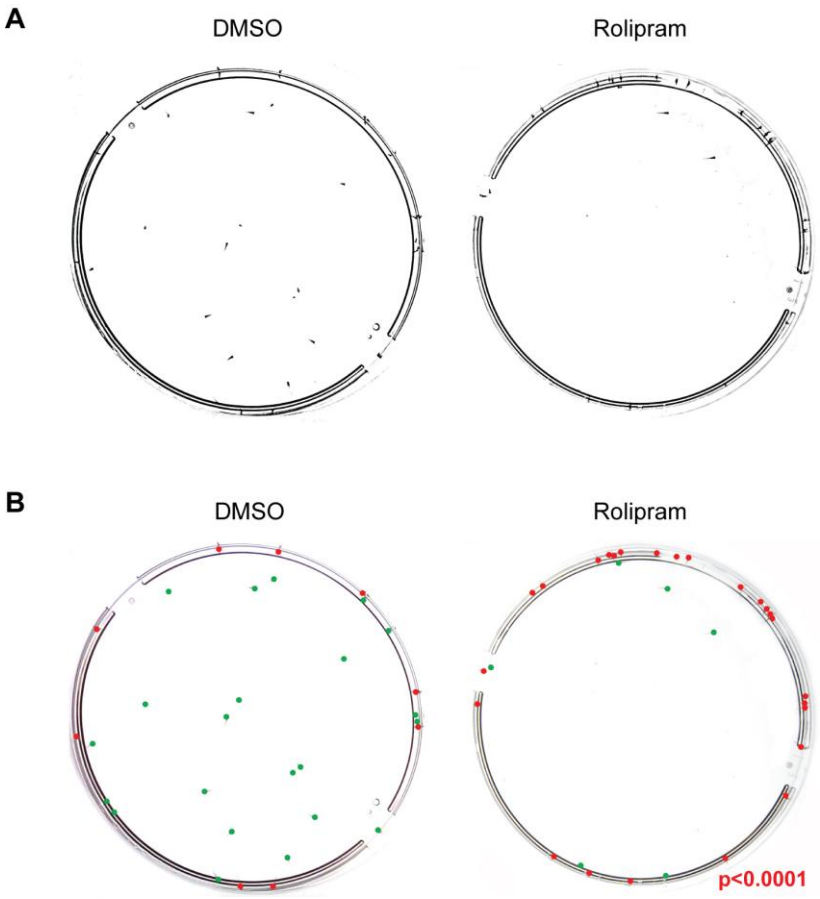

Figure 4.2.2 *Rolipram promotes the "edge effect"*

A Enhanced contrast brightfield images showing the distribution of 3dpf embryos in their plates. Incubation of 31 wild-type embryos in 15µM Rolipram induced embryos to exhibit the "edge effect". Their 31 DMSO-treated siblings were randomly distributed across the plate surface.

B Highlighted position of embryos in the same brightfield images as in A. For clarity purposes the position of the embryos in subsequent figures will be highlighted by a coloured dot. Randomly positioned embryos will be illustrated by a green dot and "edge effect"-positive embryos will be illustrated by a red dot. The p value below the Rolipram-treated embryos was calculated using Fisher's exact test with the DMSO embryos as controls and was significant to the $p<0.05$ level.

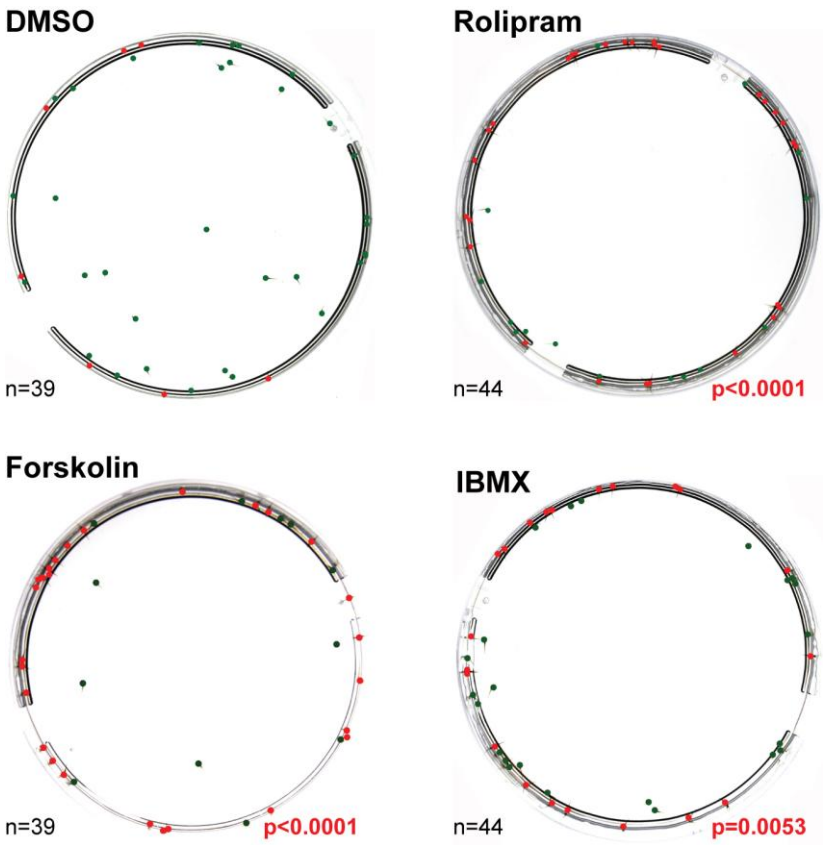

Figure 4.2.3 *The "edge effect" is phenocopied by cAMP elevators*

The "edge effect" first identified after Rolipram addition was fully and partially phenocopied by the cAMP elevators Forskolin and IBMX, respectively. In each case the drugs promoted a statistically significant change of behaviour compared to the DMSO control embryos at the $p<0.05$ level. The p values were calculated using Fisher's exact test with DMSO-treated embryos as the control.

4.2.3. Forskolin and IBMX phenocopy Rolipram

Rolipram-driven PDE4 inhibition promotes an increase in cAMP levels. To confirm that Rolipram-induced cAMP elevation was responsible for the "edge effect" the role of IBMX, an inhibitor of all PDEs, and Forskolin, an adenylyl cyclase activator (**Figure 4.1.1**), on zebrafish behaviour were investigated. I was able to reproduce previous findings (MSc thesis, Grant). Incubation of 3dpf embryos in 7.5µM Forskolin fully phenocopied Rolipram and a fraction of embryos treated with 15µM IBMX exhibited the "edge effect" (**Figure 4.2.3**). Treatment with all three cAMP elevators promoted a significantly different behaviour than the one observed in

DMSO control-treated embryos. This data confirms previous work and suggests that cAMP elevation is sufficient to influence zebrafish behaviour and enhance the "edge effect".

4.2.4. A role for MAPK in behaviour

There is a strong link between cAMP activation, human learning and behavioural disease, such as depression (Li *et al*., 2011; Rutten *et al*., 2011). Recently, however, mutations along the Mapk pathway have been correlated with alterations in learning and behaviour in Drosophila melanogaster (Pagani *et al*., 2009). The cAMP and the MAPK pathways act in parallel and there has been evidence supporting cross-talk between the signalling cascades (reviewed in Gerits *et al*., 2008). Taken together this data suggests that Mapk activation may play a role in the endorsement of the "edge effect" phenotype.

4.2.4.1. Rolipram treatment promotes Erk activation

To test whether Mapk activity levels play a role in the establishment of the "edge effect" whole embryos exhibiting the "edge effect" were lysed and their pErk levels were assessed by western blotting. Immunoblotting revealed that increasing concentrations of Rolipram correlated with Erk activation in a dose-dependent manner (**Figure 4.2.5**), consistent with a mechanistic link between pErk elevation and the "edge effect".

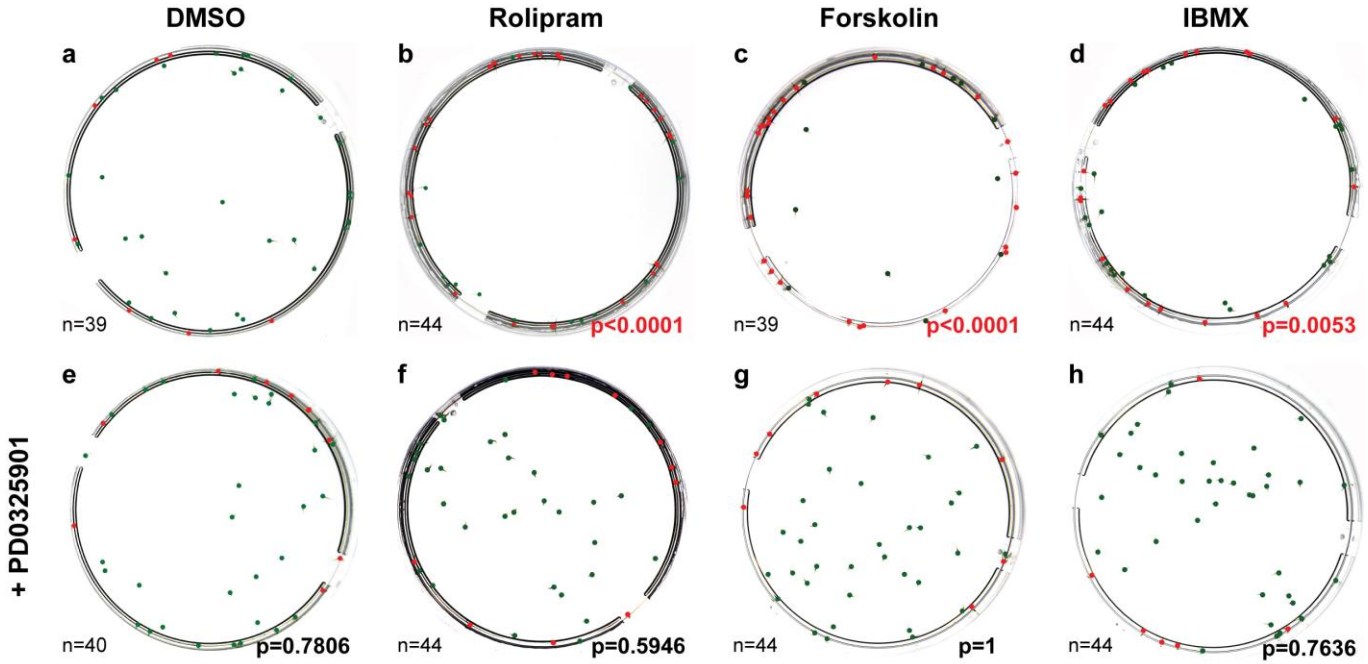

Figure 4.2.4 *PD0325901 rescues the "edge effect"*

Co-treatment of cAMP elevators Rolipram (f), Forskolin (g) and IBMX (h) with the MEK inhibitor PD0325901 rescued the "edge effect" phenotype observed with the single treatments (b, c, d, respectively). Panels a-d are identical to Figure 4.2.3 .The p values at the bottom right corner of every image were calculated using Fisher's exact test with the DMSO-treated samples as the control. P values in red are significant at $p<0.05$ and values in black are not.

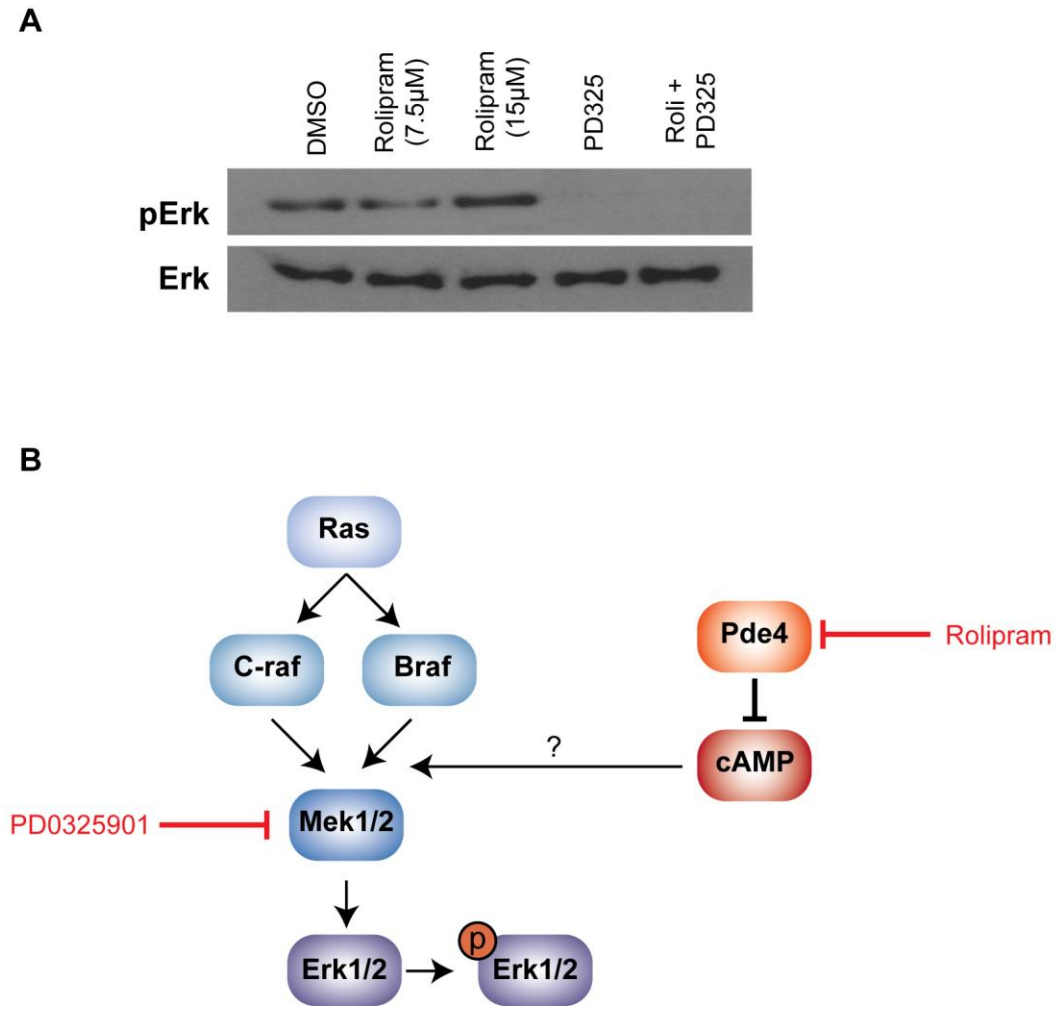

Figure 4.2.5 *The "edge effect" affects Erk activity*

A Immunoblotting of 10hpf wild-type zebrafish embryos treated for six hours with different combinations of drugs. Increasing doses of Rolipram promote increasing activation of Erk. Conversely, administration of the MEK inhibitor PD0325901 alone or in combination with a high dose of Rolipram (15µM) reduces the levels of pErk.
B Simplified schematic illustration of mode of action of small molecule inhibitors of the MAPK and cAMP pathways. Addition of Rolipram increases intracellular cAMP, which in turn activates the Ras/Mapk pathway upstream of Mek. Addition of the specific MEK inhibitor PD0325901 blocks the cAMP-driven pErk elevation.

4.2.4.2. MEK inhibition rescues the Rolipram-induced edge effect

Previous screening of the Enzo Life Sciences Kinase Inhibitor Library revealed a suppressive role of a MEK inhibitor against the Rolipram-induced "edge effect" (MSc Thesis, Grant). Having established that pErk is a component associated with the behavioural phenotype and knowing that the "edge effect" was reversible after

Mapk disruption, I wanted to assess whether the specific MEK inhibitor PD0325901 was behaviourally active. To this end, 3dpf embryos were initially treated with Rolipram, Forskolin and IBMX until the "edge effect" was established. The MEK inhibitor PD0325901 was subsequently added to a final dilution of 1µM (**Chapter 3**), the plate was agitated and the position of the embryos was scored 15 minutes post-treatment. Mek inhibition rescued the "edge effect" phenotype in all treatment groups (**Figure 4.2.4**) and decreased the pErk levels (**Figure 4.2.5**). Thus, blocking the Mapk pathway at the Mek level was sufficient to restore normal behaviour.

4.2.5. Study of genetic elevation of cAMP

4.2.5.1. PDE4D is highly conserved between humans and zebrafish

In order to genetically validate the effect of Rolipram, I studied the behaviour of pde4d$^{+/-}$ and pde4d$^{-/-}$ mutant fish. There are multiple PDE4D splice variants both in humans and zebrafish. The N- and C-regions of the coded transcript are species- and tissue-specific but the catalytic region of the protein is highly conserved amongst vertebrates. The high sequence identity (90.53%) between the human *PDE4D-001* and the zebrafish pde4d-001 (**Figure 4.2.6C**) further highlights the importance of the *PDE4D* function.

The zebrafish pde4d$^{+/-}$ mutant line was identified after a large-scale mutagenesis screen in the Sanger Institute. A single nonsense point mutation (A to T) at the beginning of the PDEase active site converts a lysine residue to a stop codon, therefore producing an incomplete catalytically inactive transcript (**Figure 4.2.6A**). Initial examination of the genetically mutant zebrafish embryos and adults (both heterozygous and homozygous) were anatomically and physically indistinguishable from wild-type individuals (data not shown).

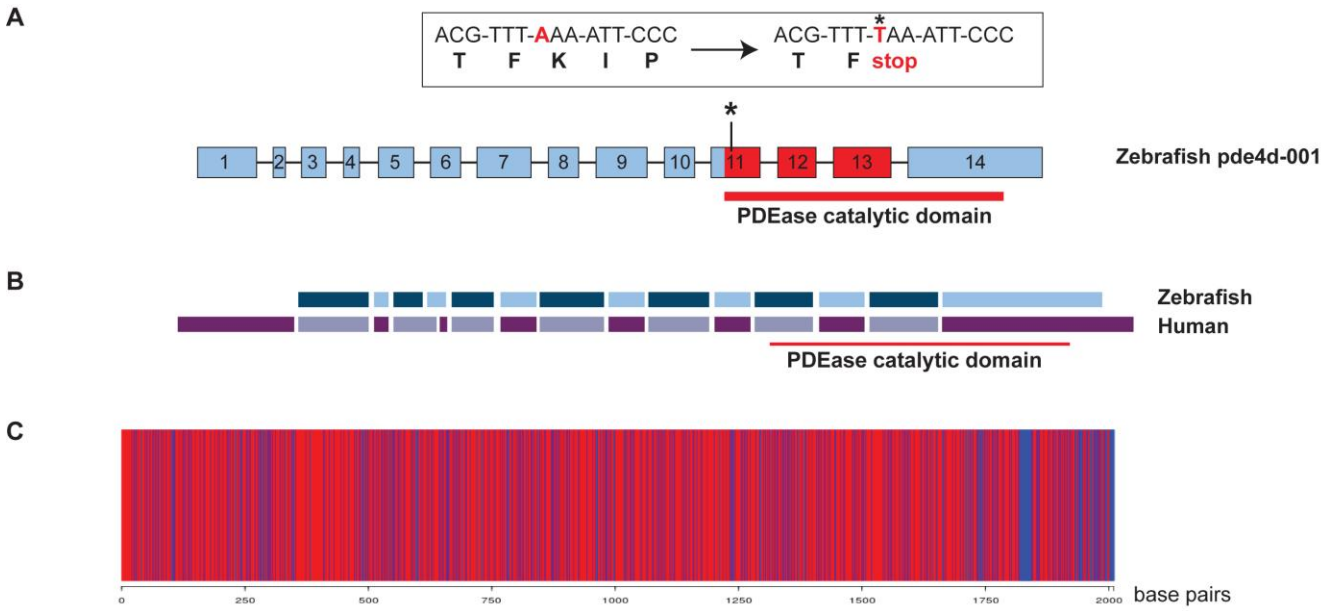

Figure 4.2.6 *Homology between zebrafish and human PDE4D*

A Schematic representation of the zebrafish pde4d-001 gene. Each numbered box represents an exon. The catalytic domain and the mutation site of the PDE4D-/- mutant line are highlighted.
B Schematic alignment of human (light and dark purple) and zebrafish (light and dark blue) PDE4D cDNA. Each box represents a single exon, the sequence of which is highly similar to that of the exon directly below it.
C Sequence alignment between zebrafish and human PDE4D cDNA reveals 90.53% sequence identity (red lines). Blue lines represent sequence mis-matches. The alignment was performed using ClustalW 2.1 and the illustration was generated in R.

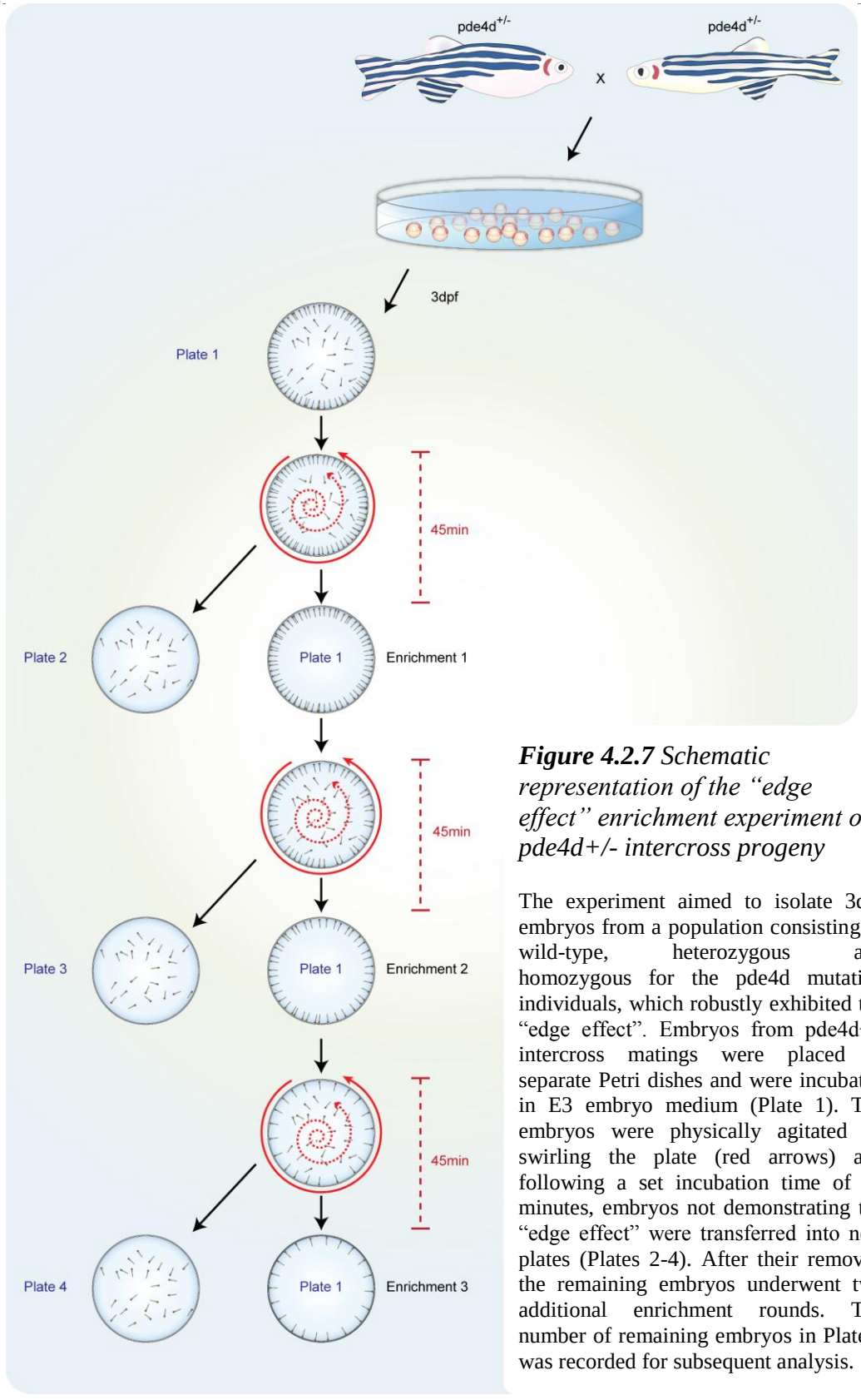

Figure 4.2.7 *Schematic representation of the "edge effect" enrichment experiment on pde4d+/- intercross progeny*

The experiment aimed to isolate 3dpf embryos from a population consisting of wild-type, heterozygous and homozygous for the pde4d mutation individuals, which robustly exhibited the "edge effect". Embryos from pde4d+/- intercross matings were placed in separate Petri dishes and were incubated in E3 embryo medium (Plate 1). The embryos were physically agitated by swirling the plate (red arrows) and following a set incubation time of 45 minutes, embryos not demonstrating the "edge effect" were transferred into new plates (Plates 2-4). After their removal, the remaining embryos underwent two additional enrichment rounds. The number of remaining embryos in Plate 1 was recorded for subsequent analysis.

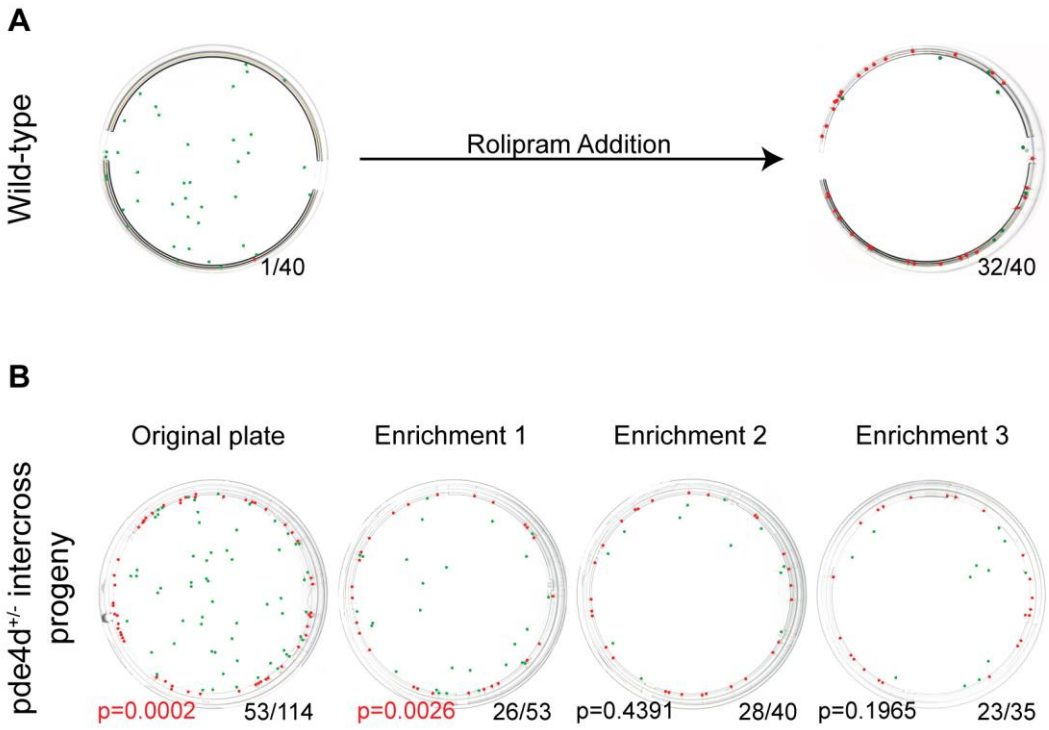

Figure 4.2.8 *A portion of pde4d+/- intercross progeny display the "edge effect"*

A 3dpf wild-type embryos before (left) and after (right) treatment with 15µM Rolipram were used as controls in the enrichment experiment. Untreated embryos position themselves randomly around the plate, whereas embryos incubated in Rolipram display the "edge effect".
B Serial enrichment of pde4d+/- intercross progeny for the "edge effect". 53 "edge effect"-positive embryos were selected from the original population (n=114) at the first enrichment, 40 embryos at the second enrichment and 35 embryos at the third enrichment round. The pictures illustrated here were taken at the end of the 45minute incubation time. The proportion of "edge effect" positive individuals gradually significantly deviates from the wild-type untreated embryos and becomes more similar to that of Rolipram-treated wild-type individuals. The p values were calculated using Fisher's exact test using the wild-type Rolipram-treated embryos as a control. Red values represent statistically significant deviation from the Rolipram-induced "edge effect" and black values a non-significant difference.
The ratios at the bottom of every picture represent the number of "edge effect"-positive individuals over the total number of embryos within each group after the 45minute incubation time.

4.2.5.2. The "edge effect" in pde4d+/- and intercross progeny

It was evident that a portion of the progeny of heterozygous mutant adult fish exhibited the "edge effect" (**Figure 4.2.8**). I carried out a phenotype enrichment experiment to establish whether the number of "edge effect"-positive individuals could be enhanced from the pool derived from an intercross of pde4d heterozygous fish (**Figure 4.2.7**). The expected outcome of the cross was that one in four offspring

would be wild-type, one in two heterozygous and one in four homozygous mutant. Despite original planning to genotype the individuals exhibiting the "edge effect" after the third enrichment, the experiment was carried out blind to *pde4d* mutation status. This was due to time limitations and the lack of a fully functioning assay to genotype single embryos and as a result the individuals were assessed solely on their "edge effect" behaviour. The frequency of the "edge effect" exhibition at each enrichment stage was compared to that of wild-type control individuals and that of wild-type Rolipram-treated embryos.

The positional behaviour of pde4d$^{+/-}$ progeny deviated significantly ($p<0.0001$) from that of wild-type control embryos even before the first enrichment for "edge effect"-exhibiting individuals. After each enrichment round, the behaviour of the "edge effect"-enriched pde4d$^{+/-}$ progeny increasingly deviated from that of wild-type untreated controls and progressively resembled that of the Rolipram-treated wild-type embryos (**Figure 4.2.8**). This data suggests that loss of *pde4d* activity influences the positional behaviour of zebrafish embryos. The behaviour of embryos removed at each enrichment round for not exhibiting the "edge effect" was not significantly different from the wild-type controls (data not shown).

4.2.5.3. Complete *pde4d* loss promotes the "edge effect"

The behaviour of 3dpf homozygous pde4d$^{-/-}$ mutants was analysed to determine if complete genetic loss of *pde4d* is sufficient to promote the "edge effect". The position of DMSO-treated pde4d$^{/-}$ embryos was significantly different than that of DMSO-treated wild-type individuals ($p<0.0001$). Interestingly, the behaviour of pde4d$^{-/-}$ embryos was indistinguishable from that of the Rolipram-treated wild-type embryos (**Figure 4.2.9)**. Thus, genetic ablation of a single *pde4* gene can reproducibly promote the "edge effect" phenotype.

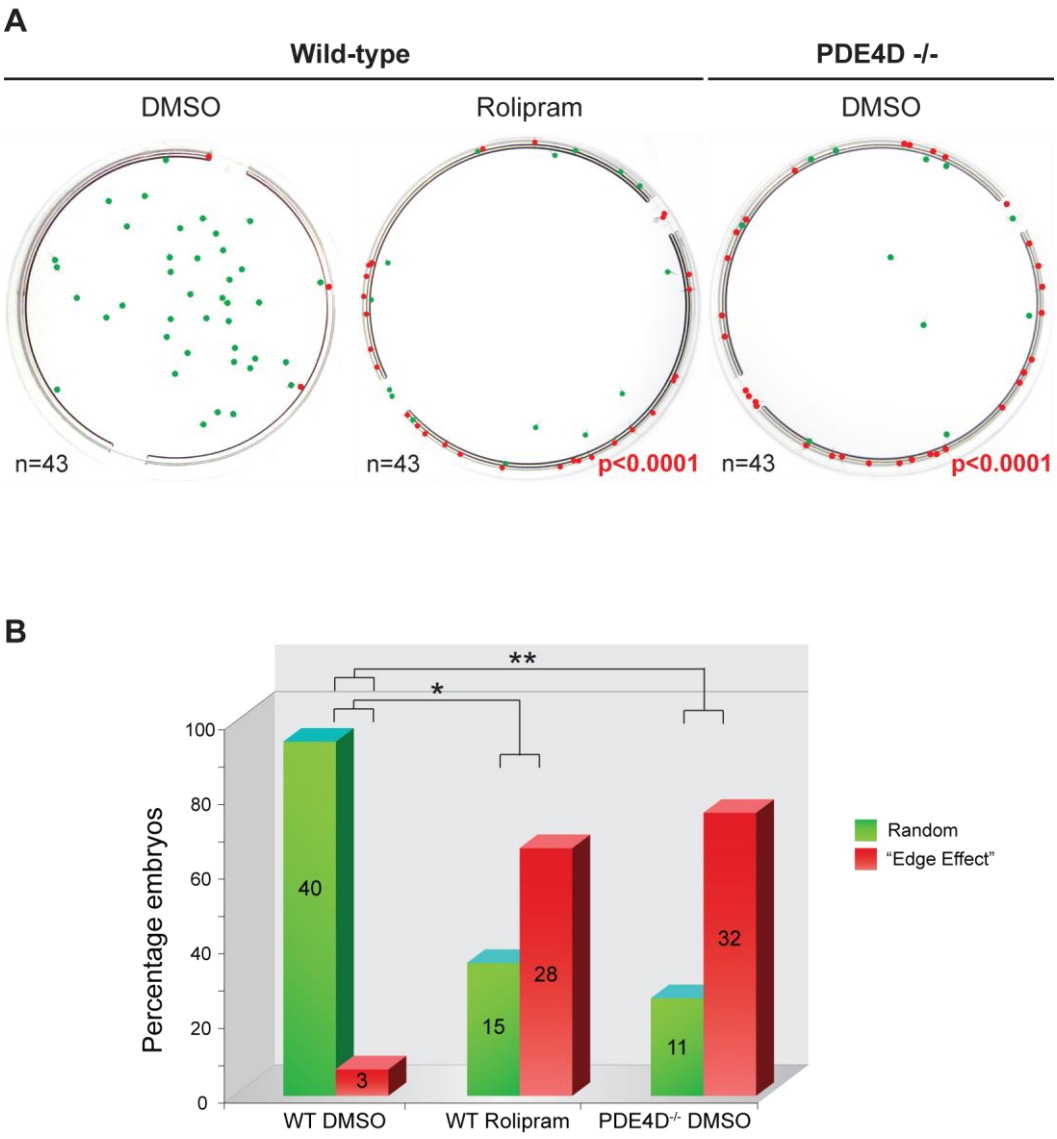

Figure 4.2.9 *Genetic loss of pde4d promotes the "edge effect" phenotype in 3dpf embryos*

A Comparison of the positioning of wild-type (wt) DMSO or Rolipram-treated and pde4d-/- DMSO-treated 3dpf embryos. Wt control embryos were randomly positioned unlike "edge effect"-exhibiting Rolipram-treated and pde4d-/- control-treated embryos. The p values were significant at the $p<0.05$ level and were calculated using Fisher's exact test with wt DMSO-treated embryos as the control.
B Comparison of positional behaviour between the different genotypes and treatments. Using Fisher's exact test, the difference of the positional behaviours was calculated to be significant between wt DMSO- and Rolipram-treated embryos and wt DMSO- and pde4d-/- DMSO-treated embryos (* $p<0.0001$). There was no significant difference between the behaviours of wt Rolipram-treated and pde4d-/- DMSO-treated individuals at the $p<0.05$ level ($p=0.4816$). (n numbers of embryos are written in the bars; green bars: random positioning; red bars: "edge effect"-positive embryos)

4.2.6. Mek inhibition in pde4d mutants does not rescue the "edge effect" phenotype

After having rescued the Rolipram-induced phenotype in wild-type embryos with PD0325901, I wanted to establish the potential of the MEK inhibitor to prevent the "edge effect" in pde4d$^{-/-}$ 3dpf embryos. Wild-type or pde4d$^{-/-}$ embryos were administered with Rolipram (15μM), PD0325901 (1μM) or with Rolipram (15μM) plus PD0325901 (1μM) (**Figure 4.2.10**). Rolipram single treatment induced similar effects irrespective of the genetic background of the fish. PD0325901 alone had no effect in the natural positioning of the wild-type embryos. Similarly, co-treatment with Rolipram and PD0325901 was not able to reverse the "edge effect" in the mutant embryos (**Figure 4.2.10A**).

Western blotting was performed on treated wild-type and pde4d$^{-/-}$ embryos to molecularly analyse the effects of all the small molecules on individuals of different genotypes (**Figure 4.2.10C**). Comparison of Mapk activity between embryos of different genetic backgrounds revealed elevated pErk levels in pde4d$^{-/-}$ mutants, thus supporting previous data correlating pde4 inhibition and Erk activation (**Figure 4.2.5A**). Additionally, PD0325901 addition reduced Erk activation in all treatment groups confirming effective Mek inhibition.

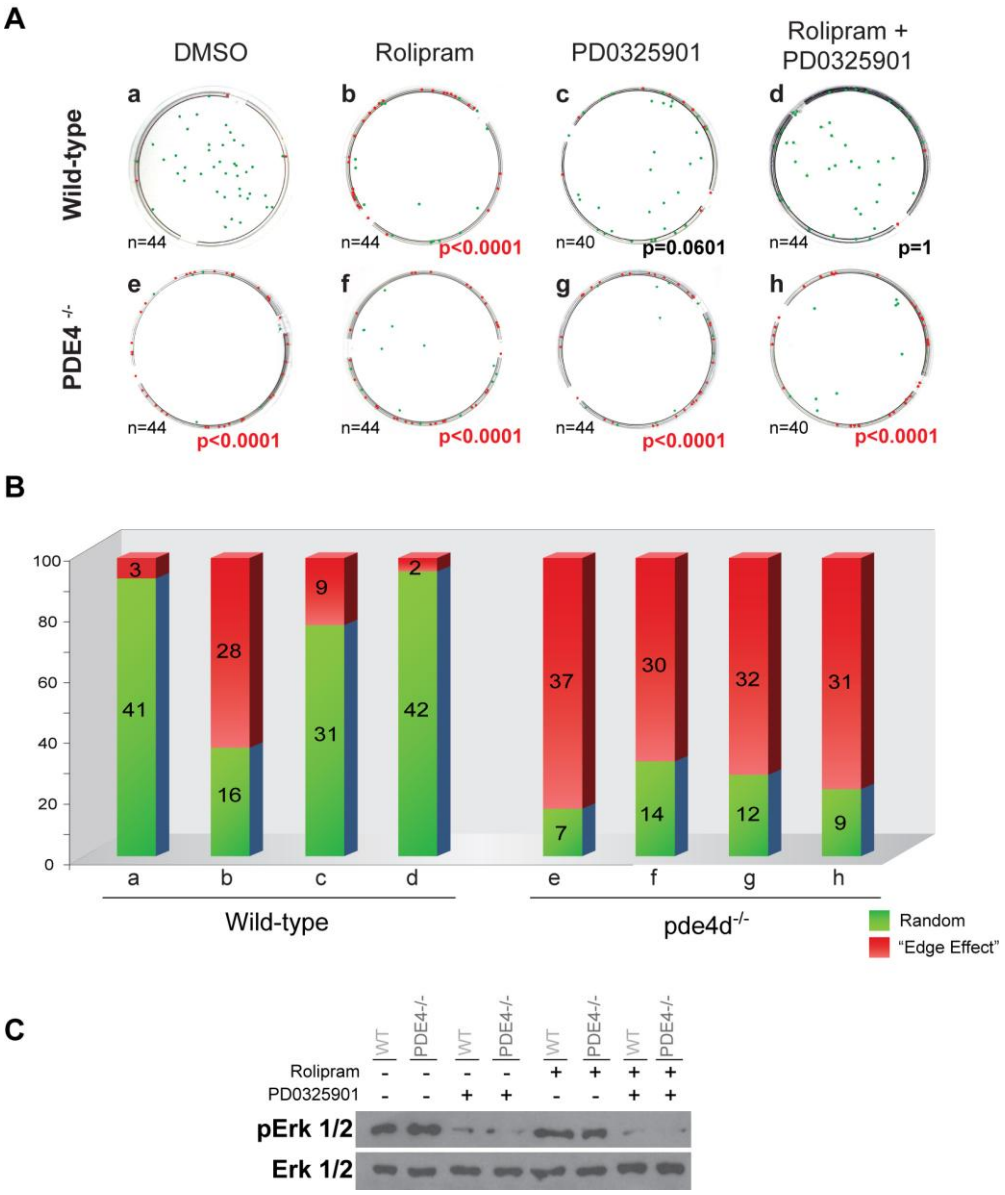

Figure 4.2.10 *MEK inhibition does not rescue the pde4d-/- "edge effect"*

A Wild-type (wt) (a-d) and pde4d-/- (e-h) 3dpf embryos were treated either with Rolipram or PD0325901 alone or with a combination of both. Neither single (f, g) nor dual treatment (h) had an effect on the behaviour of pde4d-/- embryos. p values were calculated using Fisher's exact test with wt DMSO-treated embryos as controls (red values: significant at the $p<0.05$ level; black values: not significant at the $p<0.05$ level).
B Histogram illustrating the proportions of embryos displaying each phenotype. The letters below the bars correspond to the treatment conditions in A. (n numbers inside bars; green: random positioning; red: "edge effect")
C Whole embryos from A were used to compare their Mapk activity levels. DMSO-treated pde4d-/- embryos exhibited increased pErk levels compared to the wt controls. Treatment with PD0325901 alone or in combination with Rolipram revealed highly reduced pErk levels confirming the activity of the drug. Erk1/2 was used as a loading control.

4.3. DISCUSSION

The results presented in this chapter are based on previous work in our lab that defined a specific zebrafish behavioural phenotype ("edge effect") and identified the pathway responsible. Here, I established a novel regulative role for the MAPK pathway in behaviour. I was able to replicate the phenocopy of the "edge effect" by cAMP elevators, rescue the phenotype after Mek inhibition and provide evidence for a direct effect of pErk on behaviour.

The cross-talk between cAMP and MAPK pathways and feedback signals linking the two cascades dictate behavioural outcomes in zebrafish swimming and positioning. Increased cAMP levels reproducibly promoted the defined "edge effect" (**Figure 4.2.1**), a phenotype that can be reversed after Mek inhibition. Genetic loss of one of the four *pde4* genes, *pde4d*, phenocopied the "edge effect" but blocking ERK activation failed to stably impede the positional behaviour of the zebrafish larvae. This study addresses the first attempt to unravel the molecular mechanism underlying the behavioural onset.

4.3.1. MAPK and behaviour

The link between the activation of the MAPK pathway and cognition has been long studied and has mostly focused on the areas of depression and memory. Triggered by the circadian clock, MAPK activation endogenously oscillates every 24h in the hippocampus (Eckel-Mahan *et al*., 2008) and peaks of cAMP and MAPK signalling induce expression of new genes, promoting long-term memory formation (Lyons *et al*., 2006). More recently, Noonan syndrome (NS) gain-of-function mutations of the Ptpn11 orthologue in *D. melanogaster* were found to drive alterations in Mapk signalling. This prolongs the resting intervals between the repeated training sessions impairing long-term memory formation (Pagani *et al*., 2009).

Importantly, RASopathies patients exhibit a range of behavioural phenotypes. Study of the adaptive behaviour of CFC and NS patients, although varied, shows some evidence for genotype-to-phenotype correlation (Pierpont *et al*., 2010). For example, all CFC patients present with cognitive impairment whereas a third of NS patients did so. Moreover, BRAF, MEK1 and MEK2 mutations are correlated with more impaired adaptive behaviour than PTPN11 mutations.

Zebrafish provide a good model organism to study and measure behavioural patterns and have been previously used to dissect general behaviour (Guo *et al*., 2004), sleep patterns (Cahill *et al*., 2002), drug addiction (Ninkovic *et al*., 2006) and learning (Best *et al*., 2008). Although specific aspects of behavioural phenotypes of the RASopathies spectrum cannot be readily assessed in our system, I aimed to establish whether MAPK output modulation had an effect on zebrafish behaviour at all. To assess the extent to which the MEK inhibitor that rescued the developmental phenotype promoted by CFC mutations (**Chapter 3**) could also affect zebrafish behaviour, I tested the behavioural effect of PD0325901 on 3dpf zebrafish larvae triggered to exhibit the previously characterised "edge effect".

4.3.2. The "edge effect" is reminiscent of murine depression

Administration of the three cAMP elevators Rolipram, Forskolin and IBMX to wild-type fish resulted in the same phenotype (**Figure 4.2.3**), suggesting that increased cAMP levels alone can promote the defined behaviour. The behaviour was not attributed to general drug administration as zebrafish are DMSO-tolerant (Goldsmith *et al*., 2004) and other drugs including the MEK inhibitor PD0325901 and lithium chloride had no observable effect (Anastasaki *et al*., manuscript in preparation). The lower phenotype induction of IBMX compared to the other two small molecules may be explained by the non-specific nature of the former, which also acts as an adenosine receptor inhibitor.

The treated embryos positioned themselves perpendicularly to the edge of their container facing outwards, actively resuming their positioning upon agitation (MSc Thesis, Grant). This phenotype was previously characterised as the "edge effect". This behaviour is reminiscent of thigmotaxis, which is the act of avoiding movement in open spaces and staying close to the wall. Thigmotaxis is commonly observed in mouse models of anxiety and depression (Miller *et al*., 2010) where the animals are characterised by seeking a darker environment and longer periods of inactivity compared to wild-type individuals. Similarly, in light conditions "edge effect"-exhibiting zebrafish are not being entirely inactive as they dynamically maintain their positioning. However, they are not explorative of their environment in the light and appear static in the absence of agitation. Preliminary data supports the possibility that the "edge effect" is effectively a stronger than normal shade-seeking strategy, as embryos in total darkness are positioned randomly within their arena (Anastasaki *et al*., manuscript in preparation). Taken together, these suggest that steep cAMP increase may stress the treated zebrafish in the light and promote an anxiety-like, shade-seeking behaviour.

4.3.3. cAMP elevation correlates with pErk increase

Activation of the MAPK pathway and prolonged stress are key factors to depression onset (reviewed in Krishnan and Nestler, 2008; Hayley *et al*., 2005). Stress swim tests on mice have demonstrated a stress-driven prominent increase in the phosphorylation level of Mek1/2 in all brain regions paralleled by a slight increase in activated Erk1/2 (Shen *et al*., 2004). Similarly, pharmacologic or genetic increase of cAMP in zebrafish induced a stress-like response ("edge effect") and an increase in pErk1/2. Increasing concentrations of Rolipram promoted higher levels of pErk (**Figure 4.2.5A**). This suggests that Erk1/2 phosphorylation is cAMP-dependent in that escalating levels of cAMP respectively increase Mapk activation.

4.3.4. Mek inhibition rescues the "edge effect"

Physiological negative regulation of Erk in mice induces a depression-like behaviour (Duric *et al*., 2010). The dominance of the effect is such that MEK inhibitors mask the behavioural outcome of antidepressants after co-treatment with the two agents (Duman *et al*., 2007). Conversely to murine studies though, administration of PD0325901 alone had no effect on larval behaviour and mobility (**Figure 4.2.4**).

However, blocking the MAPK cascade can promote therapeutic effects in models of depression and stress. For example, antipsychotic agents, such as clozapine, selectively activate the MEK/ERK pathway and inhibition of the MAPK signalling upstream and downstream of RAF reverses the behavioural outcome of the drug (Browning *et al*., 2005). Conversely, the level of Mapk activation is inherently doubled in the amygdala of depressed-like rats demonstrating long periods of immobility. In that case, pharmacological inhibition of Mek1/2 can restore normal phosphorylation and mobility levels (Huang and Lin, 2006). In accordance to these findings, the MEK inhibitor PD0325901 was able to counter-act the immobility (light-avoidance) effect of Rolipram, Forskolin and IBMX in wild-type larvae (**Figure 4.2.4**).

4.3.5. pde4d$^{-/-}$ mutants exhibit the "edge effect" but respond differently to wild-type larvae to MAPK inhibition

Pde4d knockout mice exhibit increased cerebral cAMP levels and reduced depression (Zhang *et al*., 2002). In light conditions, pde4d$^{-/-}$ zebrafish larvae phenocopied the effect of Rolipram. Progressive loss of *pde4d* copies correlated with an increase of "edge effect"-positive embryos. Moreover, *pde4d* loss caused an increase in pErk levels, similar to immobilised rats (Huang and Lin, 2006). Although the possibility of an antidepressant-like effect in pde4d$^{-/-}$ adult fish is still being assessed, study of zebrafish embryos points towards the opposite direction. This could be partly explained by the fact that in this study the activity of zebrafish was

only observed during light conditions and close examination of the phenotypes exhibited in the dark will clarify the understanding of *pde4d* mechanism in zebrafish.

Treatment of pde4d$^{-/-}$ embryos with the MEK inhibitor failed to reproduce the level of rescue observed in wild type larvae. The reason MEK inhibition was not as effective as in wild-type individuals in preventing the "edge effect" possibly lies in the fact that genetic loss of a *pde4* gene disturbs cAMP regulation more robustly. It is possible that global elevation of cAMP, and respectively pERK, triggers the activation of another signalling cascade, unaccounted for in this study.

The increase in cAMP is, also, molecularly portrayed in the pErk elevation of the Rolipram-treated pde4d$^{-/-}$ embryos compared to that of the WT embryos. PD0325901 is potently inhibiting ERK phosphorylation at the administered dose, indicating that the drug was acting effectively and that the "edge effect" observed in pde4d$^{-/-}$ embryos was, at least partially, MAPK-independent. It became apparent that in this system the behavioural outcome and molecular readout were not always correlated and that the cross-talk between cAMP and MAPK pathways in the establishment of the "edge effect" is not simplistic or linear.

4.3.6. Conclusions

The theory that cAMP feeds back to BRAF in order to activate MAPK does not fully explain the lack of the phenotype rescue in pde4d mutants by PD0325901. Based on my results, I can conclude that pErk levels alone are not the optimal readout to explain embryonic behaviour. Firstly, Mek inhibition (reducing pErk levels) rescued the "edge effect" (increased pErk levels) in wild-type larvae but not in pde4d$^{-/-}$ mutants (increased pErk levels). There is a clear mechanistic difference between wild-type and mutant individuals that can possibly be explained by the constantly high levels of cAMP in pde4d$^{-/-}$ embryos. In support of this, continuous incubation of wild type fish in Rolipram (constant increased levels of cAMP) recapitulates the edge effect. However, this phenotype cannot be rescued by the MEK inhibitor, similarly to the pde4d-/- mutants (data not shown).

The chemical intervention of the cAMP molecular cascade and the genetic ablation of a pathway component (pde4d) give rise to the same phenotype but presumably promote the same measurable end effect through distinct processes. The pde4d$^{-/-}$ system is somehow compensating for the permanently higher cAMP signalling output in a non Mapk-related way. Although pde4d loss is paralleled by an increase in pErk and confirming the interaction between the two cascades, blocking the Mapk pathway seizes to have an effect on pde4-/- embryo behaviour. This suggests that the cAMP-dependent molecular trigger of the "edge effect" phenotype lies either downstream of Erk or in an parallel signalling pathway.

Preliminary results from adult pde4d-/- zebrafish studies suggest that the adult mutant phenotype is rescued by PD0325901, unlike the embryonic behaviour. This finding could suggest that two separate effects of the cAMP elevation are being observed. One effect could be causing motor neuron deficiency impeding the fish from swimming properly, an effect that could be partly overcome in adults as they had more time to develop new tissue. Indeed, pde4-/- embryos and adults swim less than their wild-type siblings (Pia Lundegaard, personal communication). The second

effect could be the exaggeration of the natural shade-seeking behaviour of larval zebrafish. Thus, one effect is light-dependent and the other swimming-dependent.

The network of interactions between the two signalling cascades is not complete leading to a lack of tools available to understand their precise function in behaviour development. Determination of cAMP and pMek1/2 levels can help elucidate the complexity of cAMP and Mapk interactions in this system. However, it is necessary to address the possible effect of a third pathway. The existence of a role for Mapk signalling in zebrafish behaviour is certain but the mechanism of its action is yet to be fully deciphered.

Chapter 5 - Concluding Remarks

“One never notices what has been done; one can only see what remains to be done” - Marie Curie

5.1. Contribution to the field

This project introduced a robust platform to study the genetic onset of the RASopathies, explore molecular interactors of the disease-causing genes as well as test potential patient treatments. The main results of the project cluster around three major areas: developmental genetics, chemical genetics and behavioural genetics.

5.1.1. Established zebrafish bioassay

Firstly, the zebrafish model provided a thorough system to establish my bioassay. Its unique advantage is that it allowed me to closely examine both the effect of individual mutations as well as to test a vast array of them (**Figure 2.2.3**). Each embryo can be followed throughout embryogenesis and every developmental aspect can be monitored and measured. That way, one can understand different developmental processes during normal pathology.

The optical transparency of the embryos and the molecular tools available rendered it easy to dissect the direct developmental effect of individual mutations. For instance, human $BRAF^{V600E}$ mRNA over-expression not only caused prominent embryo dorsalisation by the end of gastrulation, like all other BRAF CFC and melanoma mutations, but also at high concentrations completely impeded the formation of eyes (**Figure 2.2.2**). Moreover, the abundance of embryos and the capacity to easily over-express mutant mRNA allows to rapidly test the effect of tens (31 in this study) but potentially hundreds of mutations in development.

5.1.2. All mutations act as gain-of-function

Secondly, this study established that all CFC mutations are acting as gain-of-function *in vivo* irrespective of their predicted *in vitro* activity. This finding is in accordance with results from *Drosophila* studies, where all SHP-2 mutations also act as gain-of-function (Oishi *et al*., 2009). The fact that all the tested CFC mutations had the same

effect can explain the phenotypic similarity between CFC and, indeed, RASopathies patients.

Not only did kinase-impaired mutations promote the same gastrulation phenotype in embryos as kinase-activating ones did, but also stable mosaic expression of the kinase-inactivating CFC allele $BRAF^{G596V}$ in zebrafish adults drove naevi formation. Ectopic melanisation requires a breach of the tightly controlled mechanism specifying pigmentation patterns and has only been observed in cases of highly activating oncogenes (such as $BRAF^{V600E}$). This result underpins the oncogenic potential possessed by all CFC mutations and, importantly, reinforces the notion that *in vitro* activity levels of proteins are not representative measures of their *in vivo* output.

5.1.3. Recycling of cancer drugs to treat developmental disorders

Thirdly, I ascertained that drugs established in other fields of treatment can be recycled to target the same pathways in different disorders. The RASopathies spectrum has a low prevalence and represents a very small target market. Hence, the potentially small financial benefit has not made the RASopathies a primary investment target for pharmaceutical companies. Nevertheless, administration of anti-cancer agents for the treatment of developmental defects in the present bioassay has been successful. I tested one FGFR and two MEK inhibitors, all of which were able to fully prevent elongation in zebrafish embryos expressing disease alleles (**Figures 3.2.1**, **3.2.4**).

Recycling anti-cancer drugs that target the MAPK pathway or its peripheral regulators presents a real possibility for RASopathies treatment. This is further supported by the fact that a number of drugs have been developed, which act specifically on known MAPK components, have established side effects and evaluated potency. However, the caveat of this approach is that children are organisms that are still undergoing development. As such, complete blockage of a key signalling pathway such as MAPK can be detrimental to their physiology.

Indeed, blocking more than 50% of the MAPK pathway output drives prominent craniofacial malformations in developing zebrafish (**Figures 3.2.9-3.2.11**). To overcome this problem, the MAPK inhibition levels need to be fine-tuned in order to simultaneously block the activity of the pathway efficiently enough to avoid the CFC allele-driven aberrant signalling as well as retain enough MAPK output for normal development and tissue formation.

To this end, I performed an initial systematic study primarily to understand the spatiotemporal requirements for active MAPK signalling in normal development. I looked at the specific molecular and developmental effects of the MEK inhibitor PD0325901 and established that increasing concentrations of the small molecule can turn the pathway off in a linear manner (evident both after dusp6-GFP transgenic line treatment **Figure 3.2.2** and after western blotting **Figure 3.2.11**). The titration series also allowed clear distinction between phenotypes of optimal and sub-optimal drug treatments.

Most importantly, after identifying a sub-optimal concentration that minimally affected development (0.2µM), I was able to alleviate the symptoms of embryos over-expressing the most common CFC allele $BRAF^{Q257R}$ after continuous sub-optimal PD0325901 treatment (**Figure 3.2.12**). The finding that a constant low dose of a MEK inhibitor can counter-act all the developmental defects promoted by CFC alleles restoring near-normality as the organism matures without greatly affecting development is integral to the potential treatment of the syndrome. The results presented here could represent the first step towards the consideration of CFC syndrome treatment with an appropriate dosage of a MEK inhibitor.

5.1.4. Targeting the cAMP pathway to modulate MAPK signalling

Lastly, this body of work identified a novel involvement of the Mapk pathway in zebrafish behaviour and introduced cAMP modulation as a possible avenue to target the MAPK pathway. The robust zebrafish “edge effect” phenotype promoted by

elevated cAMP signalling was molecularly translated to an increase in Mapk activation and inhibition of Mek was able to fully reverse the effect. The behaviour itself was suggestive of sudden anxiety or possible shade-seeking but future work will characterise this further.

Intriguingly, the already non-linear image of cAMP and Mapk signalling interactions became more complex. Both the difficulty in fully understanding the network cross-talk between the two cascades as well as the dissimilar phenotypes demonstrated by different PDE4D genetic mutants across species urge further studies of the cAMP-driven behaviour. Preliminary data supports that light conditions have a significant effect in the positioning and motility of zebrafish experiencing increased cAMP levels. Future work will focus on examining detailed behavioural and molecular alterations in adult and embryonic genetic mutants in variable environments.

Modifying cAMP levels is a very new treatment approach for paediatric disease therapy. It was not until recently that cAMP was considered a potential target, mostly because it is expressed in a variety of tissues and plays major roles in very distinct processes. It was feared that blocking or enhancing the activation of cAMP could have multiple side-effects due to the involvement of a great number of downstream signalling pathways, some of which are probably unknown. Additionally, cascade cross-talks are very tissue-specific, complex and, most importantly, not delineated. As discussed above, complete ablation of a signalling cascade can have profound unwanted side effects and, in the case of cAMP, predominantly in neuronal tissues. Topical application of drugs presents a possibility for tumour treatment. However, local injection of a drug to a developing organism such as a child is not a realistic option. Thus, combinations of sub- optimal dosages of drugs that target upstream or downstream effectors of the disease-driving genes can be helpful.

Drug combination can work in two ways. First, drug resistance can be avoided, as low doses of drugs acting on the same or parallel pathways can have a moderate effect on their targets without completely inhibiting their action. Secondly, altering signalling in the “periphery” of the target pathway can have beneficial results. It is

clear that molecular pathways are not acting in a simplistic manner as originally described. Complex inter-connections and feedback mechanisms that are not yet established are the medium via which mutations in one pathway can cause alterations in signalling output of another. Blocking components peripheral to the key driving factors can moderate the intensity of the key signalling output and restore levels of signalling that an organism can cope with.

The relationship between the MAPK and cAMP pathways has been discussed in detail in **Chapter 4.1**. In the framework of the RASopathies though, dual targeting of MAPK and cAMP pathways has the potential to be beneficial in terms of memory/learning, social behaviour/anxiety and circadian rhythms/sleeping patterns. However, the exact behavioural phenotypes of RASopathies patients are not yet fully characterised. Additionally, one of the intrinsic problems with examining behaviour is trying to dissect the underlying mechanism. A stable adult model of the syndromes would help both with establishing behavioural phenotypes and with identifying molecular drivers of mutant behaviour.

5.2. Future directions

5.2.1. Establishing a genotype-to-phenotype relationship

At this stage, a precise genotype-to-phenotype correlation has not been established in CFC patients, with the exception of BRAF mutations that are thought to mostly involve skin malformation. However, KRAS-driven phenotypes are difficult to categorise but are generally associated with extreme severity of symptoms. A possible explanation for this is that unlike BRAF and MEK that have limited molecular targets, KRAS signals to more effector proteins leading to a larger set of symptoms that are harder to define. It is plausible that the higher a gene is in a signalling cascade, the broader the spectrum of its effects molecularly and phenotypically. Future studies based on my bioassay coupled with close examination of individual tissues can elucidate the role of Kras in zebrafish development.

Study of their effect in early development revealed that expression of a collection of CFC, melanoma and engineered BRAF and MEK alleles caused a severe gastrulation phenotype in zebrafish. Having determined that the phenotypic effect was mechanistically promoted by convergence movement defects, future studies can explore the molecular targets of the allelic variants. Performing a microarray analysis could clarify the molecular effects of each individual mutation in KRAS, BRAF, MEK1 and MEK2. This approach would highlight genes or pathways affected by individual mutations. Preliminary studies on zebrafish over-expressing a small panel of BRAF, MEK1 and MEK2 CFC alleles already show distinct regulation of downstream effectors depending. More extensive analysis can identify both common downstream effectors and differentially regulated targets of KRAS, BRAF, MEK1 and MEK2.

5.2.2. Generation of an adult model of CFC syndrome

Generation of a stable line of zebrafish expressing germ-line $KRAS^{CFC}$, $BRAF^{CFC}$ and MEK^{CFC} mutations would be an ideal system to fully study and comprehend the mode of action of CFC disease alleles. A stable zebrafish line would have the advantage of endogenously expressing the mutant proteins throughout development at physiological levels similarly to human CFC patients. The CFC zebrafish could be assessed genetically, physically, histopathologically, molecularly and in terms of behaviour at different stages of their development, a study that could shed light in unexplored aspects of the disorder. Most importantly, CFC zebrafish would offer a model to assess the effectiveness of individual or combinations of drugs on alleviating the severity of CFC symptoms.

Chapter 6 - Materials and Methods

6.1. List of Abbreviations

6.1.1. Reagents

Acrylamide/ Bis Solution : N, N' –methylene- bisacrylamide for electrophoresis

APS : Ammonium persulfate for electrophoresis, 98%

BSA : Bovine serum albumen

ddH_2O : Distilled deionised water

DMSO : Dimethyl Sulfoxide

E3 : Embryo growth medium

EDTA : Ethylenediaminetetraacetic acid

EtOH : Ethanol

H_2O_2 : Hydrogen peroxide

HCl : Hydrochloric acid

IBMX : 3-Isobutyl-1-Methylxanthine

KCl : Potassium chloride

KOH : Potassium hydroxide

LB Broth : Lysogeny Broth; Luria-Bertani medium

MeOH : Methanol

NaCl : Sodium chloride

NaF : Sodium fluoride

NaOH : Sodium hydroxide

NP40 : Tergitol-type NP-40, which is nonyl phenoxypolyethoxylethanol

PBS : Phosphate Buffered Saline

PBST : Phosphate Buffered Saline with Tween 20

PFA : Paraformldehyde

RIPA Buffer : Radioimmunoprecipitation assay buffer

SDS : Sodium Dodecyl Sulphate

SSC : Sodium chloride: Sodium Citrate Buffer

SU 5402 : 2-[(1,2-Dihydro-2-oxo-3*H*-indol-3-ylidene)methyl]-4-methyl-1*H*-pyrrole-3-propanoic acid

TBE : Tris/Borate/EDTA; Tris, Boric acid, EDTA

TBS : Tris Buffered Saline

TBST : Tris Buffered Saline with Tween 20

Tris Base : tris(hydroxymethyl)aminomethane

Tris- HCl: tris(hydroxymethyl)aminomethane hydrochloride

tRNA : Purified *Torulla* yeast RNA

6.1.2. Genes

BRAF : Raf-1 murine leukaemia viral oncogene homolog B1

cAMP : Cyclic Adenosine Monophosphate

CRAF; RAF-1 : Raf-1 murine leukaemia viral oncogene homolog 1

DLX3 : Distal-less homeobox 3

ERK 1; MAPK1 : mitogen-activated protein kinase 1

ERK2; MAPK2 : mitogen-activated protein kinase 2

FGF : Fibroblast Growth Factor

HGG1 : Hatching Gland 1; aka Cathepsin L, 1

MAPK : mitogen-activated protein kinase

MEK1; MAP2K1 : mitogen-activated protein kinase-kinase 1

MEK2 ; MAP2K2 : mitogen-activated protein kinase-kinase 2

MITF : Micropthalmia-associated Transcription Factor

p53 : Tumour protein 53

PDE4 : Phosphodiesterase 4

pERK1 : phospho-mitogen-activated protein kinase 1

pERK2 : phospho-mitogen-activated protein kinase 2

pMEK1 ; phospho-mitogen-activated protein kinase-kinase 1

pMEK2 : phospho-mitogen-activated protein kinase-kinase 2

PDE4 : phosphodiesterase 4

RAS – HRAS, KRAS, ARAS :

6.1.3. Processes

Dpf : days postfertilisation

Hpf : hours postfertilisation

ISH : *In situ* hybridisation

SDS-PAGE : Sodium Dodecyl Sulphate- Polyacrylamide Gel Electrophoresis

WB : Western Blotting

6.1.4. Units of measurement

L: litre

ml : millilitre

µl : microlitre

M : molar

mM : millimolar

µM : micromolar

ng/µl : nanograms per microlitre

µg/ml : microgram per millilitre

mg/ml : milligrams per millilitre

m : meter

cm : centimetre

mm : millimter

µm : micrometer

bp : Base pairs

kb : Kilobases

Mb : Megabases

g : gram

mg: milligram

µg : microgram

ng : nanogram

pg : picogram

pH : power of hydrogen

ºC : degrees Celcius

rpm : revolutions per minute

V: Volts

mA: milliamperes

Dpi: Dots per inch

6.1.5. Zebrafish Strains

WT : Wild-type

AB : Strain A crossed to Strain B

TL : Top-Long

pde4d$^{+/-}$; $^{-/-}$: Phosphodiesterase 4 heterozygous/homozygous mutants

6.2. General Use Buffers - Recipes

PBS (pH 7.4) (1L)

NaCl	8 g
KCl	0.2 g
Na_2HPO_4	1.44 g
KH_2PO_4	0.24 g
ddH_2O	up to 1L

Autoclave to sterilise

TBS 10x Stock Solution (1L)

NaCl	87.66 g
Tris Base	12.11 g
ddH_2O	800 ml

Adjust pH to 8.0
Fill up to 1L with ddH_2O

1M Tris Buffer (1 L)

Tris Base	121.1 g
ddH_2O	800 ml

Adjust pH accordingly to 6.8; 7; 8.8 with 10M HCl
Fill up to 1L with ddH_2O and autoclave to sterilise.

0.5M EDTA (pH 8.0) (1L)

Na_2EDTA	186.1 g
ddH_2O	500 ml

Adjust pH to 8.0 with 10M NaOH.
Fill up to 1L with ddH_2O and autoclave to sterilise.

TBE 10x Stock Solution (1L)

Tris Base	108 g
Boric Acid	55 g
0.5M EDTA (pH 8.0)	40 ml
ddH_2O	up to 1L

E3 Embryo Medium 60x Stock Solution (1L)

NaCl	17.2 g
KCl	0.76 g
$CaCl_2 \cdot 2H_2O$	2.9 g
$MgSO_4 \cdot 7H_2O$	4.9 g
ddH_2O	up to 1L

E3 Embryo Medium 1x Solution (6L)

60x E3 Stock Solution	100 ml
ddH_2O	5.9 L
Methyl Blue	2 drops

6.3. Zebrafish Husbandry

Detailed zebrafish husbandry techniques can be found at *The zebrafish book. A guide for the laboratory use of zebrafish (Danio rerio)* (Westerfield, M., 2000) and *Zebrafish* (Nusslein-Volhard and Dahm, 2002).

6.3.1. General Zebrafish Care and Line Maintenance

Embryos up to 5dpf were routinely maintained in 90mm diameter Petri dishes (Sterilin) filled with E3 embryo medium. Chemically treated embryos were, unless otherwise stated, incubated in tissue culture-treated, gamma-sterilised, RNase and DNase-free 6-well (Technoplastics Products) plates in a total volume of 10ml of E3 enriched with the appropriate small molecule. All embryos were grown in a 28.5ºC incubator. The media were refreshed daily and the plates were monitored at least once per day to record phenotypes and discard of dead embryos.

5dpf embryos were put in a flowing current aquatic system in a density of approximately 30 embryos per 2L tank. Juvenile fish (14dpf-1 month old) were transferred to tanks of larger volumes in order to ensure proper growth of the animals. Adult fish (older than 3 months) were either kept in the same tanks or were transferred in larger capacity tanks, depending on the fish density, to promote better mating.

6.3.2. Zebrafish Feeding

All the fish in the aquatic system were fed three times a day during weekdays and twice during the weekend. Their diet was age dependent and followed the scheme below:

Larvae (5dpf – 14dpf)
Dry food: Half a spatula-full of a mixture made up by equal parts of ZM000 and ZM100 (3 feeds)

Juveniles (14dpf – 1 month old)

Dry food: 1 pinch of ground granular food constituted of equal parts of ZM200, ZM small granular, Zeiger adult diet and Hikari tropical micropellets (2 feeds)

Approximately 2ml of freshly harvested brine shrimp solution (2 feeds)

Adults (>1 month old)

Dry food: 1 pinch of ground granular food constituted of equal parts of ZM200, ZM small granular, Zeiger adult diet and Hikari tropical micropellets (2 feeds)

Approximately 2ml of freshly harvested brine shrimp solution (2 feeds)

6.3.3. Embryo Collection and Bleaching

Embryos that were to be raised past 5dpf in the aquarium had to be bleached, in order to minimise introduction of infection to the system.

Bleaching Solution (500ml)

10-15% Sodium hypochlorite (Sigma)	180 µl
ddH_2O	500 ml

Up to 200 embryos were transferred into a plastic sieve that was serially submerged in five separate trays containing different solutions in the following order. Care was taken to avoid embryos overflowing out of the sieve.

Tray 1 - Bleaching solution	5 mins
Tray 2 - ddH_2O	5 mins
Tray 3 - Bleaching solution	5 mins
Tray 4 - ddH_2O	5 mins
Tray 5 - E3 Embryo medium	5 mins

After the last step, the embryos were transferred in a new 90mm Petri dish (Sterilin) in fresh embryo medium and were raised normally.

6.3.4. Anaesthesia and Schedule I

To image embryos or adults, zebrafish had to be anaesthetised temporarily in tricaine (3-amino benzoic acid ethyl ester; ethyl 3-aminobenzoate) (Sigma-Aldrich).

Tricaine Anaesthetic Solution (100ml)

Tricaine powder	400 mg
ddH_2O	97.9 ml
1M Tris (pH 9.0)	2.1 ml

500µl of tricaine anaesthetic solution was added in 30ml of embryo media to anaesthetise embryos in 90mm Petri dishes almost immediately. Adult zebrafish were transferred, one at a time, in a tank containing 4.2ml of tricaine solution and 95.8ml of fresh aquatic system water until fully anaesthetised. The duration of this step depended on the size of the fish and ranged from 1 to 5 minutes. The fish recovered rapidly when transferred to fresh embryo medium or system water, respectively.

6.4. *Embryo Micro-injection*

6.4.1. Pulling Needles

The needles used for injections were pulled using a P-97 Flaming/Brown Micropipette Puller (Sutter Instrument, Novato CA, USA). That was accomplished by heating up the middle section of 1mm outer diameter, 0.8mm inner diameter, 10cm long single glass capillaries without filament (Intrafil) and then pulling the two ends of the capillary to opposite directions to create two needles. The ends of the two needles were automatically sealed as a result of the high temperature and the thin nature of the capillaries.

6.4.2. DNA and RNA Solutions for Injections

All DNA and RNA solutions prepared for injections were dissolved in ddH_2O. Routinely, DNA solutions were injected at 100ng/µl to avoid toxic side-effects. As RNA abundance tolerated by embryos varies depending on the nature of the protein encoded for, the optimal end concentration used for BRAF, MEK1 and MEK2 capped mRNA was 35ng/µl and the sub-optimal concentration was 15ng/µl

6.4.3. Adjusting Needle Size and Position

2-5µl of each construct to be injected was loaded to the end of the sealed needle using Microloader pipette tips (Eppendorf, UK). A P/N standard straight holder (Intracel, Herts, UK) adjusted onto a micromanipulator (Narishige International Limited, London, UK), held the capillaries in place. The position of the micromanipulator could be manually modified as its movement could be finely and precisely controlled in three planes. The needle holder was connected to a nitrogen-powered Picospritzer III microinjector (Intracel) by a polyethylene tube and allowed air and, hence, pressure to pass through.

Individual needle tips were broken steeply creating a non-blunt end using forceps, just prior to injection. The liquid automatically migrated to the end of the needle after the tip was broken due to capillary action. The amount of glass that was broken off the tip of the needle was estimated empirically, so that the capillary could penetrate the embryonic chorion without bending. The droplet size, however, was calculated to be 1nl by calculating the diameter of the droplet using a graticule, converting this to volume and adjusting the pressure and the duration of the injection (usually ranging from 5-15msec) until the desired volume was achieved.

6.4.4. Injecting the Embryos

Single-cell stage embryos were collected from mating tanks and transferred in clean Petri dishes in fresh E3 medium. Using a clean wide-tip 2ml graduated pastette a single file of embryos was positioned along the outer edge of a clean histology slide, which was, in turn, wedged within a 90mm Petri dish (as shown in the figure below). The injector was conjugated to a Nikon SMZ 1000 stereomicroscope illuminated from below, which allowed optimal alignment of the embryos and the needle and clear visualisation of the injection process. Most of the embryo medium around the embryos was removed in order to stop embryos from shifting positions during the injection process, with a few drops of liquid left surrounding them to prevent drying out. The embryos were manoeuvred either with forceps or with the needle itself so that the cell was facing the needle and the yolk sac was against the slide.

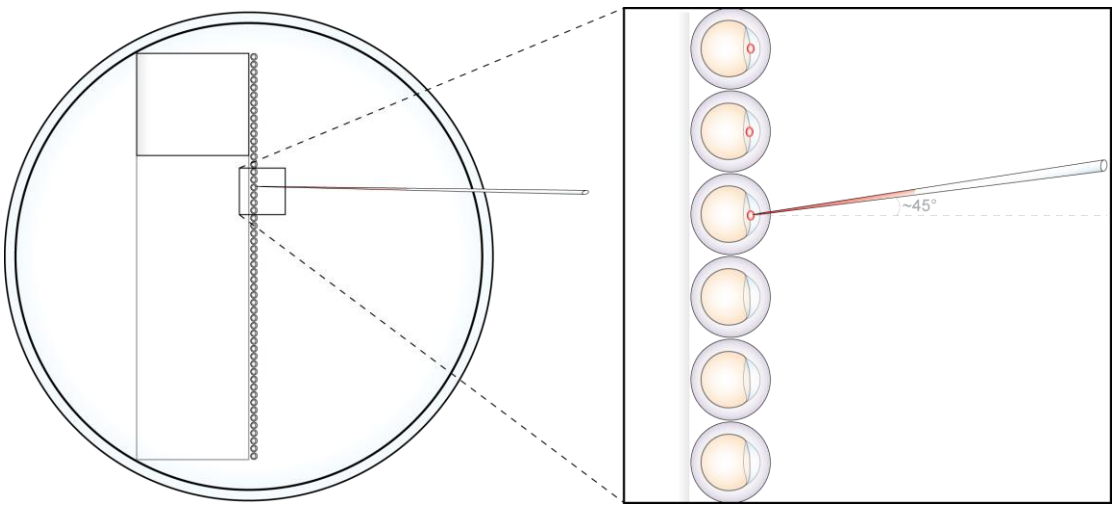

Figure 6.1
Microinjection of embryos

The microscope was focused on the embryo to be injected and the needle was driven, in a single move, through the chorion directly into the cytoplasm of the cell. Using the foot switch the solution was visibly injected and the needle was swiftly retracted from the embryo. The dish was moved manually upwards in order to inject the next embryo in line and the procedure was repeated for all of the embryos in that set. All embryos were only injected once. It is important to note that the same needle was used between experimental and control injection sets, when possible, to ensure the injected volume was identical.

6.4.5. Post-Injection Care

Injected embryos were sensitive to post-injection infections and as such were routinely checked 3-4 hours after their injection to clean up their media and discard severely deformed or dead samples. This procedure promoted healthy development and well-being of the all individuals in the plate.

6.5. Drug Treatments

6.5.1. MEK Inhibition

Two specific MEK1/2 inhibitors were used throughout the course of this project. CI1040 (previously referred to as PD184352) was provided by Richard Marais (ICR, London, UK) and PD0325901 was purchased from Dundee University.

1mg of CI-1040 (molecular weight: 478.67) was dissolved in 208.91µl of DMSO (Sigma-Aldrich) to achieve a final molarity of a 10mM stock solution. The solution was aliquoted and stored at -80ºC for up to one year. Once an aliquot was thawed it was not re-frozen, as it affected the activity of the small molecule. CI-1040 was used only for mRNA-promoted elongation prevention experiments (**Chapter 3**). It was used at a final molarity of 0.5µM or 1.0µM in 10ml E3. The drug was administered once to injected and uninjected embryos at 4hpf. The embryos were incubated in the small molecule for a maximum of 4.5 days, at which point the larvae were killed in an overdose of anaesthetic tricaine, following the Schedule I for the Animals Scientific Procedures of the Home Office/ Animal Procedures Committee (see above).

1mg of PD0325901 (molecular weight: 482.2) was dissolved in 207.38µl of DMSO to achieve a final molarity of a 10mM stock solution. The stock was aliquoted and stored stably at -20ºC for up to 2 years. Freezing an aliquot after thawing the solution was avoided but did not have an overt effect on the activity of the compound.

For the elongation prevention experiments, 10ml of PD0325901 were administered once at 0.5µM and 1.0µM at different stages during gastrulation: 4.5hpf, 5.5hpf, 6.5hpf, 7.5hpf, 8.5hpf, 9.5hpf and 10.5hpf (**Chapter 3**). The mRNA-injected embryos were incubated in the drug until 24hpf. For the systematic study of the effects of MEK inhibition during normal development, 10ml of PD0325901 were

prepared fresh and were refreshed daily at the following molarities: 0.1μM, 0.2μM, 0.3μM, 0.4μM, 0.5μM, 0.6μM, 0.7μM, 0.8μM, 0.9μM and 1.0μM. For the behavioural studies (**Chapter 4**), PD0325901 was administered in combination with other drugs according to **Table 6.1**. A total volume of 10ml was prepared for embryos treated at 4hpf and of 30ml for 3dpf embryos.

6.5.2. FGFR Inhibition

1mg of the FGFR inhibitor SU5402 (Tocris-Bioscience) powder (molecular weight: 296.32) was dissolved in 33.75μl of DMSO to achieve a final molarity of a 100mM stock solution. The stock solution was aliquoted in 50μl tubes protected from light and stored at -20ºC for up to 2 years. Embryos injected with BRAF, MEK1 and MEK2 capped mRNA used for rescue experiments (**Chapter 3**) were treated with 10ml of freshly prepared 0.5μM SU5402 in E3.

	cAMP elevator	*MAPK inhibitor*	*Time of Addition*
Rolipram + PD0325901	15μM	1μM	4hpf; 3dpf
Forskolin + PD0325901	7.5μM	1μM	3dpf
Forskolin + PD0325901	7.5μM	2μM	3dpf
Forskolin + PD0325901	15μM	1μM	4hpf; 3dpf
IBMX + PD325901	15μM	1μM	4hpf; 3dpf

Table 6.1 *Final molarities of drugs used for dual treatments.*

6.5.3. Rolipram Treatment

10mg of Rolipram (Tocris Bioscience) powder (molecular weight: 275.35) were diluted in 363.17μl DMSO to achieve a final molarity of a 100mM stock solution.

The stock was aliquoted and stored at -20ºC for 3-6 months. 4hpf embryos were treated in 10ml Rolipram or Rolipram+PD0325901 (**Table 6.1**) in a 6-well plate for six hours before being collected for Western blot analysis. 10hpf and 3dpf embryos were treated in 30ml Rolipram or Rolipram+PD032590 in a 90mm plate for up to 10hpf before being imaged and collected for Western blot analysis.

6.5.4. Forskolin Treatment

10mg of Forskolin (Tocris Bioscience) powder (molecular weight: 410.51) were diluted in 487.2µl of DMSO to achieve a final molarity of a 50mM stock solution. The solution was aliquoted and stored at -20ºC for 6 months. 4hpf embryos were treated in 10ml Forskolin or Forskolin+PD0325901 in 6-well plates and 3dpf embryos were treated in 30ml Forskolin or Forskolin+PD0325901 in 90mm Petri dishes (**Table 6.1**).

6.5.5. IBMX Treatment

50mg of IBMX (Tocris Bioscience) powder (molecular weight: 222.24) were diluted in 4.49ml DMSO to achieve a final molarity of a 50mM stock solution. The stock was aliquoted and stored at -20ºC for 6 months. 4hpf embryos were treated in 10ml IBMX or IBMX+PD0325901 in a 6-well plate. 3dpf embryos were treated in 30ml IBMX or IBMX+PD0325901 in 90mm Petri dishes (**Table 6.1**).

6.6. Immunoblotting - Recipes

6.6.1. Protein Extraction

RIPA Buffer (10 ml)

ddH_2O	9.250 ml
2M Tris-HCl pH 7.5	250 µl
5M NaCl	300 µl
1% NP40 (Sigma Aldrich)	100 µl
10% SDS	100 µl
Sodium deoxycholate	50mg

10% SDS (1L)

SDS	100 g
ddH_2O	1 L
Heat to 68ºC	
Adjust pH to 6.6	

Lysis Buffer (1 ml)

RIPA Buffer	925 µl
NaF	10 µl
Beta-glycosyl phosphate	25 µl
25x Phosphatase inhibitors mix (Roche)	40 µl

6.6.2. Preparing the SDS Gels

1M Tris pH8.8 (500 ml)

Tris base	60.55 g
ddH_2O	400 ml
Adjust pH to 8.8 with 10M HCl	
Make up to 500ml with ddH_2O	

0.5M Tris pH6.8 (200 ml)

Tris base	12.1 g
ddH_2O	150 ml
Adjust the pH to 6.8 with 10M HCl	
Make up to 200ml with ddH_2O	

25% APS (1 ml)

APS	0.25 g
ddH_2O	1 ml

Store at 4ºC and use within 3 weeks

8% SDS Resolving Gel (10 ml)

ddH_2O	3.47 ml
1M Tris pH 8.8	3.73 ml
30% Acrylamide/ Bis (BioRad)	2.7 ml
10% SDS	100 µl
TEMED (Sigma Aldrich)	10 µl
25% APS	40 µl

SDS Stacking Gel (4 ml)

ddH_2O	2.8 ml
0.5M Tris pH 6.8	500 µl
30% Acrylamide/ Bis (BioRad)	670 µl
10% SDS	40 µl
TEMED (Sigma Aldrich)	10 µl
25% APS	20 µl

6.6.3. Loading

3x Sample Buffer (*Cell Signaling)*

3x Sample Buffer	100 µl
30x DTT	10 µl

6.6.4. Running the Gel

SDS Running Buffer 10x stock solution (1L)

Glycine	144 g
Tris Base	36.3 g
SDS	10 g

Adjust pH to 8.3

6.6.5. Transferring the Proteins

Transfer Buffer 10x stock solution (1L)

Glycine	144 g
Tris Base	29 g

1x Transfer Buffer (1L)

10x Transfer Buffer stock solution	100 ml
100% MeOH	100 ml
ddH_2O	800 ml

6.6.6. Post-transfer Procedures

1x TBS with Tween20/ TBST (1L)

10xTBS stock solution	100 ml
Tween 20	500 µl
ddH_2O	900 ml

0.5% Ponceau Solution (100 ml)

Ponceau S (Sigma Aldrich)	0.5 g
Glacial acetic acid	1 ml
ddH_2O	99 ml

Blocking Solution (100 ml)

Dried milk	2 g (2%) or 0.2 g (0.2%)
1xTBST	100 ml

Stripping Buffer (1L)

Glycine	15 g
SDS	1 g
Tween 20	10 ml
ddH_2O	800 ml
Adjust pH to 2.2	
Make up to 1L with ddH_2O	

6.7. *Immunoblotting - Methodology*

6.7.1. Protein Extraction from Embryos for SDS-PAGE Analysis

6.7.1.1. Collection and storage of samples

Ten embryos were hand-dechorionated at the appropriate developmental stage. Embryos younger than 24hpf were placed in 1.7ml sterile microcentrifuge tubes in minimal liquid medium. Embryos older than 24hpf were placed in 2ml sterile ribbed skirted tubes in minimal medium. All samples were snap frozen in a dry ice/ MeOH mix and were stored at -80ºC.

6.7.1.2. Embryo Lysis

For samples of embryos younger than 24hpf, 40µl of lysis buffer was added in each tube and the embryos were homogenised by pipetting repetitively up and down.

For samples of embryos older than 24hpf, 40µl of lysis buffer and approximately 50 acid-washed glass beads were added in each skirted tube. The samples were ribolysed for 6 seconds at a 6.5 speed in a ribolyser. Following a 15-minute incubation on ice, the samples were centrifuged at maximum speed for 15 minutes at 4ºC on an Eppendorf 5415R table-top centrifuge. The supernatant was transferred on a clean sterile 1.7ml microcentrifuge tube. The protein content of the samples was measured by calculating the A_{380} absorbance of the samples, normalised to the lysis buffer using a NanoDrop 2000 spectrophotometer.

6.7.1.3. Embryo Denaturation

Respective amounts of Sample Buffer (made freshly following manufacturer's instructions) were added in each sample according to their protein content to achieve a total volume of 50µl. Each sample was denatured at 95ºC for 5 minutes and loaded on the well warm.

6.7.2. Performing Western Blots of Zebrafish Embryos

6.7.2.1. Making the Gel

0.75mm SDS polyacrylamide gels were prepared following the above recipes. Three quarters of the glass plates (BioRad) were, initially, filled with approximately 4ml of the resolving gel mix. In order to accelerate the polymerisation process and ensure that no bubbles formed at the top of the gel, after pouring the resolving gel between the plates, 1ml of isopropanol was added on top. When the gel polymerised the isopropanol was poured off and filter paper was used to drain any remnants of it. At that time, approximately 1.5ml of the stacking gel mix was poured on top of the resolving gel and a 15-well comb was immediately placed between the plates.

6.7.2.2. Running the Gel

The gel tank was placed in a bigger tank filled with ice to lower the temperature of the running buffer and promote proper running of the high lipid content samples. The gel was run in a 1xSDS Running Buffer at 80V until the samples reached the bottom of the stacking gel. The voltage was increased to 120V until the samples ran out of the gel.

6.7.2.3. Wet Protein Transfer

The gels containing the protein extracts were placed in a wet-transfer assembly cassette (Bio-Rad) containing a Hybond-C nitrocellulose membrane. All components of the cassette were pre-soaked in 1x Transfer buffer. An ice tray was placed in the transfer tank to lower the temperature of the buffer. The transfer was performed at a constant current of 400mA for 1 hour at room temperature. To ensure full transfer and visually monitor protein abundance, the membranes were stained with 0.5% Ponceau solution for 5 minutes at room temperature, with mild agitation. The membranes were, then, serially washed in TBST to remove the dye.

6.7.2.4. Blocking

Following successful transfer, each membrane was incubated in approximately 25ml of 2% milk in TBST (blocking solution) for 30 minutes at room temperature with mild agitation.

6.7.2.5. Primary antibody incubation

Each membrane was incubated in a heat-sealed plastic sleeve, in approximately 5ml of primary antibody dissolved in 2% Blocking solution, overnight at 4ºC, with mild agitation. The table lists all the antibodies used and their respective working dilutions.

Antibody	*Animal Source*	*Dilution*	*Company/ Product Code*
Phospho- ERK 1/2 (E10)	Mouse (monoclonal)	1:2000	Cell Signaling / 9106
ERK 1/2	Rabbit (Polyclonal)	1:1000	Cell Signaling / 9102
Phospho- MEK 1/2	Rabbit (monoclonal)	1:1000	Cell Signaling / 2338
MEK 1	Rabbit (polyclonal)	1:1000	Cell Signaling / 9124
c-myc	Mouse (monoclonal)	1:2000	Sigma / M4439
β-tubulin (9F3)	Rabbit (monoclonal)	1:5000	Cell Signaling / 2128
α- tubulin (B-5-1-2)	Mouse (monoclonal)	1:10000	Santa Cruz Biotechnology / sc-23948

Table 6.2 *List of antibodies used for immunoblotting*

6.7.2.6. Primary antibody washes

After disposing of the antibody, the membranes were washed with 0.2% blocking solution for 2 minutes at room temperature, with mild agitation. They were, subsequently, washed three times in 1xTBST, each time for 5 minutes at room temperature, with mild agitation.

6.7.2.7. Secondary antibody incubation

The respective secondary antibodies were prepared in 1:2000 dilution in 2% Blocking solution. Each membrane was incubated in approximately 5ml of secondary antibody solution for 45 minutes to1 hour at room temperature, with mild agitation.

6.7.2.8. Secondary antibody washes

The membranes were washed 4 times for 5 minutes in TBST at room temperature, with mild agitation.

6.7.2.9. Exposure and development of the membranes

The membranes were briefly air-dried and the protein-side of the membranes was incubated with 1ml of ECL Plus (GE Healthcare) for 5 minutes at room temperature, following manufacturer's instructions. The membranes were, next, sealed with clear cling film and directly exposed on x-ray film in a developing cassette for varying lengths of time, depending on the signal intensity. The x-ray films were developed and the films were scanned using an HP ScanJet 4300C scanner at 600dpi.

6.7.2.10. Stripping the membranes

To incubate already used membranes in a new antibody, eliminate the signal from the first antibody, the membranes were mildly stripped in 1x Stripping buffer for 10 minutes at room temperature. The buffer was discarded and the membranes were incubated for further 10 minutes in fresh buffer at room temperature. The membranes were, then, washed twice in PBST for 10 minutes at room temperature and twice in TBST for 5 minutes at room temperature. At that point, the membranes were blocked in 2% blocking solution for 30 minutes at room temperature and primary antibody incubation was performed as described above.

6.8. Wholemount in situ *hybridisation – Recipes*

6.8.1. Day 1 ISH Recipes

20x SSC (1 L)

NaCl	175.3 g
Sodium Citrate	88.2 g
ddH_2O	800 ml

Adjust the pH to 7.0 and fill up to 1L with ddH_2O.

Hybridisation Buffer (+)/ Hyb (+) (100 ml)

Formamide	50 ml
20x SSC	25 ml
tRNA	50 mg
Heparin	50 mg
1M Citric Acid	920 µl
Tween 20	500 µl
ddH_2O	22.5 ml

pH to 6.0

6.8.2. Day 2 ISH Recipes

Hybridisation Buffer (-)/ Hyb (-) (100 ml)

Formamide	50 ml
20x SSC	25 ml
1M Citric Acid	920 µl
Tween 20	500 µl
ddH_2O	22.5 ml

pH to 6.0

2x SSC (1L)

20x SSC	100 ml
ddH_2O	900 ml

0.2xSSC (1L)

2x SSC	100 ml
ddH_2O	900 ml

6.8.3. Hyb (-) ; SSC Wash Buffers

75% Hyb (-) : 25 % SSC (50 ml)

Hyb (-)	37.5 ml
2x SSC	12.5 ml

50% Hyb (-) : 50% SSC (50 ml)

Hyb (-)	25 ml
2x SSC	25 ml

25% Hyb (-) : 75% SSC (50 ml)

Hyb (-)	12.5 ml
2x SSC	37.5 ml

6.8.4. Maleic Acid Wash Buffers

Maleic Acid Buffer (MAB) (500ml)

Maleic acid	8.31 g
NaCl	4.38 g
ddH_2O	400ml

Adjust pH to 7.5 with NaOH pellets. Fill up to 500 ml with ddH_2O.

MAB with Tween (MABT) (500 ml)

MAB	500 ml
Tween 20	500 µl

6.8.5. SSC ; MAB Wash Buffers

75% SSC: 25% MAB (50 ml)

0.2x SSC	37.5 ml
MABT	12.5 ml

50% SSC: 50% MAB (50 ml)

0.2x SSC	25 ml
MABT	25 ml

25% SSC: 75% MAB (50 ml)

0.2xSSC	12.5 ml
MABT	25 ml

6.8.6. Blocking and Antibody Staining

MAB Block (100 ml)

MAB	100 ml
Roche Blocking Reagent	2g

Dissolve at 85ºC for 30 minutes

Antibody in MAB+ Block 1:5000 dilution (50 ml)

Anti-DIG AP Antiserum*	10 µl
MAB with Block	50 ml

* Anti-Digoxigenin Alkaline Phosphatase Sheep Antiserum (Roche)

6.8.7. Day 3 ISH Recipes

Staining Buffer (150 ml)

1M Tris-HCl (pH 9.5)	15 ml
0.5M $MgCl_2$	15 ml
5M NaCl	3 ml
20% Tween 20	750 µl
ddH_2O	up to 150 ml

Stop Solution/ EDTA in PBST (100 ml)

0.5M EDTA	4 ml
PBST	96 ml

6.9. Wholemount in Situ *Hybridisation - Methodology*

6.9.1. Day 0

6.9.1.1. Embryo preparation

Embryos were collected at the appropriate stage and were moved in a 2ml sterile microcentrifuge tube in minimal solution. They were immediately fixed in fresh 4% paraformaldehyde in PBS overnight at 4ºC with mild agitation. The samples were not left in PFA for longer than 20 hours.

The next day, PFA was discarded and fixed embryos that had not hatched from their chorions, were hand-dechorionated in PBST buffer in a new Petri dish.

The samples were, subsequently placed in new microcentrifuge tubes and were serially dehydrated in PBST:Methanol solutions in the following order:

5 minutes 75% PBST; 25% MeOH
5 minutes 50% PBST; 50% MeOH
5 minutes 25% PBST; 75% MeOH
5 minutes 100% MeOH

All steps were carried out at room temperature on a rocker for mild agitation, to avoid embryos sticking together. The embryos were stored in fresh 100% MeOH and were stored for a minimum of 24 hours at -20ºC.

6.9.1.2. Riboprobe production

Plasmid recovery

DNA plasmids DNA containing the templates of interest were purified traditionally using a QIAGEN® QIAprep Spin® Miniprep/ Maxiprep Kit following manufacturer's instructions. Following plasmid purification, the DNA was eluted in 30µl of RNase-free ddH_2O. Each insert was constituted of a 900bp fragment of the gene of interest.

That short stretch of DNA was selected as having a unique enough sequence to be specific to its respective gene.

Template linearisation

The plasmids were linearised for 2 hours at 37ºC, in a 30µl reaction, using the appropriate restriction enzyme, according to the table below. Plasmids cut at the 5' end of the inserts served as DNA templates for antisense RNA probe transcription. Respectively, plasmids digested at the 3' end of the gene fragment were used to produce control sense riboprobes.

Template	*Endonuclease*	*Direction of probe*	*Transcriptional promoter*
HggI	BamHI	antisense	T7
Dlx3	SalI	antisense	T7

Table 6.3 *Transcription of hggI and dlx3 riboprobes*

Digestion reaction (30 µl)

Plasmid DNA	4ug
10x Enzyme buffer	3 µl
Enzyme	1 µl
ddH_2O	to 30 µl

Ethanol precipitation of the digest

Linear plasmid DNA was purified by ethanol precipitation. One tenth of the total volume of the restriction reaction (3µl) of 3M Sodium Acetate and twice the total volume of the restriction reaction (60µl) of 100% EtOH were added in the reaction. The 93µl mix was left at room temperature for 15 minutes. The mix was, then, centrifuged at maximum speed (13,2000 rpm) for 10 minutes at 4ºC. The supernatant was discarded and the DNA pellet was washed with 1ml of 70% EtOH. The mix was centrifuged at maximum speed for 5 minutes at 4ºC. The supernatant was, once, again, discarded and the pellet was air-dried for a few minutes. The DNA was re-suspended in 30µl of ddH_2O and was stored at -20ºC until needed.

In vitro *RNA transcription*

A total of 20µl transcription reaction was assembled on ice in RNase-free conditions. The transcription reaction was incubated at 37ºC for a minimum of 2 hours.

Transcription reaction (20 µl)

Linear purified DNA	10 µl
10x Transcription Buffer (Roche)*	2 µl
0.1M DTT	2 µl
ddH_2O	2 µl
DIG UTP mix (Roche)	2 µl
RNase inhibitor (Roche)	1 µl
RNA Polymerase (Roche)*	1 µl

* The appropriate RNA polymerase enzymes and their respective transcription buffers were used according to **Table 6.3.**

Stopping the transcription reaction

1µl of DNase (Roche) was added in the reaction and was incubated at 37ºC for 15 minutes to digest the un-transcribed DNA template. 1µl of 0.5M EDTA was added to effectively halt the enzyme activity.

RNA precipitation

1.4µl of 7.5M $LiCl_2$ and 100µl of 100% EtOH were added in the reaction and were mixed in by inverting the tube a few times gently. RNA was precipitated for a minimum of 30 minutes at -20ºC or overnight at -80ºC. The samples were, then, centrifuged at maximum speed at 4ºC for 40 minutes. The supernatant was carefully removed and the remaining RNA pellet was washed with 70% EtOH. The samples were centrifuged, again, at maximum speed at 4ºC for 10 minutes. The supernatant was discarded carefully and the RNA pellet was briefly air-dried before being re-suspended in a mix of 25µl Hyb (+) and 25µl formamide at a total volume of 50µl. The probes were stored at -20ºC and were used within 2 months.

Concentration quantification

The concentration of the eluted probes was quantified using a NanoDrop spectrophotometer, normalised to the absorption of 1:1 Hyb (+):Formamide mix, and was recorded for future reference.

6.9.2. Day 1

This protocol is a slightly modified version of the wholemount *in situ* hybridisation protocol by Thisse and Thisse (Thisse and Thisse, 2008).

The stored embryos were transferred in RNase-free in situ baskets that allowed easy transfer of the embryos between different wells with no loss of samples. The procedure was set up at room temperature, in a 24-well plate, with each well containing 1ml of the respective solution. 12 wells were used, in total, for each sample.

6.9.2.1. Re-hydration

Initially, the samples were serially re-hydrated in PBST:MeOH solutions for 5 minutes in each of 75% MeOH; 25% PBST, 50% MeOH; 50% PBST and 25% MeOH; 75% PBST.

6.9.2.2. Washes

The embryos were then washed three times, for 5 minutes each, in PBST.

6.9.2.3. Digestion

1µl of the 20mg/ml stock of Proteinase K solution was diluted in 2ml of PBST to achieve a final concentration of 10ug/ml Proteinase K. The embryos were digested in Proteinase K according to the following table.

Embryonic Stage	*Duration of Proteinase K Digestion*
Blastula- end of gastrulation stage	30 sec
1-14 Somite stage	1 min
14-22 Somite stage	5 min
1 dpf embryos	15 min
2-3 dpf embryos	30 min

Table 6.4 *Proteinase K treatment duration*

6.9.2.4. Fixing

The samples were fixed, again, for 20 minutes in 4% PFA and were washed four times in PBST, for 5 minutes each time.

6.9.2.5. Pre-hybridisation

The samples were transferred out of the baskets into sterile RNase-free tubes and were incubated in 1ml of Hyb (+) solution in a 70ºC water-bath for a minimum of 2 hours.

If necessary, the samples were stably stored at -20ºC in pre-hybridisation solution for a few days.

6.9.2.6. Hybridisation

The Hyb (+) buffer was discarded and the samples were incubated in 200µl of Probe: Hyb (+) mix, in the following optimised dilutions, at 70ºC overnight.

Hyb (+) and riboprobes (200 µl)

HggI probe	1 µl (100 ng)
Dlx3 probe	3 µl (200 ng)
Hyb (+)	196 µl

6.9.3. Day 2

The hybridised embryos were transferred in fresh RNase-free baskets and placed in specialised ISH trays that kept the baskets in place during the agitation of the motile stage of the ISH machine. The following steps were followed in the automated Biolane HTI ISH machine. 50 ml of each solution was used for each step. The steps and timings were as follows.

Solution	*Temperature*	*Duration*	*Repetitions*
Stringency Washes			
100% Hyb (-)	65ºC	10 min	1x
75% Hyb (-); 25% SSC	65ºC	10 min	1x
50% Hyb (-); 50% SSC	65ºC	10 min	1x
25% Hyb (-); 75% SSC	65ºC	10 min	1x
2x SSC	65ºC	10 min	1x
0.2x SSC	65ºC	15 min	4x
75% SSC; 25% MABT	24ºC	10 min	1x
50% SSC; 50% MABT	24ºC	10 min	1x
25% SSC; 75% MABT	24ºC	10 min	1x
MABT	24ºC	15 min	1x
Blocking and antibody incubation			
MAB Block	24ºC	1 h	1x
Anti-DIG Antibody	4ºC	12 h/ overnight	1x

6.9.4. Day 3

6.9.4.1. Washes

Following antibody absorption, the embryos were thoroughly washed and incubated in staining buffer as follows.

Solution	*Temperature*	*Duration*	*Repetitions*
Washes			
MABT	24ºC	15 min	8x
Staining			
Staining buffer	24ºC	5 min	3x

6.9.4.2. Staining

The embryos were transferred out of their tray in a 24-well ISH developing plate where they were incubated in 500µl of BM Purple staining solution (Roche) at room temperature, in the dark to avoid over-exposure, with mild agitation. The embryos were monitored at frequent intervals using a dissecting microscope and the optimal exposure time for the used probes was set to 45 minutes.

6.9.4.3. Stopping Signal Development

Once the desired signal intensity was reached, the embryos were washed three times, for 15 minutes each, in Stop solution at room temperature. As the embryos were younger than 24hpf, they were transferred in low pH PBST (pH 3.0) for 5 minutes at room temperature.

6.9.4.4. Storage

The embryos were transferred out of their baskets into six well plates, all of the PBST was removed and the samples were mounted in 100% glycerol. The embryos were stably stored in glycerol in the dark (in a dark box) at 4ºC for months. At this point, the embryos were readily imaged, illuminated from above using a Nikon SMZ 1500 stereomicroscope conjugated with a Nikon coolpix camera and were edited using Adobe Photoshop® Creative Suite 4 software package.

6.10. General DNA Techniques

6.10.1. Bacterial DNA transformation

In order to maintain bacterial stocks containing plasmids of interest, chemically competent DH5α and TOP10® (Invitrogen) *Escherichia coli* (*E. coli*) were transformed with circular plasmid DNA.

Routinely, 1-2µl of plasmid DNA was incubated in 50µl of *E. coli* on ice for a minimum of 30 minutes, in sterile 1.7ml screw-top tubes, avoiding excessive pipetting and disturbance of the cells. The bacteria were, then, heat-shocked at 42ºC for 20 seconds to promote DNA uptake and were transferred back on ice for a further 2 minutes. 250µl of pre-warmed to 37ºC, autoclaved LB broth was added in each tube and each sample was transferred in a 37ºC shaker were they were allowed to grow for 2 hours whilst horizontally being shaken at 270rpm. During this time, LB-Agar plates with selective antibiotics were being warmed in a 37ºC incubator. At the end of the 2h shaking time, the samples were centrifuged for 10 minutes at 9,000 rpm. 150µl of the supernatant were discarded and the pellet was re-suspended in the rest of the 150µl solution by pipetting up and down gently. This step concentrates the bacterial culture.

The next steps were performed within a 30cm radius of a burning blue flame of a Bunsen burner to avoid contamination of the samples. Two selective plates were used for each bacterial culture. 20µl and 100µl of the re-suspended culture were aseptically plated on the pre-warmed plates containing the appropriate selective antibiotic, corresponding to the antibiotic resistance that the plasmid confers to the bacteria. The plates were placed overnight in the 37ºC incubator.

LB Broth (1L)

Bacto-tryptone	10 g
Yeast extract	5 g
NaCl	10 g
ddH_2O	800 µl

Adjust pH to 7.5 with NaOH
Fill up to 1 L with ddH_2O and sterilise by autoclaving

LB- Agar (1L)

Bacto-tryptone	10 g
Yeast extract	5 g
NaCl	10 g
ddH_2O	800 µl

Adjust pH to 7.5 with NaOH

Agar	15 g

Melt agar in microwave
Fill up to 1L with ddH_2O and sterilise by autoclaving

Single colonies were picked from the plates with autoclaved cocktail sticks and were incubated in 5ml of LB enriched with the equivalent antibiotic at 37ºC overnight in a shaker rotating at 250rpm. This bacterial culture was further used for bacterial stock production or plasmid purification, as described below.

Antibiotic concentrations used in LB Broth and LB Agar plates	
Ampicillin	100 µg/ml
Chloramphenicol	25 µg/ml
Kanamycin	50 µg/ml

6.10.2. Plasmid DNA isolation

The 5ml bacterial cultures were directly used as a starter culture to perform a miniprep if low quantities of DNA were required or a maxiprep if larger amounts of DNA were of essence, according to manufacturer's instructions (QIAprep® Spin Miniprep/ Maxiprep Kit Protocols, QIAGEN).

6.10.3. Bacterial stock preparation

500µl of the 5ml overnight bacterial culture solution was transferred in a new sterile microcentrifuge tube. 500µl of sterile 80% glycerol was added in the tube and the solution was mixed. The samples were stably stored for long-term purposes at -80ºC.

6.10.4. DNA concentration quantification

The optical density of DNA was measured using a NanoDrop® 2000 spectrophotometer, which calculated the sample absorbance at 260nm (A_{260}). The purity of the DNA was determined by calculating the A_{260}/A_{280} ratio, which should be between 1.8 and 2.0. Values smaller than 1.8 indicated protein contamination, whereas values larger than 2.0 suggested RNA contamination.

DNA Endonuclease Digestion

Plasmid DNA	5 µg
10x Endonuclease Buffer	5 µl
Endonuclease	1 µl
ddH_2O	up to 50 µl

The ddH_2O and DNA were added first and the endonuclease was added last. If the restriction enzyme required BSA addition for optimal activity, 0.5µl of 100x BSA were added to the mix. In the case of double digestions, 0.5µl of each enzyme were added to minimise the glycerol concentration of the end reaction.

6.10.5. DNA purification after digestion

Using QIAGEN® PCR Purification Kit

Manufacturer's instructions for the above kit (using a table-top centrifuge) were followed to clean-up DNA restriction reactions using purification columns. In the final step, the DNA was eluted into 30µl of ddH_2O

Using Millipore® Microcon YM-30 purification columns

The reaction was topped up with the appropriate amount of ddH_2O to make up a total volume of 500µl and the entire mix was transferred in the Microcon tubes with the column inserts. The samples were centrifuged for 12 minutes at 10,000rpm. When the centrifugation had ended, 10 µl were added directly on the membrane of the column and the column was immediately turned upside down and placed in a new sterile collection tube. The samples were centrifuged at maximum speed (14,500 rpm) for 1 minute and the purified DNA concentration was recorded using a NanoDrop spectrophotometer, normalised to ddH_2O.

6.10.6. Sub-cloning Using the GATEWAY® System

Single-Site LR Reaction

According to manufacturer's instructions (Invitrogen) the LR® reaction was performed in a total volume of 10µl as follows:

Entry clone 50-150ng	1-7 µl
Destination vector	1 µl
TE Buffer pH 8.0	up to 8 µl
LR Clonase II enzyme	2 µl

The reaction was incubated at room temperature overnight. To stop the enzymatic activity 1µl of proteinase K was added and the mix was incubated at 37ºC for 10 minutes. 1µl of the reaction was, subsequently, transformed into chemically competent cells as described above.

Entry vectors

Construct Name	*Backbone Vector*	*Antibiotic Resistance*	*Host Cells*
BRAF WT**	pENTR3C	Kanamycin	DH5α
BRAF A246P**	pENTR3C	Kanamycin	DH5α
BRAF Q257R**	pENTR3C	Kanamycin	DH5α
BRAF G464V**	pENTR3C	Kanamycin	DH5α
BRAF S467A**	pENTR3C	Kanamycin	DH5α
BRAF K483M**	pENTR3C	Kanamycin	TOP10
BRAF K499E**	pENTR3C	Kanamycin	DH5α
BRAF G534R**	pENTR3C	Kanamycin	DH5α
BRAF N581D**	pENTR3C	Kanamycin	DH5α
BRAF D594V**	pENTR3C	Kanamycin	DH5α
BRAF G596V**	pENTR3C	Kanamycin	DH5α
BRAF T599E/S602D**	pENTR3C	Kanamycin	DH5α
BRAF V600E**	pENTR3C	Kanamycin	DH5α
BRAF D638E**	pENTR3C	Kanamycin	DH5α
MEK1 WT**	pENTR3C	Kanamycin	DH5α
MEK1 F53S**	pENTR3C	Kanamycin	DH5α
MEK1 F53L**	pENTR3C	Kanamycin	DH5α
MEK1T55P**	pENTR3C	Kanamycin	DH5α
MEK1 K97M**	pENTR3C	Kanamycin	DH5α
MEK1 G128V**	pENTR3C	Kanamycin	DH5α
MEK1 Y130C**	pENTR3C	Kanamycin	DH5α
MEK1 S218D/S222D**	pENTR3C	Kanamycin	DH5α
MEK1 constitutively active**	pENTR3C	Kanamycin	TOP10
MEK2 WT**	pENTR3C	Kanamycin	DH5α
MEK2 F57C**	pENTR3C	Kanamycin	DH5α
MEK2 A62P**	pENTR3C	Kanamycin	DH5α
MEK2 K101M**	pENTR3C	Kanamycin	DH5α
MEK2 G132V**	pENTR3C	Kanamycin	DH5α
MEK2 Y134C**	pENTR3C	Kanamycin	DH5α
MEK2 S222D/S226D**	pENTR3C	Kanamycin	DH5α
MEK2 K273R**	pENTR3C	Kanamycin	DH5α
HRAS WT**	pENTR3C	Kanamycin	DH5α
HRAS G12V**	pENTR3C	Kanamycin	DH5α
HRAS G12S**	pENTR3C	Kanamycin	TOP10
HRAS G12A**	pENTR3C	Kanamycin	TOP10
HRAS G12V**	pENTR3C	Kanamycin	TOP10
HRAS G13C**	pENTR3C	Kanamycin	DH5α
HRAS G13D**	pENTR3C	Kanamycin	DH5α
HRAS Q22K**	pENTR3C	Kanamycin	DH5α
HRAS Q61L**	pENTR3C	Kanamycin	TOP10
HRAS E63K**	pENTR3C	Kanamycin	TOP10
HRAS K117R**	pENTR3C	Kanamycin	TOP10
HRAS A146T**	pENTR3C	Kanamycin	TOP10

** Sent as part of a collaboration with Katherine A. Rauen (UCSF)

Destination Vectors

Construct Name	*Backbone Vector*	*Antibiotic Resistance*	*Host Cells*
BRAF WT	pDEST17	Ampicillin	TOP10
BRAF A246P	pDEST17	Ampicillin	DH5α
BRAF Q257R	pDEST17	Ampicillin	DH5α
BRAF G464V	pDEST17	Ampicillin	DH5α
BRAF S467A	pDEST17	Ampicillin	TOP10
BRAF K483M	pDEST17	Ampicillin	TOP10
BRAF K499E	pDEST17	Ampicillin	DH5α
BRAF G534R	pDEST17	Ampicillin	DH5α
BRAF N581D	pDEST17	Ampicillin	DH5α
BRAF D594V	pDEST17	Ampicillin	TOP10
BRAF G596V	pDEST17	Ampicillin	TOP10
BRAF T599E/S602D	pDEST17	Ampicillin	DH5α
BRAF V600E	pDEST17	Ampicillin	TOP10
BRAF D638E	pDEST17	Ampicillin	DH5α
MEK1 WT	pDEST17	Ampicillin	DH5α
MEK1 F53S	pDEST17	Ampicillin	DH5α
MEK1 F53L	pDEST17	Ampicillin	DH5α
MEK1T55P	pDEST17	Ampicillin	DH5α
MEK1 K97M	pDEST17	Ampicillin	DH5α
MEK1 G128V	pDEST17	Ampicillin	DH5α
MEK1 Y130C	pDEST17	Ampicillin	DH5α
MEK1 S218D/S222D	pDEST17	Ampicillin	DH5α
MEK1 constitutively active	pDEST17	Ampicillin	TOP10
MEK2 WT	pDEST17	Ampicillin	DH5α
MEK2 F57C	pDEST17	Ampicillin	DH5α
MEK2 A62P	pDEST17	Ampicillin	DH5α
MEK2 K101M	pDEST17	Ampicillin	DH5α
MEK2 G132V	pDEST17	Ampicillin	DH5α
MEK2 Y134C	pDEST17	Ampicillin	DH5α
MEK2 S222D/S226D	pDEST17	Ampicillin	DH5α
MEK2 K273R	pDEST17	Ampicillin	DH5α
pT2Kmin-NP Dest RfA*		Ampicillin	DH5α
mitfa- BRAF WT	pT2min-NP Dest	Ampicillin	Top 10
mitfa- BRAF Q257R	pT2min-NP Dest	Ampicillin	Top 10
mitfa- BRAF S467A	pT2min-NP Dest	Ampicillin	Top 10
mitfa- BRAF D594V	pT2min-NP Dest	Ampicillin	Top 10
mitfa- BRAF G596V	pT2min-NP Dest	Ampicillin	Top 10
mitfa- BRAF V600E	pT2min-NP Dest	Ampicillin	Top 10

* Sent by James Lister (Virginia Commonwealth University)

6.11. Capped mRNA production

Capped mRNA synthesis was performed using AMBION® mMESSAGE mMACHINE SP6 and T7 Ultra kits. The in vitro transcribed synthetic mRNA was capped with a 7-methyl guanosine, a structure that could only be incorporated at the 5' end of the construct.

Linear purified DNA (as described above) that did not exceed 2Kb in length served as a template for in vitro transcription of sense mRNA following manufacturer's instructions. A total volume of 20µl was achieved by assembling the reaction at room temperature, in the following order to avoid reagents precipitating out.

2x NTP/Cap mix (pre-mixed to a 1:4 final ratio)	10 µl
10x Enzyme Buffer mix	2 µl
DNA linearised purified	6 µl
T7/SP6 Enzyme mix	2 µl

The reaction was incubated at 37ºC for 2hours and was stopped by adding 30µl ddH_2O and 30µl of LiCl solution (7.5M LiCl in 50mM EDTA). The RNA was precipitated by transferring the mix at -20ºC for a minimum of 40 minutes. The samples were, then, centrifuged at maximum speed (13,200 rpm) at 4ºC for 15 minutes. The supernatant was discarded and the resulting RNA pellet was washed with 70% EtOH to remove any residual ribonucleotides. The samples were centrifuged for a further 10 minutes at maximum speed. The EtOH was removed and the RNA pellet was re-suspended in 30µl ddH_2O. The RNA concentration was determined using a NanoDrop 2000 spectrophotometer and the RNA quality was checked both by calculating the A_{260}/A_{280} ratio on the NanoDrop and by running an aliquot of each sample on a 1% agarose Ethidium Bromide gel at 120V for 20minutes.

6.12. Alcian Blue Staining of Cartilage

Calculation of exact volumes was not necessary for the cartilage staining protocol, unless otherwise stated. It was important, however, that the embryos were always fully immersed in their equivalent solutions to avoid damage of the tissue, drying out and lack of staining.

6.12.1. Embryo collection and fixing

Embryos were collected at 5dpf and were transferred in a well of a 6-well plate, to ensure maximum solution penetration and to avoid embryos sticking together. After the maximum amount of embryo medium was removed, the embryos were immediately fixed in freshly prepared 4% PFA in PBS. The samples were fixed at room temperature with mild agitation for 7 hours. It was important that the embryos were not fixed for longer than 10 hours as that would affect the tissue permeability and, hence, the staining results.

6.12.2. Post-fixing washes

The PFA was discarded and the embryos were quickly rinsed in PBST before being transferred into a new well, to avoid PFA carry-over. The embryos were, subsequently, washed three times, for 5 minutes each, in PBST. If required, the embryos were stored overnight in PBST at 4ºC at this point.

6.12.3. Staining

The PBST was removed and the embryos were incubated in freshly made, syringe-filtered 0.1% Alcian Blue solution for approximately 7 hours at room temperature. As the duration of this incubation step varied from 5-10 hours, depending on the

samples, the embryos were monitored every 30 minutes under a light microscope after 4 hours of staining were completed, to avoid over-staining.

0.1% PBST (100ml)

PBS	100 ml
Tween- 20	100 µl

0.1% Alcian Blue Staining Solution (100 ml)

Alcian Blue 8GX (Sigma Aldrich)	100 mg
100% EtOH	80 ml
1M Glacial Acetic Acid	20 ml

6.12.4. Post-staining washes

The stain was discarded and the embryos were rinsed in 100% EtOH for a few seconds. The samples were, then, serially rehydrated in PBST in the following order, for 5 minutes each, at room temperature.

70% EtOH; 30% PBST
50% EtOH; 50% PBST
30% EtOH; 70% PBST
100% PBST

The stained embryos were stored in 100% PBST at 4ºC overnight.

6.12.5. Tissue clearing

PBST was discarded and was replaced by 0.05% GIBCO® Trypsin (Invitrogen) in PBS. The samples were incubated in trypsin at 30ºC for a minimum of 2 hours and were regularly monitored to avoid over-digestion of the embryos. The reaction was completed when the brain tissue was completely clear.

6.12.6. Bleaching, washes and storage

After removing the trypsin, all residual embryo pigmentation was cleared by adding fresh bleaching solution. This step was rapid (approximately 5 minutes) and was performed under constant monitoring under a stereomicroscope at room temperature. The bleaching was halted when the eye pigmentation was completely gone.

1% Bleaching Solution in 3% H_2O_2 (50 ml)

KOH pellets	500 mg
30% Hydrogen peroxide (Sigma)	5 ml
PBST	45 ml

To stop the bleaching reaction, the solution was replaced with PBST and the embryos were washed three times, for 5 minutes each time, in fresh PBST.

The samples were, then serially mounted in glycerol at room temperature, in the following order.

70% PBST; 30% Glycerol for 5 minutes
50% PBST; 50% Glycerol for 5 minutes
30% PBST; 70% Glycerol for 5 minutes

The embryos were stably stored in the 70% Glycerol solution at 4ºC for a few months.

6.12.7. Imaging

The mounted embryos were micro-dissected with dissection forceps in order to remove all the tissue surrounding the craniofacial cartilage. Only the stained jaw structures were kept whilst the rest of the tissue was discarded. The mounted cartilage was imaged using a Nikon microscope and IP Lab imaging software and the images were edited using Adobe Photoshop® Creative Suite 4 software package.

References

- **Abe, M. K., Saelzler, M. P., Espinosa, R., 3rd, Kahle, K. T., Hershenson, M. B., Le Beau, M. M. and Rosner, M. R.** (2002). ERK8, a new member of the mitogen-activated protein kinase family. *J Biol Chem* **277**, 16733-43.
- **Abu-Issa, R., Smyth, G., Smoak, I., Yamamura, K. and Meyers, E. N.** (2002). Fgf8 is required for pharyngeal arch and cardiovascular development in the mouse. *Development* **129**, 4613-25.
- **Ahn, N. G., Nahreini, T. S., Tolwinski, N. S. and Resing, K. A.** (2001). Pharmacologic inhibitors of MKK1 and MKK2. *Methods Enzymol* **332**, 417-31.
- **Allen, L. F., Sebolt-Leopold, J. and Meyer, M. B.** (2003). CI-1040 (PD184352), a targeted signal transduction inhibitor of MEK (MAPKK). *Semin Oncol* **30**, 105-16.
- **Alsina, M., Fonseca, R., Wilson, E. F., Belle, A. N., Gerbino, E., Price-Troska, T., Overton, R. M., Ahmann, G., Bruzek, L. M., Adjei, A. A. et al.** (2004). Farnesyltransferase inhibitor tipifarnib is well tolerated, induces stabilization of disease, and inhibits farnesylation and oncogenic/tumor survival pathways in patients with advanced multiple myeloma. *Blood* **103**, 3271-7.
- **Aman, A. and Piotrowski, T.** (2009). Multiple signaling interactions coordinate collective cell migration of the posterior lateral line primordium. *Cell Adh Migr* **3**, 365-8.
- **Amatruda, J. F., Shepard, J. L., Stern, H. M. and Zon, L. I.** (2002). Zebrafish as a cancer model system. *Cancer Cell* **1**, 229-31.
- **Amsterdam, A. and Hopkins, N.** (2006). Mutagenesis strategies in zebrafish for identifying genes involved in development and disease. *Trends Genet* **22**, 473-8.
- **Anderson, J., Burns, H. D., Enriquez-Harris, P., Wilkie, A. O. and Heath, J. K.** (1998). Apert syndrome mutations in fibroblast growth factor receptor 2 exhibit increased affinity for FGF ligand. *Hum Mol Genet* **7**, 1475-83.
- **Aoki, Y., Niihori, T., Kawame, H., Kurosawa, K., Ohashi, H., Tanaka, Y., Filocamo, M., Kato, K., Suzuki, Y., Kure, S. et al.** (2005). Germline mutations in HRAS proto-oncogene cause Costello syndrome. *Nat Genet* **37**, 1038-40.
- **Aoki, Y., Niihori, T., Narumi, Y., Kure, S. and Matsubara, Y.** (2008). The RAS/MAPK syndromes: novel roles of the RAS pathway in human genetic disorders. *Hum Mutat* **29**, 992-1006.
- **Auman, H. J. and Yelon, D.** (2004). Vertebrate organogenesis: getting the heart into shape. *Curr Biol* **14**, R152-3.
- **authors, n. l.** (2011). Deal watch: HGS and FivePrime in FGF 'ligand trap' deal. *Nat Rev Drug Discov* **10**, 328.
- **Axelrad, M. E., Glidden, R., Nicholson, L. and Gripp, K. W.** (2004). Adaptive skills, cognitive, and behavioral characteristics of Costello

syndrome. *Am J Med Genet A* **128A**, 396-400.

- **Azam, M., Seeliger, M. A., Gray, N. S., Kuriyan, J. and Daley, G. Q.** (2008). Activation of tyrosine kinases by mutation of the gatekeeper threonine. *Nat Struct Mol Biol* **15**, 1109-18.
- **Baccarini, M.** (2005). Second nature: biological functions of the Raf-1 "kinase". *FEBS Lett* **579**, 3271-7.
- **Bader-Meunier, B., Tchernia, G., Mielot, F., Fontaine, J. L., Thomas, C., Lyonnet, S., Lavergne, J. M. and Dommergues, J. P.** (1997). Occurrence of myeloproliferative disorder in patients with Noonan syndrome. *J Pediatr* **130**, 885-9.
- **Baillie, G. S., MacKenzie, S. J., McPhee, I. and Houslay, M. D.** (2000). Sub-family selective actions in the ability of Erk2 MAP kinase to phosphorylate and regulate the activity of PDE4 cyclic AMP-specific phosphodiesterases. *Br J Pharmacol* **131**, 811-9.
- **Ballester, R., Marchuk, D., Boguski, M., Saulino, A., Letcher, R., Wigler, M. and Collins, F.** (1990). The NF1 locus encodes a protein functionally related to mammalian GAP and yeast IRA proteins. *Cell* **63**, 851-9.
- **Barkan, B., Starinsky, S., Friedman, E., Stein, R. and Kloog, Y.** (2006). The Ras inhibitor farnesylthiosalicylic acid as a potential therapy for neurofibromatosis type 1. *Clin Cancer Res* **12**, 5533-42.
- **Barrett, S. D., Bridges, A. J., Dudley, D. T., Saltiel, A. R., Fergus, J. H., Flamme, C. M., Delaney, A. M., Kaufman, M., LePage, S., Leopold, W. R. et al.** (2008). The discovery of the benzhydroxamate MEK inhibitors CI-1040 and PD 0325901. *Bioorg Med Chem Lett* **18**, 6501-4.
- **Beavo, J. A. and Brunton, L. L.** (2002). Cyclic nucleotide research -- still expanding after half a century. *Nat Rev Mol Cell Biol* **3**, 710-8.
- **Bedogni, B., Welford, S. M., Kwan, A. C., Ranger-Moore, J., Saboda, K. and Powell, M. B.** (2006). Inhibition of phosphatidylinositol-3-kinase and mitogen-activated protein kinase kinase 1/2 prevents melanoma development and promotes melanoma regression in the transgenic TPRas mouse model. *Mol Cancer Ther* **5**, 3071-7.
- **Bennett, D. C.** (2003). Human melanocyte senescence and melanoma susceptibility genes. *Oncogene* **22**, 3063-9.
- **Bentires-Alj, M., Kontaridis, M. I. and Neel, B. G.** (2006). Stops along the RAS pathway in human genetic disease. *Nat Med* **12**, 283-5.
- **Berbari, N. F., Lewis, J. S., Bishop, G. A., Askwith, C. C. and Mykytyn, K.** (2008). Bardet-Biedl syndrome proteins are required for the localization of G protein-coupled receptors to primary cilia. *Proc Natl Acad Sci U S A* **105**, 4242-6.
- **Bergo, M. O., Gavino, B. J., Hong, C., Beigneux, A. P., McMahon, M., Casey, P. J. and Young, S. G.** (2004). Inactivation of Icmt inhibits transformation by oncogenic K-Ras and B-Raf. *J Clin Invest* **113**, 539-50.
- **Bertola, D. R., Kim, C. A., Pereira, A. C., Mota, G. F., Krieger, J. E., Vieira, I. C., Valente, M., Loreto, M. R., Magalhaes, R. P. and Gonzalez,**

C. H. (2001). Are Noonan syndrome and Noonan-like/multiple giant cell lesion syndrome distinct entities? *Am J Med Genet* **98**, 230-4.

- **Bertola, D. R., Pereira, A. C., Passetti, F., de Oliveira, P. S., Messiaen, L., Gelb, B. D., Kim, C. A. and Krieger, J. E.** (2005). Neurofibromatosis-Noonan syndrome: molecular evidence of the concurrence of both disorders in a patient. *Am J Med Genet A* **136**, 242-5.
- **Best, J. D., Berghmans, S., Hunt, J. J., Clarke, S. C., Fleming, A., Goldsmith, P. and Roach, A. G.** (2008). Non-associative learning in larval zebrafish. *Neuropsychopharmacology* **33**, 1206-15.
- **Bian, D., Su, S., Mahanivong, C., Cheng, R. K., Han, Q., Pan, Z. K., Sun, P. and Huang, S.** (2004). Lysophosphatidic Acid Stimulates Ovarian Cancer Cell Migration via a Ras-MEK Kinase 1 Pathway. *Cancer Res* **64**, 4209-17.
- **Bishop, A. C.** (2004). A hot spot for protein kinase inhibitor sensitivity. *Chem Biol* **11**, 587-9.
- **Bogoyevitch, M. A. and Court, N. W.** (2004). Counting on mitogen-activated protein kinases--ERKs 3, 4, 5, 6, 7 and 8. *Cell Signal* **16**, 1345-54.
- **Bolger, G. B., Erdogan, S., Jones, R. E., Loughney, K., Scotland, G., Hoffmann, R., Wilkinson, I., Farrell, C. and Houslay, M. D.** (1997). Characterization of five different proteins produced by alternatively spliced mRNAs from the human cAMP-specific phosphodiesterase PDE4D gene. *Biochem J* **328 (Pt 2)**, 539-48.
- **Bollag, G., Freeman, S., Lyons, J. F. and Post, L. E.** (2003). Raf pathway inhibitors in oncology. *Curr Opin Investig Drugs* **4**, 1436-41.
- **Boolell, M., Allen, M. J., Ballard, S. A., Gepi-Attee, S., Muirhead, G. J., Naylor, A. M., Osterloh, I. H. and Gingell, C.** (1996). Sildenafil: an orally active type 5 cyclic GMP-specific phosphodiesterase inhibitor for the treatment of penile erectile dysfunction. *Int J Impot Res* **8**, 47-52.
- **Brems, H., Chmara, M., Sahbatou, M., Denayer, E., Taniguchi, K., Kato, R., Somers, R., Messiaen, L., De Schepper, S., Fryns, J. P. et al.** (2007). Germline loss-of-function mutations in SPRED1 cause a neurofibromatosis 1-like phenotype. *Nat Genet* **39**, 1120-6.
- **Brown, J. A., Gianino, S. M. and Gutmann, D. H.** (2010). Defective cAMP generation underlies the sensitivity of CNS neurons to neurofibromatosis-1 heterozygosity. *J Neurosci* **30**, 5579-89.
- **Browning, J. L., Patel, T., Brandt, P. C., Young, K. A., Holcomb, L. A. and Hicks, P. B.** (2005). Clozapine and the mitogen-activated protein kinase signal transduction pathway: implications for antipsychotic actions. *Biol Psychiatry* **57**, 617-23.
- **Burkitt Wright, E. M. and Kerr, B.** (2010). RAS-MAPK pathway disorders: important causes of congenital heart disease, feeding difficulties, developmental delay and short stature. *Arch Dis Child* **95**, 724-30.
- **Burns, A. J. and Pachnis, V.** (2009). Development of the enteric nervous system: bringing together cells, signals and genes. *Neurogastroenterol Motil* **21**, 100-2.

- **Bustinza-Linares, E., Kurzrock, R. and Tsimberidou, A. M.** (2010). Salirasib in the treatment of pancreatic cancer. *Future Oncol* **6**, 885-91.
- **Cahill, G. M.** (2002). Clock mechanisms in zebrafish. *Cell Tissue Res* **309**, 27-34.
- **Cappellen, D., De Oliveira, C., Ricol, D., de Medina, S., Bourdin, J., Sastre-Garau, X., Chopin, D., Thiery, J. P. and Radvanyi, F.** (1999). Frequent activating mutations of FGFR3 in human bladder and cervix carcinomas. *Nat Genet* **23**, 18-20.
- **Cavanaugh, J. E., Ham, J., Hetman, M., Poser, S., Yan, C. and Xia, Z.** (2001). Differential regulation of mitogen-activated protein kinases ERK1/2 and ERK5 by neurotrophins, neuronal activity, and cAMP in neurons. *J Neurosci* **21**, 434-43.
- **Chai, Y., Jiang, X., Ito, Y., Bringas, P., Jr., Han, J., Rowitch, D. H., Soriano, P., McMahon, A. P. and Sucov, H. M.** (2000). Fate of the mammalian cranial neural crest during tooth and mandibular morphogenesis. *Development* **127**, 1671-9.
- **Chang, L. and Karin, M.** (2001). Mammalian MAP kinase signalling cascades. *Nature* **410**, 37-40.
- **Chapman, M. S. and Miner, J. N.** (2011). Novel mitogen-activated protein kinase kinase inhibitors. *Expert Opin Investig Drugs* **20**, 209-20.
- **Chen, P. C., Wakimoto, H., Conner, D., Araki, T., Yuan, T., Roberts, A., Seidman, C. E., Bronson, R., Neel, B. G., Seidman, J. G. et al.** (2010). Activation of multiple signaling pathways causes developmental defects in mice with a Noonan syndrome-associated Sos1 mutation. *J Clin Invest* **120**, 4353-65.
- **Cheung, M., Chaboissier, M. C., Mynett, A., Hirst, E., Schedl, A. and Briscoe, J.** (2005). The transcriptional control of trunk neural crest induction, survival, and delamination. *Dev Cell* **8**, 179-92.
- **Chiappini, F., Cunha, L. L., Harris, J. C. and Hollenberg, A. N.** (2011). Lack of cAMP-response element-binding protein 1 in the hypothalamus causes obesity. *J Biol Chem* **286**, 8094-105.
- **Chizhikov, V. V. and Millen, K. J.** (2004). Mechanisms of roof plate formation in the vertebrate CNS. *Nat Rev Neurosci* **5**, 808-12.
- **Choong, K., Freedman, M. H., Chitayat, D., Kelly, E. N., Taylor, G. and Zipursky, A.** (1999). Juvenile myelomonocytic leukemia and Noonan syndrome. *J Pediatr Hematol Oncol* **21**, 523-7.
- **Cirstea, I. C., Kutsche, K., Dvorsky, R., Gremer, L., Carta, C., Horn, D., Roberts, A. E., Lepri, F., Merbitz-Zahradnik, T., Konig, R. et al.** (2010). A restricted spectrum of NRAS mutations causes Noonan syndrome. *Nat Genet* **42**, 27-9.
- **Clark, J. W., Eder, J. P., Ryan, D., Lathia, C. and Lenz, H. J.** (2005). Safety and pharmacokinetics of the dual action Raf kinase and vascular endothelial growth factor receptor inhibitor, BAY 43-9006, in patients with advanced, refractory solid tumors. *Clin Cancer Res* **11**, 5472-80.

- **Corcoran, R. B., Dias-Santagata, D., Bergethon, K., Iafrate, A. J., Settleman, J. and Engelman, J. A.** (2010). BRAF gene amplification can promote acquired resistance to MEK inhibitors in cancer cells harboring the BRAF V600E mutation. *Sci Signal* **3**, ra84.
- **Cordero, D. R., Brugmann, S., Chu, Y., Bajpai, R., Jame, M. and Helms, J. A.** (2010). Cranial neural crest cells on the move: Their roles in craniofacial development. *Am J Med Genet A*.
- **Corson, L. B., Yamanaka, Y., Lai, K. M. and Rossant, J.** (2003). Spatial and temporal patterns of ERK signaling during mouse embryogenesis. *Development* **130**, 4527-37.
- **Cortes, J. and Kantarjian, H.** (2003). Advanced-phase chronic myeloid leukemia. *Semin Hematol* **40**, 79-86.
- **Costello, J. M.** (1977). A new syndrome: mental subnormality and nasal papillomata. *Aust Paediatr J* **13**, 114-8.
- **Costello, J. M.** (1996). Costello syndrome: update on the original cases and commentary. *Am J Med Genet* **62**, 199-201.
- **Coulombe, P. and Meloche, S.** (2007). Atypical mitogen-activated protein kinases: structure, regulation and functions. *Biochim Biophys Acta* **1773**, 1376-87.
- **Cowley, S., Paterson, H., Kemp, P. and Marshall, C. J.** (1994). Activation of MAP kinase kinase is necessary and sufficient for PC12 differentiation and for transformation of NIH 3T3 cells. *Cell* **77**, 841-52.
- **Creuzet, S., Schuler, B., Couly, G. and Le Douarin, N. M.** (2004). Reciprocal relationships between Fgf8 and neural crest cells in facial and forebrain development. *Proc Natl Acad Sci U S A* **101**, 4843-7.
- **Croonen, E. A., van der Burgt, I., Kapusta, L. and Draaisma, J. M.** (2008). Electrocardiography in Noonan syndrome PTPN11 gene mutation--phenotype characterization. *Am J Med Genet A* **146**, 350-3.
- **Crump, J. G., Maves, L., Lawson, N. D., Weinstein, B. M. and Kimmel, C. B.** (2004). An essential role for Fgfs in endodermal pouch formation influences later craniofacial skeletal patterning. *Development* **131**, 5703-16.
- **Daginakatte, G. C. and Gutmann, D. H.** (2007). Neurofibromatosis-1 (Nf1) heterozygous brain microglia elaborate paracrine factors that promote Nf1-deficient astrocyte and glioma growth. *Hum Mol Genet* **16**, 1098-112.
- **Dankort, D., Curley, D. P., Cartlidge, R. A., Nelson, B., Karnezis, A. N., Damsky, W. E., Jr., You, M. J., DePinho, R. A., McMahon, M. and Bosenberg, M.** (2009). Braf(V600E) cooperates with Pten loss to induce metastatic melanoma. *Nat Genet* **41**, 544-52.
- **Dasgupta, B., Li, W., Perry, A. and Gutmann, D. H.** (2005). Glioma formation in neurofibromatosis 1 reflects preferential activation of K-RAS in astrocytes. *Cancer Res* **65**, 236-45.
- **David, N. B., Saint-Etienne, L., Tsang, M., Schilling, T. F. and Rosa, F. M.** (2002). Requirement for endoderm and FGF3 in ventral head skeleton formation. *Development* **129**, 4457-68.

- **Davies, H., Bignell, G. R., Cox, C., Stephens, P., Edkins, S., Clegg, S., Teague, J., Woffendin, H., Garnett, M. J., Bottomley, W. et al.** (2002). Mutations of the BRAF gene in human cancer. *Nature* **417**, 949-54.
- **Davies, S. P., Reddy, H., Caivano, M. and Cohen, P.** (2000). Specificity and mechanism of action of some commonly used protein kinase inhibitors. *Biochem J* **351**, 95-105.
- **De Luca, A., Bottillo, I., Sarkozy, A., Carta, C., Neri, C., Bellacchio, E., Schirinzi, A., Conti, E., Zampino, G., Battaglia, A. et al.** (2005). NF1 gene mutations represent the major molecular event underlying neurofibromatosis-Noonan syndrome. *Am J Hum Genet* **77**, 1092-101.
- **Digilio, M. C., Conti, E., Sarkozy, A., Mingarelli, R., Dottorini, T., Marino, B., Pizzuti, A. and Dallapiccola, B.** (2002). Grouping of multiple-lentigines/LEOPARD and Noonan syndromes on the PTPN11 gene. *Am J Hum Genet* **71**, 389-94.
- **Digilio, M. C., Sarkozy, A., de Zorzi, A., Pacileo, G., Limongelli, G., Mingarelli, R., Calabro, R., Marino, B. and Dallapiccola, B.** (2006). LEOPARD syndrome: clinical diagnosis in the first year of life. *Am J Med Genet A* **140**, 740-6.
- **Driever, W., Solnica-Krezel, L., Schier, A. F., Neuhauss, S. C., Malicki, J., Stemple, D. L., Stainier, D. Y., Zwartkruis, F., Abdelilah, S., Rangini, Z. et al.** (1996). A genetic screen for mutations affecting embryogenesis in zebrafish. *Development* **123**, 37-46.
- **Dudley, D. T., Pang, L., Decker, S. J., Bridges, A. J. and Saltiel, A. R.** (1995). A synthetic inhibitor of the mitogen-activated protein kinase cascade. *Proc Natl Acad Sci U S A* **92**, 7686-9.
- **Duman, C. H., Schlesinger, L., Kodama, M., Russell, D. S. and Duman, R. S.** (2007). A role for MAP kinase signaling in behavioral models of depression and antidepressant treatment. *Biol Psychiatry* **61**, 661-70.
- **Dumaz, N., Hayward, R., Martin, J., Ogilvie, L., Hedley, D., Curtin, J. A., Bastian, B. C., Springer, C. and Marais, R.** (2006). In melanoma, RAS mutations are accompanied by switching signaling from BRAF to CRAF and disrupted cyclic AMP signaling. *Cancer Res* **66**, 9483-91.
- **Dumaz, N. and Marais, R.** (2003). Protein kinase A blocks Raf-1 activity by stimulating 14-3-3 binding and blocking Raf-1 interaction with Ras. *J Biol Chem* **278**, 29819-23.
- **Duric, V., Banasr, M., Licznerski, P., Schmidt, H. D., Stockmeier, C. A., Simen, A. A., Newton, S. S. and Duman, R. S.** (2010). A negative regulator of MAP kinase causes depressive behavior. *Nat Med* **16**, 1328-32.
- **Dutton, K. A., Pauliny, A., Lopes, S. S., Elworthy, S., Carney, T. J., Rauch, J., Geisler, R., Haffter, P. and Kelsh, R. N.** (2001). Zebrafish colourless encodes sox10 and specifies non-ectomesenchymal neural crest fates. *Development* **128**, 4113-25.
- **Eblen, S. T., Slack-Davis, J. K., Tarcsafalvi, A., Parsons, J. T., Weber, M. J. and Catling, A. D.** (2004). Mitogen-activated protein kinase feedback

phosphorylation regulates MEK1 complex formation and activation during cellular adhesion. *Mol Cell Biol* **24**, 2308-17.

- **Eckel-Mahan, K. L., Phan, T., Han, S., Wang, H., Chan, G. C., Scheiner, Z. S. and Storm, D. R.** (2008). Circadian oscillation of hippocampal MAPK activity and cAmp: implications for memory persistence. *Nat Neurosci* **11**, 1074-82.
- **Edouard, T., Montagner, A., Dance, M., Conte, F., Yart, A., Parfait, B., Tauber, M., Salles, J. P. and Raynal, P.** (2007). How do Shp2 mutations that oppositely influence its biochemical activity result in syndromes with overlapping symptoms? *Cell Mol Life Sci* **64**, 1585-90.
- **Escudier, B., Eisen, T., Stadler, W. M., Szczylik, C., Oudard, S., Siebels, M., Negrier, S., Chevreau, C., Solska, E., Desai, A. A. et al.** (2007). Sorafenib in advanced clear-cell renal-cell carcinoma. *N Engl J Med* **356**, 125-34.
- **Escudier, B., Eisen, T., Stadler, W. M., Szczylik, C., Oudard, S., Staehler, M., Negrier, S., Chevreau, C., Desai, A. A., Rolland, F. et al.** (2009). Sorafenib for treatment of renal cell carcinoma: Final efficacy and safety results of the phase III treatment approaches in renal cancer global evaluation trial. *J Clin Oncol* **27**, 3312-8.
- **Estep, A. L., Palmer, C., McCormick, F. and Rauen, K. A.** (2007). Mutation analysis of BRAF, MEK1 and MEK2 in 15 ovarian cancer cell lines: implications for therapy. *PLoS One* **2**, e1279.
- **Evensen, L., Link, W. and Lorens, J. B.** (2010). Imaged-based high-throughput screening for anti-angiogenic drug discovery. *Curr Pharm Des* **16**, 3958-63.
- **Fagman, H. and Nilsson, M.** (2010). Morphogenesis of the thyroid gland. *Mol Cell Endocrinol* **323**, 35-54.
- **Favata, M. F., Horiuchi, K. Y., Manos, E. J., Daulerio, A. J., Stradley, D. A., Feeser, W. S., Van Dyk, D. E., Pitts, W. J., Earl, R. A., Hobbs, F. et al.** (1998). Identification of a novel inhibitor of mitogen-activated protein kinase kinase. *J Biol Chem* **273**, 18623-32.
- **Feingold, M.** (1999). Costello syndrome and rhabdomyosarcoma. *J Med Genet* **36**, 582-3.
- **Ferner, R. E.** (2007). Neurofibromatosis 1. *Eur J Hum Genet* **15**, 131-8.
- **Ferrero, G. B., Baldassarre, G., Delmonaco, A. G., Biamino, E., Banaudi, E., Carta, C., Rossi, C. and Silengo, M. C.** (2008). Clinical and molecular characterization of 40 patients with Noonan syndrome. *Eur J Med Genet* **51**, 566-72.
- **Fischer, H., Taylor, N., Allerstorfer, S., Grusch, M., Sonvilla, G., Holzmann, K., Setinek, U., Elbling, L., Cantonati, H., Grasl-Kraupp, B. et al.** (2008). Fibroblast growth factor receptor-mediated signals contribute to the malignant phenotype of non-small cell lung cancer cells: therapeutic implications and synergism with epidermal growth factor receptor inhibition. *Mol Cancer Ther* **7**, 3408-19.

- **Franceschini, P., Licata, D., Di Cara, G., Guala, A., Bianchi, M., Ingrosso, G. and Franceschini, D.** (1999). Bladder carcinoma in Costello syndrome: report on a patient born to consanguineous parents and review. *Am J Med Genet* **86**, 174-9.
- **Friday, B. B. and Adjei, A. A.** (2008). Advances in targeting the Ras/Raf/MEK/Erk mitogen-activated protein kinase cascade with MEK inhibitors for cancer therapy. *Clin Cancer Res* **14**, 342-6.
- **Friedman, A. and Perrimon, N.** (2006). A functional RNAi screen for regulators of receptor tyrosine kinase and ERK signalling. *Nature* **444**, 230-4.
- **Fukuda, M., Horibe, K., Miyajima, Y., Matsumoto, K. and Nagashima, M.** (1997). Spontaneous remission of juvenile chronic myelomonocytic leukemia in an infant with Noonan syndrome. *J Pediatr Hematol Oncol* **19**, 177-9.
- **Furthauer, M., Lin, W., Ang, S. L., Thisse, B. and Thisse, C.** (2002). Sef is a feedback-induced antagonist of Ras/MAPK-mediated FGF signalling. *Nat Cell Biol* **4**, 170-4.
- **Furthauer, M., Thisse, C. and Thisse, B.** (1997). A role for FGF-8 in the dorsoventral patterning of the zebrafish gastrula. *Development* **124**, 4253-64.
- **Furthauer, M., Van Celst, J., Thisse, C. and Thisse, B.** (2004). Fgf signalling controls the dorsoventral patterning of the zebrafish embryo. *Development* **131**, 2853-64.
- **Gana-Weisz, M., Halaschek-Wiener, J., Jansen, B., Elad, G., Haklai, R. and Kloog, Y.** (2002). The Ras inhibitor S-trans,trans-farnesylthiosalicylic acid chemosensitizes human tumor cells without causing resistance. *Clin Cancer Res* **8**, 555-65.
- **Garcia-Vargas, A., Hafner, C., Perez-Rodriguez, A. G., Rodriguez-Rojas, L. X., Gonzalez-Esqueda, P., Stoehr, R., Hernandez-Torres, M. and Happle, R.** (2008). An epidermal nevus syndrome with cerebral involvement caused by a mosaic FGFR3 mutation. *Am J Med Genet A* **146A**, 2275-9.
- **Garnett, M. J., Rana, S., Paterson, H., Barford, D. and Marais, R.** (2005). Wild-type and mutant B-RAF activate C-RAF through distinct mechanisms involving heterodimerization. *Mol Cell* **20**, 963-9.
- **Garrington, T. P. and Johnson, G. L.** (1999). Organization and regulation of mitogen-activated protein kinase signaling pathways. *Curr Opin Cell Biol* **11**, 211-8.
- **Gedaly, R., Angulo, P., Hundley, J., Daily, M. F., Chen, C., Koch, A. and Evers, B. M.** (2010). PI-103 and sorafenib inhibit hepatocellular carcinoma cell proliferation by blocking Ras/Raf/MAPK and PI3K/AKT/mTOR pathways. *Anticancer Res* **30**, 4951-8.
- **Gerdes, J. M., Liu, Y., Zaghloul, N. A., Leitch, C. C., Lawson, S. S., Kato, M., Beachy, P. A., Beales, P. L., DeMartino, G. N., Fisher, S. et al.** (2007). Disruption of the basal body compromises proteasomal function and perturbs intracellular Wnt response. *Nat Genet* **39**, 1350-60.
- **Gerits, N., Kostenko, S., Shiryaev, A., Johannessen, M. and Moens, U.**

(2008). Relations between the mitogen-activated protein kinase and the cAMP-dependent protein kinase pathways: comradeship and hostility. *Cell Signal* **20**, 1592-607.

- **Gerstner, J. R., Lyons, L. C., Wright, K. P., Jr., Loh, D. H., Rawashdeh, O., Eckel-Mahan, K. L. and Roman, G. W.** (2009). Cycling behavior and memory formation. *J Neurosci* **29**, 12824-30.
- **Goldhoff, P., Warrington, N. M., Limbrick, D. D., Jr., Hope, A., Woerner, B. M., Jackson, E., Perry, A., Piwnica-Worms, D. and Rubin, J. B.** (2008). Targeted inhibition of cyclic AMP phosphodiesterase-4 promotes brain tumor regression. *Clin Cancer Res* **14**, 7717-25.
- **Gopal, Y. N., Deng, W., Woodman, S. E., Komurov, K., Ram, P., Smith, P. D. and Davies, M. A.** (2010). Basal and treatment-induced activation of AKT mediates resistance to cell death by AZD6244 (ARRY-142886) in Braf-mutant human cutaneous melanoma cells. *Cancer Res* **70**, 8736-47.
- **Gorden, A., Osman, I., Gai, W., He, D., Huang, W., Davidson, A., Houghton, A. N., Busam, K. and Polsky, D.** (2003). Analysis of BRAF and N-RAS mutations in metastatic melanoma tissues. *Cancer Res* **63**, 3955-7.
- **Gorlin, R. and Gorlin, W. B.** (1990). Further reconciliation between pathoanatomy and pathophysiology of stenotic cardiac valves. *J Am Coll Cardiol* **15**, 1181-2.
- **Gorlin, R. J., Anderson, R. C. and Blaw, M.** (1969). Multiple lentigenes syndrome. *Am J Dis Child* **117**, 652-62.
- **Gorre, M. E., Mohammed, M., Ellwood, K., Hsu, N., Paquette, R., Rao, P. N. and Sawyers, C. L.** (2001). Clinical resistance to STI-571 cancer therapy caused by BCR-ABL gene mutation or amplification. *Science* **293**, 876-80.
- **Grand, E. K., Chase, A. J., Heath, C., Rahemtulla, A. and Cross, N. C.** (2004). Targeting FGFR3 in multiple myeloma: inhibition of t(4;14)-positive cells by SU5402 and PD173074. *Leukemia* **18**, 962-6.
- **Gripp, K. W.** (2005). Tumor predisposition in Costello syndrome. *Am J Med Genet C Semin Med Genet* **137C**, 72-7.
- **Gripp, K. W., Scott, C. I., Jr., Nicholson, L. and Figueroa, T. E.** (2000). Second case of bladder carcinoma in a patient with Costello syndrome. *Am J Med Genet* **90**, 256-9.
- **Gripp, K. W., Scott, C. I., Jr., Nicholson, L., McDonald-McGinn, D. M., Ozeran, J. D., Jones, M. C., Lin, A. E. and Zackai, E. H.** (2002). Five additional Costello syndrome patients with rhabdomyosarcoma: proposal for a tumor screening protocol. *Am J Med Genet* **108**, 80-7.
- **Gross, J. B. and Hanken, J.** (2008). Review of fate-mapping studies of osteogenic cranial neural crest in vertebrates. *Dev Biol* **317**, 389-400.
- **Grzmil, M., Whiting, D., Maule, J., Anastasaki, C., Amatruda, J. F., Kelsh, R. N., Norbury, C. J. and Patton, E. E.** (2007). The INT6 cancer gene and MEK signaling pathways converge during zebrafish development. *PLoS One* **2**, e959.

- **Guo, S.** (2004). Linking genes to brain, behavior and neurological diseases: what can we learn from zebrafish? *Genes Brain Behav* **3**, 63-74.
- **Haklai, R., Elad-Sfadia, G., Egozi, Y. and Kloog, Y.** (2008). Orally administered FTS (salirasib) inhibits human pancreatic tumor growth in nude mice. *Cancer Chemother Pharmacol* **61**, 89-96.
- **Haklai, R., Weisz, M. G., Elad, G., Paz, A., Marciano, D., Egozi, Y., Ben-Baruch, G. and Kloog, Y.** (1998). Dislodgment and accelerated degradation of Ras. *Biochemistry* **37**, 1306-14.
- **Haura, E. B., Ricart, A. D., Larson, T. G., Stella, P. J., Bazhenova, L., Miller, V. A., Cohen, R. B., Eisenberg, P. D., Selaru, P., Wilner, K. D. et al.** (2010). A phase II study of PD-0325901, an oral MEK inhibitor, in previously treated patients with advanced non-small cell lung cancer. *Clin Cancer Res* **16**, 2450-7.
- **Hayley, S., Poulter, M. O., Merali, Z. and Anisman, H.** (2005). The pathogenesis of clinical depression: stressor- and cytokine-induced alterations of neuroplasticity. *Neuroscience* **135**, 659-78.
- **Hegedus, B., Dasgupta, B., Shin, J. E., Emnett, R. J., Hart-Mahon, E. K., Elghazi, L., Bernal-Mizrachi, E. and Gutmann, D. H.** (2007). Neurofibromatosis-1 regulates neuronal and glial cell differentiation from neuroglial progenitors in vivo by both cAMP- and Ras-dependent mechanisms. *Cell Stem Cell* **1**, 443-57.
- **Hennekam, R. C.** (2003). Costello syndrome: an overview. *Am J Med Genet C Semin Med Genet* **117C**, 42-8.
- **Hewer, R. C., Sala-Newby, G. B., Wu, Y. J., Newby, A. C. and Bond, M.** (2011). PKA and Epac synergistically inhibit smooth muscle cell proliferation. *J Mol Cell Cardiol* **50**, 87-98.
- **Hoshino, R., Chatani, Y., Yamori, T., Tsuruo, T., Oka, H., Yoshida, O., Shimada, Y., Ari-i, S., Wada, H., Fujimoto, J. et al.** (1999). Constitutive activation of the 41-/43-kDa mitogen-activated protein kinase signaling pathway in human tumors. *Oncogene* **18**, 813-22.
- **Hotte, S. J. and Hirte, H. W.** (2002). BAY 43-9006: early clinical data in patients with advanced solid malignancies. *Curr Pharm Des* **8**, 2249-53.
- **Houslay, M. D.** (2010). Underpinning compartmentalised cAMP signalling through targeted cAMP breakdown. *Trends Biochem Sci* **35**, 91-100.
- **Houslay, M. D. and Adams, D. R.** (2003). PDE4 cAMP phosphodiesterases: modular enzymes that orchestrate signalling cross-talk, desensitization and compartmentalization. *Biochem J* **370**, 1-18.
- **Houslay, M. D. and Kolch, W.** (2000). Cell-type specific integration of cross-talk between extracellular signal-regulated kinase and cAMP signaling. *Mol Pharmacol* **58**, 659-68.
- **Houslay, M. D., Schafer, P. and Zhang, K. Y.** (2005). Keynote review: phosphodiesterase-4 as a therapeutic target. *Drug Discov Today* **10**, 1503-19.
- **Hu, N., Sedmera, D., Yost, H. J. and Clark, E. B.** (2000). Structure and function of the developing zebrafish heart. *Anat Rec* **260**, 148-57.

- **Huang, T. Y. and Lin, C. H.** (2006). Role of amygdala MAPK activation on immobility behavior of forced swim rats. *Behav Brain Res* **173**, 104-11.
- **Huson, S.** (2008). Neurofibromatosis: emerging phenotypes, mechanisms and management. *Clin Med* **8**, 611-7.
- **Insel, P. A. and Ostrom, R. S.** (2003). Forskolin as a tool for examining adenylyl cyclase expression, regulation, and G protein signaling. *Cell Mol Neurobiol* **23**, 305-14.
- **Ion, A., Tartaglia, M., Song, X., Kalidas, K., van der Burgt, I., Shaw, A. C., Ming, J. E., Zampino, G., Zackai, E. H., Dean, J. C. et al.** (2002). Absence of PTPN11 mutations in 28 cases of cardiofaciocutaneous (CFC) syndrome. *Hum Genet* **111**, 421-7.
- **Ishizaki, H., Spitzer, M., Wildenhain, J., Anastasaki, C., Zeng, Z., Dolma, S., Shaw, M., Madsen, E., Gitlin, J., Marais, R. et al.** (2010). Combined zebrafish-yeast chemical-genetic screens reveal gene-copper-nutrition interactions that modulate melanocyte pigmentation. *Dis Model Mech* **3**, 639-51.
- **Jabs, E. W., Li, X., Scott, A. F., Meyers, G., Chen, W., Eccles, M., Mao, J. I., Charnas, L. R., Jackson, C. E. and Jaye, M.** (1994). Jackson-Weiss and Crouzon syndromes are allelic with mutations in fibroblast growth factor receptor 2. *Nat Genet* **8**, 275-9.
- **Jain, R., Engleka, K. A., Rentschler, S. L., Manderfield, L. J., Li, L., Yuan, L. and Epstein, J. A.** (2011). Cardiac neural crest orchestrates remodeling and functional maturation of mouse semilunar valves. *J Clin Invest* **121**, 422-30.
- **James, G. L., Goldstein, J. L., Brown, M. S., Rawson, T. E., Somers, T. C., McDowell, R. S., Crowley, C. W., Lucas, B. K., Levinson, A. D. and Marsters, J. C., Jr.** (1993). Benzodiazepine peptidomimetics: potent inhibitors of Ras farnesylation in animal cells. *Science* **260**, 1937-42.
- **Jansen, B., Schlagbauer-Wadl, H., Kahr, H., Heere-Ress, E., Mayer, B. X., Eichler, H., Pehamberger, H., Gana-Weisz, M., Ben-David, E., Kloog, Y. et al.** (1999). Novel Ras antagonist blocks human melanoma growth. *Proc Natl Acad Sci U S A* **96**, 14019-24.
- **Jeffrey, K. L., Camps, M., Rommel, C. and Mackay, C. R.** (2007). Targeting dual-specificity phosphatases: manipulating MAP kinase signalling and immune responses. *Nat Rev Drug Discov* **6**, 391-403.
- **Jeon, Y. H., Heo, Y. S., Kim, C. M., Hyun, Y. L., Lee, T. G., Ro, S. and Cho, J. M.** (2005). Phosphodiesterase: overview of protein structures, potential therapeutic applications and recent progress in drug development. *Cell Mol Life Sci* **62**, 1198-220.
- **Johannessen, C. M., Boehm, J. S., Kim, S. Y., Thomas, S. R., Wardwell, L., Johnson, L. A., Emery, C. M., Stransky, N., Cogdill, A. P., Barretina, J. et al.** (2010). COT drives resistance to RAF inhibition through MAP kinase pathway reactivation. *Nature* **468**, 968-72.
- **Johnston, L. A., Erdogan, S., Cheung, Y. F., Sullivan, M., Barber, R.,**

Lynch, M. J., Baillie, G. S., Van Heeke, G., Adams, D. R., Huston, E. et al. (2004). Expression, intracellular distribution and basis for lack of catalytic activity of the PDE4A7 isoform encoded by the human PDE4A cAMP-specific phosphodiesterase gene. *Biochem J* **380**, 371-84.

- **Joly, J. S., Joly, C., Schulte-Merker, S., Boulekbache, H. and Condamine, H.** (1993). The ventral and posterior expression of the zebrafish homeobox gene eve1 is perturbed in dorsalized and mutant embryos. *Development* **119**, 1261-75.
- **Jopling, C., van Geemen, D. and den Hertog, J.** (2007). Shp2 knockdown and Noonan/LEOPARD mutant Shp2-induced gastrulation defects. *PLoS Genet* **3**, e225.
- **Kaji, T. and Artinger, K. B.** (2004). dlx3b and dlx4b function in the development of Rohon-Beard sensory neurons and trigeminal placode in the zebrafish neurula. *Dev Biol* **276**, 523-40.
- **Kamioka, Y., Yasuda, S., Fujita, Y., Aoki, K. and Matsuda, M.** (2010). Multiple decisive phosphorylation sites for the negative feedback regulation of SOS1 via ERK. *J Biol Chem* **285**, 33540-8.
- **Kan, S. H., Elanko, N., Johnson, D., Cornejo-Roldan, L., Cook, J., Reich, E. W., Tomkins, S., Verloes, A., Twigg, S. R., Rannan-Eliya, S. et al.** (2002). Genomic screening of fibroblast growth-factor receptor 2 reveals a wide spectrum of mutations in patients with syndromic craniosynostosis. *Am J Hum Genet* **70**, 472-86.
- **Karreth, F. A., DeNicola, G. M., Winter, S. P. and Tuveson, D. A.** (2009). C-Raf inhibits MAPK activation and transformation by B-Raf(V600E). *Mol Cell* **36**, 477-86.
- **Kaulen, P., Bruning, G., Schneider, H. H., Sarter, M. and Baumgarten, H. G.** (1989). Autoradiographic mapping of a selective cyclic adenosine monophosphate phosphodiesterase in rat brain with the antidepressant [3H]rolipram. *Brain Res* **503**, 229-45.
- **Kavamura, M. I., Peres, C. A., Alchorne, M. M. and Brunoni, D.** (2002). CFC index for the diagnosis of cardiofaciocutaneous syndrome. *Am J Med Genet* **112**, 12-6.
- **Kavamura, M. I., Pomponi, M. G., Zollino, M., Lecce, R., Murdolo, M., Brunoni, D., Alchorne, M. M., Opitz, J. M. and Neri, G.** (2003). PTPN11 mutations are not responsible for the Cardiofaciocutaneous (CFC) syndrome. *Eur J Hum Genet* **11**, 64-8.
- **Kawakami, K.** (2004). Transgenesis and gene trap methods in zebrafish by using the Tol2 transposable element. *Methods Cell Biol* **77**, 201-22.
- **Kawame, H., Matsui, M., Kurosawa, K., Matsuo, M., Masuno, M., Ohashi, H., Fueki, N., Aoyama, K., Miyatsuka, Y., Suzuki, K. et al.** (2003). Further delineation of the behavioral and neurologic features in Costello syndrome. *Am J Med Genet A* **118A**, 8-14.
- **Keilhack, H., David, F. S., McGregor, M., Cantley, L. C. and Neel, B. G.** (2005). Diverse biochemical properties of Shp2 mutants. Implications for

disease phenotypes. *J Biol Chem* **280**, 30984-93.

- **Kelsh, R. N. and Eisen, J. S.** (2000). The zebrafish colourless gene regulates development of non-ectomesenchymal neural crest derivatives. *Development* **127**, 515-25.
- **Kerr, B., Allanson, J., Delrue, M. A., Gripp, K. W., Lacombe, D., Lin, A. E. and Rauen, K. A.** (2008). The diagnosis of Costello syndrome: nomenclature in Ras/MAPK pathway disorders. *Am J Med Genet A* **146A**, 1218-20.
- **Kerr, B., Eden, O. B., Dandamudi, R., Shannon, N., Quarrell, O., Emmerson, A., Ladusans, E., Gerrard, M. and Donnai, D.** (1998). Costello syndrome: two cases with embryonal rhabdomyosarcoma. *J Med Genet* **35**, 1036-9.
- **Kim, H. A., Ling, B. and Ratner, N.** (1997). Nf1-deficient mouse Schwann cells are angiogenic and invasive and can be induced to hyperproliferate: reversion of some phenotypes by an inhibitor of farnesyl protein transferase. *Mol Cell Biol* **17**, 862-72.
- **Kim, J., Lee, J. E., Heynen-Genel, S., Suyama, E., Ono, K., Lee, K., Ideker, T., Aza-Blanc, P. and Gleeson, J. G.** (2010). Functional genomic screen for modulators of ciliogenesis and cilium length. *Nature* **464**, 1048-51.
- **Kimmel, C. B., Ballard, W. W., Kimmel, S. R., Ullmann, B. and Schilling, T. F.** (1995). Stages of embryonic development of the zebrafish. *Dev Dyn* **203**, 253-310.
- **Kimmel, C. B., Miller, C. T. and Moens, C. B.** (2001). Specification and morphogenesis of the zebrafish larval head skeleton. *Dev Biol* **233**, 239-57.
- **Kimmel, C. B., Warga, R. M. and Schilling, T. F.** (1990). Origin and organization of the zebrafish fate map. *Development* **108**, 581-94.
- **Kimura, E. T., Nikiforova, M. N., Zhu, Z., Knauf, J. A., Nikiforov, Y. E. and Fagin, J. A.** (2003). High prevalence of BRAF mutations in thyroid cancer: genetic evidence for constitutive activation of the RET/PTC-RAS-BRAF signaling pathway in papillary thyroid carcinoma. *Cancer Res* **63**, 1454-7.
- **King, A. A., Debaun, M. R., Riccardi, V. M. and Gutmann, D. H.** (2000). Malignant peripheral nerve sheath tumors in neurofibromatosis 1. *Am J Med Genet* **93**, 388-92.
- **Knecht, A. K. and Bronner-Fraser, M.** (2002). Induction of the neural crest: a multigene process. *Nat Rev Genet* **3**, 453-61.
- **Knight, R. D. and Schilling, T. F.** (2006). Cranial neural crest and development of the head skeleton. *Adv Exp Med Biol* **589**, 120-33.
- **Kobayashi, T., Sakamoto, K., Takimura, T., Sekine, R., Kelly, V. P., Kamata, K., Nishimura, S. and Yokoyama, S.** (2005). Structural basis of nonnatural amino acid recognition by an engineered aminoacyl-tRNA synthetase for genetic code expansion. *Proc Natl Acad Sci U S A* **102**, 1366-71.
- **Kohl, N. E., Mosser, S. D., deSolms, S. J., Giuliani, E. A., Pompliano, D.**

L., Graham, S. L., Smith, R. L., Scolnick, E. M., Oliff, A. and Gibbs, J. B. (1993). Selective inhibition of ras-dependent transformation by a farnesyltransferase inhibitor. *Science* **260**, 1934-7.

- **Kolch, W., Mischak, H. and Pitt, A. R.** (2005). The molecular make-up of a tumour: proteomics in cancer research. *Clin Sci (Lond)* **108**, 369-83.
- **Komatsu, K., Buchanan, F. G., Otaka, M., Jin, M., Odashima, M., Horikawa, Y., Watanabe, S. and Dubois, R. N.** (2006). Gene expression profiling following constitutive activation of MEK1 and transformation of rat intestinal epithelial cells. *Mol Cancer* **5**, 63.
- **Komisarczuk, A. Z., Topp, S., Stigloher, C., Kapsimali, M., Bally-Cuif, L. and Becker, T. S.** (2008). Enhancer detection and developmental expression of zebrafish sprouty1, a member of the fgf8 synexpression group. *Dev Dyn* **237**, 2594-603.
- **Konstantinopoulos, P. A., Karamouzis, M. V. and Papavassiliou, A. G.** (2007). Post-translational modifications and regulation of the RAS superfamily of GTPases as anticancer targets. *Nat Rev Drug Discov* **6**, 541-55.
- **Kontaridis, M. I., Swanson, K. D., David, F. S., Barford, D. and Neel, B. G.** (2006). PTPN11 (Shp2) mutations in LEOPARD syndrome have dominant negative, not activating, effects. *J Biol Chem* **281**, 6785-92.
- **Koziczak, M., Holbro, T. and Hynes, N. E.** (2004). Blocking of FGFR signaling inhibits breast cancer cell proliferation through downregulation of D-type cyclins. *Oncogene* **23**, 3501-8.
- **Kratz, C. P., Zampino, G., Kriek, M., Kant, S. G., Leoni, C., Pantaleoni, F., Oudesluys-Murphy, A. M., Di Rocco, C., Kloska, S. P., Tartaglia, M. et al.** (2009). Craniosynostosis in patients with Noonan syndrome caused by germline KRAS mutations. *Am J Med Genet A* **149A**, 1036-40.
- **Krens, L. L., Baas, J. M., Gelderblom, H. and Guchelaar, H. J.** (2010). Therapeutic modulation of k-ras signaling in colorectal cancer. *Drug Discov Today* **15**, 502-16.
- **Krens, S. F., He, S., Lamers, G. E., Meijer, A. H., Bakkers, J., Schmidt, T., Spaink, H. P. and Snaar-Jagalska, B. E.** (2008). Distinct functions for ERK1 and ERK2 in cell migration processes during zebrafish gastrulation. *Dev Biol* **319**, 370-83.
- **Krens, S. F., He, S., Spaink, H. P. and Snaar-Jagalska, B. E.** (2006). Characterization and expression patterns of the MAPK family in zebrafish. *Gene Expr Patterns* **6**, 1019-26.
- **Krishnan, V. and Nestler, E. J.** (2008). The molecular neurobiology of depression. *Nature* **455**, 894-902.
- **Lajeunie, E., Heuertz, S., El Ghouzzi, V., Martinovic, J., Renier, D., Le Merrer, M. and Bonaventure, J.** (2006). Mutation screening in patients with syndromic craniosynostoses indicates that a limited number of recurrent FGFR2 mutations accounts for severe forms of Pfeiffer syndrome. *Eur J Hum Genet* **14**, 289-98.

- **Lamont, F. R., Tomlinson, D. C., Cooper, P. A., Shnyder, S. D., Chester, J. D. and Knowles, M. A.** (2011). Small molecule FGF receptor inhibitors block FGFR-dependent urothelial carcinoma growth in vitro and in vivo. *Br J Cancer* **104**, 75-82.
- **Langenau, D. M., Keefe, M. D., Storer, N. Y., Guyon, J. R., Kutok, J. L., Le, X., Goessling, W., Neuberg, D. S., Kunkel, L. M. and Zon, L. I.** (2007). Effects of RAS on the genesis of embryonal rhabdomyosarcoma. *Genes Dev* **21**, 1382-95.
- **Lasithiotakis, K. G., Sinnberg, T. W., Schittek, B., Flaherty, K. T., Kulms, D., Maczey, E., Garbe, C. and Meier, F. E.** (2008). Combined inhibition of MAPK and mTOR signaling inhibits growth, induces cell death, and abrogates invasive growth of melanoma cells. *J Invest Dermatol* **128**, 2013-23.
- **Laux, D., Kratz, C. and Sauerbrey, A.** (2008). Common acute lymphoblastic leukemia in a girl with genetically confirmed LEOPARD syndrome. *J Pediatr Hematol Oncol* **30**, 602-4.
- **Lee, J. T. and McCubrey, J. A.** (2003). BAY-43-9006 Bayer/Onyx. *Curr Opin Investig Drugs* **4**, 757-63.
- **Lemieux, E., Bergeron, S., Durand, V., Asselin, C., Saucier, C. and Rivard, N.** (2009). Constitutively active MEK1 is sufficient to induce epithelial-to-mesenchymal transition in intestinal epithelial cells and to promote tumor invasion and metastasis. *Int J Cancer* **125**, 1575-86.
- **Lepage, S. E. and Bruce, A. E.** (2010). Zebrafish epiboly: mechanics and mechanisms. *Int J Dev Biol* **54**, 1213-28.
- **Li, Y. F., Cheng, Y. F., Huang, Y., Conti, M., Wilson, S. P., O'Donnell, J. M. and Zhang, H. T.** (2011). Phosphodiesterase-4D knock-out and RNA interference-mediated knock-down enhance memory and increase hippocampal neurogenesis via increased cAMP signaling. *J Neurosci* **31**, 172-83.
- **Lim, J., Pahlke, G. and Conti, M.** (1999). Activation of the cAMP-specific phosphodiesterase PDE4D3 by phosphorylation. Identification and function of an inhibitory domain. *J Biol Chem* **274**, 19677-85.
- **Limongelli, G., Pacileo, G., Marino, B., Digilio, M. C., Sarkozy, A., Elliott, P., Versacci, P., Calabro, P., De Zorzi, A., Di Salvo, G. et al.** (2007). Prevalence and clinical significance of cardiovascular abnormalities in patients with the LEOPARD syndrome. *Am J Cardiol* **100**, 736-41.
- **Lin, A. E., Grossfeld, P. D., Hamilton, R. M., Smoot, L., Gripp, K. W., Proud, V., Weksberg, R., Wheeler, P., Picker, J., Irons, M. et al.** (2002). Further delineation of cardiac abnormalities in Costello syndrome. *Am J Med Genet* **111**, 115-29.
- **Liu, D., Liu, Z., Jiang, D., Dackiw, A. P. and Xing, M.** (2007). Inhibitory effects of the mitogen-activated protein kinase kinase inhibitor CI-1040 on the proliferation and tumor growth of thyroid cancer cells with BRAF or RAS mutations. *J Clin Endocrinol Metab* **92**, 4686-95.

- **Liu, J. J., Nakajima, K., Hirano, T. and Yang-Yen, H. F.** (1998). Activation of Stat3 by v-Src is through a Ras-independent pathway. *J Biomed Sci* **5**, 446-50.
- **Liu, L., Zhu, S., Gong, Z. and Low, B. C.** (2008). K-ras/PI3K-Akt signaling is essential for zebrafish hematopoiesis and angiogenesis. *PLoS One* **3**, e2850.
- **Liu, R. Z., Denovan-Wright, E. M. and Wright, J. M.** (2003). Structure, linkage mapping and expression of the heart-type fatty acid-binding protein gene (fabp3) from zebrafish (Danio rerio). *Eur J Biochem* **270**, 3223-34.
- **Lopes, C. A., Prosser, S. L., Romio, L., Hirst, R. A., O'Callaghan, C., Woolf, A. S. and Fry, A. M.** (2011). Centriolar satellites are assembly points for proteins implicated in human ciliopathies, including oral-facial-digital syndrome 1. *J Cell Sci* **124**, 600-12.
- **Loriot, Y., Massard, C., Angevin, E., Lambotte, O., Escudier, B. and Soria, J. C.** (2010). FGFR inhibitor induced peripheral neuropathy in patients with advanced RCC. *Ann Oncol* **21**, 1559-60.
- **LoRusso, P. M., Krishnamurthi, S. S., Rinehart, J. J., Nabell, L. M., Malburg, L., Chapman, P. B., DePrimo, S. E., Bentivegna, S., Wilner, K. D., Tan, W. et al.** (2010). Phase I pharmacokinetic and pharmacodynamic study of the oral MAPK/ERK kinase inhibitor PD-0325901 in patients with advanced cancers. *Clin Cancer Res* **16**, 1924-37.
- **Lynch, M. J., Hill, E. V. and Houslay, M. D.** (2006). Intracellular targeting of phosphodiesterase-4 underpins compartmentalized cAMP signaling. *Curr Top Dev Biol* **75**, 225-59.
- **Lyons, J. F., Wilhelm, S., Hibner, B. and Bollag, G.** (2001). Discovery of a novel Raf kinase inhibitor. *Endocr Relat Cancer* **8**, 219-25.
- **Lyons, L. C., Collado, M. S., Khabour, O., Green, C. L. and Eskin, A.** (2006). The circadian clock modulates core steps in long-term memory formation in Aplysia. *J Neurosci* **26**, 8662-71.
- **MacKenzie, S. J., Baillie, G. S., McPhee, I., Bolger, G. B. and Houslay, M. D.** (2000). ERK2 mitogen-activated protein kinase binding, phosphorylation, and regulation of the PDE4D cAMP-specific phosphodiesterases. The involvement of COOH-terminal docking sites and NH2-terminal UCR regions. *J Biol Chem* **275**, 16609-17.
- **Mahgoub, N., Taylor, B. R., Gratiot, M., Kohl, N. E., Gibbs, J. B., Jacks, T. and Shannon, K. M.** (1999). In vitro and in vivo effects of a farnesyltransferase inhibitor on Nf1-deficient hematopoietic cells. *Blood* **94**, 2469-76.
- **Makita, Y., Narumi, Y., Yoshida, M., Niihori, T., Kure, S., Fujieda, K., Matsubara, Y. and Aoki, Y.** (2007). Leukemia in Cardio-facio-cutaneous (CFC) syndrome: a patient with a germline mutation in BRAF proto-oncogene. *J Pediatr Hematol Oncol* **29**, 287-90.
- **Mansour, S. J., Matten, W. T., Hermann, A. S., Candia, J. M., Rong, S., Fukasawa, K., Vande Woude, G. F. and Ahn, N. G.** (1994).

Transformation of mammalian cells by constitutively active MAP kinase kinase. *Science* **265**, 966-70.

- **Margolin, K., Longmate, J., Baratta, T., Synold, T., Christensen, S., Weber, J., Gajewski, T., Quirt, I. and Doroshow, J. H.** (2005). CCI-779 in metastatic melanoma: a phase II trial of the California Cancer Consortium. *Cancer* **104**, 1045-8.
- **Marko, D., Pahlke, G., Merz, K. H. and Eisenbrand, G.** (2000). Cyclic 3',5'-nucleotide phosphodiesterases: potential targets for anticancer therapy. *Chem Res Toxicol* **13**, 944-8.
- **Martin, G. A., Viskochil, D., Bollag, G., McCabe, P. C., Crosier, W. J., Haubruck, H., Conroy, L., Clark, R., O'Connell, P., Cawthon, R. M. et al.** (1990). The GAP-related domain of the neurofibromatosis type 1 gene product interacts with ras p21. *Cell* **63**, 843-9.
- **Maschhoff, K. L. and Baldwin, H. S.** (2000). Molecular determinants of neural crest migration. *Am J Med Genet* **97**, 280-8.
- **McCahill, A. C., Huston, E., Li, X. and Houslay, M. D.** (2008). PDE4 associates with different scaffolding proteins: modulating interactions as treatment for certain diseases. *Handb Exp Pharmacol*, 125-66.
- **McEwan, D. G., Brunton, V. G., Baillie, G. S., Leslie, N. R., Houslay, M. D. and Frame, M. C.** (2007). Chemoresistant KM12C colon cancer cells are addicted to low cyclic AMP levels in a phosphodiesterase 4-regulated compartment via effects on phosphoinositide 3-kinase. *Cancer Res* **67**, 5248-57.
- **McIntosh, I., Bellus, G. A. and Jab, E. W.** (2000). The pleiotropic effects of fibroblast growth factor receptors in mammalian development. *Cell Struct Funct* **25**, 85-96.
- **Meier, F., Busch, S., Lasithiotakis, K., Kulms, D., Garbe, C., Maczey, E., Herlyn, M. and Schittek, B.** (2007). Combined targeting of MAPK and AKT signalling pathways is a promising strategy for melanoma treatment. *Br J Dermatol* **156**, 1204-13.
- **Merks, J. H., Caron, H. N. and Hennekam, R. C.** (2005). High incidence of malformation syndromes in a series of 1,073 children with cancer. *Am J Med Genet A* **134A**, 132-43.
- **Michailidou, C., Jones, M., Walker, P., Kamarashev, J., Kelly, A. and Hurlstone, A. F.** (2009). Dissecting the roles of Raf- and PI3K-signalling pathways in melanoma formation and progression in a zebrafish model. *Dis Model Mech* **2**, 399-411.
- **Michaloglou, C., Vredeveld, L. C., Soengas, M. S., Denoyelle, C., Kuilman, T., van der Horst, C. M., Majoor, D. M., Shay, J. W., Mooi, W. J. and Peeper, D. S.** (2005). BRAFE600-associated senescence-like cell cycle arrest of human naevi. *Nature* **436**, 720-4.
- **Miller, B. H., Schultz, L. E., Gulati, A., Su, A. I. and Pletcher, M. T.** (2010). Phenotypic characterization of a genetically diverse panel of mice for behavioral despair and anxiety. *PLoS One* **5**, e14458.

- **Miller, J. C., Holmes, M. C., Wang, J., Guschin, D. Y., Lee, Y. L., Rupniewski, I., Beausejour, C. M., Waite, A. J., Wang, N. S., Kim, K. A. et al.** (2007). An improved zinc-finger nuclease architecture for highly specific genome editing. *Nat Biotechnol* **25**, 778-85.
- **Miller, N. Y. and Gerlai, R.** (2011). Shoaling in zebrafish: what we don't know. *Rev Neurosci* **22**, 17-25.
- **Minoux, M. and Rijli, F. M.** (2010). Molecular mechanisms of cranial neural crest cell migration and patterning in craniofacial development. *Development* **137**, 2605-21.
- **Mody, N., Leitch, J., Armstrong, C., Dixon, J. and Cohen, P.** (2001). Effects of MAP kinase cascade inhibitors on the MKK5/ERK5 pathway. *FEBS Lett* **502**, 21-4.
- **Mohammadi, M., Froum, S., Hamby, J. M., Schroeder, M. C., Panek, R. L., Lu, G. H., Eliseenkova, A. V., Green, D., Schlessinger, J. and Hubbard, S. R.** (1998). Crystal structure of an angiogenesis inhibitor bound to the FGF receptor tyrosine kinase domain. *Embo J* **17**, 5896-904.
- **Mohammadi, M., McMahon, G., Sun, L., Tang, C., Hirth, P., Yeh, B. K., Hubbard, S. R. and Schlessinger, J.** (1997). Structures of the tyrosine kinase domain of fibroblast growth factor receptor in complex with inhibitors. *Science* **276**, 955-60.
- **Molina, G. A., Watkins, S. C. and Tsang, M.** (2007). Generation of FGF reporter transgenic zebrafish and their utility in chemical screens. *BMC Dev Biol* **7**, 62.
- **Moloney, D. M., Slaney, S. F., Oldridge, M., Wall, S. A., Sahlin, P., Stenman, G. and Wilkie, A. O.** (1996). Exclusive paternal origin of new mutations in Apert syndrome. *Nat Genet* **13**, 48-53.
- **Montagut, C., Sharma, S. V., Shioda, T., McDermott, U., Ulman, M., Ulkus, L. E., Dias-Santagata, D., Stubbs, H., Lee, D. Y., Singh, A. et al.** (2008). Elevated CRAF as a potential mechanism of acquired resistance to BRAF inhibition in melanoma. *Cancer Res* **68**, 4853-61.
- **Morgan, M. A., Wegner, J., Aydilek, E., Ganser, A. and Reuter, C. W.** (2003). Synergistic cytotoxic effects in myeloid leukemia cells upon cotreatment with farnesyltransferase and geranylgeranyl transferase-I inhibitors. *Leukemia* **17**, 1508-20.
- **Mullins, M. C., Hammerschmidt, M., Kane, D. A., Odenthal, J., Brand, M., van Eeden, F. J., Furutani-Seiki, M., Granato, M., Haffter, P., Heisenberg, C. P. et al.** (1996). Genes establishing dorsoventral pattern formation in the zebrafish embryo: the ventral specifying genes. *Development* **123**, 81-93.
- **Musante, L., Kehl, H. G., Majewski, F., Meinecke, P., Schweiger, S., Gillessen-Kaesbach, G., Wieczorek, D., Hinkel, G. K., Tinschert, S., Hoeltzenbein, M. et al.** (2003). Spectrum of mutations in PTPN11 and genotype-phenotype correlation in 96 patients with Noonan syndrome and five patients with cardio-facio-cutaneous syndrome. *Eur J Hum Genet* **11**,

201-6.

- **Nakayama, N., Nakayama, K., Yeasmin, S., Ishibashi, M., Katagiri, A., Iida, K., Fukumoto, M. and Miyazaki, K.** (2008). KRAS or BRAF mutation status is a useful predictor of sensitivity to MEK inhibition in ovarian cancer. *Br J Cancer* **99**, 2020-8.
- **Nazarian, R., Shi, H., Wang, Q., Kong, X., Koya, R. C., Lee, H., Chen, Z., Lee, M. K., Attar, N., Sazegar, H. et al.** (2010). Melanomas acquire resistance to B-RAF(V600E) inhibition by RTK or N-RAS upregulation. *Nature* **468**, 973-7.
- **Nechiporuk, A., Linbo, T., Poss, K. D. and Raible, D. W.** (2007). Specification of epibranchial placodes in zebrafish. *Development* **134**, 611-23.
- **Nguyen, T. K., Rahmani, M., Gao, N., Kramer, L., Corbin, A. S., Druker, B. J., Dent, P. and Grant, S.** (2006). Synergistic interactions between DMAG and mitogen-activated protein kinase kinase 1/2 inhibitors in Bcr/abl+ leukemia cells sensitive and resistant to imatinib mesylate. *Clin Cancer Res* **12**, 2239-47.
- **Niessner, H., Beck, D., Sinnberg, T., Lasithiotakis, K., Maczey, E., Gogel, J., Venturelli, S., Berger, A., Mauthe, M., Toulany, M. et al.** (2011). The farnesyl transferase inhibitor lonafarnib inhibits mTOR signaling and enforces sorafenib-induced apoptosis in melanoma cells. *J Invest Dermatol* **131**, 468-79.
- **Niihori, T., Aoki, Y., Narumi, Y., Neri, G., Cave, H., Verloes, A., Okamoto, N., Hennekam, R. C., Gillessen-Kaesbach, G., Wieczorek, D. et al.** (2006). Germline KRAS and BRAF mutations in cardio-facio-cutaneous syndrome. *Nat Genet* **38**, 294-6.
- **Nikulina, E., Tidwell, J. L., Dai, H. N., Bregman, B. S. and Filbin, M. T.** (2004). The phosphodiesterase inhibitor rolipram delivered after a spinal cord lesion promotes axonal regeneration and functional recovery. *Proc Natl Acad Sci U S A* **101**, 8786-90.
- **Ninkovic, J. and Bally-Cuif, L.** (2006). The zebrafish as a model system for assessing the reinforcing properties of drugs of abuse. *Methods* **39**, 262-74.
- **Noonan, J. A.** (1968). Hypertelorism with Turner phenotype. A new syndrome with associated congenital heart disease. *Am J Dis Child* **116**, 373-80.
- **North, K.** (2000). Neurofibromatosis type 1. *Am J Med Genet* **97**, 119-27.
- **Norton, W. and Bally-Cuif, L.** (2010). Adult zebrafish as a model organism for behavioural genetics. *BMC Neurosci* **11**, 90.
- **Nusslein-Volhard, C. and Dahm, R.** (2002). Zebrafish : a practical approach. Oxford: Oxford University Press.
- **Ohren, J. F., Chen, H., Pavlovsky, A., Whitehead, C., Zhang, E., Kuffa, P., Yan, C., McConnell, P., Spessard, C., Banotai, C. et al.** (2004). Structures of human MAP kinase kinase 1 (MEK1) and MEK2 describe novel noncompetitive kinase inhibition. *Nat Struct Mol Biol* **11**, 1192-7.

- **Oishi, K., Gaengel, K., Krishnamoorthy, S., Kamiya, K., Kim, I. K., Ying, H., Weber, U., Perkins, L. A., Tartaglia, M., Mlodzik, M. et al.** (2006). Transgenic Drosophila models of Noonan syndrome causing PTPN11 gain-of-function mutations. *Hum Mol Genet* **15**, 543-53.
- **Oishi, K., Zhang, H., Gault, W. J., Wang, C. J., Tan, C. C., Kim, I. K., Ying, H., Rahman, T., Pica, N., Tartaglia, M. et al.** (2009). Phosphatase-defective LEOPARD syndrome mutations in PTPN11 gene have gain-of-function effects during Drosophila development. *Hum Mol Genet* **18**, 193-201.
- **Orton, R. J., Sturm, O. E., Vyshemirsky, V., Calder, M., Gilbert, D. R. and Kolch, W.** (2005). Computational modelling of the receptor-tyrosine-kinase-activated MAPK pathway. *Biochem J* **392**, 249-61.
- **Padmanabhan, A., Lee, J. S., Ismat, F. A., Lu, M. M., Lawson, N. D., Kanki, J. P., Look, A. T. and Epstein, J. A.** (2009). Cardiac and vascular functions of the zebrafish orthologues of the type I neurofibromatosis gene NFI. *Proc Natl Acad Sci U S A* **106**, 22305-10.
- **Paez, J. G., Janne, P. A., Lee, J. C., Tracy, S., Greulich, H., Gabriel, S., Herman, P., Kaye, F. J., Lindeman, N., Boggon, T. J. et al.** (2004). EGFR mutations in lung cancer: correlation with clinical response to gefitinib therapy. *Science* **304**, 1497-500.
- **Pagani, M. R., Oishi, K., Gelb, B. D. and Zhong, Y.** (2009). The phosphatase SHP2 regulates the spacing effect for long-term memory induction. *Cell* **139**, 186-98.
- **Pandit, B., Sarkozy, A., Pennacchio, L. A., Carta, C., Oishi, K., Martinelli, S., Pogna, E. A., Schackwitz, W., Ustaszewska, A., Landstrom, A. et al.** (2007). Gain-of-function RAF1 mutations cause Noonan and LEOPARD syndromes with hypertrophic cardiomyopathy. *Nat Genet* **39**, 1007-12.
- **Pao, W., Miller, V. A., Politi, K. A., Riely, G. J., Somwar, R., Zakowski, M. F., Kris, M. G. and Varmus, H.** (2005). Acquired resistance of lung adenocarcinomas to gefitinib or erlotinib is associated with a second mutation in the EGFR kinase domain. *PLoS Med* **2**, e73.
- **Park, W. J., Theda, C., Maestri, N. E., Meyers, G. A., Fryburg, J. S., Dufresne, C., Cohen, M. M., Jr. and Jabs, E. W.** (1995). Analysis of phenotypic features and FGFR2 mutations in Apert syndrome. *Am J Hum Genet* **57**, 321-8.
- **Parkes, J. D., Thompson, C., Brennan, L., Gajraj, N., Howcroft, B. and Ruiz, J.** (1984). Rolipram in Parkinson's disease. *Adv Neurol* **40**, 563-5.
- **Parsa, C. F., Hoyt, C. S., Lesser, R. L., Weinstein, J. M., Strother, C. M., Muci-Mendoza, R., Ramella, M., Manor, R. S., Fletcher, W. A., Repka, M. X. et al.** (2001). Spontaneous regression of optic gliomas: thirteen cases documented by serial neuroimaging. *Arch Ophthalmol* **119**, 516-29.
- **Pasmant, E., Sabbagh, A., Hanna, N., Masliah-Planchon, J., Jolly, E., Goussard, P., Ballerini, P., Cartault, F., Barbarot, S., Landman-Parker,**

J. et al. (2009). SPRED1 germline mutations caused a neurofibromatosis type 1 overlapping phenotype. *J Med Genet* **46**, 425-30.

- **Paterson, J. L., Li, Z., Wen, X. Y., Masih-Khan, E., Chang, H., Pollett, J. B., Trudel, S. and Stewart, A. K.** (2004). Preclinical studies of fibroblast growth factor receptor 3 as a therapeutic target in multiple myeloma. *Br J Haematol* **124**, 595-603.
- **Patton, E. E., Widlund, H. R., Kutok, J. L., Kopani, K. R., Amatruda, J. F., Murphey, R. D., Berghmans, S., Mayhall, E. A., Traver, D., Fletcher, C. D. et al.** (2005). BRAF mutations are sufficient to promote nevi formation and cooperate with p53 in the genesis of melanoma. *Curr Biol* **15**, 249-54.
- **Patton, E. E. and Zon, L. I.** (2005). Taking human cancer genes to the fish: a transgenic model of melanoma in zebrafish. *Zebrafish* **1**, 363-8.
- **Pearson, G., Robinson, F., Beers Gibson, T., Xu, B. E., Karandikar, M., Berman, K. and Cobb, M. H.** (2001). Mitogen-activated protein (MAP) kinase pathways: regulation and physiological functions. *Endocr Rev* **22**, 153-83.
- **Perlyn, C. A., Morriss-Kay, G., Darvann, T., Tenenbaum, M. and Ornitz, D. M.** (2006). A model for the pharmacological treatment of crouzon syndrome. *Neurosurgery* **59**, 210-5; discussion 210-5.
- **Pertuit, M., Barlier, A., Enjalbert, A. and Gerard, C.** (2009). Signalling pathway alterations in pituitary adenomas: involvement of Gsalpha, cAMP and mitogen-activated protein kinases. *J Neuroendocrinol* **21**, 869-77.
- **Pierpont, E. I., Pierpont, M. E., Mendelsohn, N. J., Roberts, A. E., Tworog-Dube, E., Rauen, K. A. and Seidenberg, M. S.** (2011). Effects of germline mutations in the Ras/MAPK signaling pathway on adaptive behavior: cardiofaciocutaneous syndrome and Noonan syndrome. *Am J Med Genet A* **152A**, 591-600.
- **Pollock, P. M., Harper, U. L., Hansen, K. S., Yudt, L. M., Stark, M., Robbins, C. M., Moses, T. Y., Hostetter, G., Wagner, U., Kakareka, J. et al.** (2003). High frequency of BRAF mutations in nevi. *Nat Genet* **33**, 19-20.
- **Poulikakos, P. I., Zhang, C., Bollag, G., Shokat, K. M. and Rosen, N.** (2010). RAF inhibitors transactivate RAF dimers and ERK signalling in cells with wild-type BRAF. *Nature* **464**, 427-30.
- **Pozios, K. C., Ding, J., Degger, B., Upton, Z. and Duan, C.** (2001). IGFs stimulate zebrafish cell proliferation by activating MAP kinase and PI3-kinase-signaling pathways. *Am J Physiol Regul Integr Comp Physiol* **280**, R1230-9.
- **Pratilas, C. A., Hanrahan, A. J., Halilovic, E., Persaud, Y., Soh, J., Chitale, D., Shigematsu, H., Yamamoto, H., Sawai, A., Janakiraman, M. et al.** (2008). Genetic predictors of MEK dependence in non-small cell lung cancer. *Cancer Res* **68**, 9375-83.
- **Pratilas, C. A. and Solit, D. B.** (2010). Targeting the mitogen-activated protein kinase pathway: physiological feedback and drug response. *Clin Cancer Res* **16**, 3329-34.

- **Qing, J., Du, X., Chen, Y., Chan, P., Li, H., Wu, P., Marsters, S., Stawicki, S., Tien, J., Totpal, K. et al.** (2009). Antibody-based targeting of FGFR3 in bladder carcinoma and t(4;14)-positive multiple myeloma in mice. *J Clin Invest* **119**, 1216-29.
- **Rauen, K. A.** (2006). Distinguishing Costello versus cardio-facio-cutaneous syndrome: BRAF mutations in patients with a Costello phenotype. *Am J Med Genet A* **140**, 1681-3.
- **Rauen, K. A., Banerjee, A., Bishop, W. R., Lauchle, J. O., McCormick, F., McMahon, M., Melese, T., Munster, P. N., Nadaf, S., Packer, R. J. et al.** (2011). Costello and cardio-facio-cutaneous syndromes: Moving toward clinical trials in RASopathies. *Am J Med Genet C Semin Med Genet* **157**, 136-46.
- **Razzaque, M. A., Nishizawa, T., Komoike, Y., Yagi, H., Furutani, M., Amo, R., Kamisago, M., Momma, K., Katayama, H., Nakagawa, M. et al.** (2007). Germline gain-of-function mutations in RAF1 cause Noonan syndrome. *Nat Genet* **39**, 1013-7.
- **Reardon, W., Winter, R. M., Rutland, P., Pulleyn, L. J., Jones, B. M. and Malcolm, S.** (1994). Mutations in the fibroblast growth factor receptor 2 gene cause Crouzon syndrome. *Nat Genet* **8**, 98-103.
- **Reuter, C. W., Morgan, M. A. and Bergmann, L.** (2000). Targeting the Ras signaling pathway: a rational, mechanism-based treatment for hematologic malignancies? *Blood* **96**, 1655-69.
- **Reynolds, J. F., Neri, G., Herrmann, J. P., Blumberg, B., Coldwell, J. G., Miles, P. V. and Opitz, J. M.** (1986). New multiple congenital anomalies/mental retardation syndrome with cardio-facio-cutaneous involvement--the CFC syndrome. *Am J Med Genet* **25**, 413-27.
- **Richter, W. and Conti, M.** (2002). Dimerization of the type 4 cAMP-specific phosphodiesterases is mediated by the upstream conserved regions (UCRs). *J Biol Chem* **277**, 40212-21.
- **Rinehart, J., Adjei, A. A., Lorusso, P. M., Waterhouse, D., Hecht, J. R., Natale, R. B., Hamid, O., Varterasian, M., Asbury, P., Kaldjian, E. P. et al.** (2004). Multicenter phase II study of the oral MEK inhibitor, CI-1040, in patients with advanced non-small-cell lung, breast, colon, and pancreatic cancer. *J Clin Oncol* **22**, 4456-62.
- **Roberts, A., Allanson, J., Jadico, S. K., Kavamura, M. I., Noonan, J., Opitz, J. M., Young, T. and Neri, G.** (2006). The cardiofaciocutaneous syndrome. *J Med Genet* **43**, 833-42.
- **Roberts, A. E., Araki, T., Swanson, K. D., Montgomery, K. T., Schiripo, T. A., Joshi, V. A., Li, L., Yassin, Y., Tamburino, A. M., Neel, B. G. et al.** (2007). Germline gain-of-function mutations in SOS1 cause Noonan syndrome. *Nat Genet* **39**, 70-4.
- **Rodriguez-Viciana, P. and Rauen, K. A.** (2008). Biochemical characterization of novel germline BRAF and MEK mutations in cardio-facio-cutaneous syndrome. *Methods Enzymol* **438**, 277-89.

- **Rodriguez-Viciana, P., Tetsu, O., Tidyman, W. E., Estep, A. L., Conger, B. A., Cruz, M. S., McCormick, F. and Rauen, K. A.** (2006). Germline mutations in genes within the MAPK pathway cause cardio-facio-cutaneous syndrome. *Science* **311**, 1287-90.
- **Rohner, N., Bercsenyi, M., Orban, L., Kolanczyk, M. E., Linke, D., Brand, M., Nusslein-Volhard, C. and Harris, M. P.** (2009). Duplication of fgfr1 permits Fgf signaling to serve as a target for selection during domestication. *Curr Biol* **19**, 1642-7.
- **Rousseau, J., Klinger, S., Rachalski, A., Turgeon, B., Deleris, P., Vigneault, E., Poirier-Heon, J. F., Davoli, M. A., Mechawar, N., El Mestikawy, S. et al.** (2010). Targeted inactivation of Mapk4 in mice reveals specific nonredundant functions of Erk3/Erk4 subfamily mitogen-activated protein kinases. *Mol Cell Biol* **30**, 5752-63.
- **Rowell, C. A., Kowalczyk, J. J., Lewis, M. D. and Garcia, A. M.** (1997). Direct demonstration of geranylgeranylation and farnesylation of Ki-Ras in vivo. *J Biol Chem* **272**, 14093-7.
- **Rushworth, L. K., Hindley, A. D., O'Neill, E. and Kolch, W.** (2006). Regulation and role of Raf-1/B-Raf heterodimerization. *Mol Cell Biol* **26**, 2262-72.
- **Rutland, P., Pulleyn, L. J., Reardon, W., Baraitser, M., Hayward, R., Jones, B., Malcolm, S., Winter, R. M., Oldridge, M., Slaney, S. F. et al.** (1995). Identical mutations in the FGFR2 gene cause both Pfeiffer and Crouzon syndrome phenotypes. *Nat Genet* **9**, 173-6.
- **Rutten, K., Wallace, T. L., Works, M., Prickaerts, J., Blokland, A., Novak, T. J., Santarelli, L. and Misner, D. L.** (2011). Enhanced long-term depression and impaired reversal learning in phosphodiesterase 4B-knockout (PDE4B(-/-)) mice. *Neuropharmacology*.
- **Sala, E., Mologni, L., Truffa, S., Gaetano, C., Bollag, G. E. and Gambacorti-Passerini, C.** (2008). BRAF silencing by short hairpin RNA or chemical blockade by PLX4032 leads to different responses in melanoma and thyroid carcinoma cells. *Mol Cancer Res* **6**, 751-9.
- **Santoriello, C., Gennaro, E., Anelli, V., Distel, M., Kelly, A., Koster, R. W., Hurlstone, A. and Mione, M.** (2010). Kita driven expression of oncogenic HRAS leads to early onset and highly penetrant melanoma in zebrafish. *PLoS One* **5**, e15170.
- **Sarker, D., Molife, R., Evans, T. R., Hardie, M., Marriott, C., Butzberger-Zimmerli, P., Morrison, R., Fox, J. A., Heise, C., Louie, S. et al.** (2008). A phase I pharmacokinetic and pharmacodynamic study of TKI258, an oral, multitargeted receptor tyrosine kinase inhibitor in patients with advanced solid tumors. *Clin Cancer Res* **14**, 2075-81.
- **Sarkozy, A., Conti, E., Digilio, M. C., Marino, B., Morini, E., Pacileo, G., Wilson, M., Calabro, R., Pizzuti, A. and Dallapiccola, B.** (2004). Clinical and molecular analysis of 30 patients with multiple lentigines LEOPARD syndrome. *J Med Genet* **41**, e68.

- **Sato, M. and Yost, H. J.** (2003). Cardiac neural crest contributes to cardiomyogenesis in zebrafish. *Dev Biol* **257**, 127-39.
- **Satyamoorthy, K., Chehab, N. H., Waterman, M. J., Lien, M. C., El-Deiry, W. S., Herlyn, M. and Halazonetis, T. D.** (2000). Aberrant regulation and function of wild-type p53 in radioresistant melanoma cells. *Cell Growth Differ* **11**, 467-74.
- **Saxena, M., Williams, S., Tasken, K. and Mustelin, T.** (1999). Crosstalk between cAMP-dependent kinase and MAP kinase through a protein tyrosine phosphatase. *Nat Cell Biol* **1**, 305-11.
- **Saxena, N., Lahiri, S. S., Hambarde, S. and Tripathi, R. P.** (2008). RAS: target for cancer therapy. *Cancer Invest* **26**, 948-55.
- **Schier, A. F. and Talbot, W. S.** (2005). Molecular genetics of axis formation in zebrafish. *Annu Rev Genet* **39**, 561-613.
- **Schilling, T. F. and Kimmel, C. B.** (1994). Segment and cell type lineage restrictions during pharyngeal arch development in the zebrafish embryo. *Development* **120**, 483-94.
- **Schubbert, S., Zenker, M., Rowe, S. L., Boll, S., Klein, C., Bollag, G., van der Burgt, I., Musante, L., Kalscheuer, V., Wehner, L. E. et al.** (2006). Germline KRAS mutations cause Noonan syndrome. *Nat Genet* **38**, 331-6.
- **Schulz, A. L., Albrecht, B., Arici, C., van der Burgt, I., Buske, A., Gillessen-Kaesbach, G., Heller, R., Horn, D., Hubner, C. A., Korenke, G. C. et al.** (2008). Mutation and phenotypic spectrum in patients with cardio-facio-cutaneous and Costello syndrome. *Clin Genet* **73**, 62-70.
- **Sebolt-Leopold, J. S.** (2008). Advances in the development of cancer therapeutics directed against the RAS-mitogen-activated protein kinase pathway. *Clin Cancer Res* **14**, 3651-6.
- **Sebolt-Leopold, J. S., Dudley, D. T., Herrera, R., Van Becelaere, K., Wiland, A., Gowan, R. C., Tecle, H., Barrett, S. D., Bridges, A., Przybranowski, S. et al.** (1999). Blockade of the MAP kinase pathway suppresses growth of colon tumors in vivo. *Nat Med* **5**, 810-6.
- **Sebolt-Leopold, J. S. and Herrera, R.** (2004). Targeting the mitogen-activated protein kinase cascade to treat cancer. *Nat Rev Cancer* **4**, 937-47.
- **Seishima, M., Mizutani, Y., Shibuya, Y., Arakawa, C., Yoshida, R. and Ogata, T.** (2007). Malignant melanoma in a woman with LEOPARD syndrome: identification of a germline PTPN11 mutation and a somatic BRAF mutation. *Br J Dermatol* **157**, 1297-9.
- **Selcen, D., Kupsky, W. J., Benjamins, D. and Nigro, M. A.** (2001). Myopathy with muscle spindle excess: A new congenital neuromuscular syndrome? *Muscle Nerve* **24**, 138-43.
- **Senawong, T., Phuchareon, J., Ohara, O., McCormick, F., Rauen, K. A. and Tetsu, O.** (2008). Germline mutations of MEK in cardio-facio-cutaneous syndrome are sensitive to MEK and RAF inhibition: implications for therapeutic options. *Hum Mol Genet* **17**, 419-30.
- **Shah, N., Rodriguez, M., Louis, D. S., Lindley, K. and Milla, P. J.** (1999).

Feeding difficulties and foregut dysmotility in Noonan's syndrome. *Arch Dis Child* **81**, 28-31.

- **Shao, Y. Y., Lin, C. C. and Yang, C. H.** (2010). Gefitinib or erlotinib in the treatment of advanced non-small cell lung cancer. *Discov Med* **9**, 538-45.
- **Sharland, M., Patton, M. A., Talbot, S., Chitolie, A. and Bevan, D. H.** (1992). Coagulation-factor deficiencies and abnormal bleeding in Noonan's syndrome. *Lancet* **339**, 19-21.
- **Shen, C. P., Tsimberg, Y., Salvadore, C. and Meller, E.** (2004). Activation of Erk and JNK MAPK pathways by acute swim stress in rat brain regions. *BMC Neurosci* **5**, 36.
- **Shin, S. Y., Rath, O., Choo, S. M., Fee, F., McFerran, B., Kolch, W. and Cho, K. H.** (2009). Positive- and negative-feedback regulations coordinate the dynamic behavior of the Ras-Raf-MEK-ERK signal transduction pathway. *J Cell Sci* **122**, 425-35.
- **Shinya, M., Koshida, S., Sawada, A., Kuroiwa, A. and Takeda, H.** (2001). Fgf signalling through MAPK cascade is required for development of the subpallial telencephalon in zebrafish embryos. *Development* **128**, 4153-64.
- **Shukla, V., Coumoul, X., Wang, R. H., Kim, H. S. and Deng, C. X.** (2007). RNA interference and inhibition of MEK-ERK signaling prevent abnormal skeletal phenotypes in a mouse model of craniosynostosis. *Nat Genet* **39**, 1145-50.
- **Siegel, D. H., McKenzie, J., Frieden, I. J. and Rauen, K. A.** (2011). Dermatological findings in 61 mutation-positive individuals with cardiofaciocutaneous syndrome. *Br J Dermatol* **164**, 521-9.
- **Singer, G., Oldt, R., 3rd, Cohen, Y., Wang, B. G., Sidransky, D., Kurman, R. J. and Shih Ie, M.** (2003). Mutations in BRAF and KRAS characterize the development of low-grade ovarian serous carcinoma. *J Natl Cancer Inst* **95**, 484-6.
- **Sleeman, M., Fraser, J., McDonald, M., Yuan, S., White, D., Grandison, P., Kumble, K., Watson, J. D. and Murison, J. G.** (2001). Identification of a new fibroblast growth factor receptor, FGFR5. *Gene* **271**, 171-82.
- **Smalley, K. S., Haass, N. K., Brafford, P. A., Lioni, M., Flaherty, K. T. and Herlyn, M.** (2006). Multiple signaling pathways must be targeted to overcome drug resistance in cell lines derived from melanoma metastases. *Mol Cancer Ther* **5**, 1136-44.
- **Smith, A., Zhang, J., Guay, D., Quint, E., Johnson, A. and Akimenko, M. A.** (2008). Gene expression analysis on sections of zebrafish regenerating fins reveals limitations in the whole-mount in situ hybridization method. *Dev Dyn* **237**, 417-25.
- **Soderling, S. H., Bayuga, S. J. and Beavo, J. A.** (1998). Identification and characterization of a novel family of cyclic nucleotide phosphodiesterases. *J Biol Chem* **273**, 15553-8.
- **Solit, D. B., Garraway, L. A., Pratilas, C. A., Sawai, A., Getz, G., Basso, A., Ye, Q., Lobo, J. M., She, Y., Osman, I. et al.** (2006). BRAF mutation

predicts sensitivity to MEK inhibition. *Nature* **439**, 358-62.
- **Solnica-Krezel, L.** (2005). Conserved patterns of cell movements during vertebrate gastrulation. *Curr Biol* **15**, R213-28.
- **Solnica-Krezel, L.** (2006). Gastrulation in zebrafish -- all just about adhesion? *Curr Opin Genet Dev* **16**, 433-41.
- **Solnica-Krezel, L., Schier, A. F. and Driever, W.** (1994). Efficient recovery of ENU-induced mutations from the zebrafish germline. *Genetics* **136**, 1401-20.
- **Somerville, J. and Bonham-Carter, R. E.** (1972). The heart in lentiginosis. *Br Heart J* **34**, 58-66.
- **Souness, J. E., Houghton, C., Sardar, N. and Withnall, M. T.** (1997). Evidence that cyclic AMP phosphodiesterase inhibitors suppress interleukin-2 release from murine splenocytes by interacting with a 'low-affinity' phosphodiesterase 4 conformer. *Br J Pharmacol* **121**, 743-50.
- **Spence, R., Gerlach, G., Lawrence, C. and Smith, C.** (2008). The behaviour and ecology of the zebrafish, Danio rerio. *Biol Rev Camb Philos Soc* **83**, 13-34.
- **Stahl, J. M., Cheung, M., Sharma, A., Trivedi, N. R., Shanmugam, S. and Robertson, G. P.** (2003). Loss of PTEN promotes tumor development in malignant melanoma. *Cancer Res* **63**, 2881-90.
- **Stemple, D. L.** (2004). TILLING--a high-throughput harvest for functional genomics. *Nat Rev Genet* **5**, 145-50.
- **Stork, P. J. and Schmitt, J. M.** (2002). Crosstalk between cAMP and MAP kinase signaling in the regulation of cell proliferation. *Trends Cell Biol* **12**, 258-66.
- **Strumberg, D., Richly, H., Hilger, R. A., Schleucher, N., Korfee, S., Tewes, M., Faghih, M., Brendel, E., Voliotis, D., Haase, C. G. et al.** (2005). Phase I clinical and pharmacokinetic study of the Novel Raf kinase and vascular endothelial growth factor receptor inhibitor BAY 43-9006 in patients with advanced refractory solid tumors. *J Clin Oncol* **23**, 965-72.
- **Sun, H., Seyer, J. M. and Patel, T. B.** (1995). A region in the cytosolic domain of the epidermal growth factor receptor antithetically regulates the stimulatory and inhibitory guanine nucleotide-binding regulatory proteins of adenylyl cyclase. *Proc Natl Acad Sci U S A* **92**, 2229-33.
- **Sun, H. D., Malabunga, M., Tonra, J. R., DiRenzo, R., Carrick, F. E., Zheng, H., Berthoud, H. R., McGuinness, O. P., Shen, J., Bohlen, P. et al.** (2007). Monoclonal antibody antagonists of hypothalamic FGFR1 cause potent but reversible hypophagia and weight loss in rodents and monkeys. *Am J Physiol Endocrinol Metab* **292**, E964-76.
- **Szabo-Rogers, H. L., Geetha-Loganathan, P., Nimmagadda, S., Fu, K. K. and Richman, J. M.** (2008). FGF signals from the nasal pit are necessary for normal facial morphogenesis. *Dev Biol* **318**, 289-302.
- **Tamborini, E., Pricl, S., Negri, T., Lagonigro, M. S., Miselli, F., Greco, A., Gronchi, A., Casali, P. G., Ferrone, M., Fermeglia, M. et al.** (2006).

Functional analyses and molecular modeling of two c-Kit mutations responsible for imatinib secondary resistance in GIST patients. *Oncogene* **25**, 6140-6.

- **Tartaglia, M. and Gelb, B. D.** (2005). Germ-line and somatic PTPN11 mutations in human disease. *Eur J Med Genet* **48**, 81-96.
- **Tartaglia, M., Pennacchio, L. A., Zhao, C., Yadav, K. K., Fodale, V., Sarkozy, A., Pandit, B., Oishi, K., Martinelli, S., Schackwitz, W. et al.** (2007). Gain-of-function SOS1 mutations cause a distinctive form of Noonan syndrome. *Nat Genet* **39**, 75-9.
- **Tartaglia, M., Zampino, G. and Gelb, B. D.** (2010). Noonan syndrome: clinical aspects and molecular pathogenesis. *Mol Syndromol* **1**, 2-26.
- **Taylor, K. L., Grant, N. J., Temperley, N. D. and Patton, E. E.** (2010). Small molecule screening in zebrafish: an in vivo approach to identifying new chemical tools and drug leads. *Cell Commun Signal* **8**, 11.
- **Tecle, H., Shao, J., Li, Y., Kothe, M., Kazmirski, S., Penzotti, J., Ding, Y. H., Ohren, J., Moshinsky, D., Coli, R. et al.** (2009). Beyond the MEK-pocket: can current MEK kinase inhibitors be utilized to synthesize novel type III NCKIs? Does the MEK-pocket exist in kinases other than MEK? *Bioorg Med Chem Lett* **19**, 226-9.
- **Thiel, C., Wilken, M., Zenker, M., Sticht, H., Fahsold, R., Gusek-Schneider, G. C. and Rauch, A.** (2009). Independent NF1 and PTPN11 mutations in a family with neurofibromatosis-Noonan syndrome. *Am J Med Genet A* **149A**, 1263-7.
- **Thisse, B., Heyer, V., Lux, A., Alunni, V., Degrave, A., Seiliez, I., Kirchner, J., Parkhill, J. P. and Thisse, C.** (2004). Spatial and temporal expression of the zebrafish genome by large-scale in situ hybridization screening. *Methods Cell Biol* **77**, 505-19.
- **Thisse, B. and Thisse, C.** (2005). Functions and regulations of fibroblast growth factor signaling during embryonic development. *Dev Biol* **287**, 390-402.
- **Thisse, C. and Thisse, B.** (2008). High-resolution in situ hybridization to whole-mount zebrafish embryos. *Nat Protoc* **3**, 59-69.
- **Tidyman, W. E. and Rauen, K. A.** (2010). Mutational and functional analysis in human Ras/MAP kinase genetic syndromes. *Methods Mol Biol* **661**, 433-47.
- **Tobin, J. L., Di Franco, M., Eichers, E., May-Simera, H., Garcia, M., Yan, J., Quinlan, R., Justice, M. J., Hennekam, R. C., Briscoe, J. et al.** (2008). Inhibition of neural crest migration underlies craniofacial dysmorphology and Hirschsprung's disease in Bardet-Biedl syndrome. *Proc Natl Acad Sci U S A* **105**, 6714-9.
- **Tortora, G., Damiano, V., Bianco, C., Baldassarre, G., Bianco, A. R., Lanfrancone, L., Pelicci, P. G. and Ciardiello, F.** (1997). The RIalpha subunit of protein kinase A (PKA) binds to Grb2 and allows PKA interaction with the activated EGF-receptor. *Oncogene* **14**, 923-8.

- **Trainor, P. A.** (2005). Specification of neural crest cell formation and migration in mouse embryos. *Semin Cell Dev Biol* **16**, 683-93.
- **Tsai, J., Lee, J. T., Wang, W., Zhang, J., Cho, H., Mamo, S., Bremer, R., Gillette, S., Kong, J., Haass, N. K. et al.** (2008). Discovery of a selective inhibitor of oncogenic B-Raf kinase with potent antimelanoma activity. *Proc Natl Acad Sci U S A* **105**, 3041-6.
- **Tsao, H., Goel, V., Wu, H., Yang, G. and Haluska, F. G.** (2004). Genetic interaction between NRAS and BRAF mutations and PTEN/MMAC1 inactivation in melanoma. *J Invest Dermatol* **122**, 337-41.
- **Tsao, H., Mihm, M. C., Jr. and Sheehan, C.** (2003). PTEN expression in normal skin, acquired melanocytic nevi, and cutaneous melanoma. *J Am Acad Dermatol* **49**, 865-72.
- **Tsimberidou, A. M., Camacho, L. H., Verstovsek, S., Ng, C., Hong, D. S., Uehara, C. K., Gutierrez, C., Daring, S., Stevens, J., Komarnitsky, P. B. et al.** (2009). A phase I clinical trial of darinaparsin in patients with refractory solid tumors. *Clin Cancer Res* **15**, 4769-76.
- **Tuma, R. S.** (2010). Getting around PLX4032: studies turn up unusual mechanisms of resistance to melanoma drug. *J Natl Cancer Inst* **103**, 170-1, 177.
- **Turner, N. and Grose, R.** (2010). Fibroblast growth factor signalling: from development to cancer. *Nat Rev Cancer* **10**, 116-29.
- **Turner, N., Lambros, M. B., Horlings, H. M., Pearson, A., Sharpe, R., Natrajan, R., Geyer, F. C., van Kouwenhove, M., Kreike, B., Mackay, A. et al.** (2010). Integrative molecular profiling of triple negative breast cancers identifies amplicon drivers and potential therapeutic targets. *Oncogene* **29**, 2013-23.
- **van Den Berg, H. and Hennekam, R. C.** (1999). Acute lymphoblastic leukaemia in a patient with cardiofaciocutaneous syndrome. *J Med Genet* **36**, 799-800.
- **van der Burgt, I.** (2007). Noonan syndrome. *Orphanet J Rare Dis* **2**, 4.
- **Van Meter, M. E. and Kim, E. S.** (2010). Bevacizumab: current updates in treatment. *Curr Opin Oncol* **22**, 586-91.
- **van Rhijn, B. W., van Tilborg, A. A., Lurkin, I., Bonaventure, J., de Vries, A., Thiery, J. P., van der Kwast, T. H., Zwarthoff, E. C. and Radvanyi, F.** (2002). Novel fibroblast growth factor receptor 3 (FGFR3) mutations in bladder cancer previously identified in non-lethal skeletal disorders. *Eur J Hum Genet* **10**, 819-24.
- **Vossler, M. R., Yao, H., York, R. D., Pan, M. G., Rim, C. S. and Stork, P. J.** (1997). cAMP activates MAP kinase and Elk-1 through a B-Raf- and Rap1-dependent pathway. *Cell* **89**, 73-82.
- **Walshe, J. and Mason, I.** (2003). Fgf signalling is required for formation of cartilage in the head. *Dev Biol* **264**, 522-36.
- **Wan, P. T., Garnett, M. J., Roe, S. M., Lee, S., Niculescu-Duvaz, D., Good, V. M., Jones, C. M., Marshall, C. J., Springer, C. J., Barford, D. et**

al. (2004). Mechanism of activation of the RAF-ERK signaling pathway by oncogenic mutations of B-RAF. *Cell* **116**, 855-67.

- **Wang, J., Zhang, X., Thomas, S. M., Grandis, J. R., Wells, A., Chen, Z. G. and Ferris, R. L.** (2005). Chemokine receptor 7 activates phosphoinositide-3 kinase-mediated invasive and prosurvival pathways in head and neck cancer cells independent of EGFR. *Oncogene* **24**, 5897-904.
- **Wang, Y., Su, B. and Xia, Z.** (2006). Brain-derived neurotrophic factor activates ERK5 in cortical neurons via a Rap1-MEKK2 signaling cascade. *J Biol Chem* **281**, 35965-74.
- **Wee, S., Jagani, Z., Xiang, K. X., Loo, A., Dorsch, M., Yao, Y. M., Sellers, W. R., Lengauer, C. and Stegmeier, F.** (2009). PI3K pathway activation mediates resistance to MEK inhibitors in KRAS mutant cancers. *Cancer Res* **69**, 4286-93.
- **Weickhardt, A. J., Tebbutt, N. C. and Mariadason, J. M.** (2010). Strategies for overcoming inherent and acquired resistance to EGFR inhibitors by targeting downstream effectors in the RAS/PI3K pathway. *Curr Cancer Drug Targets* **10**, 824-33.
- **Weinberg, E., Zeldich, E., Weinreb, M. M., Moses, O., Nemcovsky, C. and Weinreb, M.** (2009). Prostaglandin E2 inhibits the proliferation of human gingival fibroblasts via the EP2 receptor and Epac. *J Cell Biochem* **108**, 207-15.
- **Weisberg, E., Choi, H. G., Ray, A., Barrett, R., Zhang, J., Sim, T., Zhou, W., Seeliger, M., Cameron, M., Azam, M. et al.** (2010). Discovery of a small-molecule type II inhibitor of wild-type and gatekeeper mutants of BCR-ABL, PDGFRalpha, Kit, and Src kinases: novel type II inhibitor of gatekeeper mutants. *Blood* **115**, 4206-16.
- **Weisz, B., Giehl, K., Gana-Weisz, M., Egozi, Y., Ben-Baruch, G., Marciano, D., Gierschik, P. and Kloog, Y.** (1999). A new functional Ras antagonist inhibits human pancreatic tumor growth in nude mice. *Oncogene* **18**, 2579-88.
- **Wellbrock, C. and Hurlstone, A.** (2010). BRAF as therapeutic target in melanoma. *Biochem Pharmacol* **80**, 561-7.
- **Wellbrock, C., Karasarides, M. and Marais, R.** (2004). The RAF proteins take centre stage. *Nat Rev Mol Cell Biol* **5**, 875-85.
- **Westerfield, M.** (2000). The Zebrafish book : a guide for the laboratory use of zebrafish (Brachydanio rerio). Eugene. Or.: University of Oregon Press.
- **White, K. E., Cabral, J. M., Davis, S. I., Fishburn, T., Evans, W. E., Ichikawa, S., Fields, J., Yu, X., Shaw, N. J., McLellan, N. J. et al.** (2005). Mutations that cause osteoglophonic dysplasia define novel roles for FGFR1 in bone elongation. *Am J Hum Genet* **76**, 361-7.
- **White, R. M., Cech, J., Ratanasirintrawoot, S., Lin, C. Y., Rahl, P. B., Burke, C. J., Langdon, E., Tomlinson, M. L., Mosher, J., Kaufman, C. et al.** (2011). DHODH modulates transcriptional elongation in the neural crest and melanoma. *Nature* **471**, 518-22.

- **White, S. M., Graham, J. M., Jr., Kerr, B., Gripp, K., Weksberg, R., Cytrynbaum, C., Reeder, J. L., Stewart, F. J., Edwards, M., Wilson, M. et al.** (2005). The adult phenotype in Costello syndrome. *Am J Med Genet A* **136**, 128-35.
- **Whyte, D. B., Kirschmeier, P., Hockenberry, T. N., Nunez-Oliva, I., James, L., Catino, J. J., Bishop, W. R. and Pai, J. K.** (1997). K- and N-Ras are geranylgeranylated in cells treated with farnesyl protein transferase inhibitors. *J Biol Chem* **272**, 14459-64.
- **Wilhelm, S., Carter, C., Lynch, M., Lowinger, T., Dumas, J., Smith, R. A., Schwartz, B., Simantov, R. and Kelley, S.** (2006). Discovery and development of sorafenib: a multikinase inhibitor for treating cancer. *Nat Rev Drug Discov* **5**, 835-44.
- **Wilhelm, S. M., Carter, C., Tang, L., Wilkie, D., McNabola, A., Rong, H., Chen, C., Zhang, X., Vincent, P., McHugh, M. et al.** (2004). BAY 43-9006 exhibits broad spectrum oral antitumor activity and targets the RAF/MEK/ERK pathway and receptor tyrosine kinases involved in tumor progression and angiogenesis. *Cancer Res* **64**, 7099-109.
- **Wilkie, A. O.** (2007). Cancer drugs to treat birth defects. *Nat Genet* **39**, 1057-9.
- **Wilkie, A. O., Slaney, S. F., Oldridge, M., Poole, M. D., Ashworth, G. J., Hockley, A. D., Hayward, R. D., David, D. J., Pulleyn, L. J., Rutland, P. et al.** (1995). Apert syndrome results from localized mutations of FGFR2 and is allelic with Crouzon syndrome. *Nat Genet* **9**, 165-72.
- **Williams, V. C., Lucas, J., Babcock, M. A., Gutmann, D. H., Korf, B. and Maria, B. L.** (2009). Neurofibromatosis type 1 revisited. *Pediatrics* **123**, 124-33.
- **Wilson, J. and Tucker, A. S.** (2004). Fgf and Bmp signals repress the expression of Bapx1 in the mandibular mesenchyme and control the position of the developing jaw joint. *Dev Biol* **266**, 138-50.
- **Windmann, S., Schonecke, O. W., Frohlig, G. and Maldener, G.** (1999). Dissociating beliefs about heart rates and actual heart rates in patients with cardiac pacemakers. *Psychophysiology* **36**, 339-42.
- **Winter-Vann, A. M., Baron, R. A., Wong, W., dela Cruz, J., York, J. D., Gooden, D. M., Bergo, M. O., Young, S. G., Toone, E. J. and Casey, P. J.** (2005). A small-molecule inhibitor of isoprenylcysteine carboxyl methyltransferase with antitumor activity in cancer cells. *Proc Natl Acad Sci U S A* **102**, 4336-41.
- **Winter-Vann, A. M. and Johnson, G. L.** (2007). Integrated activation of MAP3Ks balances cell fate in response to stress. *J Cell Biochem* **102**, 848-58.
- **Wu, X., Simpson, J., Hong, J. H., Kim, K. H., Thavarajah, N. K., Backx, P. H., Neel, B. G. and Araki, T.** MEK-ERK pathway modulation ameliorates disease phenotypes in a mouse model of Noonan syndrome associated with the Raf1(L613V) mutation. *J Clin Invest* **121**, 1009-25.
- **Yan, N., Ricca, C., Fletcher, J., Glover, T., Seizinger, B. R. and Manne,**

V. (1995). Farnesyltransferase inhibitors block the neurofibromatosis type I (NF1) malignant phenotype. *Cancer Res* **55**, 3569-75.

- **Yang, L., Jackson, E., Woerner, B. M., Perry, A., Piwnica-Worms, D. and Rubin, J. B.** (2007). Blocking CXCR4-mediated cyclic AMP suppression inhibits brain tumor growth in vivo. *Cancer Res* **67**, 651-8.
- **Yao, H., York, R. D., Misra-Press, A., Carr, D. W. and Stork, P. J.** (1998). The cyclic adenosine monophosphate-dependent protein kinase (PKA) is required for the sustained activation of mitogen-activated kinases and gene expression by nerve growth factor. *J Biol Chem* **273**, 8240-7.
- **Yeh, J. R., Munson, K. M., Elagib, K. E., Goldfarb, A. N., Sweetser, D. A. and Peterson, R. T.** (2009). Discovering chemical modifiers of oncogene-regulated hematopoietic differentiation. *Nat Chem Biol* **5**, 236-43.
- **Yeung, K., Janosch, P., McFerran, B., Rose, D. W., Mischak, H., Sedivy, J. M. and Kolch, W.** (2000). Mechanism of suppression of the Raf/MEK/extracellular signal-regulated kinase pathway by the raf kinase inhibitor protein. *Mol Cell Biol* **20**, 3079-85.
- **Yoon, S. and Seger, R.** (2006). The extracellular signal-regulated kinase: multiple substrates regulate diverse cellular functions. *Growth Factors* **24**, 21-44.
- **Yuen, S. T., Davies, H., Chan, T. L., Ho, J. W., Bignell, G. R., Cox, C., Stephens, P., Edkins, S., Tsui, W. W., Chan, A. S. et al.** (2002). Similarity of the phenotypic patterns associated with BRAF and KRAS mutations in colorectal neoplasia. *Cancer Res* **62**, 6451-5.
- **Zampino, G., Pantaleoni, F., Carta, C., Cobellis, G., Vasta, I., Neri, C., Pogna, E. A., De Feo, E., Delogu, A., Sarkozy, A. et al.** (2007). Diversity, parental germline origin, and phenotypic spectrum of de novo HRAS missense changes in Costello syndrome. *Hum Mutat* **28**, 265-72.
- **Zeller, E., Stief, H. J., Pflug, B. and Sastre-y-Hernandez, M.** (1984). Results of a phase II study of the antidepressant effect of rolipram. *Pharmacopsychiatry* **17**, 188-90.
- **Zenker, M., Lehmann, K., Schulz, A. L., Barth, H., Hansmann, D., Koenig, R., Korinthenberg, R., Kreiss-Nachtsheim, M., Meinecke, P., Morlot, S. et al.** (2007). Expansion of the genotypic and phenotypic spectrum in patients with KRAS germline mutations. *J Med Genet* **44**, 131-5.
- **Zhang, F. L., Kirschmeier, P., Carr, D., James, L., Bond, R. W., Wang, L., Patton, R., Windsor, W. T., Syto, R., Zhang, R. et al.** (1997). Characterization of Ha-ras, N-ras, Ki-Ras4A, and Ki-Ras4B as in vitro substrates for farnesyl protein transferase and geranylgeranyl protein transferase type I. *J Biol Chem* **272**, 10232-9.
- **Zhang, H. T., Crissman, A. M., Dorairaj, N. R., Chandler, L. J. and O'Donnell, J. M.** (2000). Inhibition of cyclic AMP phosphodiesterase (PDE4) reverses memory deficits associated with NMDA receptor antagonism. *Neuropsychopharmacology* **23**, 198-204.
- **Zhang, H. T., Zhao, Y., Huang, Y., Deng, C., Hopper, A. T., De Vivo, M.,**

Rose, G. M. and O'Donnell, J. M. (2006). Antidepressant-like effects of PDE4 inhibitors mediated by the high-affinity rolipram binding state (HARBS) of the phosphodiesterase-4 enzyme (PDE4) in rats. *Psychopharmacology (Berl)* **186**, 209-17.

- **Zhang, H. T., Zhao, Y., Huang, Y., Dorairaj, N. R., Chandler, L. J. and O'Donnell, J. M.** (2004). Inhibition of the phosphodiesterase 4 (PDE4) enzyme reverses memory deficits produced by infusion of the MEK inhibitor U0126 into the CA1 subregion of the rat hippocampus. *Neuropsychopharmacology* **29**, 1432-9.
- **Zhang, W. and Liu, H. T.** (2002). MAPK signal pathways in the regulation of cell proliferation in mammalian cells. *Cell Res* **12**, 9-18.
- **Zhang, Z., Kobayashi, S., Borczuk, A. C., Leidner, R. S., Laframboise, T., Levine, A. D. and Halmos, B.** (2010). Dual specificity phosphatase 6 (DUSP6) is an ETS-regulated negative feedback mediator of oncogenic ERK signaling in lung cancer cells. *Carcinogenesis* **31**, 577-86.
- **Zhao, Y., Zhang, H. T. and O'Donnell, J. M.** (2003). Antidepressant-induced increase in high-affinity rolipram binding sites in rat brain: dependence on noradrenergic and serotonergic function. *J Pharmacol Exp Ther* **307**, 246-53.
- **Zinnamosca, L., Petramala, L., Cotesta, D., Marinelli, C., Schina, M., Cianci, R., Giustini, S., Sciomer, S., Anastasi, E., Calvieri, S. et al.** (2010). Neurofibromatosis type 1 (NF1) and pheochromocytoma: prevalence, clinical and cardiovascular aspects. *Arch Dermatol Res*.
- **Zundelevich, A., Elad-Sfadia, G., Haklai, R. and Kloog, Y.** (2007). Suppression of lung cancer tumor growth in a nude mouse model by the Ras inhibitor salirasib (farnesylthiosalicylic acid). *Mol Cancer Ther* **6**, 1765-73.

Appendix I – Supplementary Data

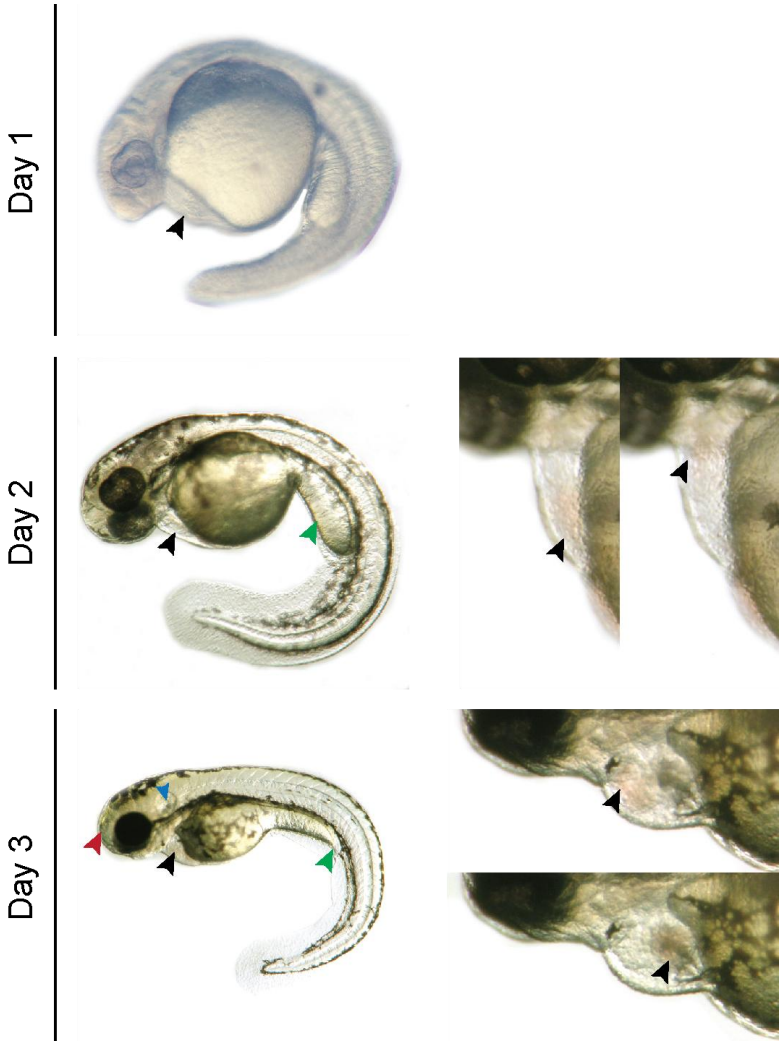

Figure A-1 *C-raf morpholino affects normal embryonic development*

Injection of wild-type zebrafish embryos with a C-raf MO promotes curling of the posterior structures, yolk extension defects (green arrow), close otolith proximity (blue arrow), development of a smaller head (red arrow) as well as an enlarged pericardium and mild atrio-ventricular anomalies (black arrows). All the morphant phenotypes were in agreement with previously published observations.

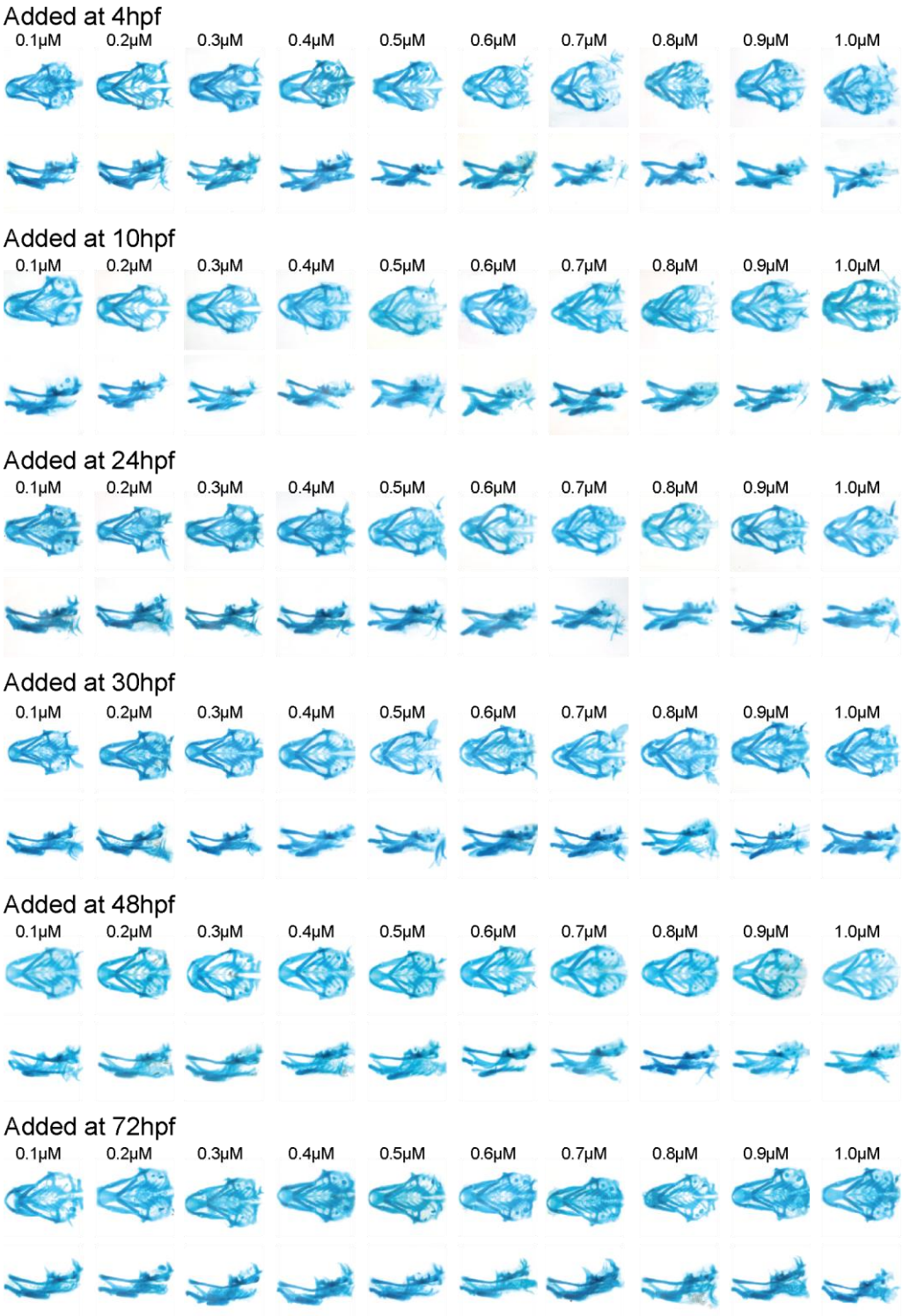

Figure A-2 *Cartilage staining of all the treated embryo groups*

Alcian blue staining of the jaw structures of all the embryos treated with increasing concentrations of PD0325901 (horizontally) at different timepoints (vertically). The top panel of each group is a ventral image of the stained cartilage and the lower panel shows the lateral image of the same embryo.

Appendix II – Relevant Publications

Human Molecular Genetics, 2009, Vol. 18, No. 14 **2543–2554**
doi:10.1093/hmg/ddp186
Advance Access published on April 17, 2009

Kinase-activating and kinase-impaired cardio-facio-cutaneous syndrome alleles have activity during zebrafish development and are sensitive to small molecule inhibitors

Corina Anastasaki[1], Anne L. Estep[2], Richard Marais[3], Katherine A. Rauen[2] and E. Elizabeth Patton[1,*]

[1]MRC Human Genetics Unit and The University of Edinburgh Institute for Genetics and Molecular Medicine, Western General Hospital, Crewe Road, Edinburgh EH4 2XU, UK, [2]Department of Pediatrics, University of California San Francisco, UCSF Helen Diller Family Comprehensive Cancer Center, 2340 Sutter Street, San Francisco, CA 94115, USA and [3]Cancer Research UK Centre for Cell and Molecular Biology, Signal Transduction Team, The Institute of Cancer Research, 237 Fulham Road, London SW3 6JB, UK

Received February 28, 2009; Revised and Accepted April 15, 2009

The Ras/MAPK pathway is critical for human development and plays a central role in the formation and progression of most cancers. Children born with germ-line mutations in BRAF, MEK1 or MEK2 develop cardio-facio-cutaneous (CFC) syndrome, an autosomal dominant syndrome characterized by a distinctive facial appearance, heart defects, skin and hair abnormalities and mental retardation. CFC syndrome mutations in BRAF promote both kinase-activating and kinase-impaired variants. CFC syndrome has a progressive phenotype, and the availability of clinically active inhibitors of the MAPK pathway prompts the important question as to whether such inhibitors might be therapeutically effective in the treatment of CFC syndrome. To study the developmental effects of CFC mutant alleles *in vivo*, we have expressed a panel of 28 BRAF and MEK alleles in zebrafish embryos to assess the function of human disease alleles and available chemical inhibitors of this pathway. We find that both kinase-activating and kinase-impaired CFC mutant alleles promote the equivalent developmental outcome when expressed during early development and that treatment of CFC-zebrafish embryos with inhibitors of the FGF-MAPK pathway can restore normal early development. Importantly, we find a developmental window in which treatment with a MEK inhibitor can restore the normal early development of the embryo, without the additional, unwanted developmental effects of the drug.

INTRODUCTION

Perception of the RAS-RAF-MEK-ERK mitogen-activated protein kinase (Ras/MAPK) signalling components, known for their role in signalling and cancer, has been altered by the discovery that germ-line mutations underlie a series of syndromes with overlapping features. These Ras/MAPK syndromes include the genetic disorders neurofibromatosis Type I, LEOPARD syndrome, Noonan syndrome, Costello syndrome, capillary malformation arteriovenous malformation syndrome and cardio-facio-cutaneous (CFC) syndrome. The overlapping clinical features, including heart defects, distinctive facial appearances, skin and hair abnormalities, short stature and mental retardation, propelled the discovery that these syndromes are caused by germ-line mutations in the same genetic pathway, and reflect a common underlying molecular pathogenesis through mutation of core components of the Ras/MAPK signalling pathway. Characteristics that distinguish between the syndromes coupled with the now available sequence-based genetic testing, has been an important

*To whom correspondence should be addressed. Tel: +44 1317773500; Fax: +44 1317773583; Email: epatton@staffmail.ed.ac.uk

step forward in diagnosis and characterization of this group of disorders (1).

With refined diagnostic tools in hand, there is a need to understand the nature of the CFC mutations *in vivo* and develop therapeutic approaches. Activated in most cancers, the Ras/MAPK signalling pathway is among the key drug targets for anti-cancer therapies (2). The pathway is activated in tumour cells through many different ways, including mutation of the components themselves, often through gain-of-function mutations. For example, the BRAF oncogene is mutated in over 60% of melanomas (3). The 'addiction' of a broad spectrum of tumours to the continued activation of Ras/MAPK signalling has made it a prime target for pharmacological intervention, and specific BRAF and MEK inhibitors are currently in clinical trails (2,4–6). Although patients with Costello syndrome are prone to developing neural crest malignancies, it is not clear if CFC patients have an elevated risk of developing cancer, with only a few individuals developing neoplasms in different tissues (1). CFC BRAF mutations have a wider mutation spectrum than BRAF-nevi/cancer mutations, yet two notable similarities emerge. First, the spectrum of CFC and nevi/cancer mutations overlap, some with identical mutations. Second, CFC and nevi/cancer disease BRAF alleles result in both kinase-activating and kinase-impaired activities *in vitro* (7–10). Although *in vitro* functional assays have established the effects of the CFC mutation on kinase activity, an outstanding question is how both activating and inactivating BRAF mutations give rise to the same clinical phenotype. We wanted to establish if CFC allele mutations promote the same phenotypic outcome *in vivo*, and which mutations are sensitive to currently available MAPK-pathway inhibitors (11,12).

Animal models play an important role in furthering our understanding of the pathogenesis associated with Ras/MAPK syndromes disease alleles. Studies in transgenic *Drosophila* have shown that both loss-of-function and gain-of-function LEOPARD and Noonan syndrome *PTPN11* mutations can give rise to similar developmental phenotypes in the eye and wing veins of the fly, suggesting a rationale for how different *PTPN11* mutations can give rise to syndromes with clinically overlapping phenotypes (13,14). In zebrafish, loss of *PTPN11* (SHP-2) and expression of Noonan and LEOPARD syndrome alleles cause early cell movement phenotypes and developmental features that overlap with the principal features of the syndromes, including growth and heart defects, craniofacial abnormalities and ocular hypertelorism (15). Adult zebrafish and mouse models of H-Ras^{G12V} reveal overlapping phenotypes with Costello syndrome patients (16,17). Both models provide insight into the syndrome. The zebrafish H-Ras^{G12V} model suggests that oncogene-induced senescence contributes to the pathogenesis of Costello syndrome (16), and the H-Ras^{G12V}-induced cardiomyopathies in the mouse can be prevented with treatment with standard anti-hypertensive therapies (17). Thus, animal models can rapidly reveal the nature of the human genetic mutation *in vivo*, their impact upon development, and provide insight into evaluating new therapeutic opportunities.

Cell culture studies have shown that CFC MEK mutant alleles are sensitive to the widely used MEK inhibitor, U0126 (12). Most CFC patients have mutations in BRAF, and it has been predicted that BRAF CFC alleles might also be sensitive to MEK inhibition (12). Given that MAPK signalling plays an important role in cell movement in zebrafish gastrulation (18), we wanted to establish the effects of BRAF and MEK CFC mutant alleles in early development. Here, we use the zebrafish system to explore the function of a panel of 28 BRAF and MEK mutant alleles in development, and to assess the potential of using small molecule inhibitors to prevent these defects. We show that the expression of both BRAF and MEK kinase-activating and kinase-impaired CFC and melanoma alleles cause similar phenotypes with significant cell movement defects in early embryogenesis. In addition, we find that the cell movement phenotypes of both the kinase-activating and kinase-impaired CFC alleles can be prevented by treatment with specific MEK inhibitors. Treatment is most effective within a developmental time window: a 1 h treatment at the start of significant convergence–extension cell movements is necessary and sufficient to prevent the CFC induced developmental effects. FGF-MAPK signalling is active during early embryogenesis, and therefore we hypothesized that the inhibition of endogenous FGFR signalling might partially prevent the developmental effects of CFC alleles in gastrulation. We show inhibition of upstream signalling is also able to restore normal development for CFC, except for the most active BRAF melanoma allele, demonstrating the importance of overall activation of the MAPK signalling during development. With sequencing-based genetic tests available to identify individuals with mutations, our work provides a rationale for varied kinase activity in the CFC allele spectrum and will contribute to the clinical discussion about the treatment strategy for individuals with CFC syndrome using currently available MAPK-pathway inhibitors.

RESULTS

CFC allele activity in zebrafish development

The Ras/MAPK pathway is highly conserved in vertebrates, and we have used the zebrafish system to examine the functional activity of CFC alleles and their response to chemical inhibition (Fig. 1), based on the important role of the FGF-MAPK pathway during early embryonic development. Within the past two decades, the zebrafish system has become established as a useful model for vertebrate developmental biology and disease (19). Organogenesis in the transparent embryos can be followed *in vivo* under the light microscope, and specific genetic and chemical models of human developmental syndromes have advanced our understanding of human disease and treatment (19–21).

Vertebrates share a conserved body plan that is established through gastrulation, the critical process that involves extensive cell movement and shapes the relatively unstructured early embryo into a gastrula with conserved germ layers (18). FGF-MAPK signalling contributes to the establishment of the dorsoventral axis, in which the highest concentration of FGF-signalling specifies the dorsal most part of the embryo and acts as a local attractive centre for convergence–extension movements within the gastrula (18). Expression of activated

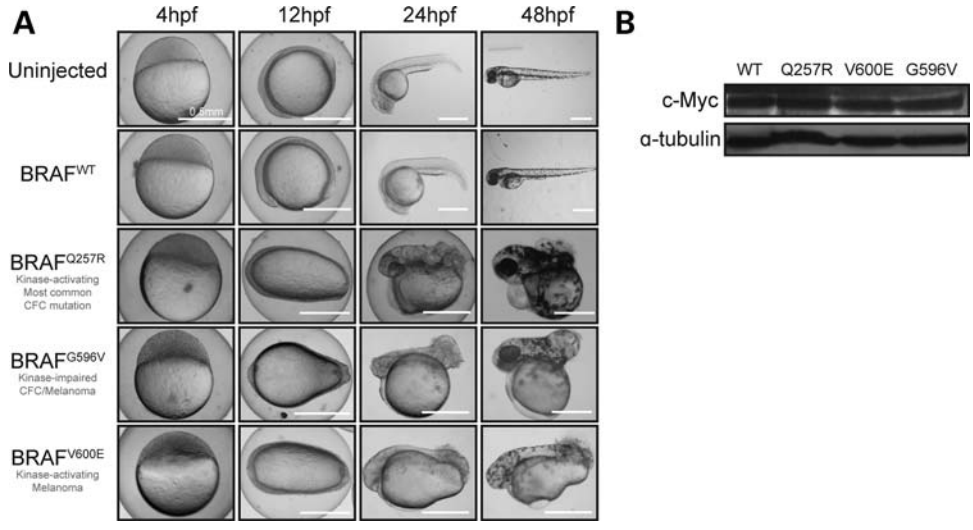

Figure 1. CFC syndrome alleles promote developmental changes during early embryogeneis. (**A**) RNA expression of CFC and melanoma variants $BRAF^{Q257R}$ (kinase-activating, CFC), $BRAF^{G596V}$ (kinase-impaired, CFC and melanoma) and $BRAF^{V600E}$ (very high-kinase, melanoma) cause elongation of the developing zebrafish embryo at 12 hpf, and severe developmental abnormalities at 24 and 48 hpf. In contrast, embryos expressing $BRAF^{WT}$ undergo normal development at all stages. No differences were detected in WT or disease allele expressing 4 hpf embryos. (**B**) Western blotting of zebrafish extracts reveals expression of the myc-tagged BRAF variants with the 9E10 antibody, and α-tubulin is a loading control.

FGF-RAS-RAF-MEK signalling in zebrafish embryo causes a loss of localized FGF-concentration that would normally promote convergence of cells towards the dorsal midline, but does not affect the continued epiboly movements and thereby results in an elongated embryo (22–24). Loss of the downstream ERK1 or ERK2 kinases in zebrafish also results in distinct convergence–extension cell migration defects during gastrulation (25), as does the expression of Noonan and LEOPARD syndrome SHP-2 alleles (15).

Building on these observations and coupled with the tractability of the zebrafish system, we reasoned that the expression of CFC mRNA in zebrafish embryos would allow us to rapidly assess the functional significance of BRAF, MEK1 and MEK2 kinase-active and kinase-impaired variants within a developmental context, and test the action of currently available FGF-MAPK-pathway inhibitors on the CFC allele phenotypic outcome (Fig. 1 and Table 1). We began by injecting mRNA into the one-cell zebrafish embryo and closely monitoring development of the effects of the high-kinase, most common variant in melanoma, $BRAF^{V600E}$, the kinase-impaired CFC/melanoma variant, $BRAF^{G596V}$ and the most common kinase-activating variant in CFC syndrome, $BRAF^{Q257R}$. Early cell-cleavage was not affected, and initial gastrulation appeared normal. However, by 12 h post-fertilization (hpf), the embryos were highly elongated (Fig. 1A). Later stages of development showed that anterior embryonic structures still formed, but that there was a lack of tail formation, similar to ectopic MAPK signalling (22–24). In addition, the embryos expressing the high-kinase $BRAF^{V600E}$ had a complete loss of eye development (Fig. 1A). Importantly, injection of normal human BRAF (wild-type, WT) into the embryo caused no evidence of elongation, suggesting that the expression of $BRAF^{WT}$ does not alter normal development, even when ectopically expressed (Fig. 1A). Western blotting confirmed expression of the myc-tagged $BRAF^{WT}$ and BRAF disease alleles (Fig. 1B).

Analysis of kinase-active and kinase-impaired CFC and melanoma alleles

The Ras/MAPK signalling pathway is highly conserved in humans and zebrafish. As in nevi/melanoma, the BRAF-CFC mutations result in both kinase-activating and kinase-impaired activities (2,7–9,26). Notably, all MEK1 and MEK2 CFC mutations are kinase active (7,27) (K.A.R., unpublished data). To assess the effects of the kinase-active and kinase-impaired melanoma and CFC alleles *in vivo*, we generated a panel of 20 BRAF and MEK disease variants in addition to the normal and engineered BRAF and MEK alleles (7,27,28) (Figs 1, 2 and Table 1), and expressed each individually by mRNA injection in the zebrafish embryo. First, we tested a panel of BRAF CFC and melanoma alleles, and found all BRAF variants promote an elongated embryonic phenotype, suggesting that *in vivo*, kinase-active and kinase-impaired BRAF alleles can promote the same developmental outcome (Fig. 2A, B and Table 1). To further test our system, we expressed normal and CFC syndrome activating MEK1 and MEK2 alleles, and also found that the disease alleles, but not the normal MEKs ($MEK1^{WT}$, $MEK2^{WT}$), promoted an elongated embryonic phenotype (Fig. 2C and Table 1). Western blotting of zebrafish embryonic lysates for total ERK protein and phospho-ERK confirmed that all BRAF and MEK alleles caused ERK activation in the zebrafish embryo (Fig. 2B, D, E). Because the $BRAF^{WT}$, $MEK1^{WT}$ and $MEK2^{WT}$ expressing embryos developed normally, but both kinase-active and kinase-impaired alleles caused altered embryonic development, this suggested to us that the *in vitro* biochemical kinase activity might not predict the potential for disease development. We found both constitutively kinase-active and kinase-inactive BRAF and MEK alleles to also promote an elongated embryonic phenotype (Fig. 2 and Table 1), suggesting that additional

Table 1. Summary of the BRAF and MEK variants expressed in zebrafish

Gene	Amino acid change	Predicted activity	Disease	Developmental phenotype in zebrafish (*n*)	Respond to treatment
BRAF	Wild-type	Wild-type	NA	No (0/40)	NA
	A246P	ND	CFC	Yes (31/57)	Yes
	Q257R	Kinase-activating	CFC	Yes (83/95)	Yes
	G464V	Kinase-activating	CFC	Yes (25/45)	Yes
	S467A	Kinase-activating	CFC	Yes (49/57)	Yes
	K483M	Kinase-inactivating	Engineered	Yes (34/44)	Yes
	K499E	Kinase-activating	CFC	Yes (23/44)	Yes
	G534R	Kinase-activating	CFC	Yes (33/38)	Yes
	N581D	ND	CFC	Yes (23/51)	Yes
	D594V	Kinase-impaired	Melanoma	yes (43/56)	yes
	G596V	Kinase-impaired	CFC and Melanoma	Yes (86/104)	Yes
	T599E/S602D	Constitutively active	Engineered	Yes (36/73)	Yes
	V600E	Kinase-activating	Melanoma	Yes (68/84)	Yes CI-1040 no SU-5402
	D638E	ND	CFC	Yes (66/89)	Yes
MEK1	Wild-type	Wild-type	NA	No (0/40)	NA
	F53L	Constitutively active	Engineered	Yes (16/33)	Yes
	F53S	Kinase-activating	CFC	Yes (20/33)	Yes
	T55P	Kinase-activating	CFC	Yes (26/45)	Yes
	K97M	Kinase-inactivating	Engineered	Yes (45/62)	Yes
	G128V	Kinase-activating	CFC	Yes (22/35)	Yes
	Y130C	Kinase-activating	CFC	Yes (30/45)	Yes
	S218D/S222D	Constitutively active	Engineered	Yes (45/55)	Yes
	ΔN3DD	Constitutively active	Engineered	Yes (41/60)	Yes
MEK2	Wild-type	Wild-type	NA	No (0/40)	N/A
	F57C	Kinase-activating	CFC	Yes (31/42)	Yes
	A62P	Kinase-activating	CFC	Yes (25/39)	Yes
	K101M	Kinase-inactivating	Engineered	Yes (39/52)	Yes
	G132V	Kinase-activating	CFC	Yes (45/72)	Yes
	Y134C	Kinase-activating	CFC	Yes (30/54)	Yes
	S222D/S226D	Constitutively active	Engineered	Yes (33/49)	Yes
	K273R	Kinase-activating	CFC	Yes (42/63)	Yes

NA, not applicable; ND, not determined; *n*, number.

interactions *in vivo*, possibly with endogenous WT BRAF and MEK, may be capable of altering normal development.

We observed control and CFC $BRAF^{Q257R}$ expressing embryos in detail and noted initial changes to embryo shape at 7.5–8.5 hpf (Fig. 3A). As FGF-MAPK signalling is critical for cell movements during gastrulation, and Noonan and LEOPARD mutant Shp2 alleles promote defective convergence and extension cell movements (15), we examined whether early gastrulation movements were affected by the expression of BRAF and MEK disease alleles using *in situ* hybridization markers (15,25). *HggI* (hatching gland, marker of anterior–posterior axis) expression remained unaffected, whereas *dlx3* (edge neural plate marker, convergence marker) was widely modified in the embryos injected with the disease, but not normal, alleles. This indicates that the CFC and melanoma alleles disrupt cell movements during gastrulation (Fig. 3B and C), similar to expression of activated FGF-MAPK signalling in zebrafish development (22–24). The convergence phenotypes appear more severe than the Shp2 Noonan and LEOPARD syndromes alleles (15), suggesting Shp2 mutations may act differently than BRAF and MEK CFC syndrome alleles during gastrulation. The ability to detect a clear phenotypic readout that could distinguish between $BRAF^{WT}$ and BRAF disease alleles, allowed us to use the zebrafish as the basis for further investigation of the CFC-pathway allele function.

BRAF kinase-active and kinase-impaired alleles can promote an additive effect during development

Our findings, that CFC kinase-impaired mutant alleles behave similar to kinase-active mutant alleles *in vivo*, are reminiscent of the action of both gain-of-function Noonan and loss-of-function LEOPARD Shp2 disease alleles to promote ectopic wing vein growth in *Drosophila* (13,14), and cell movement phenotypes in zebrafish (15). In zebrafish, Shp2 Noonan and LEOPARD mutant alleles are not additive, and do not lead to an increase in the number of embryos with a phenotype in early development (15). This suggests that Noonan and LEOPARD Shp2 mutations induce the same phenotype by activating or inhibiting pathway signalling. We investigated how BRAF kinase-activating and kinase-impaired alleles promote similar phenotypes during embryogenesis. We co-injected suboptimal levels of the kinase-active $BRAF^{Q257R}$ allele, the kinase-active $BRAF^{S467A}$ or the kinase-impaired $BRAF^{G596V}$ allele alone or with the $BRAF^{WT}$ allele (Fig. 4). Co-injection of BRAF CFC mutant alleles with $BRAF^{WT}$ did not significantly affect the number of embryos with a phenotype compared with the injection of the suboptimal BRAF CFC allele alone. Only 60–66% of the embryos have an early embryonic phenotype when expressing only one BRAF CFC allele, or in combination with $BRAF^{WT}$. In contrast, co-injection of kinase-active $BRAF^{Q257R}$ with kinase-active

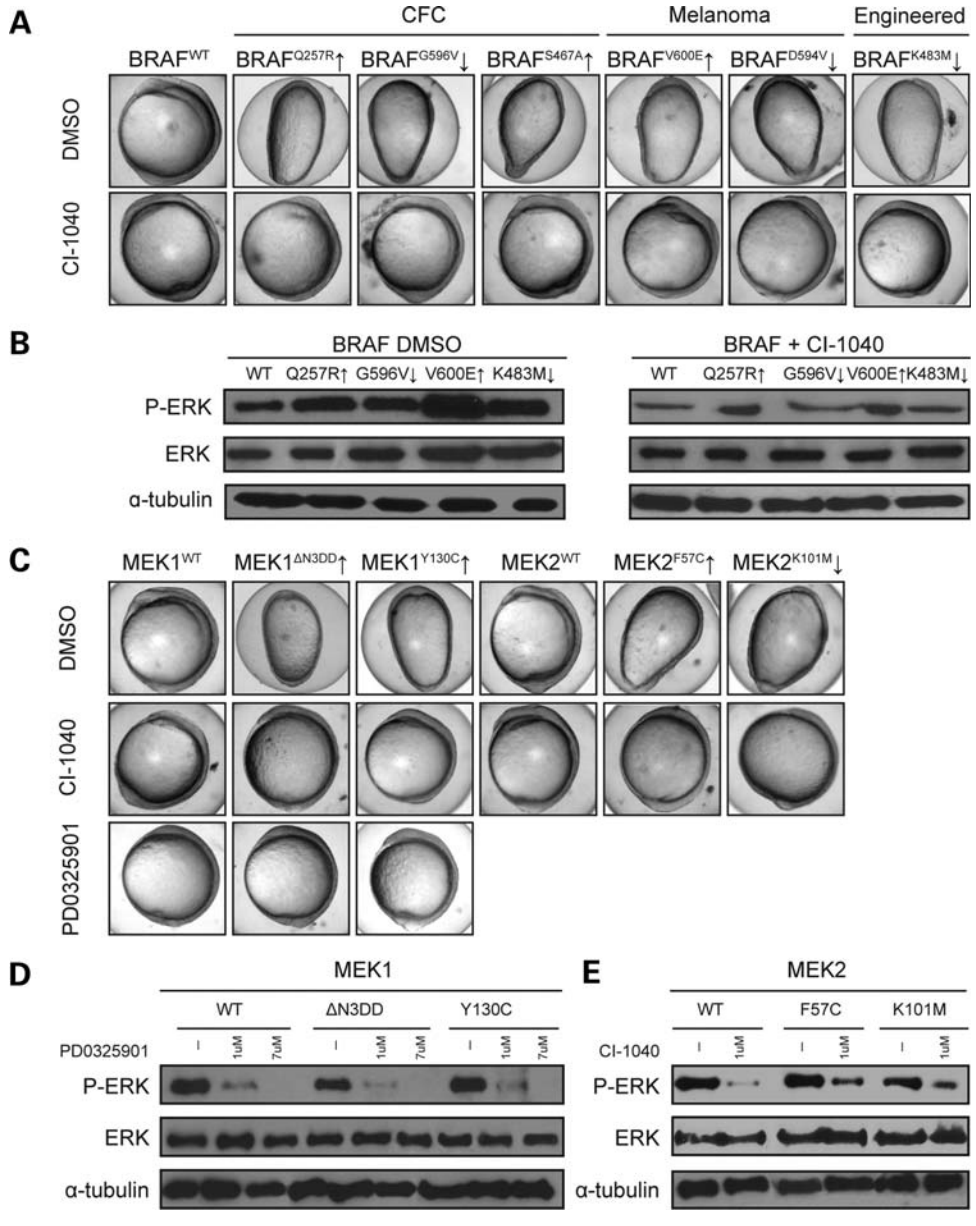

Figure 2. Analysis and treatment of kinase-activating and kinase-impaired BRAF and MEK disease variants. (**A**) RNA expression of BRAF CFC and melanoma variants, as well as engineered BRAF mutations, promotes an elongated embryo phenotype. RNA expression of wild-type BRAF has no effect on development. The developmental phenotypes caused by the BRAF variants are prevented by treatment with the MEK inhibitor, CI-1040 and the embryo has a normal rounded shape. (**B**) Western blotting of zebrafish lysates with anti-ERK and anti-phospho-ERK antibodies reveals a reduction in the ratio of phospho-ERK to total ERK protein in treated embryos, and α-tubulin is a loading control. (**C**) RNA expression of CFC MEK variants, the MEK1 constitutively activating (ΔN3DD) and the MEK2 kinase-inactivating K101M mutations promotes elongation in the developing embryo. Expression of wild-type MEK1 and MEK2 do not affect development. The developmental phenotypes caused by the MEK alleles are prevented by treatment with the MEK inhibitors, CI-1040 and PD0325901. (**D** and **E**) Western blotting of zebrafish lysates with anti-ERK and anti-phospho-ERK antibodies reveals downstream activity of phospho-ERK and confirms the potency of the MEK inhibitors, and α-tubulin is a loading control.

$BRAF^{S467A}$ resulted in a significant enhancement of the number of embryos with an elongated phenotype. In addition, co-injection of kinase-active $BRAF^{Q257R}$ with kinase-impaired $BRAF^{G596V}$ also resulted in a significant increase in the number of elongated embryos. The number of embryos with a phenotype induced by $BRAF^{Q257R/S467A}$ (91.9%) or $BRAF^{Q257R/G596V}$ (88.2%) is consistent with the 82–87% of embryos that develop a developmental phenotype when the optimal dose is used (Table 1). Our results are consistent with both the kinase-active and the kinase-impaired BRAF CFC mutations acting as gain-of-function mutations during development.

MEK inhibitors can prevent the effects of CFC alleles

We wanted to assess whether currently available MAPK-pathway inhibitors might prevent the effects of CFC disease alleles in development. Previous studies have shown that

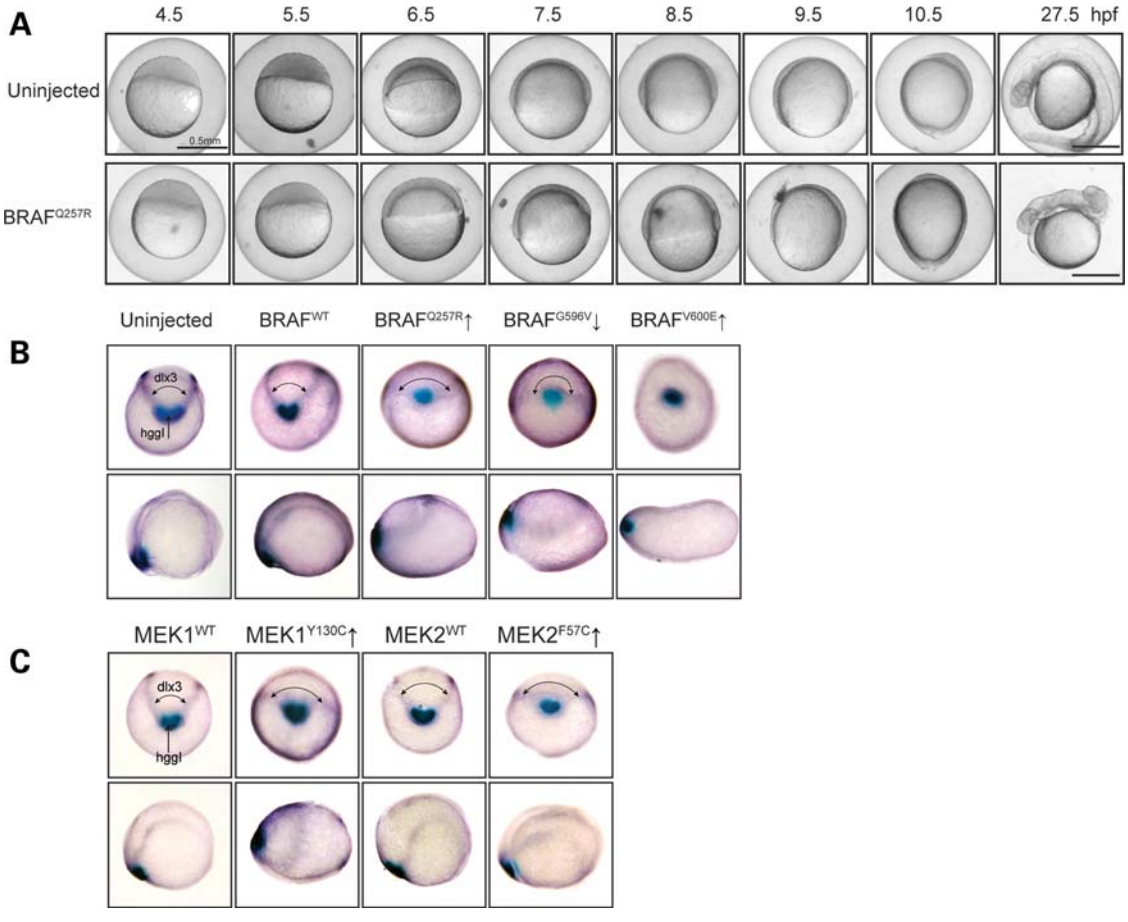

Figure 3. BRAF and MEK disease alleles promote cell movement phenotypes. (**A**) The most common CFC varient, $BRAF^{Q257R}$, was expressed in developing embryos, and the embryos imaged every hour. Development of the embryos begins to become affected by $BRAF^{Q257R}$ expression between 7.5 and 8.5 hpf. (**B**) BRAF and (**C**) MEK disease variants promote significant changes in cell movement, as revealed by *in situ* hybridization. The gene expression domain of *dlx3* is altered for both expression pattern and intensity of signal, such that there is no *dlx3* detected in the $BRAF^{V600E}$ expressing embryos. *HggI* expression remains unaffected. The bottom panel shows the lateral view of the same embryos.

cancers with activated BRAF are highly sensitive to MEK inhibitors (29) and that CFC MEK alleles in cell culture are sensitive to the widely used MEK inhibitor, U0126 (12). However, it was unknown whether the CFC kinase-activating and kinase-impaired BRAF and MEK variants would be sensitive to the inhibition of MEK during development. We expressed BRAF CFC and melanoma alleles in developing embryos as before, and at 4 hpf added CI-1040, a clinically active MEK inhibitor that is the basis for new second-generation MEK inhibitors (5,6) to the embryo medium. We found that chemical inhibition of MEK was able to restore normal development until 10.5 hpf in all embryos expressing BRAF CFC and melanoma disease alleles (Fig. 2A). We found a similar result when we expressed CFC and engineered MEK1 and MEK2 alleles in zebrafish embryos, and treated with CI-1040 or PD0325901, a derivative of CI-1040 (Fig. 2C). With both BRAF and MEK variants, western blotting confirmed that the ratio of phosphorylated ERK to total ERK protein was reduced after chemical inhibition of MEK (Fig. 2B, D, E).

MEK signalling is critical for development, and we have previously shown that prolonged treatment (up to day 4 pf) with the pharmacological inhibition of MEK using CI-1040 causes severe axis, heart and craniofacial developmental abnormalities (30), and we find a similar effect using PD0325901 (C.A., E.E.P., unpublished data). Although we were able to restore normal gastrulation in CFC embryos with CI-1040 and PD0325901 (Fig. 2A and C), treated embryos subsequently developed axis abnormalities associated with the effects of the inhibitor later in development (30). To circumvent this problem, we exposed the most common $BRAF^{Q257R}$ CFC allele expressing embryos to the MEK inhibitor for 12 different treatments that varied for the time of exposure. We found that although all experimental treatments that involved adding the inhibitor early in development prevented embryo elongation (10.5 hpf) (Fig. 5A treatments A–F), a 1 h treatment within a 4.5–5.5 hpf developmental window was sufficient to restore normal development at 24 hpf (Fig. 5A treatment A), without the additional, subsequent unwanted abnormalities caused by the inhibitor (Fig. 5A treatments C–F). Treatment within this early developmental window was necessary, as a 1 h treatment later in development (Fig. 5B treatment F) was unable to prevent CFC mutant allele phenotypes, as were the treatments

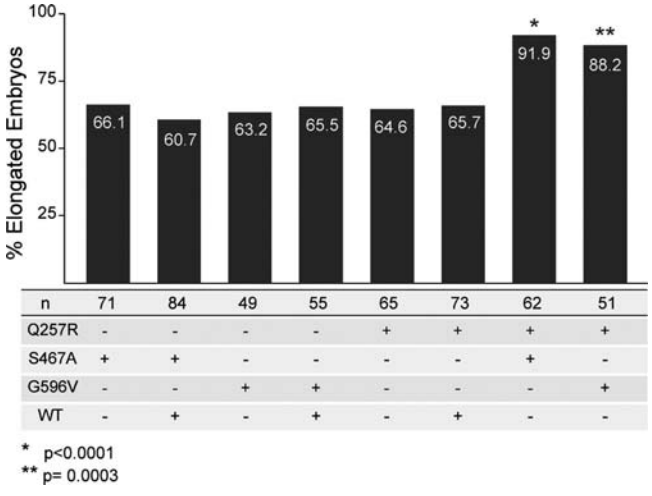

Figure 4. BRAF kinase-active and kinase-impaired alleles can promote an additive effect during development. Embryos co-expressing combinations of suboptimal doses (15 pg) of kinase-active ($BRAF^{Q257R}$, $BRAF^{S467A}$) and kinase-impaired ($BRAF^{G596V}$) CFC alleles or $BRAF^{WT}$ mRNA were assessed for the elongation phenotype at 10 hpf. The number of elongated embryos did not change significantly upon expression of a single BRAF CFC allele (15 pg), or in combination with $BRAF^{WT}$ (for a total of 30 pg). A significant increase in the mutant phenotype was induced by co-injections of $BRAF^{Q257R}$ with $BRAF^{S467A}$ ($P < 0.0001$) or $BRAF^{Q257R}$ with $BRAF^{G596V}$ ($P = 0.0003$) compared with the BRAF CFC allele co-injected with $BRAF^{WT}$ as indicated by χ^2 tests. The numbers in the bars indicates the percentages of elongated embryos; *n* is the number of injected embryos.

that had CI-1040 throughout the experiment, with the exception of the 4.5–5.5 hpf developmental window (Fig. 5B treatment B).

Distinguishing between BRAF alleles for sensitivity to pathway inhibition

The ability to treat kinase-active and kinase-impaired CFC embryos suggests correction of signalling downstream of the CFC mutation is sufficient to restore normal development. This is consistent with the sensitivity of cancers expressing RAS and RAF high-kinase oncogenes to MEK inhibitors (5,6,29), and the sensitivity of CFC MEK alleles to MEK inhibition in cell culture (12). FGF-MAPK signalling plays an important role during embryonic cell movements in zebrafish. Unlike in a cancer cell with a BRAF mutation, a developing animal with a BRAF or MEK CFC mutation also has endogenous FGFR signalling. We hypothesized that total MAPK signalling may underlie CFC syndrome development and that suppression of endogenous FGFR signalling could partially suppress the activity of the effects of the downstream CFC alleles. As with the MEK inhibitor, we treated 4 hpf embryos expressing BRAF (Fig. 6A) and MEK (Fig. 6B) CFC and melanoma mutant alleles with SU-5402, an inhibitor of the FGF receptor 1 (FGFR1). Western blotting confirmed reduction of phosphorylated ERK after SU-5402 treatment (Fig. 6C). We found the development to be normal for all treated embryos expressing BRAF and MEK disease alleles at 10.5 hpf, with the exception of the very high-kinase activity melanoma mutant $BRAF^{V600E}$ (Fig. 6A and B). The most common mutation in melanoma and nevi, $BRAF^{V600E}$ is one of the highest kinase activity mutants, has transforming activity and is sufficient to promote nevi and melanoma development, as well as other cancers, in animal models (3,26,31–34). This suggests that total levels of MAPK signalling may be responsible for the action of the CFC alleles, and reduction of either endogenous FGF signalling or downstream MEK signalling can prevent some of the pathological function of the alleles.

DISCUSSION

Our study addresses the *in vivo* action of CFC mutant alleles and may point to a potential therapeutic approach for individuals with CFC syndrome. First, we have demonstrated that CFC mutant alleles cause similar developmental phenotypes in an *in vivo* zebrafish model system, despite their *in vitro* kinase activity. Second, we have used our model system to explore the therapeutic potential of small molecule inhibitors to prevent the *in vivo* activity of CFC mutations during early development. We have evaluated both the developmental activity and the therapeutic potential of 18 human CFC and three melanoma disease alleles, as well as three different small molecule inhibitors, in 12 treatment conditions. In this work, zebrafish embryos are injected at the single cell stage with RNA of the human disease allele, or with control RNA, and the phenotype of the embryo assessed by 10 h (Figs 1, 3 and 7A). Embryos normally express FGF-MAPK signalling during development in a localized manner to shape the development of the embryos during gastrulation (18). We found BRAF and MEK kinase-active and kinase-impaired disease variants interfere with convergence–extension cell movements during gastrulation (Fig. 1), providing insight into how similar clinical CFC phenotypes are caused by kinase-activating and kinase-impaired alleles. Future studies will reveal how the effects on early cell movement (Fig. 1) correlate with disease allele penetrance and disease presentation in humans.

In our *in vivo* animal system, and in the context of endogenous signalling, we find CFC alleles with kinase-inactivating mutations, as defined *in vitro*, promote the same phenotype as kinase-active alleles. One possibility is that BRAF kinase-impaired proteins interact with CRAF to stimulate MEK-ERK signalling (9,10,35). Kinases frequently act through dimerization, including BRAF and CRAF (10,36), and crystal structures of MEK predict MEK1 and MEK2 self associate via a homodimerization interface to form stable dimers (37). Such mechanisms may be at work in our zebrafish studies, providing the molecular context for kinase-impaired BRAF and MEK alleles to be able to promote active signalling of the pathway, including the engineered kinase-inactive alleles (36) as determined by *in vitro* kinase assays (Fig. 3). Another possibility is that dysregulation of Ras/MAPK signalling through gain-of-function or loss-of-function mutations may cause similar disease phenotypes (38). As an important example, the disease spectrum associated with varying SHP-2 mutations in Noonan syndrome and cancer argue against SHP-2 activity as the defining predictor of disease outcome (39). Both loss-of-function and gain-of-function mutations in SHP-2 lead to the clinically

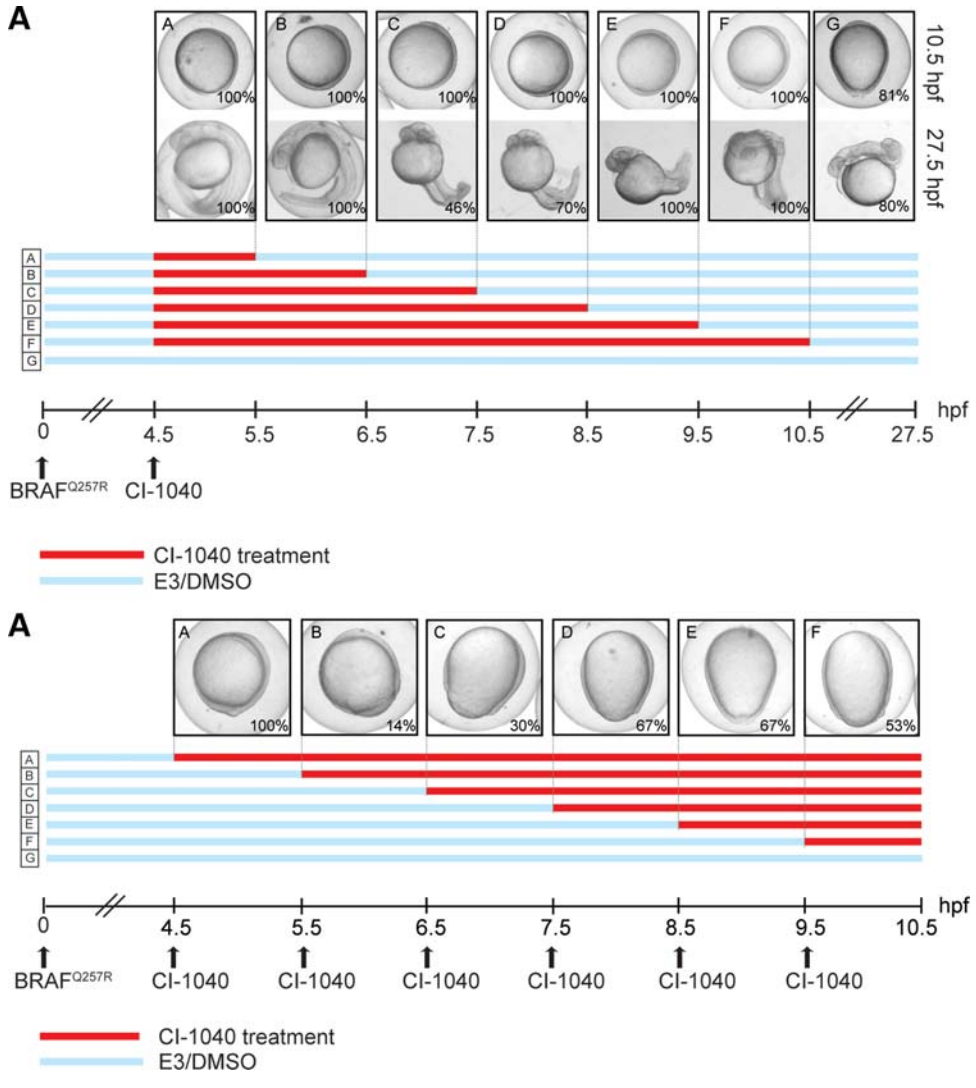

Figure 5. Identification of a zebrafish-CFC treatment window. (**A**) Six CI-1040 treatments (A–F) and a control treatment (G) for zebrafish embryos expressing CFC variant $BRAF^{Q257R}$ reveal that all drug treatments restore normal development at 10.5 hpf (treatments A–F), whereas only treatments A and B restore normal development both at 10.5 and 27.5 hpf. Other drug treatments (C–F) cause additional developmental defects at 27.5 hpf, most notably, reduced posterior development. (**B**) Six additional drug treatments (A–F) and a control treatment (G) for zebrafish-CFC variant $BRAF^{Q257R}$ show that the 4.5–5.5 hpf developmental window is necessary for the prevention of zebrafish-CFC early phenotypes. The percentage of embryos displaying the phenotype is given at the lower right of each image (a minimal of $n = 30$/experiment). Blue bars represent embryo medium, whereas red bars represent CI-1040 treatment.

similar LEOPARD and Noonan syndromes, and expression of LEOPARD and Noonan syndrome alleles in zebrafish and *Drosophila* produce equivalent developmental phenotypes (15–17). Our work suggests that both kinase-active and kinase-impaired CFC alleles are effectively gain-of-function mutations and activate the pathway because combinations of active and impaired BRAF mutant alleles can promote an additive effect during early development (Fig. 4).

Designing new therapies for rare birth disorders is problematic due to the great costs and research efforts of drug development, and the required clinical safety and efficacy testing for new therapeutics (40). Since the Ras/MAPK pathway has been a prime target for cancer therapeutics, application of these small molecule inhibitors presents a possible therapeutic avenue, since the underlying molecular dysfunction is common. Previously, the activity of CFC MEK alleles has been shown to be sensitive to MEK inhibitors in cells (12). Direct testing of the effects of anti-cancer therapeutics on BRAF and MEK CFC characteristics in zebrafish is an important next step in exploring the therapeutic potential for CFC syndrome. Using our model, we have tested the ability of FGF-MAPK inhibitors to prevent the developmental effects of CFC and melanoma disease alleles (Fig. 7B). We found that MEK inhibitors prevent the cell migration defects caused by the disease alleles, and also that additional developmental side-effects of the drug could be avoided by treating the embryos within a specific developmental time-window (Fig. 5A). These results suggest that future studies in pre-clinical models of CFC should explore if similar drug treatment time windows may help ease the developmental abnormalities and symptoms associated with CFC progression. However,

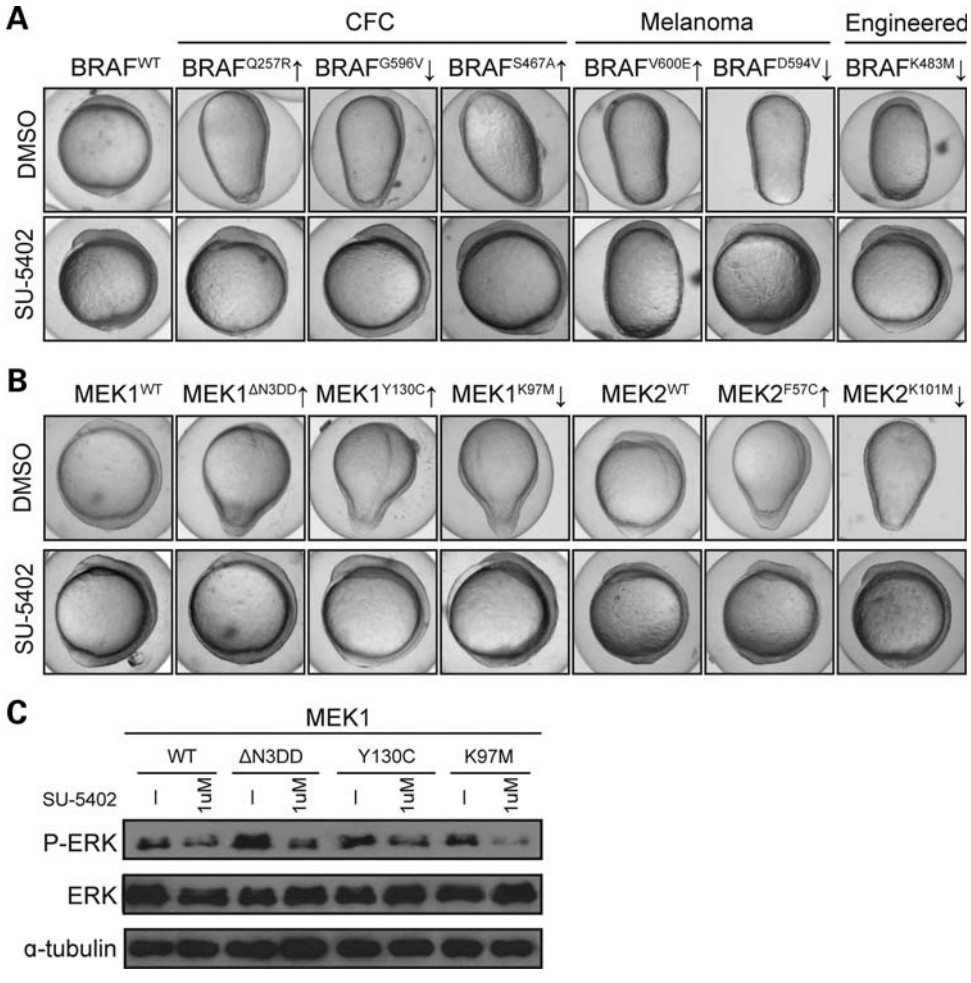

Figure 6. Treatment of BRAF, MEK1 and MEK2 variants with SU-5402. (**A**) The mutant phenotypes promoted by the RNA expression of BRAF variants are prevented by pharmacological treatment with the FGFR1 inhibitor SU-5402, with the exception of the developmental phenotype caused by $BRAF^{V600E}$. (**B**) Similarly, the elongation promoted by MEK1 and MEK2 disease variants is prevented by SU-5402 treatment. (**C**) Western blotting of total zebrafish lysates for ERK and phospho-ERK protein shows that SU-5402 treatment causes reduction of ERK phosphorylation, with α-tubulin as a loading control.

because CFC mutations affect gastrulation (Fig. 1–3), and have an early developmental treatment window (Fig. 5), application of MEK inhibitors for CFC syndrome patients may be severely limited. Nonetheless, because CFC syndrome has a progressive phenotype, and many of the phenotypic effects develop post-natally, patients may still be helped by systemic therapies after birth (1).

We also provide evidence that the developmental effects of the disease alleles can be prevented by the inhibition of endogenous FGFR-signalling, with the exception of one of the highest kinase-activating melanoma mutations, $BRAF^{V600E}$ (Fig. 6). We reason that as normal gastrulation involves endogenous FGFR signalling, FGFR inhibition reduces the total level of defective CFC BRAF or MEK signalling, thereby preventing the altered cell movement phenotype. This supports the idea that total MAPK signalling is important in CFC development (Fig. 4), and also emphasizes the importance of testing the action of developmental syndrome mutant alleles and inhibitors in a developing animal. *In vitro*, the CFC $BRAF^{Q257R}$ and melanoma $BRAF^{V600E}$ mutant alleles both promote similar high-kinase activity (7), and yet no individual with CFC syndrome has been identified with a $BRAF^{V600E}$ mutation. This demonstrates, for the first time, that the $BRAF^{V600E}$ mutation is probably stronger *in vivo* than the CFC mutations.

The high conservation of the MAPK signalling pathway means that our CFC chemical-genetic studies in zebrafish embryos will be relevant to the development of future preclinical models of CFC. For example, mice exhibiting Apert-like syndrome from dominant mutations in fibroblast growth factor receptor-2 can be treated pre- and post-natally with the small molecule MEK inhibitor, U0126 (41). We note, however, that similar comprehensive CFC allele comparisons, coupled with multiple treatment testing, within the short-time span described here, is not currently feasible in mouse models. This makes the zebrafish system a tractable tool for medical and research geneticists to explore allele activity and therapeutic potential. This work establishes a foundation to propel forward the clinical discussion and scientific strategy for assessing the suitability of using currently available cancer drugs to treat the progressive phenotypes of CFC in children.

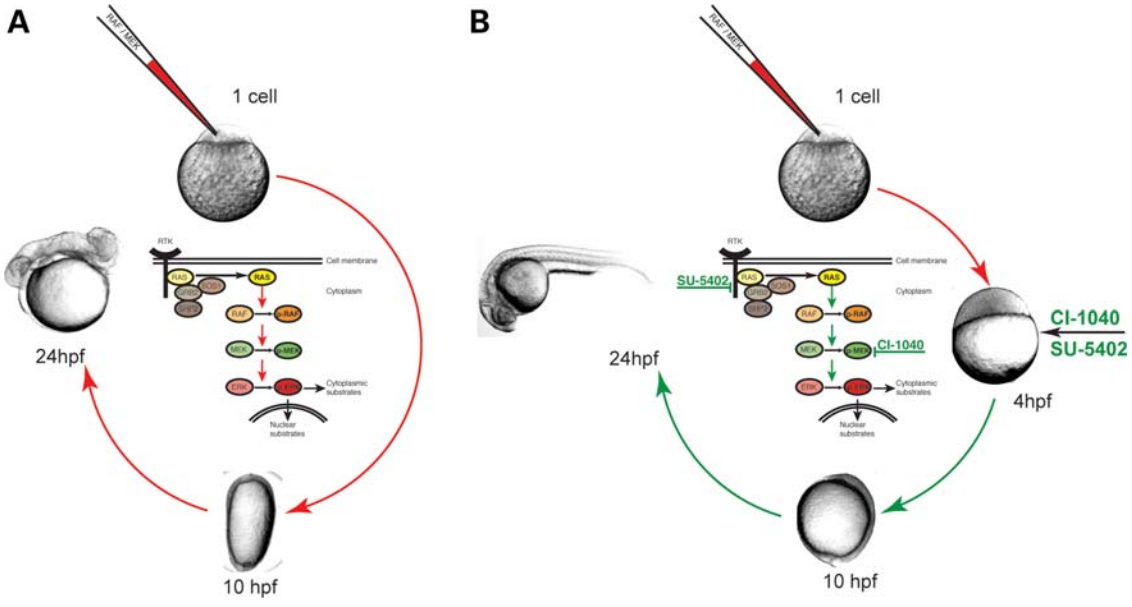

Figure 7. Evaluation of CFC-disease variant *in vivo* activity and potential treatment. Schematic representation of the zebrafish-based approach designed to examine the *in vivo* significance of BRAF and MEK CFC disease mutations. (**A**) Microinjection of BRAF or MEK CFC variant mRNA into the single-cell zebrafish embryo promoted an elongated zebrafish embryo at 10 hpf that gives rise to an animal with severe development defects, including axis formation, and heart defects at 24 hpf (red arrow). (**B**) Treatment of CFC-microinjected embryos with inhibitors of the FGF-MAPK signalling pathway (green) restores normal development to the CFC-zebrafish embryo, possibly by restoring appropriate total levels of MAPK-signalling (green arrows).

MATERIALS AND METHODS

Animal husbandry

Adults and zebrafish embryos were raised and maintained at 28.5°C. Embryos were acquired by pair matings of AB* and TL zebrafish lines.

Cloning and RNA production

Patient and engineered BRAF, MEK1 and MEK2 DNA were cloned into pENTR 3C (Invitrogen), and using the Gateway® (Invitrogen) technology the DNA sequences were subcloned into the pDEST17 (Invitrogen) vector. Expression vectors were linearized, and *in vitro* transcription of synthetic capped mRNA was performed using the T7 RNA polymerase mMESSAGE mMACHINE Kit (Ambion).

Microinjection of embryos

Injections were performed on WT zebrafish embryos using a nitrogen-powered Picospritzer III microinjector (Intracel) conjugated to a Nikon SMZ 1000 stereomicroscope. One-cell stage embryos were injected with 35 pg (optimal) or 15 pg (suboptimal) of capped mRNA and were monitored until throughout the first 24 h of development.

Pharmacological inhibition of FGF and MAPK signalling

To test the prevention of the mRNA-promoted phenotype, 4 hpf embryos injected with mRNA were treated with small molecule inhibitors. To inhibit FGFR1 activity, embryos were incubated in SU5402 (Calbiochem) at 1 μM in E3 embryo medium (42) at 28.5°C in the dark. To inhibit MEK1/2, embryos were treated with 1 μM CI-1040 and 1or 7 μM PD-0325901 (University of Dundee) in E3 embryo medium at 28.5°C as previously described (30).

Whole-mount RNA in situ hybridization

Embryos collected at the tail-bud stage were fixed overnight in 4% parafolmaldehyde/PBS at 4°C, were hand-dechorionated and dehydrated overnight in methanol at −20°C. *In vitro* transcribed digoxigenin-labelled antisense RNA probes were synthesised (Roche). *Dlx3* and *HggI* riboprobes (15) and whole-mount *in situ* hybridization were carried out following previously described protocols (43). Anti-digoxigenin antiserum alkaline phosphatase was incubated in a 1:5000 dilution overnight and the samples were washed in BCL3 solution (1 M Tris pH 9.5, 5 M NaCl, 0.5 M $MgCl_2$, 20% Tween 20). The embryos were, subsequently, stained in 500 μl of BM Purple alkaline phosphatase (Roche) for 30–45 min and the reaction was stopped in 20 mM EDTA/PBS. Processed embryos were imaged using a Nikon SMZ1500 stereomicroscope in conjunction with a Nikon Coolpix 5400 camera.

Protein blotting

Embryo buffer was removed, and tail-bud stage embryos were frozen at −80°C. Samples were ribolyzed for 5 s in protein extraction buffer [2 M Tris pH 7.5, 5 M NaCl, 1% NP40, Na deoxycholate, 10% SDS, 0.5 M NaF, 1 M β-glycosyl phosphate, protease inhibitor cocktail tablet (Roche)]. The protein content was measured and the samples were normalized. Total protein extracts were analyzed by western blotting, probed with antibodies raised in rabbit [p44/42 MAPK (1:2000) (Cell Signaling)] and in mouse [phospho p44/42

MAPK (E10) (1:2000), c-myc (9E10) (1:2000) (Sigma), α-tubulin B-5-1-2 (1:50000) (Santa Cruz)]. Secondary antibodies conjugated to horseradish peroxidase were used to detect the proteins.

ACKNOWLEDGEMENTS

We are grateful to CFC International, and to Professors Ian Jackson, Veronica van Heyningen, David Fitzpatrick, David Harrison and Nick Hastie (Edinburgh, UK) for scientific advice and assistance with the manuscript. We thank Professor Jeroen den Hertog (Utrecht, NL) for plasmids, and Dr James Amatruda (Dallas, USA) for critical reading of the manuscript.

Conflict of Interest statement. None declared.

FUNDING

This work was supported by a National Institutes of Health grant HD048502 to K.A.R., and a Medical Research Council Career Development Award and a Wellcome Trust Grant to E. E. P. Funding to pay the Open Access charge was provided by the Wellcome Trust.

REFERENCES

1. Tidyman, W.E. and Rauen, K.A. (2008) Noonan, Costello and cardio-facio-cutaneous syndromes: dysregulation of the Ras-MAPK pathway. *Expert Rev. Mol. Med.*, **10**, e37.
2. Sebolt-Leopold, J.S. and Herrera, R. (2004) Targeting the mitogen-activated protein kinase cascade to treat cancer. *Nat. Rev. Cancer*, **4**, 937–947.
3. Davies, H., Bignell, G.R., Cox, C., Stephens, P., Edkins, S., Clegg, S., Teague, J., Woffendin, H., Garnett, M.J., Bottomley, W. *et al.* (2002) Mutations of the *BRAF* gene in human cancer. *Nature*, **417**, 949–954.
4. Sebolt-Leopold, J.S. and English, J.M. (2006) Mechanisms of drug inhibition of signalling molecules. *Nature*, **441**, 457–462.
5. Sebolt-Leopold, J.S. (2008) Advances in the development of cancer therapeutics directed against the RAS-mitogen-activated protein kinase pathway. *Clin. Cancer Res.*, **14**, 3651–3656.
6. Gray-Schopfer, V., Wellbrock, C. and Marais, R. (2007) Melanoma biology and new targeted therapy. *Nature*, **445**, 851–857.
7. Rodriguez-Viciana, P., Tetsu, O., Tidyman, W.E., Estep, A.L., Conger, B.A., Cruz, M.S., McCormick, F. and Rauen, K.A. (2006) Germline mutations in genes within the MAPK pathway cause cardio-facio-cutaneous syndrome. *Science*, **311**, 1287–1290.
8. Niihori, T., Aoki, Y., Narumi, Y., Neri, G., Cavé, H., Verloes, A., Okamoto, N., Hennekam, R.C., Gillessen-Kaesbach, G., Wieczorek, D. *et al.* (2006) Germline KRAS and BRAF mutations in cardio-facio-cutaneous syndrome. *Nat. Genet.*, **38**, 294–296.
9. Wan, P.T., Garnett, M.J., Roe, S.M., Lee, S., Niculescu-Duvaz, D., Good, V.M., Jones, C.M., Marshall, C.J., Springer, C.J., Barford, D. *et al.* (2004) Mechanism of activation of the RAF-ERK signaling pathway by oncogenic mutations of B-RAF. *Cell*, **116**, 855–867.
10. Garnett, M.J., Rana, S., Paterson, H., Barford, D. and Marais, R. (2005) Wild-type and mutant B-RAF activate C-RAF through distinct mechanisms involving heterodimerization. *Mol. Cell*, **20**, 963–969.
11. Rauen, K.A., Hefner, E., Carrillo, K., Taylor, J., Messier, L., Aoki, Y., Gripp, K.W., Matsubara, Y., Proud, V.K., Hammond, P. *et al.* (2008) Molecular aspects, clinical aspects and possible treatment modalities for Costello syndrome: Proceedings from the First International Costello Syndrome Research Symposium 2007. *Am. J. Med. Genet. A.*, **146A**, 1205–1217.
12. Senawong, T., Phuchareon, J., Ohara, O., McCormick, F., Rauen, K.A. and Tetsu, O. (2008) Germline mutations of MEK in cardio-facio-cutaneous syndrome are sensitive to MEK and RAF inhibition: implications for therapeutic options. *Hum. Mol. Genet.*, **17**, 419–430.
13. Oishi, K., Gaengel, K., Krishnamoorthy, S., Kamiya, K., Kim, I.K., Ying, H., Weber, U., Perkins, L.A., Tartaglia, M., Mlodzik, M. *et al.* (2006) Transgenic *Drosophila* models of Noonan syndrome causing PTPN11 gain-of-function mutations. *Hum. Mol. Genet.*, **15**, 543–553.
14. Oishi, K., Zhang, H., Gault, W.J., Wang, C.J., Tan, C.C., Kim, I.K., Ying, H., Rahman, T., Pica, N., Tartaglia, M. *et al.* (2009) Phosphatase-defective LEOPARD syndrome mutations in *PTPN11* gene have gain-of-function effects during *Drosophila* development. *Hum. Mol. Genet.*, **18**, 193–201.
15. Jopling, C., van Geemen, D. and den Hertog, J. (2007) Shp2 knockdown and Noonan/LEOPARD mutant Shp2-induced gastrulation defects. *PLoS Genet.*, **3**, e225.
16. Santoriello, C., Deflorian, G., Pezzimenti, F., Kawakami, K., Lanfrancone, L., d'Adda di Fagagna, F. and Mione, M. (2009) Expression of H-RASV12 in a zebrafish model of Costello syndrome causes cellular senescence in adult proliferating cells. *Dis. Model Mech.*, **2**, 56–67.
17. Schuhmaher, A.J., Guerra, C., Sauzeau, V., Cañamero, M., Bustelo, X.R. and Barbacid, M. (2008) A mouse model for Costello syndrome reveals an Ang II-mediated hypertensive condition. *J. Clin. Invest.*, **118**, 2169–2179.
18. Solnica-Krezel, L. (2005) Conserved patterns of cell movements during vertebrate gastrulation. *Curr. Biol.*, **15**, R213–R228.
19. Grunwald, D.J. and Eisen, J.S. (2002) Headwaters of the zebrafish—emergence of a new model vertebrate. *Nat. Rev. Genet.*, **3**, 717–724.
20. Patton, E.E. and Zon, L.I. (2001) The art and design of genetic screens: zebrafish. *Nat. Rev. Genet.*, **2**, 956–966.
21. Zon, L.I. and Peterson, R.T. (2005) *In vivo* drug discovery in the zebrafish. *Nat. Rev. Drug Discov.*, **4**, 35–44.
22. Furthauer, M., Thisse, C. and Thisse, B. (1997) A role for FGF-8 in the dorsoventral patterning of the zebrafish gastrula. *Development*, **124**, 4253–4264.
23. Furthauer, M., Lin, W., Ang, S.L., Thisse, B. and Thisse, C. (2002) Sef is a feedback-induced antagonist of Ras/MAPK-mediated FGF signaling. *Nat. Cell Biol.*, **4**, 170–174.
24. Furthauer, M., Van Celst, J., Thisse, C. and Thisse, B. (2004) Fgf signalling controls the dorsoventral patterning of the zebrafish embryo. *Development*, **131**, 2853–2864.
25. Krens, S.F., He, S., Lamers, G.E., Meijer, A.H., Bakkers, J., Schmidt, T., Spaink, H.P. and Snaar-Jagalska, B.E. (2008) Distinct functions for ERK1 and ERK2 in cell migration processes during zebrafish gastrulation. *Dev. Biol.*, **319**, 370–383.
26. Pollock, P.M., Harper, U.L., Hansen, K.S., Yudt, L.M., Stark, M., Robbins, C.M., Moses, T.Y., Hostetter, G., Wagner, U., Kakareka, J. *et al.* (2003) High frequency of BRAF mutations in nevi. *Nat. Genet.*, **33**, 19–20.
27. Rodriguez-Viciana, P. and Rauen, K.A. (2008) Biochemical characterization of novel germline BRAF and MEK mutations in cardio-facio-cutaneous syndrome. *Methods Enzymol.*, **438**, 277–289.
28. Rauen, K.A. (2006) Distinguishing Costello versus cardio-facio-cutaneous syndrome: BRAF mutations in patients with a Costello phenotype. *Am. J. Med. Genet. A.*, **140**, 1681–1683.
29. Solit, D.B., Garraway, L.A., Pratilas, C.A., Sawai, A., Getz, G., Basso, A., Ye, Q., Lobo, J.M., She, Y., Osman, I. *et al.* (2006) BRAF mutation predicts sensitivity to MEK inhibition. *Nature*, **439**, 358–362.
30. Grzmil, M., Whiting, D., Maule, J., Anastasaki, C., Amatruda, J.F., Kelsh, R.N., Norbury, C.J. and Patton, E.E. (2007) The INT6 cancer gene and MEK signaling pathways converge during zebrafish development. *PLoS ONE*, **2**, e959.
31. Patton, E.E., Widlund, H.R., Kutok, J.L., Kopani, K.R., Amatruda, J.F., Murphey, R.D., Berghmans, S., Mayhall, E.A., Traver, D., Fletcher, C.D. *et al.* (2005) BRAF mutations are sufficient to promote nevi formation and cooperate with p53 in the genesis of melanoma. *Curr. Biol.*, **15**, 249–254.
32. Pritchard, C., Carragher, L., Aldridge, V., Giblett, S., Jin, H., Foster, C., Andreadi, C. and Kamata, T. (2007) Mouse models for BRAF-induced cancers. *Biochem. Soc. Trans.*, **35**, 1329–1333.
33. Mercer, K., Giblett, S., Green, S., Lloyd, D., DaRocha Dias, S., Plumb, M., Marais, R. and Pritchard, C. (2005) Expression of endogenous oncogenic V600EB-raf induces proliferation and developmental defects in mice and transformation of primary fibroblasts. *Cancer Res.*, **65**, 11493–11500.
34. Dankort, D., Filenova, E., Collado, M., Serrano, M., Jones, K. and McMahon, M. (2007) A new mouse model to explore the initiation, progression, and therapy of BRAFV600E-induced lung tumors. *Genes Dev.*, **21**, 379–384.

35. Dumaz, N., Hayward, R., Martin, J., Ogilvie, L., Hedley, D., Curtin, J.A., Bastian, B.C., Springer, C. and Marais, R. (2006) In melanoma, RAS mutations are accompanied by switching signaling from BRAF to CRAF and disrupted cyclic AMP signaling. *Cancer Res.*, **66**, 9483–9491.
36. Rushworth, L.K., Hindley, A.D., O'Neill, E. and Kolch, W. (2006) Regulation and role of Raf-1/B-Raf heterodimerization. *Mol. Cell. Biol.*, **26**, 2262–2272.
37. Ohren, J.F., Chen, H., Pavlovsky, A., Whitehead, C., Zhang, E., Kuffa, P., Yan, C., McConnell, P., Spessard, C., Banotai, C. *et al.* (2004) Structures of human MAP kinase kinase 1 (MEK1) and MEK2 describe novel noncompetitive kinase inhibition. *Nat. Struct. Mol. Biol.*, **11**, 1192–1197.
38. Bentires-Alj, M., Kontaridis, M.I. and Neel, B.G. (2006) Stops along the RAS pathway in human genetic disease. *Nat. Med.*, **12**, 283–285.
39. Keilhack, H., David, F.S., McGregor, M., Cantley, L.C. and Neel, B.G. (2005) Diverse biochemical properties of Shp2 mutants. Implications for disease phenotypes. *J. Biol. Chem.*, **280**, 30984–30993.
40. Wilkie, A.O. (2007) Cancer drugs to treat birth defects. *Nat. Genet.*, **39**, 1057–1059.
41. Shukla, V., Coumoul, X., Wang, R.H., Kim, H.S. and Deng, C.X. (2007) RNA interference and inhibition of MEK-ERK signaling prevent abnormal skeletal phenotypes in a mouse model of craniosynostosis. *Nat. Genet.*, **39**, 1145–1150.
42. Westerfield, M. (1995) *The Zebrafish Book*, 3rd edn. The University of Oregon Press.
43. Thisse, C. and Thisse, B. (2008) High-resolution *in situ* hybridization to whole-mount zebrafish embryos. *Nat. Protoc.*, **3**, 59–69.